BEST AVAILABLE IMAGES

Defective images within this document are accurate representations of the original documents submitted by the applicant.

Defects in the images may include (but are not limited to):

- BLACK BORDERS
- TEXT CUT OFF AT TOP, BOTTOM OR SIDES
- FADED TEXT
- ILLEGIBLE TEXT
- SKEWED/SLANTED IMAGES
- COLORED PHOTOS
- BLACK OR VERY BLACK AND WHITE DARK PHOTOS
- GRAY SCALE DOCUMENTS

IMAGES ARE BEST AVAILABLE COPY.

As rescanning documents *will not* correct images, please do not report the images to the Image Problem Mailbox.

STIC-ILL

TP248.13.C74

From: Steadman, David (AU1652)
Sent: Friday, August 10, 2001 8:42 AM
To: STIC-ILL
Subject: Literature/ILL Request

Art Unit: 1652
Room #: 10D-04
Mailbox #: 10C-01 M3
Serial #:09/621,448

Please provide the following references:

1) Antonie Van Leeuwenhoek 1993-94;64(2):145-63
Molecular aspects of lysine, threonine, and isoleucine biosynthesis in Corynebacterium glutamicum.
Eikmanns BJ, Eggeling L, Sahm H.

2) Crit Rev Biotechnol 1995;15(1):73-103
Recent advances in the physiology and genetics of amino acid-producing bacteria.
Jetten MS, Sinskey AJ.

3) Ann N Y Acad Sci 1996 May 15;782:25-39
Construction of L-lysine-, L-threonine-, and L-isoleucine-overproducing strains of Corynebacterium glutamicum.
Sahm H, Eggeling L, Eikmanns B, Kramer R.

Thank you very much,
David Steadman

Critical Reviews in Biotechnology, 15(1):73–103 (1995)

Recent Advances in the Physiology and Genetics of Amino Acid-Producing Bacteria

Mike S. M. Jetten[1] and Anthony J. Sinskey[2]

[1]Department of Microbiology and Enzymology, Kluyver Laboratory for Biotechnology, Delft University of Technology, Julianalaan 67, 2628 BC Delft, The Netherlands; [2]Department of Biology, Room 68-370, Massachusetts Institute of Technology, 77 Massachusetts Avenue, Cambridge, MA 02139

ABSTRACT: *Corynebacterium glutamicum* and its close relatives, *C. flavum* and *C. lactofermentum*, have been used for over 3 decades in the industrial production of amino acids by fermentation. Since 1984, several research groups have started programs to develop metabolic engineering principles for amino acid-producing *Corynebacterium* strains. Initially, the programs concentrated on the isolation of genes encoding (deregulated) biosynthetic enzymes and the development of general molecular biology tools such as cloning vectors and DNA transfer methods. With most of the genes and tools now available, recombinant DNA technology can be applied in strain improvement. To accomplish these improvements, it is critical and advantageous to understand the mechanisms of gene expression and regulation as well as the biochemistry and physiology of the species being engineered. This review explores the advances made in the understanding and application of amino acid-producing bacteria in the early 1990s.

KEY WORDS: *Corynebacterium glutamicum*, lysine, glutamate, pyruvate kinase, aspartokinase, metabolic engineering.

I. INTRODUCTION

Amino acids have a wide variety of applications. Monosodium glutamate (MSG) and glycine are used as flavor enhancers in food, while some essential amino acids such as lysine, threonine, tryptophan, and methionine are supplemented in animal feed (Flodin, 1993). Phenylalanine and aspartate are used in the production of artificial sweeteners, and many other amino acids serve as therapeutic agents in nutritional and metabolic disorders or as raw material for the synthesis of cosmetics, toothpaste, shampoo, and detergents (Martin et al., 1987).

Amino acids are produced via chemical synthesis, hydrolysis of natural proteins, and bacterial fermentations (Kinoshita, 1985). Only a limited number of bacterial species are used to obtain production strains for the industrial manufacture of amino acids (Aida et al., 1986). The detailed genetic information and well-developed host-vector systems of *Escherichia coli* made this organism very suitable to construct amino acid-excreting strains via recombinant DNA technology (Beppu, 1986). In this way, *E. coli* strains were constructed that produce considerable amounts of threonine, tryptophan, or valine (Aiba et al., 1980, 1982; Beppu, 1986; Debadov, 1983; Miwa et al., 1983). Strains secreting proline, threonine, or isoleucine were derived from *Serratia marcescens* by using classic mutagenesis and screening procedures in combination with transduction of deregulated genes (Aida et al., 1986; Nakamori et al., 1986). Several *Bacillus* species have been used to breed strains that produce aromatic amino acids (Shiio, 1986).

However, the bacteria most widely used for the industrial production of amino acids belong to the *Corynebacterium-Brevibacterium* group of coryneform bacteria (Archer et al., 1989; Batt et al., 1985a; Eikmanns et al., 1993; Follettie et al., 1991; Jetten et al., 1993; Kinoshita, 1985; Liebl,

0738-8551/95/$.50

1991; Wohlleben et al., 1993). Recent DNA-DNA hybridization studies show that there are only very minor differences between the *B. flavum*, *B.. lactofermentum*, and *C. glutamicum* species (Liebl et al., 1991; Eikmanns et al., 1991). These differences do not justify the use of different genus names, and it has been proposed to consider them as one *C. glutamicum* species (Liebl et al., 1991). Throughout this paper, we therefore will use the name *Corynebacterium*. *Corynebacterium* species are Gram-positive, irregular, non-sporulating, strictly aerobic, food-grade organisms that have long occupied a central role in the manufacture of amino acids, such as glutamate, lysine, threonine, tryptophan, and phenylalanine (Kinoshita, 1985). The world-wide production in 1992 of the flavor enhancer MSG and the food-supplement L-lysine/HCl by *C. glutamicum* was estimated at approximately 800,000 and 400,000 metric tons, respectively (Randell and Andreas, 1992).

In this review, recent findings that contribute to the understanding of the relevant physiology, biochemistry, and molecular biology of *C. glutamicum* and closely related organisms, with particular emphasis on the biosynthetic pathway for the aromatic and aspartate-derived amino acids, are reviewed. Where possible, reports about other organisms and amino acids are referenced.

II. BASIC CLONING TECHNIQUES FOR *CORYNEBACTERIUM GLUTAMICUM*

Although the production of amino acid by *C. glutamicum* and close relatives has been known for more than 30 years, the first reports on the metabolic engineering of *C. glutamicum* only appeared in 1984 (Miwa et al., 1984; Santamaria et al., 1985). Since that time, several research groups have independently initiated research programs focusing on the development of metabolic engineering tools for *Corynebacterium* species (Jetten et al., 1993; Martin et al., 1987; Wohlleben et al., 1992). Essential prerequisites for the metabolic engineering of *Corynebacterium* are the availability of vectors derived from endogenous plasmids and efficient DNA transfer systems. The availability of these tools allows the cloning, expression, disruption, or replacement of genes. By using these procedures, the metabolic processes that are of biotechnological importance can be optimized and used for the construction of more efficient production strains, as has been shown for *E. coli* and *S. marcescens* (Beppu, 1986).

A. *Corynebacterium* Plasmids and Cloning Vectors

Numerous *Corynebacterium* strains have been screened for the presence of endogenous plasmids (Martin et al., 1987; Sonnen et al., 1991; Wohlleben et al., 1992). Small, cryptic plasmids were independently detected in various *Corynebacterium* strains. Some of the plasmids are very similar and to avoid confusion have been grouped into four different families (Sonnen et al., 1991). An overview is presented in Table 1.

The complete nucleotide sequences of representatives of three plasmid families (pBL1, pSR1, and pNG2) are available at the moment (Archer and Sinskey, 1993; Filipula et al., 1986; Serwold-Davis et al., 1990; Yamaguchi et al., 1986). pBL1 (4.45 kb, isolated from *C. lactofermentum*) and pHYM1519/pSR1 (3.1 kb, isolated from *C. glutamicum*) families are most popular among the research groups involved in the metabolic engineering of *Corynebacterium* strains (Archer and Sinskey, 1993; Eikmanns et al., 1991c; Jetten et al., 1994a; Miwa et al., 1985; Sandoval et al., 1985). Both plasmids have been used to construct a multitude of cloning vectors, which replicate in *Corynebacterium* strains and/or *E. coli*. Although a few endogenous antibiotic resistance genes (streptomycin, tetracycline, and trimethoprim) have been found in *Corynebacterium* (Batt et al., 1985b; Katsumata et al., 1984; Takagi et al., 1986; Takeda et al., 1990), several heterologous, more convenient antibiotic resistance markers (erythromycin, chloramphenicol, and kanamycin) are expressed efficiently in *Corynebacterium* and therefore commonly used (Cardenas et al., 1991; Chan et al., 1991; Guerrero et al., 1992; Martin et al., 1987; Santamaria et al., 1987; Serwold-Davis et al., 1987; Yoshihama et al., 1985).

A comprehensive study on the host range of the various plasmids is still lacking, but of all the *Corynebacterium* plasmids tested, pNG2 and its

TABLE 1
Overview of Plasmids Isolated from *Corynebacterium* Strains

Group	Plasmid	Bacterial source		Size (kb)	Sequenced	Markers	Ref.
pCC1	pCC1	*C. callunae*	2243	4.2	No	Cryptic	Sandoval et al., 1984
	pCC100		NCIB[a] 10318	4.2	No	Cryptic	Shaw, 1989
pBL1	pBL1	*C. lactofermentum*	ATCC[b] 21798	4.4	Yes	Cryptic	Santamaria et al., 1984
	pAM330		ATCC13869	4.5	Yes	Cryptic	Miwa et al., 1984
							Yamaguchi et al., 1986
	pWS101		ATCC 13869	4.4	No	Cryptic	Yoshihama et al., 1985
	pGX1901		ATCC 13869	4.45	Yes	Cryptic	Smith et al., 1986
							Filipula et al., 1986
	pBL100		ATCC 13869	4.5	No	Cryptic	Shaw and Hartley, 1988
	pX18		ATCC 21086	4.4	No	Cryptic	Yeh et al., 1986
pHM1519	pHM1519	*C. glutamicum*	ATCC 13058	3.0	No	Cryptic	Miwa et al., 1984
	pSR1		ATCC 13058	3.1	No	Cryptic	Yoshihama et al., 1985
			ATCC 19223	3.0	Yes	Cryptic	Archer and Sinskey, 1993
	pCG100		ATCC 13058	3.0	No	Cryptic	Shaw and Hartley, 1988
							Trautwetter and Blanco, 1991
	pCG1		ATCC 31808	3.2	No	Cryptic	Ozaki et al., 1984
pNG2	pNG2	*C. diphtheriae*	C7	14.4	Yes	E_m^R	Serwold-Davis et al., 1989
pGA1	pGA1	*C. glutamicum*	LP-6	4.9	No	Cryptic	Sonnen et al., 1991

[a] NCIB, National Collection of Industrial Bacteria, Aberdeen, Scotland.
[b] ATCC, American Type Culture Collection, Rockville, MD.

relatives have the widest host range (Serwold-Davis et al., 1987). Recently, however, a broad host-range derivative of pSR1 has been described (Archer and Sinskey, 1993) that is able to replicate in both *E. coli* and *Corynebacterium* species.

B. Mobilizable Vectors

Recently, a special class of integration vectors has been developed and is now very frequently used for gene disruption and gene replacement experiments in *Corynebacterium* (Schäfer et al., 1990; Schwarzer and Puehler, 1991). These so-called suicide vectors lack a functional *Corynebacterium* replicon, and can therefore only be maintained when integration occurs via homologous recombination into the chromosome. To employ these vectors, very efficient DNA transfer via transconjugation or electroporation is required.

C. DNA Transfer Methods

At the moment, several methods for the introduction of cloning vectors and exogenous DNA into *Corynebacterium* are available. These include protoplast transformation, transduction, electroporation, and transconjugation.

1. Protoplast Transformation and Transduction

Protoplast transformations developed for amino acid-producing *Corynebacterium* were based on the polyethyleneglycol (PEG)-mediated standard procedures used for other Gram-positive bacteria (Katsumata et al., 1985; Santamaria et al., 1985; Yoshihama et al., 1985). The efficiency of this procedure is rather low (10^5 transformants per milligram of DNA), and the regeneration of protoplasts is often problematic. Several reports have claimed that the protoplasts generated with the PEG method can also be used in protoplast-fusion experiments (Karasawa et al., 1986). The improvements obtained with this method are rather dubious, and the method appears to be very inefficient. So far only a few reports have appeared that described phage-based transduction of *Corynebacterium* strains (Momose et al., 1976; Ozaki et al., 1984; Patek et al., 1988; Sachez et al., 1986). However, the discovery and characterization of both temperate nonlytic phage phiGA1 and virulent corynephages CL31 and Cog may be a good starting point to develop new tools for the use of transduction in *C. glutamicum* (Sonnen, 1992; Sonnet et al., 1990a,b; Trautwetter et al., 1987a,b).

2. Electroporation

Instead of protoplast transformation, electroporation and transconjugation are now used as more convenient and much more efficient methods for transformation. Different research groups have each developed their own procedure for electroporation (Bonamy et al., 1990; Bonnassie et al., 1990; Dunican and Shivnam, 1990; Follettie et al., 1993; Hyanes and Britz, 1989, 1990). Normally, cells used for electroporation are grown in rich medium for 3 to 5 h, harvested at the early logarithmic phase (OD: 600 nm below 2), washed extensively with low-salt buffers containing 5 to 20% glycerol, and concentrated to approximately 10^{10} cells per milliliter before use. To increase the efficiency of electroporation, several compounds (penicillin G, ampicillin, isonicotinic acid, or Tween 80) can be added to the growth medium to make the cells more permeable for exogenous DNA (Bonassie et al., 1990; Follettie et al., 1993; Haynes and Britz, 1990; Wolf et al., 1990). Generally, 100-µl aliquots of the cells are equilibrated with 0.1 to 1 µg of DNA and subjected to a field strength of 12.5 kV/cm for about 3 to 8 msec. Thereafter, the cells are immediately mixed with 0.9 ml of an isotonic medium, incubated for 1 to 1.5 h to express the antibiotic marker, and plated on a sorbitol/sucrose/brain heart infusion medium. Transformants generally appear within 48 h. The maximum number of transformants obtained with this method varies between 4 and 5×10^7 per microgram of DNA (Haynes and Britz, 1989; Follettie et al., 1993).

3. Transconjugation

Another very efficient method for the introduction of DNA into *Corynebacterium* is the transconjugation of mobilizable suicide plasmids from *E. coli* to various *Corynebacterium* strains (Schäfer et al., 1990, 1994). This method is frequently used for gene disruption and gene replacement in *C. glutamicum* (Jäger et al., 1992; Labarre et al., 1993; Reyes et al., 1991; Schäfer et al., 1990; Schwarzer and Puehler, 1991). The system depends on the mobilization function of the broad host-range plasmids derived from RP4 to transfer plasmids from specialized *E. coli* strains (e.g., S17-1) to Gram-positive *Corynebacterium* strains. Special strains with defined deletion mutations, which lack all vector and antibiotic resistance marker sequences, can be constructed by combining the techniques of gene disruption and replacement. Strains constructed in this manner are very likely to be considered safe with respect to environmental release or industrial use. Several examples of the application of these techniques, summarized in Table 2, are reviewed in this article.

Numerous observations made during transformation and transconjugation experiments indicate the presence of restriction or modification systems in *Corynebacterium* strains (Follettie et al., 1991; Liebl, 1991; Wohlleben et al., 1992). The problems caused by these systems for cloning experiments can be overcome by the use of restriction-deficient host strains, by heating the cells for 9 min at 50°C or exposing the cells to environmental stress such as pH, ethanol, or SDS (Bonassie et al., 1990; Liebl, 1991; Follettie et al., 1991; Schäfer et al., 1990, 1994).

D. Gene Expression

A large number of both homologous and heterologous genes have been successfully expressed in *Corynebacterium*, although comprehensive knowledge about translation and transcription initiation signals in this organism is still lacking. To date there are no indications that translation initiation signals from other bacteria do not function in *Corynebacterium*. The information available on endogenous transcription initiation is only slowly emerging. So far only about ten transcription start points have been mapped (Follettie et al., 1991). Visual inspection indicated that there are major differences between these promoters and those from, for example, *E. coli* and *Bacillus subtilis*. The most conserved sequence in the promoter region was a TGTGT motif approximately 20 base pairs upstream of the transcription initiation site (Follettie et al., 1991). A TATAAT sequence analogous to other bacterial promoters around the –10 position was only moderately conserved. Recently, McCormick et al. (1993) presented a study in which the TGTGT motif of the *thr*C promoter was targeted by site-directed mutagenesis. In this way, 14 single base-pair substitutions in the TGTGT region were obtained and analyzed by comparing the differences of the β-galactosidase activity of these *thr*C-*lac*Z constructs. Of the 14 mutations, only three had a significant effect on promoter strength; a change of the TGTGT to TGCTG resulted in a two-fold increase in activity, whereas TGTCT or TGTTG resulted in a 50% decrease in promoter strength. These results are encouraging, but DNA footprinting and characterization of more *C. glutamicum* promoters will be necessary to obtain a full understanding of transcription initiation in this organism.

The efficiency and regulatory properties of very strong *E. coli* promoters such as P_{tac} were found to exhibit similar properties in *Corynebacterium* (Tsuchiya and Morinaga, 1988). Using the *lac*Iq/P_{tac} system, several inducible, high-expression vectors were constructed (Eikmanns et al., 1991c; Liebl et al., 1992; Gubler, unpublished results). In contrast to highly efficient promoters, strong transcription termination signals of *E. coli* do not seem to function in *Corynebacterium* (Wohlleben et al., 1993).

E. Isolation of *Corynebacterium Glutamicum* Genes

The availability of the aforementioned cloning systems in *Corynebacterium* has greatly facilitated the cloning of genes involved in both intermediate metabolism and several amino acid

TABLE 2
Genes Disrupted or Integrated Via Transconjugation in *C. glutamicum*

Target gene	Disrupted or integrated	Phenotype	Ref.
ask	Integrated	Increased internal lysine	Broër and Krämer, 1993
	Disrupted	No lysine production	Schrumpf et al., 1992
	Integrated	Increased lysine production	Jetten et al., 1994a
	Disrupted	No lysine production	Jetten et al., 1994a
cspA	Disrupted	No S-layer formation	Peyret et al., 1993
dapE	Disrupted	Decreased lysine production	Wehrmann et al., 1993
ddh	Disrupted	Decreased lysine production	Schrumpf et al., 1991
gdh	Disrupted	No apparent effect	Labarre et al., 1993
			Bormann et al., 1993
gltA	Disrupted	No apparent effect	Reyes et al., 1991
hom^{dr}-thrC	Integrated	Increased threonine production	Reinscheid et al., 1994
ilvA	Disrupted	Isoleucine auxotrophy	Boles et al., 1993
	Disrupted	No threonine degradation	Jetten, unpublished
lysA	Disrupted	Lysine auxotrophy	Schwarzer and Puehler, 1990
ppc	Disrupted	No apparent effect	Gubler et al., 1994a
			Peterschwinde et al., 1993
pyk	Disrupted	Decreased lysine production	Gubler, 1994b

biosynthetic pathways. Table 3 summarizes the genes cloned from *C. glutamicum*. Three strategies have been followed for cloning *Corynebacterium* genes: heterologous complementation, homologous complementation, and screening of libraries with degenerate oligonucleotides.

Complementation of *E. coli* auxotrophs by a gene bank of *C. glutamicum* made in *E. coli* using either plasmid or cosmid vectors has been used successfully in the cloning of biosynthetic genes for tryptophan, lysine, isoleucine, and threonine, and of genes encoding the glyoxylate bypass and PEP carboxylase (Table 3). A second approach has been the direct cloning of genes in *C. glutamicum* by complementation of amino acid auxotrophs of this organism. In this way, several genes of the phenylalanine and threonine pathway have been obtained (Table 3).

A third strategy, which has been used only sporadically, is the use of nucleotide probes derived from either N-terminal or internal peptide sequences of purified proteins. Recently, Gubler et al. (1994) used a combination of the aforedescribed methods to clone the pyruvate kinase gene of *C. glutamicum*. On the basis of homology between published pyruvate amino acids sequences, two degenerate oligonucleotides were designed and used to synthesize a 126-bp internal fragment of the *C. glutamicum* pyruvate kinase gene (*pyk*) via a polymerase chain reaction. This internal fragment was cloned in an RP4-derived suicide vector and used to generate defined Pyk$^-$ mutants of *C. glutamicum*. The *pyk* gene thereafter was obtained via complementation of the mutant on minimal medium containing ribose as carbon source.

Genes obtained via one of the aforementioned methods can be used to improve production strains by raising the activity of rate-limiting enzymes or removing the feedback regulation of critical enzymes. Use of such genes also allows for specific probes to be utilized in order to determine rate-limiting steps in the biosynthesis of a product of interest.

The biosynthetic pathway of several amino acids in *C. glutamicum* is used to illustrate the aforementioned technology.

III. PRECURSOR SUPPLY

A. Introduction

Although great progress has been made in the understanding of the molecular organization of biosynthetic genes (Jetten et al., 1993;

TABLE 3
Genes cloned from *C. glutamicum*

Gene	Function/gene product	Cloning method[a]	Sequenced	Ref.
*ace*A	Isocitrate lyase	CEC	Yes	Reinscheid et al., 1994b; Lee et al., 1994
*ace*B	Malate synthase	CEC	Yes	Reinscheid et al., 1993; Lee et al., 1994
*aec*D	AEC lyase	AEC^R	No	Rossol and Puehler, 1991
*arg*S	Arginyl-tRNA synthetase	SEQH	Yes	Sharp and Mitchel, 1993; Oguiza et al., 1993
aro	DAHP synthase	CEC	Yes	Chen et al., 1993
ask	Aspartokinase	CEC/AEC^R	Yes	Kalinowski et al., 1990; Follettie et al., 1993
ask^{fbr}	Feedback-resistant *ask*	CEC/AEC^R	Yes	Kalinowski et al., 1991; Follettie et al., 1993; Jetten et al., 1993
asd	ASA dehydrogenase	CEC	Yes	Kalinowski et al., 1990; Follettie et al., 1993; Jetten et al., 1994a
*csp*A	S-layer protein	NT	Yes	Peyret et al., 1993
*dap*A	DHP synthase	CEC	Yes	Bonnassie et al., 1990b; Cremer et al., 1988; Pisabaro et al., 1993; Yeh et al., 1988
*dap*B	DHP reductase	CEC	Yes	Cremer et al., 1988; Yeh et al., 1988
ddh	DAP dehydrogenase	CEC	Yes	Ishino et al., 1989; Yeh et al., 1988
*dap*E	DAP epimerase	CEC	No	Wehrmann et al., 1993
fda	Fructose-diP_i aldolase	CEC	Yes	van der Osten et al., 1990
gap	Glycerol-3P_i dehydrogenase	SEQH	Yes	Eikmanns, 1991
gdh	Glutamate dehydrogenase	CEC	Yes	Takeda et al., 1990; Bormann et al., 1992
*glt*A	Citrate synthase	UK	No	Schwinde et al., 1993
gnd	Exonuclease	NT	Yes	Liebl, 1991; Gubler, unpublished results
hom	Homoserine dehydrogenase	CEC	Yes	Follettie et al., 1988
hom^{dr}	Feedback-resistant *hom*	AHV^R	Yes	Archer et al., 1992; Reinscheid et al., 1991
*ilv*ABCN	Isoleucine biosynthesis	CEC	Yes	Cordes et al., 1992; Moeckel et al., 1992; Keilhauer et al., 1993
leu	Leucine biosynthesis	CCG	Yes	Patek et al., 1994
*lys*A	DAP decarboxylase	CEC	Yes	Marcel et al., 1990; Yeh et al., 1988
*lys*I	Lysine uptake	CEC	Yes	Seep-Feldhaus et al., 1992
pgk	Phosphoglycerate kinase	SEQH	Yes	Eikmanns, 1991
*phe*A	Prephenate dehydratase	CEC	No	Follettie and Sinskey, 1986
ppc	PEP carboxylase	CEC	Yes	Eikmanns et al., 1989; O'Regan et al., 1989
*pts*II	Enzyme II PTS system	CEC	No	Yoon et al., 1993
pyk	Pyruvate kinase	CCG	Yes	Gubler et al., 1994b; Jetten et al., 1994c
*thr*B	Homoserine kinase	CCG	Yes	Follettie et al., 1988; Peoples et al., 1988
*thr*C	Threonine synthase	CCG	Yes	Han et al., 1989
tpi	Triosephosphate isomerase	SEQH	Yes	Eikmanns, 1991
*trp*EDCBA	Tryptophan biosynthesis	CEC	Partial	Del Real et al., 1985; Follettie and Sinskey,1986; Heery and Dunican, 1993; Katsumata and Ikeda, 1992; Ozaki et al., 1985

[a] AEC^R, screening for aminoethylcystein resistance; AHV^R, screening for aminohydroxyvaline resistance; CEC, complementation of *E. coli* auxotroph; CCG, complementation of *C. glutamicum* auxotroph; NT, screening with N-terminal probe; SEQH, sequence homology.

Eikmanns et al., 1993), relatively little is known about the enzymes involved in the central carbon metabolism (Figure 1) of *C. glutamicum* (Jetten et al., 1993, 1994a, b; Krulwich and Pellicone, 1979). With the limited information available, several attempts have been made to

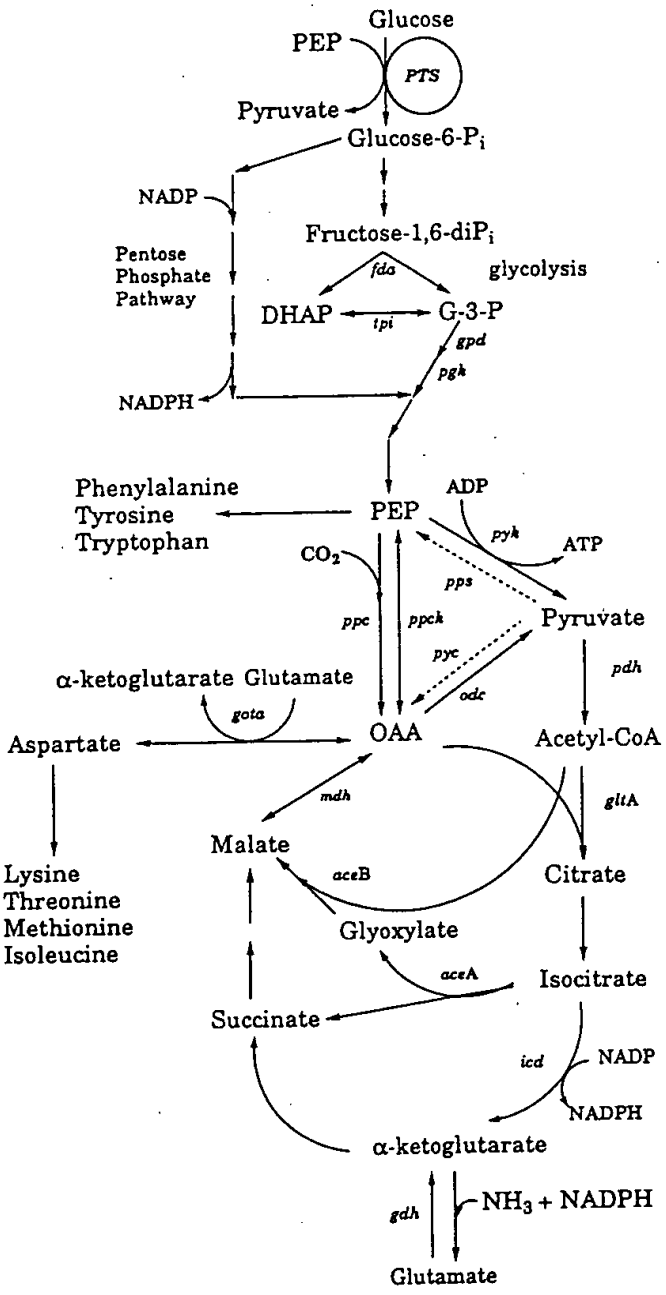

FIGURE 1. Central metabolism of *C. glutamicum*. OAA, oxaloacetate; PEP, phosphoenol pyruvate; PTS, PEP: sugar phosphotransferase system; gota, glutamate: OAA transaminase; *icd*, isocitrate dehydrogenase; *mdh*, malate dehydronase; *odc*, OAA decarboxylase; *pdh*, pyruvate dehydrogenase complex; *ppck*, PEP carboxykinase; *pps*, PEP synthetase; *pyc*, pyruvate carboxylase; abbreviations for other genes in Table 3.

estimate critical branch points and carbon fluxes during amino acid production by *C. glutamicum* (Kiss and Stephanopoulos, 1992; Stephanopoulos and Valino, 1991; Valino and Stephanopoulos, 1993). This flux analysis suggested that the regulation of carbon flow at the phosphoenol pyruvate (PEP) branch point is the limiting factor in lysine production. At this point, three different enzyme systems compete for the available PEP, pyruvate kinase, PEP: sugar phosphotransferase system (PTS), and PEP carboxylase, as outlined in Figure 1. To optimize, for example, lysine production, it seemed beneficial to amplify the PEP carboxylase (*ppc*) gene in a strain with a disrupted pyruvate kinase *pyk* gene. In such a strain, nearly all the carbon could be diverted by PEP carboxylase toward the synthesis of oxaloacetate (OAA) and aspartate, and little or no carbon would flow to the TCA cycle. In addition to diversion of the carbon flow to OAA, it would be necessary to inhibit the action of enzymes such as citrate synthase or OAA decarboxylase, which convert OAA into undesirable products. In order to direct even more carbon toward the synthesis of OAA, it also seemed beneficial to explore the presence of other enzyme systems such as the glyoxylate bypass or pyruvate carboxylase in *C. glutamicum*. Recent studies concerning several of the aforementioned aspects of the intermediate metabolism of *C. glutamicum* are summarized below.

B. Pyruvate Kinase

1. Protein Purification

Pyruvate kinase converts PEP with ADP, irreversibly to pyruvate and ATP, thereby directing the available carbon toward the TCA cycle and energy generation. Using a combination of anion exchange and affinity chromatography, pyruvate kinase from *C. glutamicum* was recently purified to homogeneity (Jetten et al., 1994c). The purified enzyme (M_r: 232 kDa) is composed of four subunits with a M_r of 59 kDa and has a very high k_{cat} (2520 s^{-1}) compared to other bacterial enzymes. The enzyme was not influenced by fructose-1,6-diphosphate and only used Mn^{2+} or Co^{2+} as cations. In addition to ADP (K_m = 0.07 m*M*), the purified enzyme also used GDP (K_m = 0.25 m*M*) and IDP (K_m = 0.12 m*M*) as substrates. The purified pyruvate kinase of *C. glutamicum* demonstrated complex sigmoidal kinetics with PEP as substrate. In the presence of the negative allosteric effector ATP, the concentration at half-maximal rate ($S_{0.5}$) increased from 1.2 to 2.8 m*M* and cooperation as expressed by the Hill coefficient increased from 2.0 to 3.2. AMP promoted the opposite effects: the $S_{0.5}$ was decreased to 0.4 m*M* and the enzyme exhibited almost no cooperation. These complex kinetics show that *C. glutamicum* is able to regulate pyruvate kinase activity to a certain extent. At high ATP levels, the enzyme is inhibited, thereby permitting the carbon flow to be directed toward biosynthesis, whereas under energy limitation, pyruvate kinase is maximally active and directs much of the carbon toward the TCA cycle and energy generation.

2. Cloning Procedure

As mentioned earlier, Gubler et al. (1994b) used a very elegant combination of several molecular genetic techniques to clone the pyruvate kinase gene of *C. glutamicum*. On the basis of several published deduced amino acids sequences, two degenerate oligonucleotides were designed and used to synthesize a 126-bp internal fragment of the *C. glutamicum* pyruvate kinase gene (*pyk*) via a polymerase chain reaction. This internal fragment was cloned in the mobilizable pSUP301 vector and used to generate defined Pyk^- mutants of *C. glutamicum* via transconjugation. Phenotypical analysis of the Pyk^- mutants revealed that they were no longer able to grow on minimal medium containing the non-PTS sugar ribose as a sole carbon and energy source. The *pyk* gene could therefore be cloned on a 2.8-kb *Bam*HI-*Pst*I fragment via complementation of the mutant on minimal ribose medium. Sequence analysis of the 2.8-kb fragment revealed an open reading frame of 1425 nucleotides encoding a 475-amino acid residue polypeptide with a subunit M_r of 59,912 Da. Sequence comparison with other bacterial pyru-

vate kinases showed an overall identity of 39 to 44%, with some very conserved regions. The information obtained from sequence analysis was used to construct more efficient mobilizable plasmids for the disruption of the *pyk* gene via marker exchange mutagenesis in lysine production strains.

3. Performance of Defined Pyk⁻ Mutants

Both Pyk⁺ and Pyk⁻ strains of *C. lactofermentum* ATCC 21799 were used in shake-flask fermentations to determine the effect of the *pyk* mutation on lysine production. The Pyk⁺ parent strain produced 26 g/l of lysine together with 3 g/l of alanine, 5 g/l of valine, and 6 g/l of acetate in 72 h from 90 g/l of glucose. The Pyk⁻ mutants only produced 15 g/l of lysine together with 3 g/l of valine and 3 g/l of alanine from 90 g/l of glucose in 72 h. In addition to 13 g/l of acetate, the Pyk⁻ strains also excreted 3 g/l of dihydroxyacetone and 4 g/l of glyceraldehyde, which might be indicative of an accumulation of glycolytic intermediates upstream of PEP. This surprising finding is in contrast to earlier reports by Mori and Shiio (1987), who claimed that the Pyk⁻ mutation was beneficial for lysine production in *C. flavum*. This and the following examples will clearly show that there is yet much to be learned about the regulation of carbon flow in this group of organisms.

C. Phosphoenol Pyruvate: Sugar Phosphotransferase (PTS) System

To date, little information exists about the functionality of the PTS system in *C. glutamicum*. Mori and Shiio (1987a, b) published two papers on the presence of a PTS in *C. glutamicum*, which was confirmed by Malin and Bourd (1991). Recently, the cloning of a PTS component was reported (Yoon et al., 1993). The unclear phenotypical behavior of previously described Pyk⁻ mutants indicates that the PTS system might not be the only way in which *C. glutamicum* is able to take up glucose.

D. Phosphoenol Pyruvate Carboxylase

PEP carboxylase converts PEP with CO_2 to oxaloacetate in order to replenish the TCA cycle with OAA, which is constantly removed from the cycle for the production of amino acids derived from aspartate. Because of this anaplerotic function, PEP carboxylase received considerable attention in the literature. The enzyme was purified and characterized by Mori and Shiio (1985), who showed that the PEP carboxylase of *C. flavum* was stimulated by acetyl-coenzyme A and inhibited by aspartate and α-ketoglutarate. The *ppc* gene encoding PEP carboxylase was cloned and sequenced later on (Eikmanns et al., 1989; O'Regan et al., 1989). Amplification of the *ppc* gene in lysine-producing *C. glutamicum*, however, did not result in higher yields. (Sano et al., 1987; Cremer et al., 1991). To elucidate the role of PEP carboxylase together pyruvate kinase in more detail, defined *ppc*⁻ and *ppc*⁻/*pyk*⁻ double mutants were constructed via marker exchange mutagenesis (Gubler et al., 1994; Jetten, unpublished results). Independently *ppc*⁻ mutants were obtained by two research groups using slightly different approaches (Gubler et al., 1994a; Peterschwinde et al., 1993). In both cases, these *ppc*⁻ mutants did not show reduced growth rates and lysine production from glucose was indistinguishable from the parent strains (Gubler et al., 1994a; Peterschwinde et al., 1993). This surprising finding is in contrast to the general opinion that *ppc* is the exclusive anaplerotic pathway in *C. glutamicum* (Mori and Shiio, 1985; Shiio et al., 1993), and indicates that other PEP-converting enzymes or even different anaplerotic reactions may play an important role in the regulation of carbon flux in *C. glutamicum*.

E. Phosphoenol Pyruvate Carboxykinase

One alternative way for the conversion of PEP was identified in both *C. glutamicum ppc*⁻ mutants and characterized in more detail (Gubler et al., 1994a; Peterschwinde et al., 1993; Jetten and Sinskey, 1993). The enzyme PEP carboxykinase was partially purified using anion exchange

chromatography to obtain PEP carboxykinase preparations free from interfering OAA-decarboxylating activities. The PEP carboxykinase activity in these preparations was completely dependent on the presence of IDP (K_m: 0.5 m*M*) with a V_{max} of 0.82 µmol/min/mg in the direction of OAA formation. ADP could not substitute for IDP, which is in contrast to the situation observed in other bacterial PEP carboxykinases. The finding that ATP inhibited 60% of the enzyme activity at 0.1 m*M* in the OAA-forming reaction indicated that the enzyme probably only functions in the gluconeogenetic direction and might be regulated by the adenosine nucleotide pools. Once the *pck* gene encoding for PEP carboxykinase becomes available and defined *pck*⁻ and *ppc*⁻/*pck*⁻ mutants can be constructed, more concrete evidence about the role of PEP carboxykinase in *C. glutamicum* can be obtained.

F. Does *C. glutamicum* Have Pyruvate Carboxylase?

Other alternative pathways for the generation of OAA besides PEP carboxykinase could be provided by pyruvate carboxylase, which converts pyruvate with CO_2 and ATP to OAA. To our knowledge, only one report exists in which the authors have claimed to be able to detect the presence of pyruvate carboxylase in *C. lactofermentum* (Tosaka et al., 1979). Several groups have tried to confirm this finding, but were unable to do so (Dominguez et al., 1993; Jetten et al., 1994a; Neuback et al., 1993). More research, especially with defined double or triple mutants (*ppc*⁻/*pyk*⁻/*pck*⁻) of *C. glutamicum* or *C. lactofermentum* might be necessary to either rule out the existence of a pyruvate carboxylase or confirm its presence. Preliminary studies with *ppc*⁻/*pyk*⁻ double mutants of strain 21799 showed that the mutants were no longer able to grow on the non-PTS sugars gluconate and ribose unless provided with pyruvate (Jetten, unpublished results). The production of lysine from pyruvate or acetate in these mutants did not seem to be impaired compared with the parent strain, which could indicate the presence of pyruvate carboxylase.

G. Glyoxylat Bypass

The glyoxylate bypass, in which isocitrate with one molecule of acetyl-coenzyme A is converted to malate and succinate via glyoxylate by the consecutive action of isocitrate lyase and malate synthase, could also function as an anaplerotic route in *C. glutamicum*. Induction and repression of the genes encoding ICL and MS (*ace*A and *ace*B) have not been studied in *C. glutamicum* (Ozaki and Shiio, 1969). When the organism is cultured on C2 (acetate) or C3 (pyruvate/lactate) compounds, the bypass seems to be fully induced, but regulation mechanisms of the isocitrate branch-point such as the isocitrate dehydrogenase kinase/phosphatase (e.g., in *E. coli*) have not been described (Ozaki and Shiio, 1969). Some reports indicate that the *ace*A-*ace*B operon is not completely repressed in the presence of excess glucose, as has been observed in *E. coli* (Gubler et al., 1994a; Ozaki and Shiio, 1969; Schrumpf et al., 1992; Reinscheid et al., 1994b). This could be due to either a different regulation mechanism or the induction of the bypass by acetate, which accumulates in the medium as a fermentation product. Recently, the genes encoding *ace*A and *ace*B have been cloned from *C. glutamicum* (Reinscheid et al., 1993; Lee et al., 1994). Preliminary results showed that the genes are organized differently in *C. glutamicum* than in *E. coli* and that the *ace*B gene of *C. glutamicum* is considerably larger than in *E. coli*. The construction of defined *ace*A⁻ mutants in combination with other mutations (*ppc*⁻/*pyk*⁻) will provide more information about carbon flow via the glyoxylate bypass and its contribution to OAA synthesis in *C. glutamicum*.

H. Oxaloacetate Decarboxylase

One other important aspect of central carbon metabolism in *C. glutamicum* is the often reported high OAA decarboxylating activities in crude extracts of this organism. Using various chromatographic procedures, the OAA-decarboxylating enzyme was purified 300-fold from a *C. glutamicum* pyruvate kinase mutant (Jetten and Sinskey, 1995). The molecular mass determined

by gel filtration was 118 kDa, while SDS-PAGE only showed one subunit of 32 kDa, indicating an α_4 subunit structure for the native enzyme. The enzyme exclusively decarboxylated OAA and did not use any other α-keto acids as substrate. Mn^{2+} was required for full activity but could be replaced by Mg^{2+}, Ni^{2+}, Co^{2+}, and Ca^{2+}. The enzyme has a low affinity for OAA (K_m = 2.1 m*M*) and Mn^{2+} (K_m = 1.2 m*M*) and V_{max} of 158 µmol/min/mg. The enzyme was not inhibited by avidin, indicating that biotin is not involved in the decarboxylation. The purified enzyme did not show any pyruvate kinase, pyruvate carboxylase, malate dehydrogenase, PEP carboxykinase, or malic enzyme activities, demonstrating that it belongs to the divalent cation-dependent OAA decarboxylases. In contrast to several other OAA decarboxylases, the enzyme from *C. glutamicum* was not inhibited by acetyl-CoA, but greatly affected by Cu^{2+}, ADP, GDP, and HSCoA. This inhibition pattern is not easily explained. One could speculate that OAA-decarboxylating activity serves to prevent the build up of OAA in the cell. In the absence of a sufficient acetyl-coenzyme A supply, a high OAA concentration may lead to an inhibition of the TCA cycle by shifting the OAA/malate equilibrium. The decarboxylation of OAA to pyruvate, together with the oxidative conversion of the formed pyruvate to acetyl-SCoA, would provide enough precursors for citrate synthase to continue the operation of the TCA cycle. To what extent the OAA decarboxylase contributes to *in vivo* OAA decarboxylation is not known (Jetten et al., 1993; Jetten and Sinskey, 1995).

I. Miscellaneous

Recently, several more genes encoding enzymes involved in central carbon metabolism have been isolated and characterized. Eikmanns (1992) located a large cluster of glycolytic genes upstream of the *ppc* gene by sequence analysis. The cluster consists of *gap* (glyceraldehyde-3-phosphate dehydrogenase), *pgk* (3-phosphoglycerate kinase), and *tpi* (triose-phosphate isomerase). Transcriptional analysis of the gene cluster by Northern blots identified four different mRNAs corresponding to *gap*, *gap-pgk-tpi*, *pgk-tpi*, and *pgk-tpi-ppc*. Primer extension analysis located the transcriptional initiation sites in front of *gap* and *pgk*. The DNA sequence of these promoter structures was aligned with previously determined transcriptional start sites of *C. glutamicum*. No homology was found with typical *E. coli* or *B. subtilis* promoters, but a tentative consensus sequence at –35 was identified as TTGACA. Mutational analysis by McCormick et al. (1993) (see also, Section II.E), however, showed a TGTGC motif as the most conserved among *C. glutamicum* promoters. This discrepancy clearly points out that additional information based on DNA footprinting is necessary before more definite conclusions concerning structure-function relationships can be made.

J. Conclusion on Precursor Supply

Although there have been many papers describing mutants defective in enzymes of central metabolism (Shiio et al., 1991), our understanding of the central metabolism in *C. glutamicum* is still very limited. Now that new, more powerful genetic tools and more genes involved in the central metabolism have become available, a new phase in the study of the intermediate metabolism can start. The construction of defined double or triple mutants will be necessary to provide strains with proper genetic backgrounds. These strains can be used to identify which enzyme systems contribute to what extent in the biosynthesis of various compounds. Similar to recent studies with *E. coli*, the effect of the overexpression of different enzymes (*ppc*, *pck*, and *pyk*) on growth rate and metabolite production in *C. glutamicum* mutants can be evaluated and used to improve amino acid production strains (Chao and Liao, 1993; Chao et al., 1993).

IV. GLUTAMATE

A. Enzymes Responsible for Glutamate Synthesis

Under certain culture conditions such as biotin limitation or addition of surfactants,

C. glutamicum is able to excrete large amounts of L-glutamate into the medium (Clement and Laneelle, 1986; Kinoshita, 1985; Shiio et al., 1963). The generally accepted explanation for this high-level accumulation is that the exit of glutamate leads to decreases in the internal pool of this amino acid, which in turn relieves feedback control mechanisms (Liebl et al., 1991). However, Frings et al. (1993) showed that glutamate and glutamine serve as osmoprotectants in *Corynebacterium* strains exposed to high salt concentrations. It has been further postulated that the low activity and high instability of the α-ketoglutarate dehydrogenase from *C. glutamicum* favors the conversion of α-ketoglutarate by glutamate dehydrogenase (GDH), especially in the presence of high NH_4^+ concentrations (Shiio and Ujigawa, 1980). Glutamate can be formed by either the previously mentioned GDH or the coupled action of glutamine synthase (GS) and glutamate synthase (GOGAT) under low NH_4^+ concentrations. All three enzymes have been detected in and purified from *C. glutamicum* strains (Takeda et al., 1990), but only recently has the gene encoding GDH been cloned from both *C. glutamicum* and *C. melassecola* (Bormann et al., 1991; Takeda et al., 1990). Sequence analysis of the *C. glutamicum* GDH reading frame showed that the *gdh* gene consists of 1344 bp encoding a 448-amino acid residue polypeptide. The deduced amino acid sequence showed between 47 and 54% identity with amino acid sequences of other organisms (Bormann et al., 1991). Physiological studies with overexpressed *gdh* revealed no indications of significant regulation of *gdh* expression. Northern blot analysis indicated a 1.7-kb monocistronic *gdh* transcript, while RNA polymerase footprinting showed a transcription initiation site 185 nucleotides upstream from the ATG start codon.

Glutamate synthesis in *C. glutamicum* is generally believed to be dependent on the activity of GDH because (1) the GS/GOGAT system is repressed under the high NH_4^+ concentrations of the fermentation media employed, (2) the GDH activity is orders of magnitude higher than the GS/GOGAT system, and (3) GDH mutants of *C. flavum* were described as glutamate auxotrophs with negligible glutamate excretion. In order to verify this hypothesis, Bormann et al. (1993) constructed defined GDH deficient mutants via marker exchange mutagenesis and strains with tenfold overexpressed GDH activity. Comparison of these two strains with the wild type revealed that GDH is dispensable for glutamate synthesis required for growth and that the level of GDH has no influence on glutamate accumulation. The authors related this surprising result to the compensatory capacity of the GS/GOGAT system and a limitation of the glutamate secretion system.

B. Glutamate Excretion

The mechanism of glutamate transport into the medium has been subject of a long controversy in the literature. Three different mechanisms have been proposed to describe glutamate efflux. The "leak" model is based on the observation that glutamate efflux can be induced by various treatments such as biotin limitation, addition of sublethal amounts of penicillin, or addition of surfactants, all of which correlate with alterations in the cell membrane (Clement and Laneelle, 1986; Duperray et al., 1992). The second hypothesis is based on a general model for many efflux processes in bacteria, namely, inversion of the uptake process induced by changes in chemical potential or regulation, or by uncoupling due to changes in the membrane structure (Clement et al., 1984). Krämer and co-workers (Gutmann et al., 1992; Hoischen and Krämer, 1989; Hoischen and Krämer, 1990; Plakunov et al., 1992; Krämer, 1994), however, have proposed a model based on the presence of a specific glutamate carrier because several of the observations did not agree with either the "leak" or the "inversion" model: (1) *C. glutamicum* cells were able to export glutamate against an existing gradient, which makes it unlikely that the internal/external glutamate ratio can be the driving force for glutamate efflux (Gutmann et al., 1992), (2) glutamate export proceeded even in the absence of a membrane potential (Gutmann et al., 1992), (3) the transport of glutamate was not coupled with the movement of H^+, K^+, or Cl^- ions, as would be expected in the "leak" model (Gutmann et al., 1992), (4) the carrier was specific for glutamate; no transport of amino acids other than

glutamate was observed (Hoischen and Krämer, 1989; Gutmann et al., 1992), (5) the observed difference between the excretion and uptake rates (Krämer and Lambert, 1991; Krämer et al., 1991) ruled out the inversion of the uptake system, (6) no changes were observed in the fatty acid or phospholipid contents when cells were switched between nonproducing and producing states (Hoischen and Krämer, 1990), and (7) there was no specific membrane component that regulated glutamate efflux (Hoischen and Krämer, 1990). In addition, Neuback et al. (1993) could not detect any differences in the anisotropy of membranes from producing or nonproducing cells. Because no change in anisotropy of membranes was observed during any period in the fermentation, Neuback et al. (1993) concluded that glutamate secretion was not coupled to differences in membrane fluidity, making the efflux of glutamate via a "leak" very unlikely.

Gutmann et al. (1992) determined that there was a positive correlation between the secretion rate and the intracellular ATP pool, indicating that ATP or a high-energy compound could be involved in the activity of the secretion system. Isolation and characterization of the specific glutamate carrier of *C. glutamicum* and cloning and characterization of the gene(s) encoding the glutamate transport system will be necessary to provide further evidence for the active transport model.

V. LYSINE

A. Aspartokinase

Lysine biosynthesis in amino acid-producing *Corynebacterium* strains proceeds via the diaminopimelate (DAP) pathway (Figure 2). Aspartokinase (ASK) and aspartate semialdehyde dehydrogenase (ASD) catalyze the initial reactions of this pathway (Follettie et al., 1993; Kalinowski et al., 1991; Tosaka and Takinami, 1978). Regulation of the multibranched biosynthetic pathway of the aspartate family of amino acids in *C. glutamicum* is relatively simple. In contrast to *E. coli* and *Bacillus* sp., which have three distinct isoenzymes, only one ASK has been observed in *C. glutamicum* so far (Follettie et al., 1993; Kalinowski et al., 1991). However, studies with a defined *ask* mutant of *C. lactofermentum*, obtained via marker exchange mutagenesis, showed that the ask mutant was still able to grow on minimal medium, indicating that more than one ASK could be present in this organism (Jetten et al., 1995). Also, there is no apparent regulation of the synthesis of any enzymes of the lysine pathway in *C. glutamicum*. Instead, this pathway is thought to be coordinated by relative specific activities, and patterns of inhibition and repression at key branch points (Follettie et al., 1993; Tosaka and Takinami, 1978). The main control of carbon flow into this pathway is mediated by concerted feedback inhibition of ASK by lysine and threonine (Shiio and Miyajima, 1969). Wild-type *C. glutamicum* does not excrete significant amounts of lysine (Schrumpf et al., 1992). Classically, lysine-producing *C. glutamicum* strains were obtained by screening for resistance to the lysine analog S-(α-aminoethyl)-D,L-cysteine (AEC) and by screening for homoserine and threonine auxotrophs (Tosaka and Takinami, 1978). Most of these resistant strains contain an ASK that is resistant to feedback inhibition by lysine and threonine (Shiio et al., 1991, 1993).

In order to elucidate the mechanism of feedback resistance of ASK in *C. glutamicum*, the *ask* genes from both wild-type and feedback resistant, lysine-producing *C. glutamicum* strains have been isolated and characterized (Kalinowski et al., 1990, 1991; Follettie et al., 1993; Jetten et al., 1995). The *ask* and *asd* genes were found to be organized in an operon and separated by a 23-base pair intercistronic region. The *ask-asd* operon can be isolated by complementation of *E. coli* strain 5080, which lacks an *asd* gene (Follettie et al., 1993; Jetten et al., 1995). This strain therefore cannot grow on LB medium, which does not contain the diaminopimelate (DAP) needed for cell wall synthesis. The complete nucleotide sequence of the *ask-asd* operation has been determined for both *C. glutamicum* and *C. flavum* strains (Kalinowski et al., 1991; Follettie et al., 1993). Computer analysis of potential protein-coding regions identifies two long open-reading frames of 421 and 344 residue proteins, respectively. Analysis of the amino acid sequence of the first open-reading frame showed

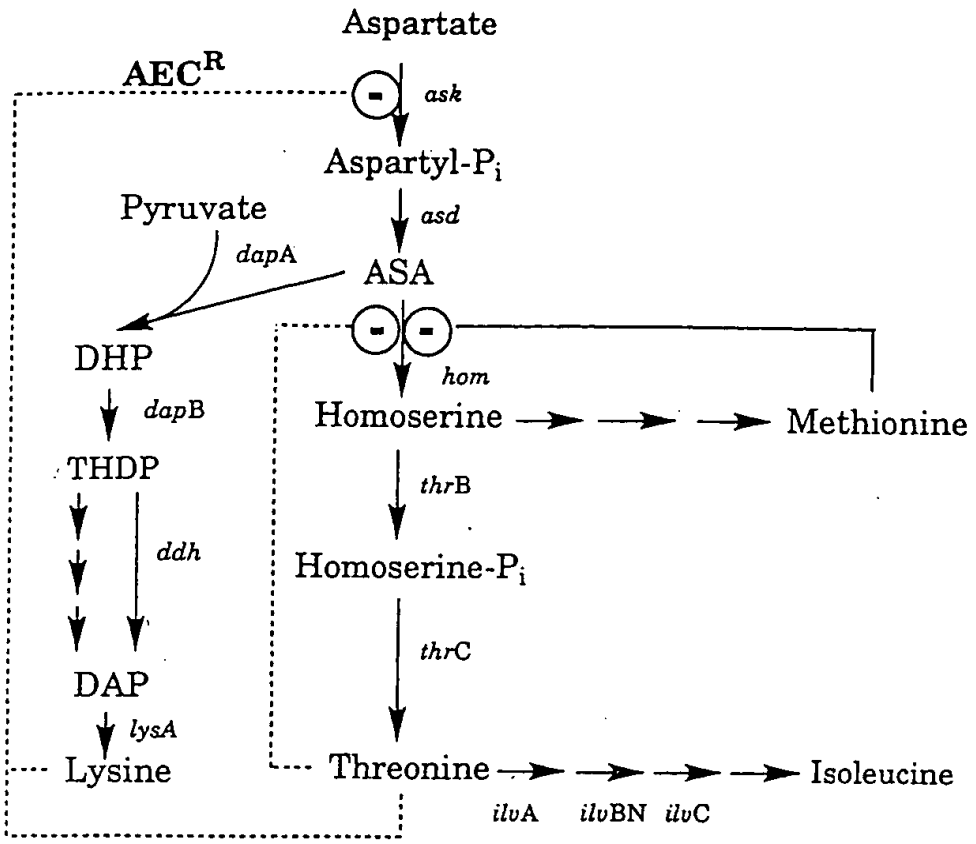

FIGURE 2. Biosynthetic pathway for aspartate-derived amino acids. AEC^R, aminoethylcysteine resistance; ASA, aspartate-β-semialdehyde; abbreviations for genes in Table 3.

significant homology and identity to previously characterized aspartokinases in other microorganisms. Deletion analysis and S1 nuclease mapping showed that two promoters are required for expression of the complete operon. Promoter P1 is located 38 nucleotides upstream of the predicted translation initiation site of the *ask* gene, while a second promoter (P2) responsible for 40% of *asd* expression was found to be located inside the *ask* gene. The presence of this second promoter, a potential ribosome-binding site at position 1105 and a GTG translation initiation codon at position 1116, provided excellent evidence that the *C. glutamicum ask* gene encoded a second polypeptide. The expression of the postulated AKα and AKβ subunits was confirmed by Western blot analysis with polyclonal antibodies generated to the C-terminal 179-amino acid residues of the *C. glutamicum* ask gene product. This organization is similar to the *ask*II gene in *B. subtilis* that encodes the α- and β-subunits required for functional aspartokinase enzyme activity.

In order to determine the molecular basis of deregulation of ASK and concomitant AEC resistance, the nucleotide sequences of wild-type and feedback-resistant *ask* genes were compared (Kalinowski et al., 1990, 1991; Follettie et al., 1993; Jetten et al., 1995). Only four of the observed mutations in the DNA sequence resulted in changes in the amino acid sequence of the feedback-resistant ASK. All four mutations are located in the coding region for the *ask* β-subunit. Analysis of hybrid *ask* genes containing one or the other of the amino acid differences demonstrated that the deregulation of the aspartokinases were due to an S301Y, G345D, or R349G substitution (Kalinowski et al., 1990; Follettie et al., 1993; Jetten et al., 1994). Because all three deregulated aspartokinases characterized so far contain muta-

tions in the carboxy terminus of the enzyme, a regulatory role of the β-subunit has been proposed by Follettie et al. (1993). More detailed analysis and site-directed mutagenesis are necessary to locate the different binding sites of threonine and lysine to the aspartokinase and to understand the mechanism of the feedback inhibition.

The effect of deregulated, feedback-resistant ASK on lysine production has been studied in various high lysine-producing *C. glutamicum* strains (Cremer et al., 1990; Schrumpf et al., 1992; Shiio et al., 1991; Jetten et al., 1995). In most cases, amplification of the *ask* gene resulted in significant increases in lysine production, indicating that in these strains ASK levels are still the limiting factor.

B. Enzymes Involved in Synthesis and Conversion of Mesodiaminopimelate

The pathway of aspartate-derived amino acids diverges after the synthesis of aspartate semialdehyde, one branch leading to the biosynthesis of DAP and lysine, the other one to threonine, methionine, and isoleucine. The condensation of ASA with pyruvate to dihydropicolinate (DHP) is the committed step in the conversion of ASA via DAP to lysine. This reaction is catalyzed by DHP synthase. The enzyme has a rather low affinity for both ASA and pyruvate (Cremer et al., 1988), compared to the enzyme competing for ASA, homoserine dehydrogenase (Archer et al., 1991; Follettie et al., 1988). The gene for DHPS, *dap*A, has been cloned by complementation of *E. coli dap*A mutants and was found to be closely linked to *dap*B, the gene encoding for the next step in the pathway, DHP reductase (Cremer et al., 1988; Pisabarro et al., 1993; Yeh et al., 1988). Neither the activity nor the expression of the DHPS seems to be affected by lysine (Cremer et al., 1988; Yeh et al., 1988). Shiio et al. (1987) reported that mutants with defective DHPS were reasonable threonine producers, but required high levels of meso-DAP for optimal growth. Although no meso-DAP transport is known to occur in *C. glutamicum*, the overproduction of threonine by these mutants would be consistent with the notion that the competition of DHPS and homoserine dehydrogenase for ASA regulates the flow of intermediates into the two main branches of this pathway.

The *dap*B gene encoding the DHP reductase of *C. glutamicum* has been cloned by complementation of *E. coli dap*B mutants and is closely linked to *dap*A (Cremer et al., 1988; Pisabarro et al., 1993; Yeh et al., 1988). The *dap*A-*dap*B genes are clustered on a 3.5-kb *Sau*3AI-*Bam*HI fragment, but separated by an open reading frame of 750 bp. Pisabarro et al. (1993) speculated that this open reading frame may encode for a 29-kDa polypeptide involved in the cyclization of dihydropicolinate.

C. glutamicum has a high level of meso-DAP dehydrogenase and contains all the enzymes of the epimerase pathway for meso-DAP synthesis (Schrumpf et al., 1991; Yeh et al., 1988). The epimerase pathway in *C. glutamicum* seems to prefer succinylated intermediates. In *C. flavum*, however, higher activities have been reported for the acetylated intermediates (Tosaka and Takinami, 1978). The gene for meso-DAP dehydrogenase (*ddh*) has been cloned by its ability to restore lysine synthesis in *E. coli dap*D mutants with a defective epimerase pathway (Ishino et al., 1987, 1988; Yeh et al., 1988). Studies with strains containing either a disrupted *ddh* gene or a disrupted *dap*E gene showed that both the epimerase and dehydrogenase pathways contribute to lysine biosynthesis (Schrumpf et al., 1991; Sonntag et al., 1993; Wehrman et al., 1993). Using ^{13}C labeled glucose, Sonntag et al. (1993) determined how the flux was distributed between the different pathways. They showed that the *ddh* pathway contributed about 30% to lysine synthesis in both wild-type and lysine production strains. Pseudo steady-state experiments also revealed that the flux partitioning over the *ddh* pathway in a production strain decreased from 70% in the initial stages of the fermentations to 0% at the end of lysine accumulation, probably due to NH_4^+ depletion. Although lysine itself had no effect on the activity of the DDH, the enzyme did not contribute to lysine synthesis when NH_4^+ was replaced by glutamate as an ammonium source, showing that this anabolic pathway is directly influenced by an extracellular medium component (Sonntag et al., 1993; Cremer et al., 1988).

The final step in the biosynthesis of lysine is the pyridoxal phosphate-dependent decarboxylation of meso-DAP to lysine, catalyzed by DAP decarboxylase. The gene encoding DAP decarboxylase (*lys*A) has considerable homology to the gene of *E. coli* (Yeh et al., 1988). The expression of *lys*A in *C. glutamicum* depends on the presence of a 2.35-kb region upstream of the *lys*A coding region (Marcel et al., 1989). On the basis of DNA homology, this region was recently identified as a possible coding sequence for arginyl-tRNA synthetase (Oguiza et al., 1993; Sharp and Mitchell, 1993). *Arg*S appears to be cotranscribed with the *lys*A gene in a single 3000-nucleotide transcript (Oguiza et al., 1993). Oguiza et al. showed that the transcription of the *arg*S-*lys*A operon was repressed by lysine and induced by arginine, indicating a peculiar pattern of interlock between these two pathways in *C. glutamicum*.

C. Lysine Transport

Wild-type *Corynebacterium* strains do not secrete significant amounts of lysine into the medium (Schrumpf et al., 1992). Effective high lysine secretion is only possible when (1) concerted feedback inhibition of lysine and threonine on aspartokinase is removed and (2) additional mutations in the lysine export system have occurred. High internal lysine concentrations and concomitant lysine secretion are thought to be the result of these mutations (Broër and Krämer, 1991, 1992a, b). The lysine secretion systems of three different lysine-producing *C. glutamicum* strains were characterized and compared to verify this hypothesis (Broër et al., 1993). A pseudo wild-type strain (KK-25) with a resistant aspartokinase gene introduced into the chromosome via conjugal transfer showed only a very low lysine export rate of 2 nmol/min/mg dry weight, and the strain did not secrete lysine when the internal concentration was below 15 m*M*. *C. glutamicum* production strains DG 52-5 and MH20-22B, obtained via classical mutagenesis and screening, had comparable high lysine secretion rates (11 nmol/min/mg dry weight) and K_m values (18 ± 5 m*M*), but showed subtle differences in dependence on ΔpH and membrane potential. On the basis of these observations, it was proposed that at least strain MH20-22B carried a mutated form of the lysine export permease. The same conclusion was reached in another study, where strain MH20-22B was characterized in more detail (Schrumpf et al., 1993). The strain was obtained after two rounds of mutagenesis and screening, the first one based on AEC resistance, the second on leucine auxotrophy and lysine production. The main differences with its predecessor are feedback-resistant aspartokinase, lack of isopropylmalate dehydratase, and a high secretion rate of lysine (10 nmol/min/mg dry weight). Application of site-directed mutagenesis to this strain revealed a key role for deregulated aspartokinase and the probable presence of a mutated secretion system, as observed by Broër and Krämer (1993).

To study the wild-type lysine secretion system of *C. glutamicum* in more detail, Erdmann et al. (1993) investigated the effect of dipeptide uptake on lysine excretion. Uptake of dipeptides containing lysine increased the internal lysine concentration, thereby triggering the secretion process. The secretion of lysine depended on the medium composition in which the cells were grown. Experiments where protein synthesis was inhibited with chloramphenicol indicated that *de novo* protein synthesis is necessary for the regulation of lysine secretion.

Because *C. glutamicum* mutants can produce up to 1 *M* of the cation lysine in the medium, export must not only proceed against a chemical gradient but also against the membrane potential. As the ATP content of the cells did not correlate with the export activity, it was proposed that lysine is presumably secreted in a symport mechanism with two OH^-, which is energetically equivalent to a lysine/$2H^+$ antiport mechanism. In this way, the positive charge of lysine is compensated for and the membrane potential can function as the driving force for excretion. Similar to elucidation of the glutamate transport in *C. glutamicum*, the availability of the gene encoding the lysine permease will greatly contribute to our current understanding of the lysine export process.

VI. THREONINE

A. Molecular Organization of the Threonin Biosynthetic Pathway

As already mentioned, the relative affinities of the competing enzymes homoserine dehydrogenase and dihydropicolinate synthase determine the distribution of the common substrate aspartate-β-semialdehyde (ASA) to the divergent threonine and lysine biosynthesis pathways (Follettie et al., 1993). Carbon flows preferentially toward the threonine pathway at the expense of lysine biosynthesis as a result of the 15-fold-higher substrate affinity and substrate conversion rate exhibited by homoserine dehydrogenase over its competing enzyme dihydropicolinate synthase (Shiio et al., 1989). The activity of homoserine dehydrogenase is highly sensitive to allosteric inhibition by L-threonine (K_i = 0.16 m*M*) and therefore, in the presence of sufficient threonine, ASA predominantly enters the lysine pathway (Figure 2).

The *C. glutamicum* genes encoding the first two enzymes in the threonine pathway, homoserine dehydrogenase and homoserine kinase, were isolated by complementation of *E. coli thr*B mutant (Follettie et al., 1988). The two genes form an operon that is expressed from a single promoter located immediately upstream of the *hom* gene (Peoples et al., 1988). The *hom-thr*B operon is genetically regulated at the level of transcription by a threefold repression by methionine via a unique attenuator system (Jetten et al., 1993). Two research groups have isolated and characterized genes encoding deregulated feedback-resistant homoserine dehydrogenase (Archer et al., 1992; Reinscheid et al., 1991) in order to investigate the molecular basis for L-threonine allosteric inhibition of homoserine dehydrogenase. The complete nucleotide sequence of both *hom*^{dr} genes was determined, and comparison with the wild-type sequence revealed that both mutations responsible for the deregulation are located in the carboxyl end of the enzyme. Archer et al. (1992) determined that the *hom*^{dr} mutation is due to a single base deletion in codon 429 within the homoserine dehydrogenase gene. The resulting frameshift mutation radically alters the structure of the carboxy terminus, leading to ten amino acid changes and a deletion of the last seven residues relative to the wild type. Similar results were obtained by Reinscheid et al. (1992), who studied the deregulated *hom*^{dr} gene of the AHV-resistant *C. glutamicum* mutant DM 368-3. A DNA fragment exchange experiment between wild-type and deregulated homoserine dehydrogenase genes showed that a 0.23-kb region close to the 3′ terminus of the *hom*^{dr} gene was responsible for the deregulation. Comparison of sequence data revealed that the mutation in the *hom*^{dr} gene was due to single transition from G to A at position 1133, leading to a replacement of glycine-378 by glutamate.

The final step in the biosynthesis of threonine is the conversion of homoserine-phosphate to threonine. This reaction is catalyzed by the enzyme threonine synthase. The *thr*C gene encoding threonine synthase was obtained by complementation of a *C. glutamicum* threonine auxotroph (Han et al., 1989). The *thr*C gene is expressed as a single 1.3-kb transcript that is translated into a polypeptide of 54.5 kDa. Expression of threonine synthase appeared to be constitutive in *C. glutamicum*. The predicted amino acid sequence of threonine synthase showed homologies of 22 and 15% with the predicted *thr*C gene products of *E. coli* and *B. subtilis*, respectively. The homology was predominantly located in the N-terminal part of the proteins, and it has been suggested that this region may bind the pyridoxal-phosphate coenzyme.

B. Threonine Production by Recombinant *C. glutamicum* Strains

In order to obtain information on the limiting steps in carbon flux to threonine and construct well-defined recombinant threonine-producing strains, the effects of the combined amplification of the threonine biosynthetic genes on amino acid production in wild-type and lysine plus threonine-producing strains has been studied (Eikmanns et al., 1991; Reinscheid et al., 1994; Colon et al., 1993). Amplification of threonine genes in wild-type *C. glutamicum* 13032 did not result in any threonine secretion, reflecting the key role of the still feedback-

inhibited aspartokinase of this strain (Eikmanns et al., 1991). Introduction of the deregulated homoserine dehydrogenase gene *hom*^{dr} together with the wild-type homoserine kinase gene *thr*B on a multicopy plasmid in lysine-producing strains resulted in unstable transformant that produced only limited amounts of threonine (Archer et al., 1992; Eikmanns et al., 1991). In order to solve the instability problems, Reinscheid et al. (1994) integrated the *hom*^{dr}-*thr*B operon into the chromosome of the lysine producer MH20-22B via conjugal transfer. In this way, they obtained strains with one, two, or three copies of the deregulated *hom*^{dr}-*thr*B operon that were stable for more than 70 generations. In the MH20-22B strains with one copy of the *hom*^{dr}-*thr*B operon, lysine production was reduced from 208 to 129 m*M* as compared to the parent strain, with concomitant production of 39 m*M* threonine, 14 m*M* homoserine, 21 m*M* isoleucine, and 33 m*M* glycine. Strains containing three copies of the deregulated operon produced 58 m*M* lysine, 65 m*M* threonine, 21 m*M* homoserine, 31 m*M* isoleucine, and 30 m*M* glycine. The authors further observed a drastic increase in the internal concentration of both threonine (100 m*M*) and homoserine (74 m*M*). It was therefore concluded that overall threonine production is most probably limited by the efflux of threonine (Reinscheid et al., 1994). Similar to the results of Reinscheid et al. (1994), Colon et al. (1993) observed increased levels of homoserine and isoleucine in cells of *C. lactofermentum* with an amplified *hom*^{dr}-*thr*B operon. The accumulation of homoserine is most likely caused by the inhibition of the *thr*B product homoserine kinase at higher threonine concentrations (Reinscheid et al., 1994). In order to prevent an intracellular build up of homoserine, Colon et al. (1993) fused the *thr*B gene to the *tac* promoter and regulated *hom*^{dr}/P*tac*-*thr*B expression by the addition of IPTG. In this way, complete conversion of homoserine to threonine was observed. Unfortunately, most of the threonine produced was either converted to isoleucine or degraded to glycine, resulting in only moderately increased threonine production. The conversion of threonine to isoleucine was prevented by the construction of defined *ilv*A mutants via marker exchange mutagenesis (Jetten, unpublished results). The degradation of threonine to glycine is not easily solved. At least two different enzyme systems have been reported to convert threonine to glycine. The first system consists of the combined action of threonine dehydrogenase and 2-amino-3-oxobutyrate-CoA ligase, which converts threonine via 2-amino-3-oxobutyrate to glycine and acetyl-CoA (Bell and Turner, 1976). The second possible mechanism is nonspecific conversion by the *gly*A gene product serine hydroxymethyltransferase (Plamann and Stauffer, 1983; Schirch et al., 1985). Unfortunately, neither of the genes for these systems have yet been characterized in *C. glutamicum*, and hence defined mutants obtained via marker exchange mutagenesis will not be available soon. The fastest way of obtaining mutants defective in either *gly*A or *tdh* would be screening for strains unable to grow on threonine or glycine as the sole carbon and nitrogen source.

Another approach to develop *C. glutamicum* threonine production strains has been amplification of the *thr* operon from *E. coli* in *C. flavum* (Ishida et al., 1993; Patek et al., 1989, 1993). Plasmids containing the *E. coli thr* operon were only maintained by applying high trimethoprim concentrations in the broth. In this way, Ishida et al. (1993) obtained a *C. flavum* strain that produced 64.4 g/l of threonine from acetate (700 g/l) and glucose (100 g/l) with a yield of 19.9% in 92 h. The strains used by Patek et al. (1993) produced 12 g/l of threonine from 180 g/l of sucrose in 48 h, which is approximately half the amount obtained by Reinscheid et al. (1994).

Many of the problems experienced in the construction of *C. glutamicum* threonine production (redirection of carbon flow, threonine degradation) have also been encountered in the breeding of either *E. coli* (Debadov, 1982) or *S. marcescens* threonine production strains (Masuda et al., 1993). Recently, Masuda et al. (1993) described the performance of *S. marcescens* strain T-2000 in batch fermentation. Strain T-2000 was obtained by transformation of strain T-1165 with plasmid pSK301 containing a mutant threonine operon. Strain T-1165 itself is defective in

two threonine-degrading enzymes and already contains the deregulated threonine operon on the chromosome. Introduction of the low-copy-number plasmid pSK301 did not give the expected increase in threonine yield. Therefore, the effect of different nitrogen sources on threonine production by strain T-200 was investigated. By changing the nitrogen source from the normally employed urea to ammonium, the authors were able to obtain an increase in threonine titers from 55 to 100 g/l from 300 g/l of sucrose, showing that maintaining sufficient levels of ammonium in the fermentation broth can be very critical. Without mentioning any specific bottlenecks, the authors even expected greater improvements in threonine yield if they could optimize the precursor flow toward the threonine pathway.

VII. ISOLEUCINE

A. Molecular Organization of Genes Involved in Isoleucine Biosynthesis

The biosynthesis of isoleucine in *C. glutamicum* and other organisms starts with the conversion of L-threonine to 2-oxobutyrate (Figure 2) catalyzed by the *ilv*A gene product L-threonine deaminase (LTD) (Möckel et al., 1992). The next step in the synthesis is performed by an acetohydroxy acid synthase (AHAS), which naturally uses both 2-oxobutyrate and 2-acetolactate as substrate. In Enterobacteriaceae, up to five different AHAS isozymes have been found, each with a different complex regulation pattern (Barak et al., 1987). To date, only one enzyme is known in *C. glutamicum* (Cordes et al., 1992; Eggeling et al., 1987).

Both LTD and AHAS are feedback inhibited by isoleucine, while AHAS is also inhibited by leucine and valine (Cordes et al., 1992). Further, the expression of AHAS seems to be regulated by all three branched-chain amino acids (Eggeling et al., 1987). Sahm and co-workers studied the production of isoleucine from 2-oxobutyrate in the late 1980s (Eggeling et al., 1987; Scheer et al., 1987), and recently described the isolation and molecular characterization of the genes involved in branched amino acid synthesis in *C. glutamicum* (Cordes et al., 1992; Keilhauer et al., 1993; Möckel et al., 1992). The genes encoding LTD, AHAS, and isomeroreductase (IRT) were cloned via complementation of *E. coli* mutants defective in one of the isoleucine biosynthetic genes (Cordes et al., 1992). Deletion analysis of the obtained clones and expression in a homologous *C. glutamicum* background showed that the *ilv*B (AHAS) and *ilv*C (IRT) genes were clustered on a 7-kb chromosomal fragment and probably are transcribed in the same direction. Southern blot analysis showed that the *ilv*A gene is localized at least 6 kb away from the *ilv*BC genes, indicating that *C. glutamicum* does not have a clustered *ilv* operon as has been reported for *E. coli*.

Analysis of overexpressed LTD showed that the enzyme is composed of four identical subunits and exhibits complex sigmoidal kinetics (Möckel et al., 1992). The negative allosteric effector isoleucine increased both the cooperativity, as expressed in terms of the Hill coefficient (n), from 2.4 to 3.7 and the substrate concentration ($S_{0.5}$), where half-maximal rates are observed, from 21 to 78 m*M* threonine. The positive effector valine promoted the opposite effects: reduction of $S_{0.5}$ to 12 m*M* threonine and no cooperativity (n = 1). Sequence analysis of the *ilv*A gene revealed an open reading frame encoding a polypeptide of 436 amino acids with an M_r of 46,599 Da, which is in agreement with the molecular mass determined for the subunit of the native enzyme. Comparison of the deduced *ilv*A amino acid sequence with sequences of other threonine deaminases showed that the *C. glutamicum* protein has a considerably reduced carboxy terminal part. On the basis of this size reduction and structural analogies with other threonine-converting enzymes, the authors postulated an important role for the carboxy terminal part in the allosteric control of threonine deaminase (Moeckel et al., 1992). DNA sequence analysis and marker exchange mutagenesis of the *ilv*BC operon revealed that the AHAS protein is encoded by two genes, *ilv*B and *ilv*N, as has been observed in other bacteria (Keilhauer et al., 1993). Northern RNA blot analysis of the *ilv*BNC cluster identified three different transcripts of 3.9, 2.3, and 1.1 kb, corresponding to

*ilv*BNC, *ilv*NC, and *ilv*C, respectively. The *ilv*C transcript encoding isomeroreductase was by far the most abundant. Deletion analysis of the operon revealed the presence of three active promoters, which, however, were not further characterized. Addition of 2-oxobutyrate to the medium resulted in increased amounts of *ilv*BNC and *ilv*NC transcripts, which correlated well with the observed increase in AHAS activity. The presence of an *ilv*NC transcript has not been observed in other bacteria. It was therefore concluded that separate synthesis of the small *ilv*N subunit of AHAS might be necessary for maximal AHAS activity and could contribute to the allosteric regulation of the enzyme, as has been postulated for *E. coli* (Weinstock et al., 1992).

B. Transport of Isoleucine

1. Excretion

In contrast to the situation described for glutamate excretion in *C. glutamicum*, no special culture conditions or difficult treatments are necessary to trigger the efflux of isoleucine. *C. glutamicum* accumulates and secretes substantial amounts of isoleucine when the precursor 2-oxobutyrate is added to the medium (Ebbinghausen et al., 1989; Eggeling et al., 1987). As described above, 2-oxobutyrate induces AHAS, thereby promoting its own conversion, and 2-oxobutyrate bypasses the regulation of LTD. Similar to glutamate transport, three mechanisms have been proposed for isoleu-cine secretion into the medium: passive diffusion, inversion of the uptake system, and active secretion by a specific carrier.

Ebbinghausen et al. (1989) found that *C. glutamicum* cells were able to export isoleucine against an existing gradient, which makes it unlikely that the internal/external isoleucine ratio can be the driving force for isoleucine efflux. Further, the transport of isoleucine was not coupled with the movement of K+ ions, showing that the cells are not "leaky". The observed difference between isoleucine excretion and uptake rates ruled out inversion of the uptake system. No amino acids other than isoleucine were excreted, indicating that a specific carrier is involved in the transport of isoleucine. Ebbinghausen et al. (1989) further showed that the membrane potential was the driving force for isoleucine excretion, making the specific carrier model even more likely.

2. Uptake

Like other Gram-positive bacteria, *C. glutamicum* possesses a single transport system for the uptake of all three branched-chain amino acids (Ebbinghausen et al., 1989b). As *C. glutamicum* is fully capable of synthesizing enough branched-chain amino acids for growth, the role of this low-activity transport system in *C. glutamicum* is not clearly understood. However, Ingraham et al. (1983) have suggested that such a system could function as a cyclic retention mechanism to scavenge amino acids leaking out of the cell. To prove the presence of separate uptake and excretion system and to study the regulation of the uptake system, Boles et al. (1993) constructed defined *ilv*A mutants via marker exchange mutagenesis. These mutants are dependent on the addition of isoleucine or 2-oxobutyrate to the medium. It was proposed that these defined mutants could be used to screen for mutants defective in isoleucine uptake by screening for growth in the presence of 2-oxobutyrate and nongrowth when supplied with limiting isoleucine. However, screening of more than 20,000 colonies did not result in mutants with the expected phenotype. The failure of the selection procedure was discovered when the isoleucine uptake rate of *ilv*A mutants was determined in the presence or absence of 2-oxobutyrate and branched-chain amino acids. It was found that increasing the internal isoleucine concentrations greatly enhanced the activity of the uptake system. The uptake system became fully induced when the internal isoleucine concentration rose above 4 to 8 m*M*. Addition of chloramphenicol to short-term fermentations with *ilv*A mutants prevented induction of the uptake system, indicating that the observed induction is due to *de novo* synthesis of the carrier protein, and not

caused by regulation of the carrier activity. The availability of such an induction system will greatly contribute to the design of isolation procedures for the specific isoleucine carrier. Boles et al. (1993) explained the observed regulation with the cycle retention model of Igraham et al. (1983), which postulates that amino acid uptake systems with low uptake rates function as an efficient way to scavenge amino acids that are lost by nonspecific efflux from the cytosol.

VIII. PHENYLALANINE, TYROSINE, AND TRYPTOPHAN

A. Molecular Organization of *C. glutamicum* Genes Involved in Aromatic Amino Acid Biosynthesis

The biosynthetic pathway of the aromatic amino acids phenylalanine, tyrosine, and tryptophan in *Corynebacterium* and other organisms involves the participation of at least 17 different enzymes and shows complex regulatory mechanisms (Figure 3). The properties of the enzymes and some of the regulatory aspects have been reviewed elsewhere (Shiio, 1986). Here, we discuss the isolation and characterization of *C. glutamicum* genes involved in the biosynthesis of aromatic amino acids and their application in the construction of production strains via recombinant DNA technology. Biosynthesis of the aromatic amino acids in *C. glutamicum* proceeds via a common pathway to chorismate, from which the pathways to phenylalanine, tyrosine, and tryptophan diverge. The control of the metabolite flow through this pathway primarily occurs via end-product inhibition of four enzymatic steps: 3-deoxy-D-arabino-heptulsonate-7-phosphate (DAHP) synthase (DS), anthranilate synthase (AS), chorismate mutase (CM), and prephenate dehydratase (PD) (Figure 3). The first enzyme of the common pathway, DAHP synthase, catalyzes the condensation of PEP and erythrose-4-phosphate to DAHP. This enzyme is synergistically inhibited by a combination of phenylalanine and tyrosine. Its expression is somewhat repressed by tyrosine (Shiio, 1986). DAHP synthase forms a polypeptide complex with chorismate mutase, which catalyzes the conversion of chorismate to prephenate. Therefore, it is not surprising that the chorismate mutase-DAHP synthase complex is also inhibited by a combination of tyrosine and phenylalanine. PD and AS, which initiate the pathways to phenylalanine and tryptophan, are subject to end-product inhibition by phenylalanine and tryptophan, respectively.

The genes encoding both wild-type feedback-sensitive and deregulated bifunctional DAHP synthase-chorismate mutase have been cloned by complementation of auxotrophic mutants (Follettie and Sinskey, 1986; Ikeda and Katsumata, 1992). Recently, the wild-type *aro* gene encoding DHAP synthase was sequenced and showed strong homology with the *aro* genes of *E. coli* and *Salmonella typhimurium* (Chen et al., 1993). Comparison of the wild-type sequence with the sequence of genes encoding deregulated DAHP synthase might reveal more details about binding sites or the inhibition mechanism. In addition to the deregulated DHAP synthase-chorismate mutase genes, Ikeda and Katsumata (1992) also isolated the gene encoding deregulated prephenate dehydratase. The three deregulated genes were assembled on one multicopy plasmid pKF1 and used to transform strain KY10865. Strain KY10865 normally produces 7 g/l of tryptophan, but when transformed with plasmid pKF1, the metabolite flow was successfully redirected toward the synthesis of phenylalanine, resulting in the production of 10 g/l of phenylalanine. The effect was even more pronounced in fed batch fermentations, where the parent strain produced 18 g/l of tryptophan and the transformant secreted 28 g/l of phenylalanine. This example shows that metabolite flow in an organism can efficiently be redirected by amplification of deregulated branch-point enzymes.

The tryptophan-specific pathway starts with conversion of chorismate to anthranilate by the *trp*E gene product anthranilate synthase. The enzyme is subject to feedback inhibition by tryptophan. Both wild-type and deregulated tryptophan genes form *C. glutamicum* and *C. lactofermentum* have been isolated via complementation of *E. coli* tryptophan auxotrophs (Del Real et al., 1985; Heery and Dunican, 1993; Follettie and Sinskey, 1986; Matsui et al., 1986, 1987). Similar to *E. coli*,

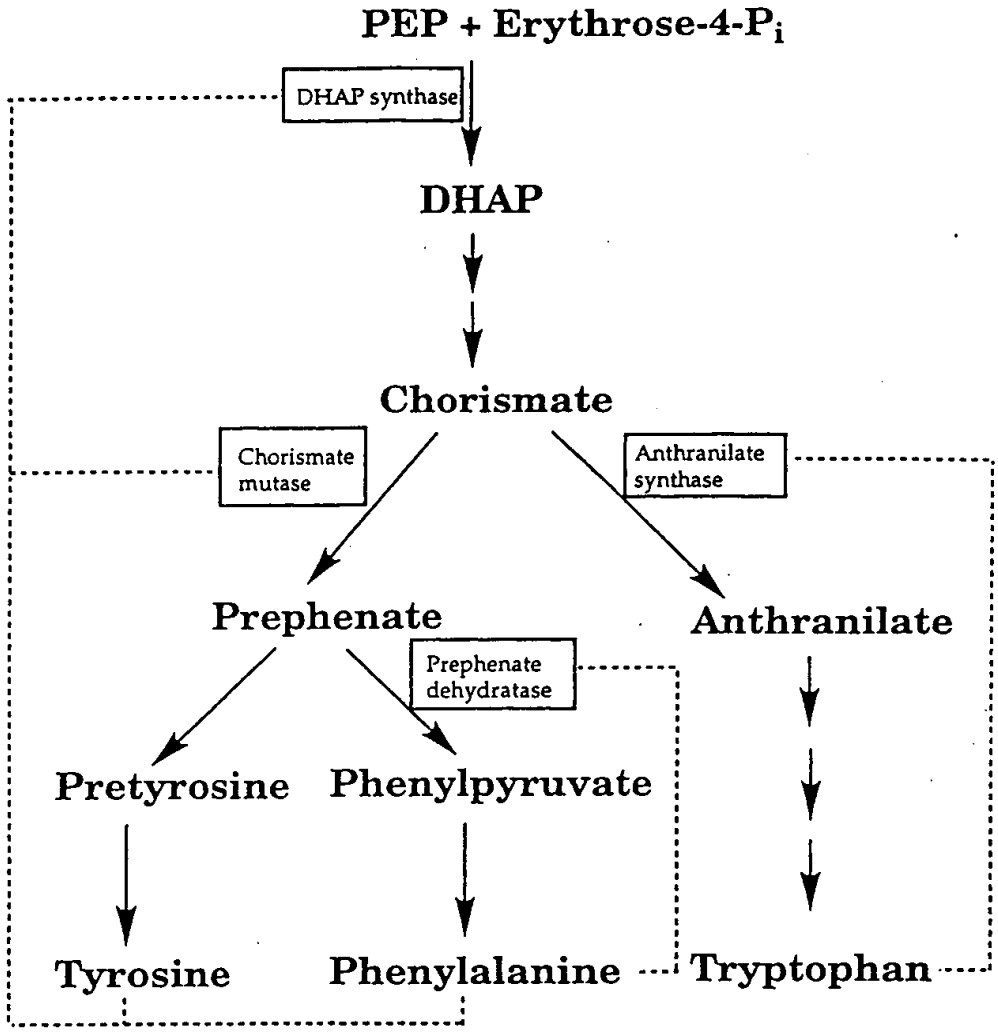

FIGURE 3. Biosynthetic pathway for aromatic amino acids. DHAP, 3-deoxy-D-arabino-heptulose-7-phosphate.

the *trp* genes of *C. glutamicum* are clustered in the order *trp*E, *trp*D, *trp*C, *trp*B, and *trp*A (Heery and Dunican, 1993). The *trp*E gene is preceded by the *trp* promoter and attenuator (Matsui et al., 1987; Sano and Matsui, 1987). The *trp* attenuator consists of a 17-codon open reading frame containing three tandem *trp* codons and is located immediately downstream of the *trp* promoter. Sequence analysis of the *C. lactofermentum trp*E gene revealed that the feedback resistance of the enzyme is caused by a missense mutation in codon 38 of the *trp*E gene (Matsui et al., 1987). However, Heery and Dunican (1993) did not observe any difference in the deduced amino acid sequence of the anthranilate synthase gene of a feedback-resistant *C. glutamicum* strain. Instead, they found that this *C. glutamicum* strain contained a nonsense mutation in the trp leader sequence that could be responsible for a constitutive antitermination response.

In order to improve tryptophan production by strain KY10894, Katsumata and Ikeda (1993) applied metabolic pathway engineering to this strain. Successive introduction of the genes encoding deregulated DAHP synthase, deregulated anthranilate synthase, and phosphoribosyl-transferase on a multicopy plasmid ultimately resulted in a 54% increase in tryptophan production, to 43 g/l. In contrast to tryptophan-producing strains of *Bacillus* and *E. coli*, this *C. glutamicum*

did not show reduced tryptophan secretion rates during the stationary phase. The authors ascribed the absence of this decline to the abundant presence of stable DAHP synthase. Because high-level tryptophan production by this strain was still dependent on the presence of selection pressure by spectinomycin, the authors will have to ensure plasmid stability in the absence of the antibiotic or use conjugal transfer to stably integrate multiple copies of the deregulated genes into the chromosome.

IX. CONCLUSIONS AND PROSPECTS

At the moment, nearly all modern molecular biology techniques are available for *C. glutamicum*. The use of these techniques in the manipulation of *Corynebacterium* strains will lead to the construction of new and hopefully better production strains for primary metabolites.

Recent studies with *Ppc*- and *Pyk*-defective mutants of *C. glutamicum* have put the regulation of carbon flow at the PEP branch point in a new perspective. Extensive metabolic flux analysis studies with double or even triple mutants will be necessary to evaluate the contribution of the individual enzyme systems to the synthesis of OAA and to obtain a more complete understanding of the regulation of central metabolism in *C. glutamicum*. This knowledge will be helpful in diverting precursor supply toward the biosynthesis of aromatic and aspartate-derived amino acids.

The studies with *gdh*$^-$ mutants of *C. glutamicum* showed that the GS/GOGAT system has enough compensatory capacity to synthesize glutamate, and that the excretion of glutamate might be limited by the secretion process. Krämer and co-workers (1993) have ended the controversy of the glutamate secretion in favor of active transport. Availability of the genes encoding glutamate and lysine transport will greatly contribute to our understanding and ability to manipulate amino acid secretion processes in *C. glutamicum*.

Studies of the *ask-asd* operon have indicated that regulation of aspartokinase may be mediated by the β-subunit of ASK. Genetic engineering of the coding region of this subunit can provide completely deregulated aspartokinases, which are an absolute prerequisite for high lysine and threonine production strains and for a better understanding of lysine- and threonine-binding sites.

The integration and amplification of a deregulated homoserine dehydrogenase gene showed that lysine-secreting strains can be manipulated to produce threonine. Before threonine hyperproducing *C. glutamicum* strains can be obtained, the threonine degradation mechanisms will need to be unraveled and inactivated.

The genes for the biosynthesis of isoleucine and the aromatic amino acids have been cloned and their expression studied. The application of genes encoding feedback-resistant enzymes of the aromatic pathway has resulted in improved production strains for phenylalanine and tryptophan.

ACKNOWLEDGMENT

Our research was supported by the Netherlands Organization for Scientific Research (NWO), the Royal Netherlands Academy of Art and Sciences (KNAW), and the Archer Daniels Midland Company. We thank M. Follettie, M. Gubler, H. Lee, O. Peoples, G. Colon, M. McCormick, S. Park, C. Shaw, S. Lee, P. Hanke, T. McMullin, and B. Eikmanns for useful discussion, critical comments, or sharing their unpublished results.

REFERENCES

Aiba, S., Imanaka, T., and Tsunekawa, H., Enhancement of tryptophan production by *Escherichia coli* as an application of genetic engineering, *Biotechol. Lett.*, **2**, 525, 1980.

Aiba, S., Tsunekawa, H., and Imanaka, T., New approach to tryptophan production by *Escherichia coli*: genetic manipulation of composite plasmids in vitro, *Appl. Environ. Microbiol.*, **43**, 289, 1982.

Aida, K., Chibita, L., Nakayama, K., Takinami, K., and Yamada, H., *Biotechnology of Amino Acids Production*, Elsevier, Amsterdam, The Netherlands, 1986.

Archer, J. A. C. and Sinskey, A. J., The DNA sequence and the minimal replicon of the *Corynebacterium glutamicum* plasmid pSR1: evidence for a common anchestor with plasmids from *C. diphtheriae*, *J. Gen. Microbiol.*, **139**, 1753, 1993.

Archer, J. A. C., Solowcordero, D. E., and Sinskey, A. J., A C-terminal deletion in *Corynebacterium glutamicum* homoserine dehydrogenase abolishes allosteric inhibition by L-threonine, *Gene*, **107**, 53, 1991.

Archer, J. A. C., Follettie, M. T., and Sinskey, A. J., Biology of *Corynebacterium glutamicum:* a molecular approach, in *Genetics and Molecular Biology of Industrial Microorganisms*, Hershberger, C. L., Queener, S. W., and Hegeman, G., Eds., ASM, Washington, D.C., 1989, 27.

Barak, Z., Chipman, D. M., and Gollop, N., Physiological implications of the specificity of acetohydroxy acid synthase isozymes in enteric bacteria, *J. Bacteriol.*, **169**, 3750, 1987.

Batt, C. A., Follettie, M. T., Shin, H. K., Yeh, P., and Sinskey, A. J., Genetic engineering of coryneform bacteria, *Trends Biotechnol.*, **3**, 305, 1985.

Batt, C. A., Shanabruch, W. S., and Sinskey, A. J., Expression of pAMa1 tetracycline resistance gene in *Corynebacterium glutamicum*, *Biotechnol. Lett.*, **7**, 717, 1985.

Bell, S. C. and Turner, J. M., Bacterial catabolism of threonine; threonine degradation initiated by L-threonine NAD^+ oxidoreductase, *Biochem. J.*, **156**, 449, 1976.

Beppu, T., Application of recombinant DNA technology in breeding of amino acid producing strains, in *Biotechnology of Amino Acids Production*, Aida, K., Chibita, L., Nakayama, K., Takinami, K., and Yamada, H., Eds., Elsevier, Amsterdam, 1986, 24.

Boles, E., Ebbinghausen, H., Eikmanns, B., and Kramer, R., Unusual regulation of the uptake system for branched-chain amino acids in *Corynebacterium glutamicum*, *Arch. Microbiol.*, **159**, 147, 1993.

Bonamy, C., Guyonvarch, A., Reyes, O., David, F., and Leblon, G., Interspecies electrotransformation in Corynebacteria, *FEMS Microbiol. Lett.*, **66**, 263, 1990.

Bonnassie, S., Burini, J. F., Oreglia, J., Trautwetter, A., Patte, and Sicard, A., Transfer of plasmid DNA to *Brevibacterium lactofermentum* by electrotransformation, *J. Gen. Microbiol.*, **136**, 2107, 1990a.

Bonnassie, S., Oreglia, J., and Sicard, A. M., Nucleotide sequence of the *dapA* gene from *Corynebacterium glutamicum*, *Nucleic Acids Res.*, **18**, 6421, 1990b.

Bormann, E. R., Eikmanns, B. J., and Sahm, H., Molecular analysis of the *Corynebacterium glutamicum gdh* gene encoding glutamate dehydrogenase, *Mol. Microbiol.*, **6**, 317, 1992.

Broër, S., Eggeling, L., and Krämer, R., Strains of *Corynebacterium glutamicum* with different lysine productivities may have different lysine excretion systems, *Appl. Environ. Microbiol.*, **59**, 316, 1993.

Broër, S. and Krämer, R., Mechanism of lysine uptake and excretion by *Corynebacterium glutamicum*, in *Molecular Mechanisms of Transport*, Quagliariello, E. and Palmieri, F., Eds., Elsevier, Amsterdam, 1991a, 67.

Broër, S. and Krämer, R., Lysine excretion by *Corynebacterium glutamicum*. I. Identification of a specific carrier system, *Eur. J. Biochem.*, **202**, 131, 1991b.

Broër, S. and Krämer, R., Lysine excretion by *Corynebacterium glutamicum*. II. Energetics and mechanism of the transport system, *Eur. J. Biochem.*, **202**, 136, 1991c.

Cardenás, R., Martin, J. F., and Gil, J. A., Construction and characterization of promoter probe vectors for Corynebacteria using the kanamycin resistance reporter gene, *Gene*, **98**, 117, 1991.

Chan, K. C., Duran, R., Arnaud, A., and Galzy, P., Cloning vectors and antibiotic resistance markers for *Brevibacterium* sp. R312, *Gene*, **105**, 119, 1991.

Chao, Y. P. and Liao, J. C., Alteration of growth yield by overexpression of phosphoenol pyruvate carboxylase and phosphoenol pyruvate carboxykinase in *Escherichia coli*, *Appl. Environ. Microbiol.*, **59**, 4261, 1993.

Chao, Y. P., Patnaik, R., Roof, W. D., Young, R. F., and Liao, J. C., Control of gluconeogenetic growth by *pps* and *pck* in *Escherichia coli*, *J. Bacteriol.*, **175**, 6939, 1993.

Chen, C. C., Liao, C. C., and Hsu, W. H., The cloning and nucleotide sequence of a *Corynebacterium glutamicum* 3-deoxy-D-arabinoheptulosonate-7-phosphate synthase gene, *FEMS Microbiol. Lett.*, **107**, 223, 1993.

Clement, Y. and Lanneelle, G., Glutamate excretion mechanism in *Corynebacterium glutamicum*: triggering by biotin starvation or surfactant addition, *J. Gen. Microbiol.*, **132**, 925, 1986.

Clement, Y., Escoffier, B., Trombe, M. C., and Lanneelle, G., Is glutamate excreted by its uptake system in *Corynebacterium glutamicum*? A working hypothesis, *J. Gen. Microbiol.*, **130**, 2589, 1984.

Colòn, G. E., Follettie, M. T., Jetten, M. S. M., Stephanopoulos, G., and Sinskey, A. J., Redirections of carbon flux at a *Corynebacterium glutamicum* threonine metabolic branch point by controlled enzyme overexpression, in Abstr. Annu. ASM Meet., 1993, 320.

Cordes, C., Mockel, B., Eggeling, L., and Sahm, H., Cloning, organization and functional analysis of *ilv*A, *ilv*B and *ilv*C Genes from *Corynebacterium glutamicum*, *Gene*, **112**, 113, 1992.

Cremer, J., Eggeling, L., and Sahm, H., Cloning of the *dapA-dapB* cluster of the lysine secretion bacterium *Corynebacterium glutamicum*, *Mol. Gen. Genet.*, **224**, 317, 1988a.

Cremer, J., Eggeling, L., and Sahm, H., Control of lysine biosynthesis sequence in *Corynebacterium glutamicum* as analyzed by overexpression of the individual corresponding genes, *Appl. Environ. Microbiol.*, **57**, 1746, 1991.

Cremer, J., Treptow, C., Eggeling, L., and Sahm, H., Regulation of enzymes of lysine biosynthesis in *Corynebacterium glutamicum*, *J. Gen. Microbiol.*, **134**, 3221, 1988b.

Debadov, J., Construction of strains producing L-threonine, in *Genetics of Industrial Microorganisms*, Ikeda, Y. and Beppu, T., Eds., Kodansha, Tokyo, 1983, 254.

Del Real, G., Aguilar, A., and Martin, J. F., Cloning and expression of the tryptophan genes from *Brevibacterium*

lactofermentum in *Escherichia coli*, *Biochem. Biophys. Res. Commun.*, **133**, 1013, 1985.

Dominguez, H., Nezondet, C., Lindley, N. D., and Cocaign, M., Modified carbon flux during oxygen limited growth of *Corynebacterium glutamicum* and the consequences for amino acid overproduction, *Biotechnol. Lett.*, **15**, 449, 1993.

Dunican, L. K. and Shivnan, E., High frequency transformation of whole cells of amino acid producing coryneform bacteria using high voltage electroporation, *Bio/Technology*, **7**, 1067, 1990.

Duperray, F., Jezequel, D., Ghazi, A., Letelier, L., and Shechter, E., Excretion of glutamate by *Corynebacterium glutamicum* triggered by surfactants, *Biochim. Biophys. Acta*, **1103**, 250, 1992.

Ebbinghausen, H., Weil, B., and Kramer, R., Isoleucine excretion in *Corynebacterium glutamicum*: evidence for a specific efflux carrier system, *Appl. Microbiol. Biotechnol.*, **31**, 184, 1989a.

Ebbinghausen, H., Weil, B., and Kramer, R., Transport of branched chain amino acids in *Corynebacterium glutamicum*, *Arch. Microbiol.*, **151**, 238, 1989b.

Eggeling, I., Cordes, C., Eggeling, L., and Sahm, H., Regulation of acetohydroxy acid synthase in *Corynebacterium glutamicum* during fermentation of 2-α-ketobutyrate to L-isoleucine, *Appl. Microbiol. Biotechnol.*, **25**, 617, 1987.

Eikmanns, B. J., Identification, sequence analysis, and expression of a *Corynebacterium glutamicum* gene cluster encoding the 3 glycolytic enzymes glyceraldehyde-3-phosphate dehydrogenase, 3-phosphoglycerate kinase, and triosephosphate isomerase, *J. Bacteriol.*, **174**, 6076, 1992.

Eikmanns, B. J., Eggeling, L., and Sahm, H., Molecular aspects of lysine, threonine, and lysine biosynthesis in *Corynebacterium glutamicum*, *Anthonie van Leeuwenhoek*, **64**, 145, 1993.

Eikmanns, B., Follettie, M. T., Griot, M. U., and Sinskey, A. J., The phosphoenol pyruvate carboxylase gene of *Corynebacterium glutamicum*: molecular cloning, nucleotide sequence, and expression, *Mol. Gen. Genet.*, **218**, 330, 1989.

Eikmanns, B., Kircher, M., and Reinscheid, D. J., Discrimination of *Corynebacterium glutamicum* and *Brevibacterium lactofermentum* by restriction pattern analysis of DNA adjacent to the *hom* gene, *FEMS Microbiol. Lett.*, **82**, 203, 1991a.

Eikmanns, B. J., Kleinertz, E., Liebl, W., and Sahm, H., A family of *Corynebacterium glutamicum/Escherichia coli* shuttle vectors for cloning, controlled gene expression, and promoter probing, *Gene*, **102**, 93, 1991b.

Eikmanns, B., Metz, M., Reinscheid, D., Kricher, M., and Sahm, H., Amplification of three threonine biosynthetic genes in *Corynebacterium glutamicum* and its influence on carbon flux in different strains, *Appl. Microbiol. Biotechnol.*, **34**, 617, 1991c.

Erdmann, A., Weil, B., and Krämer, R., Lysine secretion by wild-type *Corynebacterium glutamicum* triggered by dipeptide uptake, *J. Gen. Microbiol.*, **139**, 3115, 1993.

Ertan, H., Some properties of glutamate dehydrogenase, glutamine synthetase and glutamate synthase from *Corynebacterium callunae*, *Arch. Microbiol.*, **158**, 35, 1992a.

Ertan, H., The effect of various culture conditions on the levels of ammonia assimilatory enzymes of *Corynebacterium callunae*, *Arch. Microbiol.*, **158**, 42, 1992b.

Filipula, D., Ally, A., and Nagle, J., Complete nucleotide sequence of a native plasmid of *Brevibacterium lactofermentum*, *Nucleic Acids Res.*, **14**, 514, 1986.

Flodin, N. W., Lysine supplementations of cereal foods — a retrospective, *J. Am. Coll. Nutr.*, **12**, 486, 1993.

Follettie, M. T., Archer, J., Peoples, O. P., and Sinskey, A. J., Metabolic engineering of *Corynebacterium*, in *Proceedings of the Sixth International Symposium on Genetics of Industrial Microorganisms*, Heslot, H., Davies, J., Florent, J., Bobichon, L., Durand, G., and Penasse, L., Eds., Societe Microbiologique Francaise, Paris, 1991, 315.

Follettie, M. T., Peoples, O. P., Agoropoulou, C., and Sinskey, A. J., Gene structure and expression of the *Corynebacterium flavum* N13 *ask-asd* operon: molecular and evolutionary analysis of aspartokinase, *J. Bacteriol.*, **175**, 4096, 1993.

Follettie, M. T., Shin, H. K., and Sinskey, A. J., Organization and regulation of the *Corynebacterium glutamicum hom-thr*B and *thr*B loci, *Mol. Microbiol.*, **2**, 53, 1988.

Follettie, M. T. and Sinskey, A. J., Molecular cloning and nucleotide sequence of the *Corynebacterium glutamicum pheA* gene, *J. Bacteriol.*, **167**, 695, 1986a.

Follettie, M. T. and Sinskey, A. J., Recombinant DNA technology for *Corynebacterium glutamicum*, *Food Technol.*, **40**, 88, 1986b.

Follettie, M. T. and Sinskey, A. J., *Corynebacterium glutamicum*: a model for the use of DNA technology in food grade organisms, in *Biotechnology and Food Safety*, Bills, D. D. and Kung, S. D., Eds., Butterworth-Heinemann, Boston, 1989, 277.

Frings, E., Kunte, H. J., and Galinski, E. A., Compatible solutes in representatives of the genera *Brevibacterium* and *Corynebacterium* — occurrence of tetrahydropyrimidines and glutamine, *FEMS Microbiol. Lett.*, **107**, 25, 1993.

Gubler, M. E., Park, S. M., Jetten, M. S. M., Stephanopoulos, G., and Sinskey, A. J., Effects of phosphoenol pyruvate carboxylase deficiency on metabolism and lysine production of *Corynebacterium glutamicum*, *Appl. Microbiol. Biotechnol.*, **40**, 857, 1994a.

Gubler, M. E., Jetten, M. S. M., Lee, S. H., and Sinskey, A. J., Cloning of pyruvate kinase gene (*pyk*) of *Corynebacterium glutamicum* and site specific inactivatin of *pyk* in a lysine producing *C. lactofermentum* strain, *Appl. Environ. Microbiol.*, 60, 2494, 1994b.

Guerrero, C., Mateos, L. M., Malumbres, M., and Martin, J. F., The bleomycin resistance gene of transpon Tn5 is an excellent marker for transformation of corynebacteria, *Appl. Microbiol. Biotechnol.*, **36**, 759, 1992.

Gutmann, M., Hoischen, C., and Kramer, R., Carrier-mediated glutamate secretion by *Corynebacterium glutamicum* under biotin limitation, *Biochim. Biophys. Acta*, **1112**, 115, 1992.

Han, K. S., Archer, J., and Sinskey, A. J., The molecular structure of the *Corynebacterium glutamicum* threonine synthase gene, *Mol. Microbiol.*, **4**, 1693, 1990.

Haynes, J. A. and Britz, M. L., Electrotransformation of *Brevibacterium lactofermentum* and *Corynebacterium glutamicum*: growth in Tween 80 increases transformation frequency obtained by electroporation, *FEMS Microbiol. Lett.*, **61**, 329, 1989.

Haynes, J. A. and Britz, M. L., The effect of growth conditions of *Corynebacterium glutamicum* on the transformation frequency obtained by electroporation, *J. Gen. Microbiol.*, **136**, 255, 1990.

Heery, D. M. and Dunican, L. K., Cloning of the *trp* gene cluster from a tryptophan-hyperproducing strain of *Corynebacterium glutamicum*: identification of a mutation in the *trp* leader sequence, *Appl. Environ. Microbiol.*, **59**, 791, 1993.

Hoischen, C. and Krämer, R., Evidence for an efflux carrier system involved in the secretion of glutamate by *Corynebacterium glutamicum*, *Arch. Microbiol.*, **151**, 342, 1989.

Hoischen, C. and Krämer, R., Membrane alteration is necessary but not sufficient for effective glutamate secretion by *Corynebacterium glutamicum*, *J. Bacteriol.*, **172**, 3409, 1990.

Ikeda, M. and Katsumata, R., Metabolic engineering to produce tyrosine or phenylalanine in a tryptophan-producing *Corynebacterium glutamicum* strain, *Appl. Environ. Microbiol.*, **58**, 781, 1992.

Ikeda, M., Ozaki, A., and Katsumata, R., Phenylalanine production by metabolically engineered *Corynebacterium glutamicum* with the *phe*A gene of *Escherichia coli*, *Appl. Microbiol. Biotechnol.*, **39**, 318, 1993.

Ingraham, J. I., Maaloe, O., and Neidhardt, F. C., *Growth of the Bacterial Cell*, Sinauer, Sunderland, MA, 1983.

Ishida, M., Sato, K., Hashiguchi, K., and Ito, H., High fermentation production of L-threonine from acetate by a *Brevibacterium flavum* stabilized strain transformed with a recombinant plasmid carrying the *Escherichia coli thr* operon, *Biosci. Biotechnol. Biochem.*, **57**, 1755, 1993.

Ishino, I., Mizukami, T., Yamagushi, K., Katzumata, R., and Araki, K., Cloning and sequencing of the meso-DAP dehydrogenase gene (*ddh*) of *Corynebacterium glutamicum*, *Agric. Biol. Chem.*, **52**, 2903, 1988.

Ishino, I., Mizukami, T., Yamagushi, K., Katzumata, R., and Araki, K., Nucleotide sequence of the meso-DAP dehydrogenase gene (*ddh*) of *Corynebacterium glutamicum*, *Nucleic Acids Res.*, **15**, 3917, 1987.

Jäger, W., Schäfer, A., Puehler, A., Labes, G., and Wohlleben, W., Expression of the *Bacillus subtilis sac*B gene leads to sucrose sensitivity in the Gram positive bacterium *Corynebacterium glutamicum* but not in *Streptomyces lividans*, *J. Bacteriol.*, **174**, 5462, 1992.

Jetten, M. S. M., Follettie, M. T., and Sinskey, A. J., Metabolic engineering of *Corynebacterium glutamicum*, in *Recombinant DNA Technology II*, Bajpai, R. and Prokop, A., Eds., Annals of the New York Academy of Science, New York, 1994a, 754.

Jetten, M. S. M., Follettie, M. T., and Sinskey, A. J., Effect of different levels of aspartokinase on the lysine production of *Corynebacterium lactofermentum*, *Appl. Microbiol. Biotechnol.*, in press, 1995.

Jetten, M. S. M., Gubler, M. E., McCormick, M. M., Colon, G. E., Follettie, M. T., and Sinskey, A. J., Molecular organization and regulation of the biosynthetic pathway for asparte derived amino acids in Corynebacterium glutamicum, in *Industrial Microorganisms: Basic and Applied Molecular Genetics*, Baltz, R. H., Hegeman, G., and Skatrud, P. L., Eds., ASM, Washington, D.C., 1993, 97.

Jetten, M. S. M., Gubler, M. E., Lee, S. H., and Sinskey, A. J., Structural and functional analysis of pyruvate kinase from *Corynebacterium glutamicum*, *Appl. Environ. Microbiol.*, 60, 2501, 1994c.

Jetten, M. S. M., Pitoc, G. A., Follettie, M. T., and Sinskey, A. J., Regulation of phosphoenol pyruvate and oxaloacetate converting enzymes in *Corynebacterium glutamicum*, *Appl. Microbiol. Biotechnol.*, **40**, 420, 1994d.

Jetten, M. S. M. and Sinskey, A. J., Characterization of phosphoenolpyruvate carboxykinase from *Corynebacterium glutamicum*, *FEMS Microbiol. Lett.*, **111**, 183, 1993.

Jetten, M. S. M. and Sinskey, A. J., Purification and properties of oxaloacetate decarboxylase from *Corynebacterium glutamicum*, *Anthonie van Leeuwenhoek*, 67, 221, 1995.

Kalinowski, J., Cremer, J., Bachmann, B., Eggeling, L., Sahm, H., and Puehler, A., Genetic and biochemical analysis of the aspartokinase from *Corynebacterium glutamicum*, *Mol. Microbiol.*, **5**, 1197, 1991.

Kalinowski, J., Bachmann, B., Thierbach, G., and Puehler, A., Aspartokinase genes *lys*Cα and *lys*Cβ overlap and are adjacent to the aspartate-semialdehyde dehydrogenase gene *asd* in *Corynebacterium glutamicum*, *Mol. Gen. Genet.*, **224**, 317, 1990.

Karasawa, M., Tosaka, O., Ikeda, S., and Yoshii, H., Application of protoplast fusion to the development of L-threonine and L-lysine producers, *Agric. Biol. Chem.*, **50**, 339, 1986.

Katsumata, R., Ozaki, A., Oka, T., and Furuya, A., Protoplast formation of glutamate-producing bacteria with plasmid DNA, *J. Bacteriol.*, **159**, 306, 1984.

Katsumata, R. and Ikeda, M., Hyperproduction of tryptophan in *Corynebacterium glutamicum* by pathway engineering, *Bio Technology*, **11**, 921, 1993.

Keilhauer, C., Eggeling, L., and Sahm, H., Isoleucine synthesis in *Corynebacterium glutamicum* molecular analysis of the *ilv*B-*ilv*N-*ilv*C operon, *J. Bacteriol.*, **175**, 5595, 1993.

Kinoshita, S., Glutamatic acid bacteria, in *Biology of Industrial Microorganisms*, Demain, A. L. and Solomon, N. A., Eds., Benjamin Cummings, London, 1985, 115.

Kiss, R. D. and Stephanopoulos, G., Culture instability of auxotrophic amino acid producers, *Biotechnol. Bioeng.*, **40**, 75, 1992.

Krämer, R., Secretion of amino acids by bacteria: physiology and mechanism, *FEMS Microbiol. Rev.*, **13**, 75, 1994.

Krämer, R. and Lambert, C., Uptake of glutamate in *Corynebacterium glutamicum*, *Eur. J. Biochem.*, **194,** 937, 1990.

Krämer, R., Lambert, C., Hoischen, C., and Ebbighausen, H., Uptake of glutamate in *Corynebacterium glutamicum*, *Eur. J. Biochem.*, **194,** 929, 1990.

Krulwich, T. A. and Pellicione, N. J., Catabolic pathways of coryneforms, nocardias and mycobacteria, *Annu. Rev. Microbiol.*, **33,** 95, 1979.

Labarre, J., Reyes, O., Guyonvarch, A., and Leblon, G., Gene replacement integration, and amplification at the *gdh*A locus of *Corynebacterium glutamicum*, *J. Bacteriol.*, **175,** 1001, 1993.

Lee, H. S., Jetten, M., Williams, R., and Sinskey, A., Molecular characterization of *ace*B, a gene encoding malate synthase in *Corynebacterium glutamicum*, *Biotechnol. Lett.*, submitted, 1994.

Liebl, W., The genus Corynebacterium — nonmedical, in *The Prokaryotes*, Balows, A., Trueper, H. G., Dworkin, M., Harder, W., and Schleifer, K. H., Eds., Springer-Verlag, Berlin, 1991, 1157.

Liebl, W., Ehrmann, M., Ludwig, W., and Schleifer, K. H., Transfer of *Brevibacterium divaricatum* DSM 2029T, *Brevibacterium flavum* DSM 20411, *Brevi-bacterium lactofermentum* DSM 20412 and DSM 1412, and *Corynebacterium lilium* DSM20317 to *Corynebacterium glutamicum* and their distinction by rDNA gene restriction patterns, *Int. J. Syst. Bacteriol.*, **41,** 255, 1991.

Liebl, W. and Schein, B., Isolation of restriction deficient mutants of *Corynebacterium glutamicum*, *Proc. Dechema Biotechnol. Conf.*, **4,** 102, 1991.

Malin, G. M. and Bourd, G. I., Phosphotransferase-dependent glucose transport in *Corynebacterium glutamicum*, *J. Appl Bacteriol.*, **71,** 517, 1991.

Marcel, T., Archer, J. A. C., Mengin-Lecreulx, M., and Sinskey, A. J., Nucleotide sequence and organization of the upstream region of *Corynebacterium glutamicum lys*A gene, *Mol. Microbiol.*, **4,** 1819, 1990.

Martin, J. F., Santamaria, R., Sandoval, H., del Real, G., Mateos, L. M., Gil, J. A., and Aguilar, A., Cloning systems in amino acid-producing corynebacteria, *Bio/Technology*, **5,** 137, 1987.

Masuda, M., Takamatsu, S., Nishimura, N., Komatsubara, S., and Tosa, T., Improvement of nitrogen supply for L-threonine production by a recombinant strain of *Serratia marcescens*, *Appl. Biochem. Biotechnol.*, **37,** 255, 1992.

Matsui, K., Miwa, K., and Sano, K., Complete nucleotide sequence and deduced amino acid sequences of the *Brevibacterium lactofermentum trp* operon, *Nucleic Acids Res.*, **14,** 10113, 1986.

Matsui, K., Miwa, K., and Sano, K., Two single base pair substitutions causing desensitization to tryptophan feedback inhibition of anthranilate synthase and enhanced expression of tryptophan genes of *Brevibacterium lactofermentum*, *J. Bacteriol.*, **109,** 5330, 1987.

McCormick, M., Follettie, M. T., and Sinskey, A. J., Characterization of the structure/function relationships of *Corynebacterium glutamicum* promoters, Abstr. Annu. ASM Meet., 331, 1993.

Miwa, K., Matsui, H., Terabe, M., Nakamori, S., Sano, K., and Momose, H., Cryptic plasmids in glutamic acid producing bacteria, *Agric. Biol. Chem.*, **48,** 2901, 1984a.

Miwa, K., Matsui, H., Terabe, M., Ito, K., Ishida, M., Takagi, H., Nakamori, S., and Sano, K., Construction of novel shuttle vectors and a cosmid vector for the glutamic acid producing bacteria *Brevibacterium lactofermentum* and *Corynebacterium glutamicum*, *Gene*, **39,** 281, 1985.

Miwa, K., Tsuchida, T., Kurahashi, D., Nakamori, S., Sano, K., and Momose, H., Construction of L-threonine overproducing strains of *Escherichia coli* K-12 using recombinant DNA techniques, *Agric. Biol. Chem.*, **47,** 2329, 1983.

Miwa, K., Nakamori, S., Sano, K., and Momose, H., Stability of recombinant plasmids carrying the threonine operon in *Escherichia coli*, *Agric. Biol. Chem.*, **48,** 2233, 1984b.

Miyajima, R. and Shiio, I., Regulation of aspartate family amino acid biosynthesis in *Brevibacterium flavum*. III. Properties of homoserine dehydrogenase, *J. Biochem.*, **68,** 311, 1970.

Mockel, B., Eggeling, L., and Sahm, H., Functional and structural analyses of threonine dehydratase from *Corynebacterium glutamicum*, *J. Bacteriol.*, **174,** 8065, 1992.

Momose, H., Miyashiro, S., and Oba, M., On the transducing phages in glutamic acid producing bacteria, *J. Gen. Appl. Microbiol.*, **22,** 119, 1976.

Mori, M. and Shiio, I., Purification and some properties of phosphoenol pyruvate carboxylase from *Brevibacterium flavum* and its aspartate overproducing mutant, *J. Biochem.*, **97,** 1119, 1985.

Mori, M. and Shiio, I., Pyruvate formation and sugar metabolism in an amino acid-producing bacterium *Brevibacterium flavum*, *Agric. Biol. Chem.*, **51,** 129, 1987a.

Mori, M. and Shiio, I., Phosphoenol pyruvate: sugar phosphotransferase system and sugar metabolism in *Brevibacterium flavum*, *Agric. Biol. Chem.*, **51,** 2671, 1987b.

Morinaga, Y., Tsuchiya, M., Miwa, K., and Sano, K., Expression of *Escherichia coli* promoters in *Brevibacterium lactofermentum* using shuttle vector pEB003, *J. Biotechnol.*, **5,** 305, 1987.

Nakamori, K., Threonine and homoserine, in *Biotechnology of Amino Acids Production*, Aida, K., Chibita, L., Nakayama, K., Takinami, K., and Yamada, H., Eds., Elsevier, Amsterdam, 1986, 173.

Nakamori, K., Ishida, M., Takagi, M., Ito, K., Miwa, K., and Sano, K., Improvement of L-threonine production by amplification of the homoserine dehydrogenase gene in *Brevibacterium lactofermentum*, *Agric. Biol. Chem.*, **51,** 87, 1987.

Neubeck, M., Prenner, E., Horvat, P., Bona, R., Hermetter, A., and Moser, A., Membrane fluidity in glutamic acid-producing bacteria *Brevibacterium* sp ATCC-13869, *Arch. Microbiol.*, **160,** 101, 1993.

Oguiza, J. A., Malumbres, M., Eriani, G., Pisabarro, A., Mateos, L. M., Martin, F., and Martin, J. F., A gene

encoding arginyl-tRNA synthetase is located in the upstream region of the *lys*A gene in *Brevibacterium lactofermentum*: regulation of *arg*S-*lys*A cluster expression by arginine, *J. Bacteriol.*, **175,** 7356, 1993.

O'Regan, M., Thierbach, G., Bachmann, B., Villeval, D., Lepage, P., Viret, J. F., and Lemoine, Y., Cloning and nucleotide sequence of the phosphoenol pyruvate carboxylase coding gene of *Corynebacterium glutamicum* ATCC 13032, Gene, **77,** 237, 1989.

Ozaki, A., Katsamata, R., Oka, T., and Furuya, A., Functional expression of the genes of *Escherichia coli* in Gram- positive *Corynebacterium glutamicum*, *Mol. Gen. Genet.*, **196,** 175, 1984.

Ozaki, A., Katsumata, R., Oka, T., and Furuya, A., Transfection of *Corynebacterium glutamicum* with temperate phage phiCG1, *Agric. Biol. Chem.*, **48,** 2597, 1985a.

Ozaki, A., Katsumata, R., Oka, T., and Furuya, A., Cloning of the genes concerned in phenylalanine biosynthesis in *Corynebacterium glutamicum* and its application to breeding of a phenylalanine-producing strain, *Agric. Biol. Chem.*, **49,** 2925, 1985b.

Ozaki, H. and Shiio, I., Regulation of the TCA and glyoxylate cycles in *Brevibacterium flavum*, *J. Biochem.*, **66,** 297, 1969.

Patek, M., Hochmannova, J., and Nesvera, J., Production of threonine by *Brevibacterium flavum* containing threonine biosynthetic genes from *Escherichia coli*, *Folia Microbiol.*, **38,** 355, 1993.

Patek, M., Krumbach, K., Eggeling, L., and Sahm, H., Leucine synthesis in *Corynebacterium glutamicum*: enzyme activities, structure of *leu*A, and effect of *leu*A inactivation on lysine synthesis, *Appl. Environ. Microbiol.*, **60,** 133, 1994.

Patek, M., Navratil, O., Hochmannova, J., Nesvera, J., Krumphanzl, V., and Bucko, M., Expression of the threonine operon from *Escherichia coli* in *Brevibacterium flavum* and *Corynebacterium glutamicum*, *Biotechnol. Lett.*, **11,** 231, 1989.

Patek, M., Nesvera, J., Hochmannova, J., and Stockrova, J., Transfection of *Brevibacterium flavum* with bacteriophage BFB10 DNA, *Folia Microbiol.*, **333,** 247, 1988.

Peoples, O. P., Liebl, W., Bodis, M., Maeng, P. J., Follettie, M. T., Archer, J. A. C., and Sinskey, A. J., Nucleotide sequence and fine structural analysis of the *Corynebacterium glutamicum hom-thr*B operon, *Mol. Microbiol.*, **2,** 63, 1988.

Peterswendisch, P. G., Eikmanns, B. J., Thierbach, G., Bachmann, B., and Sahm, H., Phosphoenol pyruvate carboxylase in *Corynebacterium glutamicum* is dispensable for growth and lysine production, *FEMS Microbiol. Lett.*, **112,** 269, 1993.

Pisabarro, A., Malumbres, M., Mateos, L. M., Oguiza, J. A., and Martin, J. F., A cluster of 3 genes (*dap*A, *orf*2, and *dap*B) of *Brevibacterium lactofermentum* encodes dihydrodipicolinate synthase, dihydrodipicolinate reductase, and a 3rd polypeptide of unknown function, *J. Bacteriol.*, **175,** 2743, 1993.

Plakunov, V. K., Volkova, I. M., and Lebedeva, Z. D., Role of excretion in the overproduction of glutamic acid by *Corynebacterium glutamicum*, *Microbiology*, **61,** 118, 1992.

Plamann, M. D. and Stauffer, G. V., Characterization of the *Escherichia coli* gene for serine hydroxymethyltransferase, Gene, **22,** 9, 1983.

Randall, J. R. and Andreas, D. O., in *Archer Daniels Midland Annual Report*, ADM, Decatur, IL, 1992, 16.

Reinscheid, D J., Eikmanns, B. J., and Sahm, H., Analysis of *Corynebacterium glutamicum hom* gene coding for a feedback resistant homoserine dehydrogenase, *J. Bacteriol.*, **173,** 3228, 1991.

Reinscheid, D. J., Eikmanns, B. J., and Sahm, H., Isolation and analysis of the *Corynebacterium glutamicum* genes encoding isocitrate lyase and malate synthase, *BioEngineering*, **9,** 32, 1993.

Reinscheid, D. J., Eikmanns, B. J., and Sahm, H., Characterization of the isocitrate lyase gene from *Corynebacterium glutamicum* and biochemical analysis of the enzyme, *J. Bacteriol.*, 176, 3474, 1994b.

Reinscheid, D. J., Kronemeyer, W., Eggeling, L., Eikmanns, B. J., and Sahm, H., Stable expression of *hom*-1-*thr*B in *Corynebacterium glutamicum* and its effect on the carbon flux to threonine and related amino acids, *Appl. Environ. Microbiol.*, **60,** 126, 1994a.

Reyes, O., Guyonvarch, A., Bonamy, C., Salti, V., David, F., and Leblon, G., Integron-bearing vectors: a method suitable for stable chromosomal integration in highly restrictive *Corynebacteria*, *Gene*, **107,** 61, 1991.

Rossol, I. and Puehler, A., The *Corynebacterium glutamicum aec*D gene encodes a C-S lyase with alphabeta-elimination activity that degrades aminoethylcysteine, *J. Bacteriol.*, **174,** 2968, 1992.

Sanchez, F., Penalva, M., Patino, C., and Rubio, V., An efficient method for the introduction of viral DNA into *Brevibacterium lactofermentum* protoplasts, *J. Gen. Microbiol.*, **132,** 1767, 1986.

Sandoval, H., Aguilar, A., Paniagua, C., and Martin, J. F., Isolation and physical characterization of plasmid pCC1 from *Corynebacterium callunnae* and construction of hybrid derivatives, *Appl. Microbiol. Biotechnol.*, **19,** 409, 1984.

Sandoval, H., Del Real, G., Mateos, L. M., Aguilar, A., and Martin, J. F., Screening of plasmids in non-pathogenic corynebacteria, *FEMS Microbiol. Lett.*, **27,** 93, 1985.

Sano, K., Ito, K., Miwa, K., and Nakamori, S., Amplification of the phosphoenol pyruvate carboxylase gene of *Brevibacterium lactofermentum* to improve amino acid production, *Agric. Biol. Chem.*, **51,** 597, 1987.

Sano, K. and Matsui, K., Structure and function of the *trp* operon control regions in *Brevibacterium lactofermentum*, a glutamic acid producing bacterium, *Gene*, **53,** 191, 1987.

Santamaria, R., Gil, J. A., and Martin, J. F., High frequency transformation of *Brevibacterium lactofermentum* protoplasts by plasmid DNA, *J. Bacteriol.*, **162,** 463, 1985.

Santamaria, R., Gil, J. A., Mesas, J. M., and Martin, J. F., Characterization of an endogeneous plasmid and devel-

opment of cloning vectors and a transformation system in *Brevibacterium lactofermentum*, *J. Gen. Microbiol.*, **130**, 2237, 1985.

Santamaria, R., Martin, J. F., and Gil, J. A., Identification of a promoter sequence in the plasmid pUL340 of *Brevibacterium lactofermentum* and construction of new cloning vectors for corynebacteria containing two selectable markers, *Gene*, **56**, 199, 1987.

Schäfer, A., Kalinowski, J., and Puehler, A., Increased fertility of *Corynebacterium glutamicum* recipients in intergenic mating with *Escherichia coli* after stress exposure, *Appl. Environ. Microbiol.*, **60**, 756, 1994.

Schäfer, A., Kalinowski, J., Simon, R., Seep-Feldhaus, R. A., and Puehler, A., High-frequency conjugal transfer from Gram-negative *Escherichia coli* to various Gram-positive coryneform bacteria, *J. Bacteriol.*, **172**, 1663, 1990.

Schirch, L., Hopkins, S., Villar, E., and Angelaccio, S., Serine hydroxy methylltransferase from *Escherichia coli*: purification and properties, *J. Bacteriol.*, **163**, 1, 1985.

Scheer, E., Cordes, C., Eggeling, L., and Sahm, H., Regulation of acetohydroxy acid synthase in *Corynebacterium glutamicum* during isoleucine formation from 2-hydroxybutyric acid, *Arch. Microbiol.*, **149**, 173, 1987.

Schrumpf, B., Eggeling, L., and Sahm, H., Isolation and prominent characteristics of an L-lysine hyperproducing strain of *Corynebacterium glutamicum*, *Appl. Microbiol. Biotechnol.*, **37**, 566, 1992.

Schrumpf, B., Schwarzer, A., Kalinowski, J., Puehler, A., Eggeling, L., and Sahm, H., A functionally split pathway for lysine synthesis in *Corynebacterium glutamicum*, *J. Bacteriol.*, **173**, 4510, 1991.

Schwarzer, A. and Puehler, A., Manipulation of *Corynebacterium glutamicum* by gene disruption and replacement, *Bio/Technology*, **9**, 84, 1991.

Schwinde, J. W., Thumschmitz, N., Eikmanns, B. J., and Sahm, H., Transcriptional analysis of the *gap-pgk-tpi-ppc* gene cluster of *Corynebacterium glutamicum*, *J. Bacteriol.*, **175**, 3905, 1993.

Seep-Feldhaus, A. H., Kalinowski, J., and Puehler, A., Molecular analysis of the *Corynebacterium glutamicum lysI* gene involved in lysine uptake, *Mol. Microbiol.*, **5**, 2995, **1991.**

Serwold-Davis, T. M., Groman, N., and Kao, C. C., Localization of an origin of replication in *Corynebacterium diphtheriae* broad host range plasmid pNG2 that also functions in *Escherichia coli*, *FEMS Microbiol. Lett.*, **66**, 119, 1990.

Serwold-Davis, T. M., Groman, N., and Rabin, M., Transformation of *Corynebacterium diphtheriae*, *Corynebacterium ulcerans*, *Corynebacterium glutamicum* and *Escherichia coli* with the *C. diphtheriae* plasmid pNG2, *Proc. Natl. Acad. Sci. U.S.A.*, **84**, 4464, 1987.

Sharp, P. M. and Mitchell, K. J., *Corynebacterium glutamicum* arginyl-transfer RNA synthetase, *Mol. Microbiol.*, **8**, 200, 1993.

Shaw, P. C., Transformation of a *Corynebacterium callunae-Escherichia coli* hybrid plasmid to various Gram-positive coryneform bacteria, *Agric. Biol. Chem.*, **53**, 1717, 1989.

Shaw, P. C. and Hartley, B. S., A host vector system for an *Arthrobacter* species, *J. Gen. Microbiol.*, **134**, 903, 1988.

Shiio, I., Tryptophan, phenylalanine and tyrosine, in *Biotechnology of Amino Acids Production*, Aida, K., Chibita, L., Nakayama, K., Takinami, K., and Yamada, H., Eds., Elsevier, Amsterdam, 1986, 188.

Shiio, I. and Miyajima, R., Concerted inhibition and its reversal by end-products of aspartokinase in *Brevibacterium flavum*, *J. Biochem.*, **65**, 849, 1969.

Shiio, I., Otsuka, S. I., and Takahashi, M., Effect of biotin on the bacterial fermentation of glutamic acid, *J. Biochem.*, **51**, 56, 1963.

Shiio, I., Sugimoto, S., and Kawamura, K., Isolation and properties of α-ketobutyrate-resistant lysine-producing mutants from *Brevibacterium flavum*, *Biosci. Biotechnol. Biochem.*, **57**, 51, 1993.

Shiio, I. and Ujigawa-Takeda, K., Presence and regulation of α-ketoglutarate dehydrogenase complex in a glutamate producing *Brevibacterium flavum*, *Agric. Biol. Chem.*, **44**, 1897, 1980.

Shiio, I., Yokota, A., Toride, Y., and Sugimoto, S., Threonine production by dihydropiconilate synthase mutant of *Brevibacterium flavum*, *Agric. Biol. Chem.*, **53**, 41, 1989.

Shiio, I., Yoshino, H., and Sugimoto, S., Isolation and properties of lysine producing mutants with feedback resistant aspartokinase derived from a *Brevibacterium flavum* strain with citrate synthase and pyruvate kinase defects and feedback resistant phosphoenol pyruvate carboxylase, *Agric. Biol. Chem.*, **54**, 3275, 1990.

Smith, M. D., Flickinger, J. L., Lieberger, P. W., and Schmid, B., Protoplast transformation in coryneform bacteria and introduction of an α-amylase gene from *Bacillus amyloliquefaciens* into *Brevibacterium lactofermentum*, *Appl. Environ. Microbiol.*, **51**, 634, 1986.

Sonnen, H., Thierbach, G., Kautz, S., Kalinowski, J., Scheider, J., Puehler, A., and Kutzner, H. J., Characterization of pGA1, a new plasmid from *Corynebacterium glutamicum* LP-6, *Gene*, **107**, 69, 1991.

Sonnen, H., Unusual phage/host relationship in the amino acid producing *Corynebacterium glutamicum*, *Bioengineering*, **3**, 53, 1992.

Sonnen, H., Schneider, J., and Kutzner, H. J., Characterization of phiGA1, an inducible phage particle from *Brevibacterium flavum*, *J. Gen. Microbiol.*, **136**, 567, 1990a.

Sonnen, H., Schneider, J., and Kutzner, H. J., Corynephage Cog, a virulent bateriophage of *Corynebacterium glutamicum*, and its relation to phiGA1, an inducible phage particle from *Brevibacterium flavum*, *J. Gen. Virol.*, **71**, 1629, 1990b.

Sonntag, K., Eggeling, L., Degraaf, A. A., and Sahm, H., Flux partitioning in the split pathway of lysine synthesis

in *Corynebacterium glutamicum*: quantification by C-13-NMR and H-1-NMR spectroscopy, *Eur. J. Biochem.*, **213**, 1325, 1993.

Stephanopoulos, G. and Vallino, J. J., Network rigidity and metabolic engineering in metabolite overproduction, *Science*, **252**, 1675, 1991.

Takagi, H., Morinaga, Y., Miwa, K., Nakamori, S., and Sano, K., Versatile cloning vectors constructed with genes indigenous to glutamic acid producer *Brevibacterium lactofermentum*, *Agric. Biol. Chem.*, **50**, 2597, 1986.

Takeda, Y., Fujii, M., Nakajyoh, Y., Nishimura, T., and Isshiki, S., Isolation of a tetracycline resistance plasmid from a glutamate producing *Corynebacterium melassecola*, *J. Fermen. Bioeng.*, **70**, 117, 1990.

Takeda, Y., Nakajyoh, Y., and Isshiki, S., Cloning and expression in *Escherichia coli* of the glutamate dehydrogenase gene, *gdh*, from *Corynebacterium melassecola*, *J. Fermen. Bioeng.*, **69**, 317, 1990.

Thierbach, G., Schwarzer, A., and Puehler, A., Transformation of spheroplasts and protoplasts of *Corynebacterium glutamicum*, *Appl. Microbiol. Biotechnol.*, **29**, 356, 1988.

Tosaka, O., Morioka, H., and Takinami, K., The role of biotin-dependent pyruvate carboxylase in L-lysine production, *Agric. Biol. Chem.*, **43**, 1513, 1979.

Tosaka, O. and Takinami, K., Pathway and regulation of lysine biosynthesis in *Brevibacterium lactofermentum*, *Agric. Biol. Chem.*, **42**, 95, 1978.

Trautwetter, A. and Blanco, C., Structural organization of the *Corynebacterium glutamicum* plasmid pGC100, *J. Gen. Microbiol.*, **137**, 2093, 1991.

Trautwetter, A., Blanco, C., and Bonnaissie, S., Characterization of the corynebacteriophage CG33, *J. Gen. Microbiol.*, **133**, 2945, 1987.

Trautwetter, A., Blanco, C., and Sicard, A. M., Structural characteristics of the *Corynebacterium lillium* bacteriophage, CL31, *J. Virol.*, **61**, 1540, 1987.

Tsuchiya, M. and Morinaga, T., Genetic control systems of *Escherichia coli* can confer inducible expression of cloned genes in coryneform bacteria, *Bio/Technology*, **6**, 428, 1988.

Vallino, J. J. and Stephanopoulos, G., Metabolic flux distribution in *Corynebacterium glutamicum* during growth and lysine overproduction, *Biotechnol. Bioeng.*, **41**, 633, 1993.

Von der Osten, C. H., Barbas, C., Wong, C., and Sinskey, A. J., Molecular cloning, nucleotide sequence and fine structural analysis of the *Corynebacterium glutamicum* *fda* gene: structural comparison of *C. glutamicum* fructose-1,6-biphosphate aldolase to class I and class I aldolases, *Mol. Microbiol.*, **3**, 1625, 1989.

Wehrmann, A., Ruether, K., Eggeling, L., and Sahm, H., Role of split pathway in lysine synthesis of *Corynebacterium glutamicum*: a genetical and physiological approach, *BioEngineering*, **9**, 33, 1993.

Weinstock, O., Sella, C., Chipman, D. M., and Barak, Z., Properties of subcloned subunits of bacterial acetohydroxy acid synthases, *J. Bacteriol.*, **174**, 5560, 1992.

Wohlleben, W., Muth, G., and Kalinowski, J., Genetic engineering of Gram positive bacteria in: *Biotechnology: Genetics and Fundamentals of Genetic Engineering*, Rehm, H. J., Reed, G., Puehler, A., and Sahm, H., Eds., VCH Puglishers, Weinheim, Germany, 1993, 477.

Wolf, H., Puehler, A., and Neumann, E., Electrotransformation of intact and osmotically sensitive cells of *Corynebacterium glutamicum*, *Appl. Microbiol. Biotechnol.*, **30**, 283, 1989.

Yamaguchi, R., Terabe, M., Miwa, K., Tshuchiya, M., Takagi, H., Morinaga, Y., Nakamori, S., Sano, K., Momose, H., and Yamazaki, A., Determination of the complete nucleotide sequence of *Brevibacterium lactofermentum* plasmid pAM330, and analysis of its genetic information, *Agric. Biol. Chem.*, **50**, 2771, 1986.

Yeh, P., Oreglia, J., Prevots, F., and Sicard, A., A shuttle vector system for *Brevibacterium lactofermentum*, *Gene*, **47**, 301, 1986.

Yeh, P., Sicard, A. M., and Sinskey, A. J., General organization of the genes specifically involved in the diaminopimelate-lysine biosynthetic pathway of *Corynebacterium glutamicum*, *Mol. Gen. Genet.*, **212**, 105, 1988.

Yeh, P., Sicard, A. M., and Sinskey, A. J., Nucleotide sequence of the *lysA* gene of *Corynebacterium glutamicum* and possible mechanism for modulation of expression, *Mol. Gen. Genet.*, **212**, 112, 1988.

Yoon, K. H., Park, S. C., and Oh, T. K., Cloning and characterization of the gene encoding enzyme II of the *Brevibacterium lactofermentum* phosphoenol pyruvate dependent sugar phosphotransferase system, in Abstr. Annu. ASM Meet., 1993, 323.

Yoshihama, M., Higashiro, K., Rao, E. A., Akedo, M., Shanabruch, W. G., Follettie, M. T., Walker, G. C., and Sinskey, A. J., Cloning vector system for *Corynebacterium glutamicum*, *J. Bacteriol.*, **162**, 591, 1985.

M tab lic Flux Distributions in *Corynebacterium glutamicum* During Growth and Lysin Overproduction

Joseph J. Vallino* and Gregory Stephanopoulos†
Chemical Engineering Department, Massachusetts Institute of Technology, Cambridge, Massachusetts 02139

Received May 1, 1992/Accepted September 28, 1992

The two main contributions of this article are the solidification of *Corynebacterium glutamicum* biochemistry guided by bioreaction network analysis, and the determination of basal metabolic flux distributions during growth and lysine synthesis. Employed methodology makes use of stoichiometrically based mass balances to determine flux distributions in the *C. glutamicum* metabolic network. Presented are a brief description of the methodology, a thorough literature review of glutamic acid bacteria biochemistry, and specific results obtained through a combination of fermentation studies and analysis-directed intracellular assays. The latter include the findings of the lack of activity of glyoxylate shunt, and that phosphoenolpyruvate carboxylase (PPC) is the only anaplerotic reaction expressed in *C. glutamicum* cultivated on glucose minimal media. Network simplifications afforded by the above findings facilitated the determination of metabolic flux distributions under a variety of culture conditions and led to the following conclusions. Both the pentose phosphate pathway and PPC support significant fluxes during growth and lysine overproduction, and that flux partitioning at the glucose-6-phosphate branch point does not appear to limit lysine synthesis. © 1993 John Wiley & Sons, Inc.
Key words: flux analysis • metabolic engineering • *Corynebacterium glutamicum* • lysine

INTRODUCTION

Standard practice for strain improvement of industrial microorganisms involves exposing a product-producing strain to a mutagen, then selecting for those mutants which exhibit a desired phenotype and testing the derived strains for improved productivity or yield.[13] In this type of procedure, the alterations of the parent strain's genome cannot be easily resolved due to the nonspecific effects of the mutagens employed, so that the genetic modifications that lead to improved strains may go undetermined or be incorrectly attributed to the phenotype selected for. Although genetic engineering techniques[3] can be used to remove the ambiguities associated with nonspecific mutagens, the enzymes that should be modified to increase product yield or productivity are often unknown, so that the extra effort required by genetic engineering techniques may not be rewarded with an equivalent improvement in strain enhancement. This is especially true when strain improvement requires modifications of the primary metabolic enzymes which are not obviously associated with the product of interest. Consequently, mutation-selection is still often a faster approach for strain improvement. As case in point involves lysine production by glutamic acid bacteria.[25]

It is well established that strains of glutamic acid bacteria (typically *Corynebacterium glutamicum, Brevibacterium flavum,* and *Brevibacterium lactofermentum*) can be obtained that produce significant amounts of lysine (ca. 30% molar yield) by selecting for mutants that exhibit *S*-(2-aminoethyl) L-cysteine resistance (AEC, a lysine antimetabolite), which dramatically enhances selecting strains with feedback-resistant aspartate kinase.[11,74] Deregulation of lysine synthesis, however, does not result in the maximum yield (75% molar),[68] so that mutation-selection techniques have focused on modifying enzymes of the primary metabolism, such as citrate synthase,[59] the pyruvate dehydrogenase complex[44,75] (PDC), pyruvate kinase[61,65] (PK), and phosphoenolpyruvate carboxylase[88] (PPC). Although these modifications have resulted in a strain that produces lysine at a 55% molar yield,[62] it is not known in what respect(s) this strain differs from the original parent strain. Indeed, genetic engineering approaches have yet to make significant improvements in lysine yield[11,32,50] due to the inability of deciphering the results obtained from mutation-selection.

Although techniques such as metabolic control theory,[15] biochemical systems theory,[67] whole-cell kinetic models,[23] stable[21] and radio[6] isotope tracers, and linear analysis[45] have been applied to metabolic networks, significant information regarding potential metabolic bottlenecks can be obtained from mass balance techniques.[36,38,46,76,80,81,83] The latter are readily applied and do not require information regarding enzyme kinetics. In this study we utilized these mass balance techniques in conjunction with intracellular assays to solidify the biochemistry of *C. glutamicum* ATCC 21253, and to examine metabolic flux distributions during growth and lysine overproduction to establish the basal case for subsequent perturbation studies.

MATERIALS AND METHODS

Microorganism and Medium

The organism *C. glutamicum* ATCC 21253, obtained from the American Type Culture Collection (ATCC, Rockville,

* Present address: Scripps Institution of Oceanography, University of California, San Diego, La Jolla, CA 92093–0202.
† To whom all correspondence should be addressed.

Biotechnology and Bioengineering, Vol. 41, Pp. 633–646 (1993)

CCC 0006-3592/93/060633-014

METABOLIC ENGINEERING 1, 35–48 (1999)
ARTICLE NO. MT980106

Response of the Central Metabolism in *Corynebacterium glutamicum* to the use of an NADH-Dependent Glutamate Dehydrogenase

Achim Marx, Bernhard J. Eikmanns, Hermann Sahm, Albert A. de Graaf, and Lothar Eggeling

Institut für Biotechnologie, Forschungszentrum Jülich GmbH, D-52425 Jülich, Germany

E-mail: l.eggeling@fz-juelich.de

Received February 23, 1998; revised June 15, 1998; accepted July 2, 1998

The extensive use of ^{13}C enrichments in precursor metabolites for flux quantification does not rely on NADPH stoichiometries and can therefore be used to quantify reducing power fluxes. As an application of this concept, the NADPH fluxes were quantified in an L-lysine producer of *Corynebacterium glutamicum* grown into metabolic and isotopic steady state with [1-^{13}C]glucose. In this case, where the organism's NADPH-dependent glutamate dehydrogenase consumes reducing power, the NADPH flux generated is 210% (molar flux relative to glucose uptake rate) with its major part (72% of the total) generated via the pentose phosphate pathway activity. An isogenic strain in which the glutamate dehydrogenase of *C. glutamicum* was replaced by the NADH-dependent glutamate dehydrogenase of *Peptostreptococcus asaccharolyticus* was made and the metabolite fluxes were again estimated. The major response to this local perturbation is a drastically reduced NADPH generation of only 139%. Most of the NADPH (62% of the total) is now generated via the tricarboxylic acid cycle activity. This shows the extraordinary flexibility of the central metabolism and provides a picture of the global regulatory properties of the central metabolism. Furthermore, a detailed analysis of the fluxes and exchange fluxes within the anaplerotic reactions is given. It is hypothesized that these reactions might also serve to balance the total reducing power budget as well as the energy budget within the cell. © 1999 Academic Press

Key Words: **reducing power supply; lysine production; anaplerotic reactions; pentose phosphate pathway; flux quantifications; isotope studies.**

1. INTRODUCTION

The fueling reactions within the central metabolism serve to provide energy as well as precursor metabolites for the cell. This dual function could be of particular importance when metabolite overproduction is attempted, since removal of precursors and an altered energy budget require a readjustment of the fluxes in this part of the metabolism. Metabolic engineering tries to make specific predictions of where increased activities could lead to a product increase. Such predictions are corroborated for reactions within assembling pathways, where allosterically controlled enzymes and branching points are major targets for obtaining flux increase (Eggeling *et al.*, 1996). Examples are the successful construction of amino-acid-producing-bacteria such as *Corynebacterium glutamicum* (Eggeling *et al.*, 1997a) or *Escherichia coli* (Eggeling and Sahm, 1998). Moreover, as a further target for improving metabolite production, a specific product exporter has recently been identified (Vrljic *et al.*, 1996). This completes the identification of the cellular control steps for converting precursors of the central metabolism into the desired extracellular product. However, in contrast to the assembling pathways and the transport process, the targets in the central metabolism to be engineered are less well defined. This is due to (i) the many branching points and cyclic and parallel reactions, (ii) the not easily accessible tools for quantifying the *in vivo* fluxes, (iii) the fact that enzyme activities in the network may be overlooked, and last but not least (iv) the very flexible responses of the living cell. Therefore, it is still a very ambitious goal to predict targets for flux increase in this part of the metabolism. A recent success in engineering the flux of glucose-derived carbons toward aromatic amino acid formation was based on more qualitative physiological knowledge (Flores *et al.*, 1996) and the successful application in producer strains has not yet been documented (Barry, 1996).

Of course, one aspect of metabolic engineering is a quantification of all fluxes. We have developed a comprehensive methodology distinguished by (i) the analysis of fluxes in the steady state, (ii) the intensive use of carbon atom quantification, made possible through [1-^{13}C]glucose and NMR spectroscopy, and (iii) metabolite balances (Marx *et al.*, 1996). This approach is completed by (iv) sophisticated mathematical tools also allowing the estimation of reverse fluxes and statistical parameters (Wiechert *et al.*, 1997). In particular, the high resolution obtained by such analyses in formulating new questions, whose answers could then in the future be utilized for metabolic engineering. This is the special benefit of intracellular flux analysis. In our previous

1096-7176/99 $30.00

investigations, we simply quantified the fluxes in isogenic *C. glutamicum* strains in a cause–effect study, where the central metabolism itself was not engineered, but only the final biosynthesis sequence or the export (Marx *et al.*, 1996, 1997). This served to probe the flexibility of the fueling reactions in response to different carbon burdens.

However, in most flux analyses no access to the reducing power budget has been possible to date. In contrast, NADP(H) stoichiometries are generally used as additional constraints to make solutions for carbon fluxes possible at all. In contrast, our approach, depending heavily on information on the fate of carbon atoms, does not require these constraints. Access to the reducing power budget is thus possible, since some carbon fluxes, e.g., through the glucose-6-phosphate dehydrogenase or the isocitrate dehydrogenase reaction, are inevitably linked to the NADPH flux. Therefore, carbon fluxes can be used to derive NADPH stoichiometries. We have already performed such calculations in previous work to a certain extent (Sonntag *et al.*, 1995). In the present paper, we describe our direct intervention in the NADPH budget to once again quantify the flexibility within the fueling reactions in a cause–effect study. Whereas we previously quantified the response of the central metabolism due to different carbon flux burdens (Marx *et al.*, 1997), this time we focus on the response of the central metabolism to different reducing power demands.

MATERIALS AND METHODS

Genetic Engineering

The *Peptostreptococcus asaccharolyticus* glutamate dehydrogenase gene was cloned according to the published sequence (Snedecor *et al.*, 1991) by use of the polymerase chain reaction and the primers 5′-ATGGATCCCCGAGT GAGAAATCACGGTG-3′ and 5′-CTGAGCTCAGCTGA TTATATGAGTTT-3′. The 1.4-kb product obtained was digested with *Bam*HI and *Sac*I and ligated with the shuttle vector pEKEx2 treated identically (Eikmanns *et al.*, 1991). Transformation of *E. coli* DH5α yielded kanamycin-resistant clones which were confirmed by restriction analyses to contain pEKExpgdh of 9.7 kb (Fig. 1). With this vector the specific glutamate dehydrogenase activity (NADH as substrate, *E. coli* as host) was increased from 0.05 to 1.1, and, after isopropyl-β-D-thiogalactoside addition, to 5.4 μmol/min and mg protein.

For construction of the gene deletion vector pK19*mobsacB*Δ*gdh*, part of the *gdh* gene was isolated as a 1.25-kb *Sph*I fragment (Börmann *et al.*, 1992) and ligated with pUC18. A *Bgl*II and *Eco*RV site within *gdh* was used to remove a 611-bp internal fragment to result in pUC18Δ*gdh*. The *Sph*I fragment, now only 0.6 kb in size, was reisolated

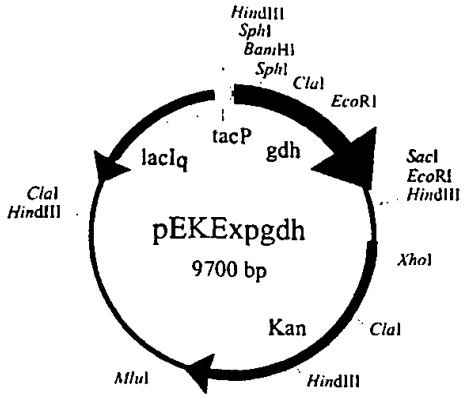

FIG. 1. The expression vector pEKEXpgdh to express the NAD-dependent *Peptostreptococcus asaccharolyticus* glutamate dehydrogenase gene *gdh* in *C. glutamicum*. Abreviations: *Kan*, kanamycine resistance; *lacI*^{q}, the constitutively expressed repressor of the *lac* operon; *tacP*, *Tac* promotor.

and ligated with the vector pK19*mobsacB*, which had been previously cleaved with *Sph*I and treated with alkaline phosphatase. The resulting vector pK19*mobsacB*Δ*gdh* was introduced into the mobilizing donor strain *E. coli* S17-1 (Simon *et al.*, 1983), and matings were performed with *C. glutamicum* MH20-22B (Schrumpf *et al.*, 1992) according to Schäfer *et al.* (1990). The single transconjugant obtained was cultivated overnight in liquid LBG for proliferation, and then dilutions were spread on LBG containing 10% sucrose (Schäfer *et al.*, 1994) to select for clones where the second recombination had taken place. One hundred Suc^r clones were assayed for their kanamycin phenotype, and eventually 15 Suc^r Kan^s clones were subjected to glutamate dehydrogenase activity determinations.

The enzymes necessary for *in vitro* recombinations were obtained from Boehringer (Mannheim, Germany) and used as recommended. Plasmids were isolated as described (Schwarzer and Pühler, 1990). *E. coli* was transformed after pretreatment with $CaCl_2$/$RbCl_2$ and *C. glutamicum* by electroporation (Liebl *et al.*, 1989).

Continuous Culture

The strains (homologous mutant strain *C. glutamicum* MH20-22BΔ*gdh* pEK1.9*gdh*-1 and heterologous mutant strain *C. glutamicum* MH20-22BΔ*gdh* pEKExpgdh) were grown in continuous culture as described elsewhere (Marx *et al.*, 1996). The medium was identical to that previously used with 43 mM glucose and 1.4 mM L-leucine, except that the ammonium sulfate concentration was 600 mM, and isopropyl-β-D-thiogalactoside (IPTG) (0.5 mM) and methionine S-sulfoximine (14.8 mM) were present. After inoculation and consumption of glucose, the medium together with [1-^{13}C]glucose was fed continuously at a rate of 0.082 h^{-1}.

TABLE 1

Extracellular Fluxes in Two L-Lysine-Producing Strains of *C. glutamicum* Differing Only in the Possession of an NAD or NADPH-Dependent Glutamate Dehydrogenase

	Glutamate dehydrogenase	
Carbon[a]	*gdh*(NAD)	*gdh*(NADP)
Glucose	100	100
Biomass	33	28
Product	18	32
CO_2	45	39
Sum	96	99
Y_{XS} ($g_X \cdot g_S^{-1}$)	0.33	0.28
Y_{PS} ($mol_P \cdot mol_S^{-1}$)	0.18	0.32
q_S ($nmol_S \cdot min^{-1} \cdot mg_{DW}^{-1}$)	23.0	26.9

Note. Abbreviations: *gdh*(NAD) are the data for the strain with the NAD-dependent glutamate dehydrogenase of *Peptostreptococcus asaccharolyticus*, *gdh*(NADP) those for the strain with the NAD-dependent enzyme. Y_{XS} (Y_{PS}) is the yield of conversion of the substrate glucose (S) to biomass (X), and product (P), respectively, q_S is the specific substrate uptake rate.

[a] Expressed as percentage of consumed glucose carbon.

CO_2 evolution as well as the dissolved oxygen concentration of the culture, was recorded on-line. In the steady state, glucose was entirely consumed. Samples of the cultures were collected to estimate lysine, growth, NADH- and NADPH-dependent glutamate dehydrogenase activities, and glutamine–oxoglutarate aminotransferase activity. In addition, in the steady state the $^{13}CO_2$ content of the effluent gas was quantitated by nondispersive infrared spectroscopy. From the analyses, the carbon balances of the cultures were derived which are given in Table 1 as percentages of flux relative to the glucose input rate.

Enzyme Determinations

Cells were harvested from the chemostat or exponentially growing cultures. They were washed with 0.9% NaCl, resuspended in the respective assay buffer, and disrupted by sonification. The cell debris was removed by centrifugation, and the resulting crude extract was used directly for glutamate dehydrogenase activity determinations. For determination of the glutamine–oxoglutarate aminotransferase activity (GOGAT), crude extract was gel-filtrated (PD-10 columns, Pharmacia) to remove ammonium salts, using as eluent buffer 0.1 M potassium phosphate (pH 7.5), 1.44 mM cysteine, 0.5 mM EDTA.

The glutamate dehydrogenase activity was assayed by following the oxoglutarate-dependent decrease in the extinction at 340 nm. The assay contained, in 1 ml, 100 μmol Tris HCl buffer (pH 8.0), 0.25 μmol NADPH (or NADH, respectively), 20 μmol NH_4Cl, and 10 μmol 2-oxoglutarate. The GOGAT activity was assayed in a system containing, in 1 ml, 100 μmol Tris/HCl buffer (pH 7.6), 0.1 μmol dithiothreitol, 0.25 μmol NADPH, 10 μmol 2-oxoglutarate, and 10 μmol glutamine. The protein concentration in the extracts was determined by the biuret method using bovine serum albumin as standard.

Determination of Fractional Enrichments in Carbon Atoms

High-resolution ^1H NMR spectra were obtained on an AMX-400 WB spectrometer (Bruker, Karlsruhe, Germany) operating at 400.13 MHz and equipped with a multichannel interface and a 5-mm inverse GRASP probe head. For the determination of ^{13}C enrichments in the protonated carbon atoms, as well as in the nonprotonated carbon atoms, ^1H NMR difference spectroscopy with and without GARP-1 composite pulse ^{13}C decoupling was used. The ^{13}C enrichments of protonated carbons were calculated as the ratio of the ^{13}C satellite signal area in the difference spectrum to the total integral of each proton in the GARP-1 decoupled spectrum. For the determination of ^{13}C enrichments in the nonprotonated carbons, spin-echo NMR spectroscopy was applied (Wendisch *et al.*, 1997). Typical settings of the inversion pulse sequence were 15-s relaxation delay, 2-s H_2O presaturation pulse; 9 μs 90° transmitter pulse; and 256-μs sine-shaped spoiler delay, with a selective 18-μs 180° transmitter pulse, and a 180° decoupler inversion pulse adjusted sample-specific. GARP-1 decoupling was optionally used.

The $^{12}CO_2$ concentration in the exhaust gas was measured on-line by non-dispersive infrared spectroscopy (URAS 10E, Hartmann & Braun, Frankfurt, Germany). The $^{13}CO_2$ concentration was quantified off-line by infrared spectroscopy with appropriate standards and settings (COI, Fischer Analysen GmbH, Leipzig, Germany).

Flux Determinations

The precursor demand for cell mass formation is as described (Marx *et al.*, 1996), as well as the biochemical model used (Marx *et al.*, 1997). The mathematical treatment has been described in detail by Wiechert *et al.* (1997) using matrix notations of the carbon-labeling balance equations. The program NMRFlux was used (Wiechert and de Graaf, 1997) to convert the biochemical equations and the equations of carbon atom transitions into the corresponding flux equations. Similarly, the experimentally determined fluxes and enrichments were incorporated. Using a sophisticated parameter-fitting algorithm (Wiechert *et al.*, 1997), which is based on the Levenberg–Marquard algorithm, a nonlinear least-squares analysis with mutiple initializations was performed to determine the global minimum.

RESULTS

Engineering of Strains

The rationale of the NADPH flexibility study in *C. glutamicum* was to use an NADH-consuming glutamate dehydrogenase instead of the original NADPH-dependent enzyme of the organism (Oshima *et al.*, 1964; Börmann *et al.*, 1992). Such an NADH-consuming enzyme is present in *P. asaccharolyticus*, where it serves catabolic purposes (Snedecor *et al.*, 1991). Of course, when dictated by the equilibrium constant, the enzyme also catalyzes the formation of glutamate. Based on the published sequence and using the polymerase chain reaction, we amplified the *P. asaccharolyticus* glutamate dehydrogenase gene from genomic DNA. A *Bam*HI site was introduced 39 bp in front of the gene and a *Sac*I site 163 bp downstream of it. This served to clone the amplified fragment into the corresponding sites of the expression vector pEKEx2 (Eikmanns *et al.*, 1991) to yield pEKExpgdh. With this vector, NAD-dependent and IPTG-inducible glutamate dehydrogenase activity was obtained in *C. glutamicum* (see below).

To delete the original NADPH-dependent enzyme from the *C. glutamicum* chromosome, the mobilizable but non-replicative vector pK19*mobsacBΔgdh* was constructed (see Materials and Methods). It carries the homologous *C. glutamicum* gene, from which an internal fragment had been deleted. It was introduced into the lysine producer *C. glutamicum* MH20-22B by intergeneric mating. This lysine producer was chosen because (i) the NADPH demand for lysine production is high, (ii) the strain is very well characterized (Schrumpf *et al.*, 1992), and (iii) we have already established several detailed flux quantifications for this high-level producer (Marx *et al.*, 1996, 1997). After mating, one transconjugant (resistant for kanamycin) was obtained with the vector integrated in the chromosomal *gdh* due to homologous recombination. This clone was subjected to a second round of positive selection (resistance for sucrose) to result in clones which had lost the vector. Fifteen of the numerous clones obtained were assayed for glutamate dehydrogenase activity, and three of them were identified as having no enzyme activity due to the appropriate location of the second recombination. The loss of the chromosomal fragment in the constructed strain *C. glutamicum* MH20-22B*Δgdh* was confirmed in a Southern blot (not shown). This strain was transformed with plasmid pEKExpgdh, encoding the heterologous *P. asaccharolyticus* enzyme. As the control, the deletion strain was transformed with pEK19*gdh*-1, encoding the homologous *C. glutamicum* enzyme (Börmann *et al.*, 1992). In the following the strains will be referred to as the heterologous mutant and the homologous mutant, respectively.

Gene Expressions

To verify expression of the glutamate dehydrogenase genes, enzyme activity determinations were performed. In the strain MH20-22B*Δgdh* with deleted dehydrogenase, no enzyme activity was detected (not shown). In the heterologous mutant with the *P. asaccharolyticus* gene, the NADH-dependent enzyme was synthesized (without IPTG addition) to yield a high specific dehydrogenase activity of 1.80 μmol/min/mg protein. In addition to the dehydrogenase activity residual glutamine–oxoglutarate aminotransferase activity was detectable in this heterologous mutant (activity of 0.033 μmol/min/mg protein); it was almost zero in the homologous mutant. Since this activity, together with the glutamine synthetase, could contribute to NADPH-dependent glutamate synthesis, the inhibitor methionine *S*-sulfoximine was used (Weisbrod and Meister, 1973). *In vivo* this inhibitor specifically prevents glutamate synthesis via the transferase/glutamine synthetase system, since growth of *C. glutamicum* with inactivated *gdh* is abolished at a concentration of 10 mM, whereas growth of the wild type is not (M. Tesch, personal communication). Consequently, both the heterologous mutant and the homologous mutant were grown in the continuous cultures in the presence of 15 mM methionine *S*-sulfoximine. As verified in extracts of cells taken from the cultures during establishment of the steady state, the dehydrogenase activities in both cultures were already comparable after 3 and 4 volume changes. In the steady state, a specific activity of 5.08 μmol/min/mg protein was determined for the NAD-dependent enzyme of the heterologous mutant, and a specific activity of 6.97 μmol/min/mg protein for the NADP-dependent enzyme of the homologous mutant was determined.

NMR Quantifications

Continuous cultures of the mutants were supplied with 99% enriched [1-^{13}C]glucose. In the steady state all glucose was consumed. Making use of the fact that in the metabolic and isotopic steady state the enrichments in the precursors within the metabolic network are identical to those in the precursors stored as building blocks in the cell material, we hydrolyzed the total cell material and isolated the building blocks on a preparative scale to allow enrichment determinations. In total, the fractional enrichments in carbon in nine amino acids, in glucosamine, and in the sugar moiety of guanosine were quantified by ^{1}H-detected NMR spectroscopy, including spin-echo NMR for non-protonated carbons of amino acids (Tables 2 and 3).

As a technique generally applicable to quantifying the enrichment in CO_2, a method for estimating the enrichment

TABLE II

Measured ^{13}C Enrichments in Cell Constituents Isolated from the Heterologous Mutant, *gdh*(NAD)

Metabolite	^{13}C enrichment (%) in carbon					
	C-1	C-2	C-3	C-4	C-5	C-6
Gly	3.2 ± 0.3	2.2 ± 0.3				
Ala	4.3 ± 1.0	4.5 ± 1.0	37.0 ± 0.8			
Glx	18.6 ± 0.6	30.1 ± 0.6	18.3 ± 0.2	37.5 ± 0.4	3.6 ± 1.0	
Arg	n.d.	30.7 ± 1.0	18.4 ± 1.0	35.1 ± 1.0	2.9 ± 1.0	16.4 ± 0.5
Thr	12.6 ± 0.8	n.d.	n.d.	16.2 ± 1.5		
Asx	n.d.	18.1 ± 1.0	30.7 ± 1.5	n.d.		
Phe[a]	n.d.	n.d.	34.3 ± 2.5	n.d.	20.5 ± 2.5	1.1 ± 1.0
Val[b]	n.d.	4.8 ± 1.0	n.d.	37.4 ± 1.5		
Lys	n.d.	13.2 ± 0.6	30.2 ± 1.0	15.5 ± 1.0	n.d.	7.6 ± 0.4
Guanosine	24.5 ± 0.8	n.d.	n.d.	n.d.	25.1 ± 1.0	
Glucosamine	78.0 ± 4.0	n.d.	n.d.	n.d.	n.d.	n.d.
CO_2	16.5 ± 0.5					

Note. n.d., not determined.

[a] The mean value for C-5 is derived from C-5 plus C-9. The enrichment in C-7 and C-8 is 1.1 ± 1.0%.

[b] The mean value for C-4 is derived from C-4 plus C-4'.

in C-6 of arginine was developed because the C-6 enrichment stems exclusively from CO_2 incorporated via carbamoylphosphate synthase activity. In a series of experiments, the spin-echo delay (TE) was varied to quantify the amplitudes of the ^{13}C satellites in the difference spectra obtained. A cosine dependency of the amplitudes of the difference spectra on TE is observed due to the evolution of the long-range *J* HCNC during the spin-echo delay (Fig. 2). According to the difference signal of 30.7% for the heterologous mutant, a spin-echo delay of 142 ms and calibration result in a fractional enrichment of 16.5 ± 0.5%. This is in excellent agreement with the enrichment in CO_2 as determined by nondispersive infrared spectroscopy (Table 2). It shows that in the culture the intracellular CO_2 is in equilibrium with the extracellular CO_2. Access to the fructose 6-phosphate enrichments was made possible by the quantifications in glucosamine. Together with the available enrichments in e4p and p5p, this further improves the flux

TABLE III

Measured ^{13}C Enrichments in Cell Constituents Isolated from the Homologous Mutant, *gdh*(NADP)

Metabolite	^{13}C enrichment (%) in carbon					
	C-1	C-2	C-3	C-4	C-5	C-6
Gly	2.0 ± 0.2	1.7 ± 0.3				
Ser	n.d.	n.d.	23.0 ± 2.0			
Ala	2.0 ± 0.5	2.2 ± 1.0	25.7 ± 0.7			
Glx	15.7 ± 0.6	21.1 ± 0.3	11.6 ± 0.3	25.8 ± 0.7	2.2 ± 1.0	
Arg	n.d.	20.5 ± 0.5	11.6 ± 1.0	23.9 ± 1.0	1.9 ± 1.0	21.3 ± 0.4
Thr	8.0 ± 0.5	12.7 ± 1.0	20.4 ± 1.7	15.3 ± 1.0		
Phe[a]	n.d.	1.1 ± 1.0	25.5 ± 1.0	n.d.	12.8 ± 2.0	1.1 ± 1.0
Val[b]	n.d.	2.6 ± 1.0	2.6 ± 1.0	26.0 ± 2.5[b]		
Lys	n.d.	8.2 ± 0.4	22.2 ± 1.0	14.8 ± 1.0	n.d.	3.7 ± 0.4
Guanosine	7.5 ± 0.4	2.9 ± 1.3	1.1 ± 1.0	1.1 ± 1.0	16.4 ± 0.6	
Glucosamine	62.3 ± 2.5	n.d.	n.d.	n.d.	n.d.	n.d.
CO_2	22.4 ± 0.5					

[a] The mean value for C-5 is derived from C-5 plus C-9. The enrichment in C-7 and C-8 is 1.1 ± 1.0%.

[b] The mean value for C-4 is derived from C-4 plus C-4'.

TABLE IV

^{13}C Enrichments in Precursor Metabolites of the Heterologous Mutant as Derived from the Experimentally Determined Enrichments (Standard Characters) and as Predicted by the Solution of the Mathematical Model for Flux Quantification (in Italics)

Metabolite	^{13}C enrichment (%) in carbon					
	C-1	C-2	C-3	C-4	C-5	C-6
f6p	78.0 ± 4.0	n.d.	n.d.	n.d.	n.d.	n.d.
f6p	*80.0*	*1.4*	*4.6*	*1.6*	*1.3*	*9.6*
p5p	24.5 ± 0.8	n.d.	n.d.	n.d.	25.1 ± 1.0	
p5p	*24.4*	*2.3*	*2.4*	*1.6*	*24.9*	
e4p	1.1 ± 1.0	1.1 ± 1.0	1.1 ± 1.0	20.5 ± 2.5		
e4p	*2.9*	*2.2*	*1.5*	*20.9*		
gap	3.2 ± 0.3	2.2 ± 0.3	n.d.			
gap	*3.1*	*1.9*	*37.9*			
pyr	4.3 ± 1.0	4.6 ± 1.0	37.2 ± 1.5			
pyr	*4.0*	*3.6*	*37.2*			
akg	18.6 ± 0.6	30.1 ± 0.6	18.3 ± 0.2	37.5 ± 0.4	3.6 ± 1.0	
akg	*16.3*	*30.6*	*18.2*	*37.2*	*3.7*	
oaa	12.6 ± 0.8	18.1 ± 1.0	30.7 ± 1.5	16.2 ± 1.5		
oaa	*11.7*	*18.2*	*30.6*	*16.3*		
lys	n.d.	13.2 ± 0.6	30.2 ± 1.0	15.5 ± 1.0	n.d.	7.6 ± 0.4
lys	*9.5*	*14.0*	*32.5*	*16.3*	*35.3*	*7.8*
CO_2	16.4 ± 0.5					
CO_2	*16.4*					

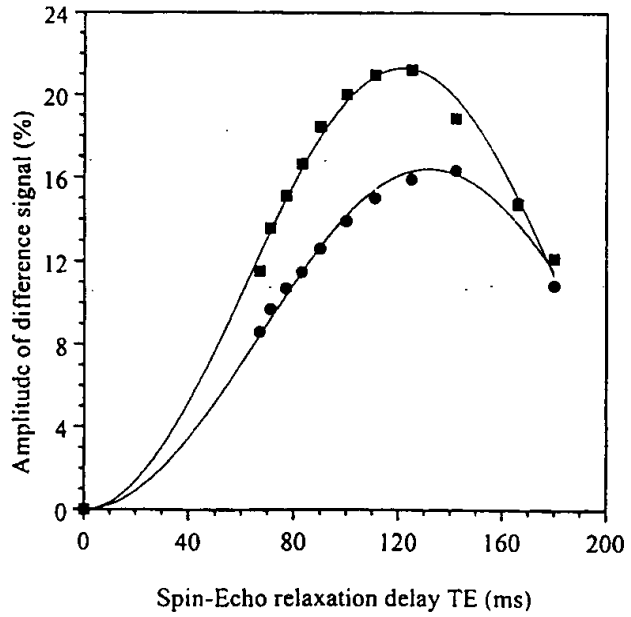

FIG. 2. Spin-echo difference signal amplitude of ^{13}C-6 satellites of H-5 of arginine as a function of the spin-echo relaxation delay, from arginine isolated from the homologous mutant (■) and from the heterologous mutant (●) after growth on [1-^{13}C]-glucose.

determinations within the pentose phosphate pathway (PPP).

The fractional enrichments in the precursor metabolites of the heterologous mutant thus derived are given in Table 4. For those positions where several data were available (for instance, C-1 pyr derived from C-1 ala and C-1 val), a weighted mean value was used. Weighting was performed according to the measurement error. In a similar manner, the data for the precursor metabolites of the homologous mutant were derived and are given in Table 5.

Estimated Carbon Fluxes

The current model used to estimate the carbon fluxes contains 14 fluxes removing or supplying metabolites from the network, with 11 of them being accumulating fluxes for biomass synthesis. Another 16 fluxes connect the 14 intracellular metabolite pools in the central metabolism (Marx *et al.*, 1997). For each experiment a detailed statistical analysis was carried out according to the procedures described by Wiechert *et al.* (1997). In particular, confidence regions and correlations were computed for the estimated fluxes (Table 6). The sums of squared deviations were 32.9 and 48.7 for the heterologous and the homologous mutant,

TABLE V

^{13}C Enrichments in Precursor Metabolites of the Homologous Mutant as Derived from the Experimentally Determined Enrichments (Standard Characters) and as Predicted by the Solution of the Mathematical Model for Flux Quantification (in Italics)

Metabolite	^{13}C enrichment (%) in carbon					
	C-1	C-2	C-3	C-4	C-5	C-6
f6p	62.3 ± 2.5	n.d.	n.d.	n.d.	n.d.	n.d.
f6p	*61.7*	*1.5*	*2.5*	*1.4*	*1.3*	*8.5*
p5p	7.5 ± 0.4	2.9 ± 1.3	1.1 ± 1.0	1.1 ± 1.0	16.4 ± 0.6	
p5p	*7.6*	*2.1*	*1.6*	*1.5*	*16.4*	
e4p	1.1 ± 1.0	1.1 ± 1.0	1.1 ± 1.0	12.8 ± 2.0		
e4p	*2.2*	*1.6*	*1.4*	*14.3*		
gap	2.0 ± 0.2	1.7 ± 0.3	23.0 ± 2.0			
gap	*2.0*	*1.7*	*26.3*			
pyr	2.0 ± 0.5	2.4 ± 1.0	25.7 ± 0.7			
pyr	*2.0*	*1.9*	*26.2*			
akg	15.7 ± 0.6	21.1 ± 0.3	11.6 ± 0.3	25.8 ± 0.7	2.2 ± 1.0	
akg	*16.2*	*21.2*	*11.6*	*26.2*	*1.9*	
oaa	8.0 ± 0.5	12.7 ± 1.0	20.4 ± 1.7	15.3 ± 1.0		
oaa	*7.9*	*11.6*	*21.2*	*16.2*		
lys	n.d.	8.2 ± 0.4	22.2 ± 1.0	14.8 ± 1.0	n.d.	3.7 ± 0.4
lys	*6.4*	*9.1*	*22.5*	*16.2*	*24.9*	*4.4*
CO2	21.3 ± 0.4					
CO_2	*23.2*					

TABLE VI

Statistical Analysis of Net or Exchange Fluxes in the Two Isogenic *C. glutamicum* Strains.

Flux	Reaction	Flux rate (%) of lower and upper boundary			
		Homologous mutant		Heterologous mutant	
v_5	Glucose-6-P DH	56.8	95.9	21.0	31.8
v_{15}	Isocitrate lyase	0.0	0.0	0.0	5.6
	Diaminopimelate DH	11.3	17.3	6.2	9.2
$v_7^{\leftrightarrow}$	Glucose-6-P isomerase	96.9	∞	0.0	∞
$v_8^{\leftrightarrow}$	Glyceraldehyde-3-P DH	79.6	∞	36.8	132.5
$v_9^{\leftrightarrow}$	TK(x5p + e4p ↔ g3p + f6p)	3.1	14.9	3.5	8.0
$v_{11}^{\leftrightarrow}$	TA	0.0	9.4	6.4	20.3
$v_{12}^{\leftrightarrow}$	TK(x5p + ri5p ↔ s7p + g3p)	54.4	74.7	30.0	46.6
$v_{14}^{\leftrightarrow}$	Fumarase	22.4	41.2	16.2	50.2
$v_{16}^{\leftrightarrow}$	Anaplerotic exchange	3.8	17.0	22.6	36.5

Note. The 90% confidence interval for the upper and lower boundary is given. The values are expressed as percentages relative to the glucose uptake flux (set to 100%). Abbreviations: DH dehydrogenase; TK, transketolase; TA, transaldolase. The fluxes are specified in detail in Marx *et al.* (1996).

respectively, showing good correspondence between measured and computed values.

The carbon fluxes estimated in the homologous mutant are shown in Fig. 3. The flux entering the PPP is as high as 76%. The excess carbon flux not required for the synthesis of polyolphosphates for biosynthetic purposes is over the nonoxidative transaldolase and transketolase reactions to f6p and gap, which thus rejoin the glycolysis. At the level of the gap 162 mol% is present out of the theoretical maximum of 200 mol%. This equals 81% of the maximum. Thus at the level of the gap, 19% of the carbon was used for biomass formation and carbon dioxide generation. In the heterologous mutant (Fig. 4), the flux entering the PPP is strongly reduced to 26%. This can be traced back to the enrichment in C-3 of pyr (compare Tables 4 and 5), since less C-1 of the substrate [1-^{13}C]glucose is removed from the network in this mutant. However, at the level of the gap, again 176 mol% is present. Thus the strong change in the oxidative part of the PPP has limited consequences for the gap availability, and for the fluxes towards pep and pyr. In both mutants the glyoxylic acid cycle carries no flux,

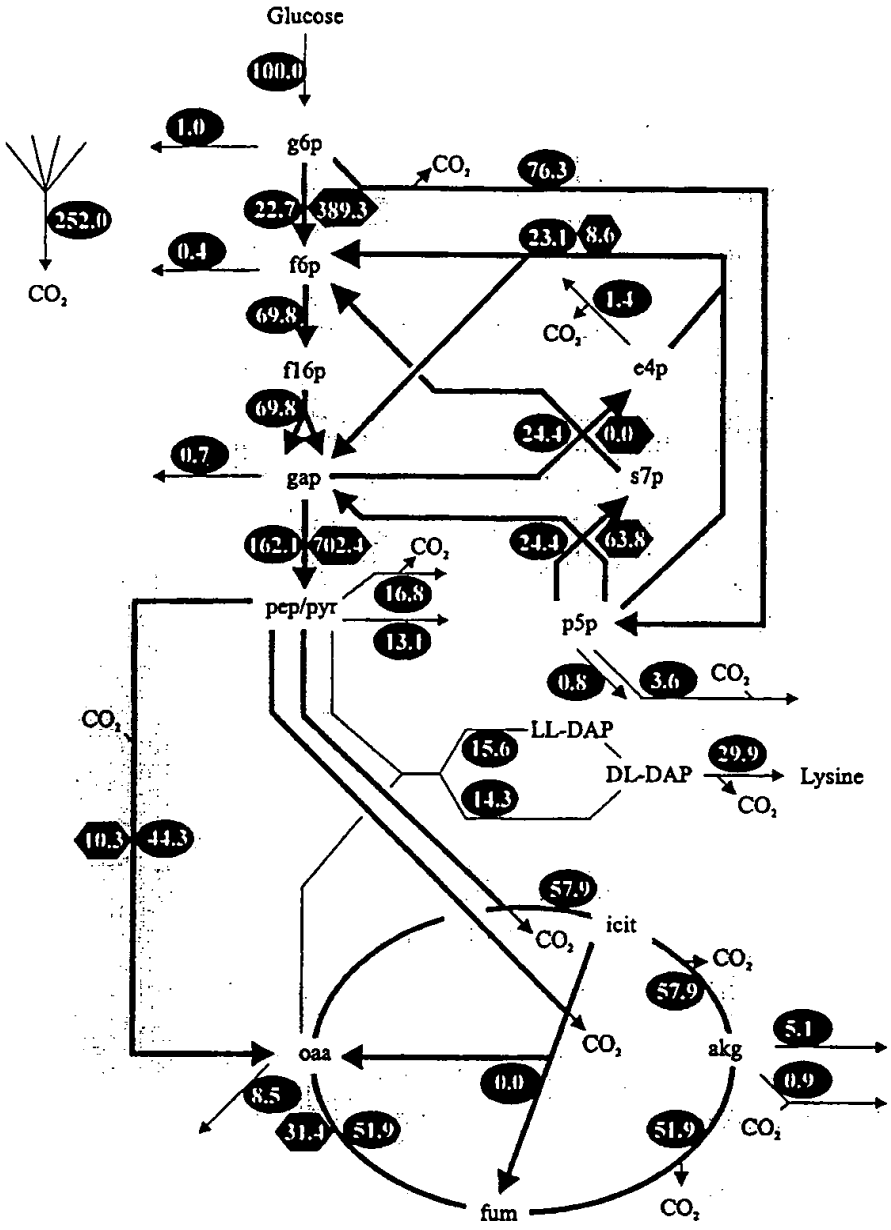

FIG. 3. *In vivo* flux distribution in the central metabolism for *C. glutamicum* MH20-22B using its NADP-dependent glutamate dehydrogenase (homologous mutant MH20-22B*Δgdh* pEK1.9*gdh*-1). Numbers in oval symbols near thick lines give the estimated net fluxes; those near the thin arrows give the measured fluxes required for biomass synthesis. Numbers in hexagons give the estimated additional exchange fluxes in reversible reactions. All fluxes are given as molar metabolite flux expressed as a percentage of the glucose uptake rate, which was 26.9 μmol/g dry. Abbreviations: g6p, glucose 6-phosphate; f16bp, fructose 1,6-bisphosphate; f6p, fructose 6-bisphosphate; gap, glyceraldehyde 3-phosphate; pep, phospho*enol*pyruvate; pyr, pyruvate; oaa, oxaloacetate; fum, fumarate; icit, isocitrate, akg, ketoglutarate; p5p, pentose 5-phosphate; s7p, sedoheptulose 7-phosphate; e4p, erythrose 4-phosphate; LL-DAP, LL-diaminopimelate; DL-DAP, DL-diaminopimelate.

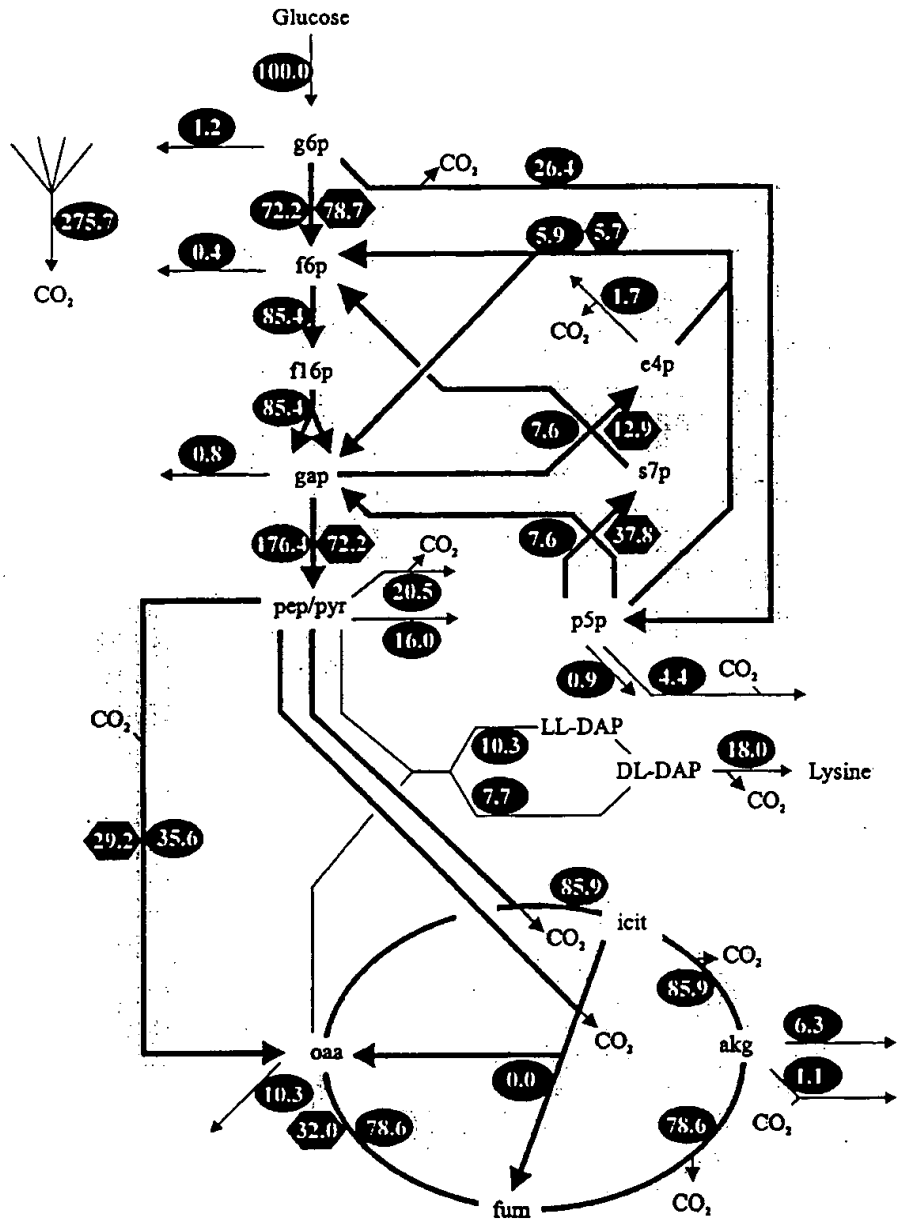

FIG. 4. *In vivo* flux distribution in the central metabolism for *C. glutamicum* MH20-22B using the NAD-dependent glutamate dehydrogenase of *P. asaccharolyticus* (heterologous mutant *C. glutamicum* MH20-22B*Δgdh* pEKEXpgdh). The glucose flux, set to 100% was 23.0 μmol/g dry. Description and abbreviations as in Fig. 3.

whereas the flux entering the tricaboxylic acid cycle (TCC) is significantly increased to 86 mol%, compared to the homologous mutant (58%). This could be due to an increased NADH demand in the heterologous mutant. In both mutants a high and comparable part of the lysine is synthesized via the dehydrogenase branch of the split pathway, which contributes 48% to total lysine synthesis in the homologous mutant and 43% in the heterologous mutant.

The exchange fluxes are shown in hexagons in Figs. 4 and 5, with their 90% confidence interval given in Table 6. For the heterologous mutant we estimated a large backflux

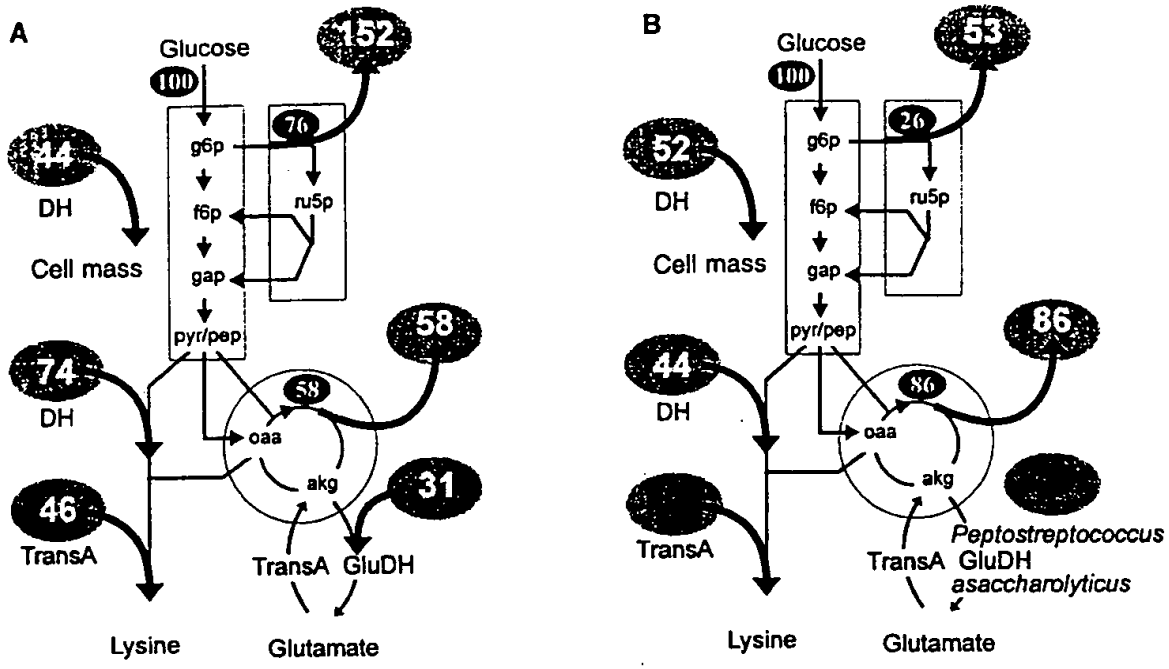

FIG. 5. The NADPH-generating and -consuming fluxes with NADPH-dependent glutamate dehydrogenase (A) and NADH-dependent glutamate dehydrogenase (B). The numbers in large ovals are the NADPH fluxes in mol% relative to the glucose uptake flux.

of 29.2 mol% (confidence interval 22.6–36.5) within the anaplerotic reactions. In the homologous mutant this value is only 10.3% (interval 3.8–17.0). This difference is reflected in the higher enrichment in C-2 of pyr in the heterologous mutant, which is due to the higher incorporation of oxaloacetate carbons via backflux into pyruvate. On the other hand, the enrichment in C-2 of oxaloacetate (oaa) decreases with high exchange flux (Fig. 6). In the computer-aided analysis all data are considered and contribute to the estimate of this exchange flux v_{16}^{-}. Further high-exchange fluxes are present within the PPP, with the transketolase reaction (p5p + p5p ↔ s7p + gap) exceeding the net flux more than threefold. In the TCC a moderate backflux from oxaloacetate to fumarate was estimated.

The Estimated NADPH Fluxes

For the NADPH-generating fluxes only three reactions are relevant. These are the glucose-6-phosphate dehydrogenase, gluconate-6-phosphate dehydrogenase and isocitrate dehydrogenase reactions, where the carbon flux is directly equivalent to molar NAPH generation (Fig. 5A). These generating fluxes add up in the homologous mutant to a molar flux of 210.5%. The malic enzyme was not considered because only a maximal value can be derived from the current flux analyses (see Discussion). To calculate the consuming fluxes we counted the required amounts of NADPH from known stoichiometries of the various biosynthetic reactions and the cell composition (Marx *et al.*, 1996). Approximately 15,500 μmol NADPH is necessary for the synthesis of 1 g dry weight. Of this amount about 50% is consumed by the glutamate dehydrogenase reaction, which functions mainly to deliver its amino group via transamination to cell mass synthesis (6350 μmol/g dry), and to a lesser extent to provide glutamate and glutamine for protein synthesis (800 μmol/g dry). Based on these stoichiometries the NADPH-consuming flux for α-ketoglutarate reduction is 31 mol%, and that directly required for reduction of cell material via dehydrogenases is 44 mol%. The fluxes for L-lysine synthesis were calculated separately. The aspartate DH and dihydrodipicolinate DH carry a flux of 29.9 mol% (Fig. 3) and the diaminopimelate DH a flux of 14.3%, adding up to 74.1%. The transaminase flux is 46 mol% (29.9% aspartate amino transferase, plus 15.6% succinylaminotransferase). It follows that the sum of the NADPH-consuming fluxes is 194.9%, which is almost identical to the generating fluxes of 210.5%.

The flux balance for the heterologous mutant is shown in Fig. 5B. Here the glutamate dehydrogenase flux does not contribute to biosynthetic purposes due to the NAD-dependent dehydrogenase of *P. asaccharolyticus*. The NADPH flux of dehydrogenases required for biosynthetic purposes is comparable (51.6%), whereas the dehydrogenases operating

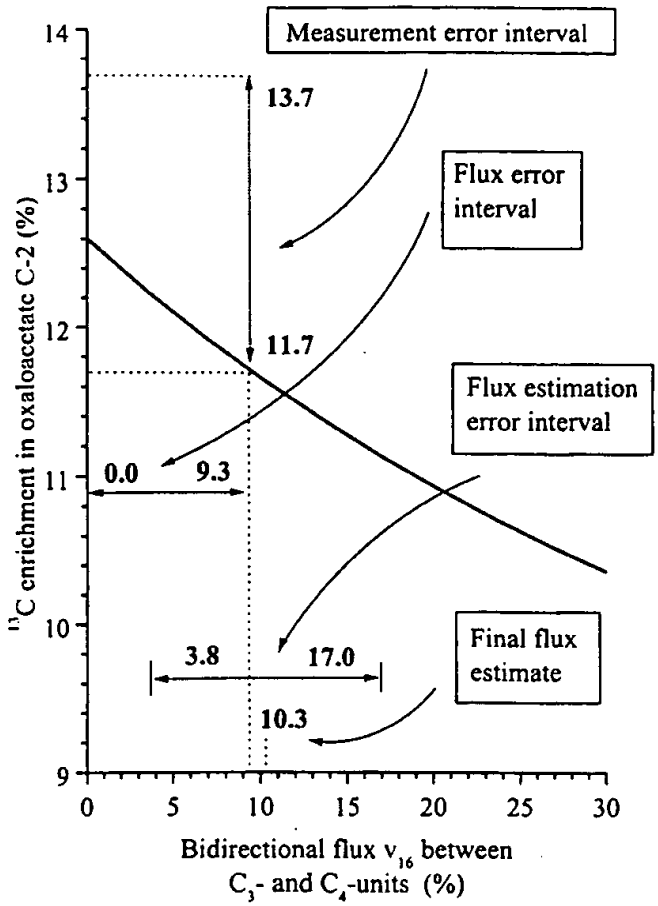

FIG. 6. Degree of ^{13}C enrichment in C-2 of oxaloacetate as a function of the exchange flux $v_{16}^{\rightleftarrows}$ (exchange between C-4 and C-3 units). The dependency is given together with measured values, estimated values, and their statistical errors.

in L-lysine synthesis consume less NADPH, since in this particular experiment the total carbon flux toward L-lysine was reduced. However, importantly, as the response of the reduced NADPH demand due to the NAD-dependent glutamate DH, the generation of NADPH is drastically reduced. The total NADPH generating flux is 138.7 mol%. The consuming flux is calculated to be 95.3%, which gives an excess of 43.4%. This flux is exclusively accessible by the given isotope analysis and its relevance will be discussed below. About one fourth of the reduced NADPH demand in the heterologous mutant can be attributed to reduced demand for biomass synthesis and three fourths to that for L-lysine synthesis.

DISCUSSION

Although it is often attempted, it is not possible to predict in a necessarily reductionist approach to describing the living cell how specific enzyme activities must be preset to result in the maximal output of the desired product. In contrast, the real benefit of such an approach is to be found elsewhere (Popper, 1974).This might be in our example the quantification of the intracellular flexibility or a deeper insight into the exchange fluxes.

We were able to identify such an exchange flux for a bacterium *in vivo* within the anaplerotic reactions (Marx *et al.*, 1996). The statistical analysis of this exchange flux in *C. glutamicum* shows that $v_{16}^{\rightleftarrows}$ (opposed carboxylating and decarboxylating reactions) is different in the two glutamate DH mutants analyzed. The 90% confidence interval for the heterologous mutant is 22.6–36.5% molar exchange flux, and the interval for the homologous mutant is 3.8–17.0% (Table 6). This difference results from the different levels of the ^{13}C content for the oxaloacetate C-2 position (Tables 4 and 5). The enrichment in this position responds very sensitivly to the $v_{16}^{\rightleftarrows}$ exchange rate. The corresponding quantitative relation for the homologous mutant is shown in Fig. 6. The measured enrichment was 12.7 ± 1.0. Therefore, the molar exchange for the individually considered flux of $v_{16}^{\rightleftarrows}$ is 0–9.3% (relative to glucose uptake). Since the simulation considers all fluxes and exchanges, the estimated exchange between the C-3 units and the C-4 precursors as integrated in the total flux system is 10.3%, with a 90% confidence interval of 3.8–17.0%. The difference in the exchange flux between the two mutants had to be given as the sum of the individual fluxes interconverting the C-3 units and the C-4 units, since the partially identical educts and products do not yet permit any individual flux quantification. The situation is even more complex, since only recently has it become possible to clone the pyruvate carboxylase-encoding gene *pyc* (Peters-Wendisch *et al.*, 1998), which is therefore, in addition to phospho*enol*pyruvate carboxylase (*ppc*), the second reaction contributing to the net synthesis of oxaloacetate (Fig. 7). As mentioned, the partition of the carboxylating flux between the two carboxylase reactions identified is not yet known, nor is the physiological role of the backflux at this extensive set of enzymes around the anaplerotic reactions. In rats the backflux from pyruvate to oxaloacetate was estimated in isotopomer studies to be of approximately the same size as that from oxaloacetate to phospho*enol*pyruvate (Katz *et al.*, 1993). The backflux in *C. glutamicum* may indeed be of fundamental physiological significance (Fig. 7). Thus, an energy-consuming futile cycle without contributing to biosynthesis (Rognstadt, 1996) may be formulated via phospho*enol*pyruvate carboxykinase and pyruvate carboxylase. The inhibition of both enzymes by ADP corresponds to the idea that the ATP- and GTP-consuming cycle is reduced at a low energy charge. In glutamate production we found a very slight futile cycle flux between C-3 units and C-4 units of

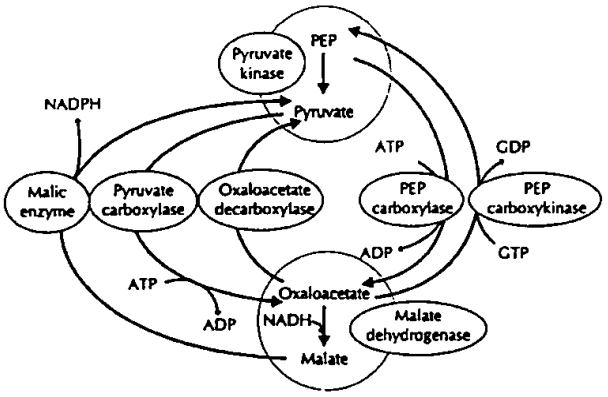

FIG. 7. Overview of the flux-carrying reactions at the anaplerotic node that could contribute to the reverse flux of 29.2% in the heterologous mutant, including a hypothetical transhydrogenase cycle and an energy-consuming cycle.

only 17.1% (Marx *et al.*, 1997). This could therefore be attributed to a low energy charge or increased conservation metabolism under the stress of biotin limitation. Another cycle which could be constructed consists of the malic enzyme and malate dehydrogenase resulting in the transfer of reducing equivalents from NAD to NADP. This cycle represents a transhydrogenase activity. There is contradictory information on *C. glutamicum* for a specific transhydrogenase (Cocaign-Bousquet and Lindley, 1996; Park *et al.*, 1997; Vallino 1991). In general, the sum of the carboxylating and decarboxylating reactions apparently serves as a fine tuning within the central metabolism to balance the fueling reactions with the catabolic reactions (Kornberg, 1966). Although the conversions between C-3 units and C-4 units seem to be important for the metabolic design of aromatic amino acid production in *E. coli* (Patnaik *et al.*, 1995), it is still unclear how they can be selectively used to increase amino acid overproduction. It is striking that with high C-4 unit formation the reverse flux is lowest in the homologous mutant of *C. glutamicum* (10.3%, see Fig. 3), as is the case under glutamate-producing conditions (Marx *et al.*, 1996). It is thus conceivable that the net conversion can be promoted not only by overexpression of, for example, pyruvate carboxylase, but also by reduction of the reverse fluxes.

As shown by the stoichiometry in Fig. 5, more NADPH is formed than is consumed. However, based on the 90% confidence interval, also the greater discrepany calculated for the heterologous mutant is still within the error range. Thus formation of an NADPH surplus cannot be quantified with certainty. Nevertheless, in all flux situations analyzed for *C. glutamicum* to date we have determined an excess of NADPH formation and never a deficit (Marx *et al.*, 1997; Sonntag *et al.*, 1995). Several additional reactions that are difficult to quantify might consume NADPH such as the system identified in *E. coli* detoxifying peroxide radicals (Luchi and Weiner, 1996), or an NAPDH-oxidizing activity which at least has been detected in extracts of *C. glutamicum* (Vallino, 1991). Also, a weak reaction of the *P. assacharolyticus* glutamate dehydrogenase using NADPH instead of NADH might be attributed to the greater discrepancy of the heterologous mutant, since the enzyme has a very low activity of 0.9% with NADPH as substrate.

In any case, the cell (Fig. 5) actually responded by reduced redox generation through our selective intervention of diminished demand for redox equivalents. There are several examples of cases where externally added electron mediators might affect the intracellular redox metabolism as inferred from an altered product spectrum (Neijssel 1977; Kwong and Rao, 1992). An internal alteration of the NADPH balance was obtained in yeast by the synthesis of an NADPH-dependent xylose reductase, which led to altered by-product formation (Meinander *et al.*, 1996). Our quantitative data show that for the directly altered NADPH demand the NADPH generation is reduced by about one-third. It thus follows that *C. glutamicum* is enormously flexible not only with respect to the carbon fluxes in the central metabolism (Marx *et al.*, 1997) but also with respect to the redox fluxes. This could be a reason for the particular suitability of this bacterium for metabolite overproduction. Since our data show that the cell adjusts the fluxes to the reduced NADPH demand and does not use a potentially available increased NADPH supply to increase lysine production, we regard this as an indication that lysine production is not essentially NADPH-limited. However, this question must be addressed in further studies by direct intracellular quantification of the involved metabolites.

In total, we have now generated a unique set of five different flux situations of isogenic strains specifying the response of the metabolism to an altered carbon or reducing power flux. Acting only on one enzyme activity, for instance, a kinase (Marx *et al.*, 1997) or a dehydrogenase (this work), results in an extreme range of fluxes in the central metabolism. The oxidative PPP carbon flux varies from 25 to 76%. As a general trend, it can be seen that at a high NADPH demand a high PPP flux results. Furthermore, there is an inverse relation of the PPP flux to the TCC flux. A global picture of flux regulation in *C. glutamicum* can thus be derived. The TCC flux is first adjusted according to the carbon requirements. The isocitrate dehydrogenase activity necessarily linked to the latter provides a basal level of NADPH flux. In extreme cases this is manifest in glutamate production, where a high input into the TCC is present due to the high α-ketoglutarate requirement. However, there is still high cycling activity due to the α-ketoglutarate DH activity present, which was originally thought to be absent in *C. glutamicum* (Kinoshita, 1985). This activity

serves to provide sufficient NADH for ATP generation. Whereas in the TCC cycle the fluxes are adjusted to the specific carbon and NADH demand, the PPP flux is adjusted according to the NADPH demand not fulfilled by the TCC. With high TCC flux (glutamate production) the PPP flux is thus reduced, whereas at low TCC flux (lysine production) the PPP flux is high to adjust the NADPH balance. The specific regulators controlling the entry into the PPP are the glucose-6-P DH and 6-P-gluconate DH, both controlled in their catalytic acitivity by the NADPH concentration via allosteric mechanisms (Sugimoto and Shiio, 1987). Due to the flexibility of the central metabolism and its design to provide precursors as well as NADPH and NADH, it appears that the major targets to be altered to obtain maximal productivities are the biosynthesis pathways themselves, together with the export of the metabolite to be produced. What might limit maximal product formation beyond these reactions cannot be predicted by mechanistic flux studies, but relates to questions concerning the cell in its entirety, for instance, the tolerance of the cell toward physical features of the product, or how controlled reduction of precursor use for biomass formation can be obtained.

ACKNOWLEDGMENTS

We thank E. Börmann, K. Krumbach, and S. Petrovic for help with constructions and analyses, M. Tesch for sharing results prior to publication, and W. Wiechert (University of Siegen), D. Molenaar (University of Düsseldorf), and V. Wendisch (University of California, Berkeley) for discussions.

REFERENCES

Berry, A. (1996). Improving production of aromatic compounds in *Escherichia coli* by metabolic engineering. *TIBTECH* 14, 250–256.

Börmann, E., Eikmanns, B. J., and Sahm, H. (1992). Molecular analysis of the *Corynebacterium glutamicum gdh* gene encoding glutamate dehydrogenase. *Mol. Microbiol.* 6, 317–326.

Cocaign-Bousquet, M., Guyonvarch, A., and Lindley, N. D. (1996). Growth-rate dependent modulation of carbon flux through central metabolism and the kinetic consequences for glucose-limited chemostat cultures of *Corynebacterium glutamicum*. *Appl. Environ. Microbiol.* 62, 429–436.

Eggeling, L., DeGraaf, A. A., and Sahm, H. (1996). Quantifying and directing metabolite flux: Application to amino acid overproduction. *Adv. Biochem. Eng.* 54, 2–30.

Eggeling, L., Oberle, S., and Sahm, H. (1997). Improved L-lysine yield with *Corynebacterium glutamicum*: Use of *dapA* resulting in increased flux combined with growth limitation. *Appl. Microbiol. Biotechnol.* 49, 24–30.

Eggeling, L., Morbach, S., and Sahm, H. (1997). The fruits of molecular physiology: Engineering the L-isoleucine biosynthesis pathway in *Corynebacterium glutamicum*. *J. Biotechnol.* 56, 167–182.

Eggeling, L., and Sahm, H. (1998). Amino acid production: Principles of metabolic engineering. *In* "Metabolic Engineering" (Y. S. Sang and E. T. Papoutsakis, Eds.), Biotechnology Intelligence Unit, R. G. Landes.

Eikmanns, B., Kleinertz, E., Liebl, W., and Sahm, H. (1991). A family of *Corynebacterium glutamicum/Escherichia coli* shuttle vectors for gene cloning, controlled gene expression, and promoter probing. *Gene* 102, 93–98.

Flores, N., Xiao, J., Berry, A., Bolivar, F., and Valle, F. (1996). Pathway engineering for the production of aromatic compounds in *Escherichia coli*. *Nature Biotechnol.* 14, 620–623.

Iuchi, S., and Weiner, L. (1996). Cellular and molecular physiology of *Escherichia coli* in the adaption to aerobic environments. *J. Biochem.* 120, 1055–1063.

Katz, J., Wals, P., and Lee, W. P. (1993). Isotopomer studies of gluconeogenesis and the Krebs cycle with ^{13}C-labeled lactate. *J. Biol. Chem.* 268, 25509–25521.

Kinoshita, S. (1985). Glutamic acid bacteria. *In* "Biology of Industrial Microorganisms" (A. L. Demain and N. A. Solomon, Eds.), pp. 115–142, Benjamin/Cummings, Redwood City, CA.

Kornberg, H. L. (1966). Anaplerotic sequences and their role in metabolism. *In* "Essays in Biochemistry" (P. N. Campbell and G. D. Grevile, Eds), Vol II, pp. 1–31, Academic Press, New York.

Kwong, S. C. W., and Rao, G. (1992). Effect of reducing agents in an aerobic amino acid fermentation. *Biotechnol. Bioeng.* 40, 851–857.

Liebl, W., Bayerl, A., Stillner, U., and Schleifer, K. H. (1989). High efficiency electroporation of intact *Corynebacterium glutamicum* cells *FEMS Microbiol. Lett.* 65, 299–304.

Marx, A., de Graaf, A. A., Wiechert, W., Eggeling, L., and Sahm, H. (1996). Determination of the fluxes in the central metabolism of *Corynebacterium glutamicum* by NMR spectroscopy combined with metabolite balancing. *Biotechnol. Bioeng.* 49, 111–129.

Marx, A., Striegel, K., de Graaf, A. A., Sahm, H., and Eggeling, L. (1997). Response of the central metabolism of *Corynebacterium glutamicum* to different flux burdens. *Biotechnol. Bioeng.* 56, 168–180.

Meinander, N., Zacchi, G., and Hah-Hägerdal, B. (1996). A heterologous reductase affects the redox balance of recombinant *Saccharomyces cerevisiae*. *Microbiology* 142, 165–172.

Mori, M., and Shiio, I. (1985). Purification and some properties of phosphoenolpyruvate carboxylase from *Brevibacterium flavum* and its aspartate-overproducing mutant. *J. Biochem. Tokyo* 97, 1119–1128.

Mori, M., and Shiio, I. (1985). Synergistic inhibition of phosphoenolpyruvate carboxylase by aspartate and 2-oxoglutarate in *Brevibacterium flavum*. *J. Biochem. Tokyo* 98, 1621–1630.

Neese, R. A., and Hellerstein, M. K. (1995). Calculations for gluconeogenesis by mass isotopomer distribution analysis. *J. Biol. Chem.* 276, 14464–14466.

Neijssel, O. M. (1977). The effect of 2,4-dinitrophenol on the growth of *Klebsiella aerogenes* NCTC 418 in aerobic chemostat cultures. *FEMS Lett.* 1, 47–50.

Oshima, K., Tanaka, K., and Kinoshita, S. (1964). Studies on L-glutamic acid fermentation. XI. Purification and properties of L-glutamic dehydrogenase from *Micrococcus glutamicus*. *Agric. Biol. Chem. Tokyo* 28, 714–722.

Park, S. M., Sinskey, A. J., and Stephanopoulos, G. (1997). Metabolic and physiological studies of *Corynebacterium glutamicum* mutants. *Biotechnol. Bioeng.* 55, 864–879.

Patnaik, R., Spitzer, R. G., and Liao, J. C. (1995). Pathway engineering for production of aromatics in *Escherichia coli*: Confirmation of stoichiometric analysis by independent modulation of AroG, TktA, and Pps activities. *Biotechnol. Bioeng.* 46, 361–370.

Peters-Wendisch, P., Kreutzer, C., Kalinowski, J., Pátek, M., Sahm, H., and Eikmanns, B. J. (1998). Pyruvate carboxylase from *Corynebacterium glutamicum*: Characterization, expression and inactivation of the *pyc* gene. *Microbiol. UK* 143, 1095–1103.

Peters-Wendisch, P. G., Wendisch, V. F., Paul, S., Eikmanns, B. J., and Sahm, H. (1997). Pyruvate carboxylase as an anaplerotic enzyme in *Corynebacterium glutamicum*. *Microbiol. UK* **143**, 1095–1103.

Popper, K. (1974). "Studies on the Philosophy of Biology." (F. J. Ayda and T. Dobzhansky, Eds.), pp. 259–283, MacMillan, London.

Rognstad, R. (1996). Futile cycling in carbohydrate metabolism. I. Background and current controversies on pyruvate cycling. *Biochem. Arch.* **12**, 71–83.

Sauer, U., Hatzimanikatis, V., Hohmann, H., Manneberg, M., van Loon, A., and Bailey (1996). Physiology and metabolic fluxes of wild-type and riboflavin-producing *Bacillus subtilis*. *Appl. Environ. Microbiol.* **62**, 3687–3696.

Schäfer, A., Kalinowski, J., Simon, R., Seep-Feldhaus, A., and Pühler, A. (1990). High-frequency conjugal plasmid transfer from gram-negative *Escherichia coli* to various gram-positive coryneform bacteria. *J. Bacteriol.* **172**, 1663–1666.

Schäfer, A., Tauch, A., Jäger, W., Kalinoski, J., Thierbach, G., and Pühler, A. (1994). Small mobilizable multi-purpose cloning vectors derived from the *Escherichia coli* plasmids pK18 and pK19: Selection of defined deletions in the chromosome of *Corynebacterium glutamicum*. *Gene* **145**, 69–73.

Schrumpf, B., Eggeling, L., and Sahm, H. (1992). Isolation and prominent characteristics of an L-lysine hyperproducing strain of *Corynebacterium glutamicum*. *Appl. Microbiol. Biotechnol.* **37**, 566–571.

Schwarzer, A., and Pühler, A. (1990). Genetic manipulation of the amino acid-producing *Corynebacterium glutamicum* strain ATCC 13032 by gene disruption and gene replacement. *Bio/Technology* **9**, 84–87.

Simon, R., Priefer, U., and Pühler, A. (1983). A broad host range mobilization system for in vivo genetic engineering: Transposon mutagenesis in gram negative bacteria. *Bio/Technology* **1**, 784–791.

Snedecor, B., Chu, H., and Chen, E. (1991). Selection, expression, and nucleotide sequencing of the glutamate dehydrogenase gene of *Peptostreptococcus asaccharolyticus*. *J. Bacteriol.* **173**, 6162–6167.

Sonntag, K., Schwinde, J., de Graaf, A. A., Marx, A., Eikmanns, B. J., Wiechert, W., and Sahm, H. (1995). 13-C NMR studies of the fluxes in the central metabolism of *Corynebacterium glutamicum* during growth and overproduction of amino acids in batch cultures. *Appl. Microbiol. Biotechnol.* **44**, 489–495.

Sugimoto, S., and Shiio, I. (1987). Regulation of glucose-6-phosphate dehydrogenase in *Brevibacterium flavum*. *Agric. Biol. Chem. Tokyo* **51**, 101–108.

Vallino, J. J. (1991). "Identification of Branch-Point Restrictions in Microbial Metabolism Through Metabolic flux Analysis and Local Network Perturbations." Ph.D. thesis, Massachusetts Insitute of Technology, Boston.

Vallino, J. J., and Stephanopoulos, G. (1993). Metabolic flux distributions in *Corynebacterium glutamicum* during growth and lysine overproduction. *Biotechnol. Bioeng.* **41**, 633–646.

Vrljic, M., Sahm, H., and Eggeling, L. (1996). A new type of transporter with a new type of cellular function: L-Lysine export in *Corynebacterium glutamicum*. *Mol. Microbiol.* **22**, 815–826.

Weisbrod, R. E., and Meister, A. (1973). Studies on glutamine synthetase from *Escherichia coli*. *J. Biol. Chem.* **248**, 3997–4002.

Wendisch, V. F., de Graaf, A. A., and Sahm, H. (1997). Accurate determination of ^{13}C enrichments in nonprotonated carbon atoms of isotopically enriched amino acids by ^{1}H nuclear magnetic resonance. *Anal. Biochem.* **245**, 196–202.

Wiechert, W., Siefke, C., de Graaf, A. A., and Marx, A. (1997). Bidirectional reaction steps in metabolic engineering. II. Flux estimation and statistical analysis. *Biotechnol. Bioeng.* **55**, 118–135.

Wiechert, W., and de Graaf, A. A. (1997). Bidirectional reaction steps in metabolic engineering: Modeling and simulation of carbon isotope labeling experiments. *Biotechnol Bioeng.* **55**, 101–117.

ISSN 1096-7176

METABOLIC ENGINEERING

EDITORS
- Gregory N. Stephanopoulos
- Anthony J. Sinskey
- Martin L. Yarmush

ASSOCIATE EDITORS
- Barry C. Buckland
- Hans Westerhoff

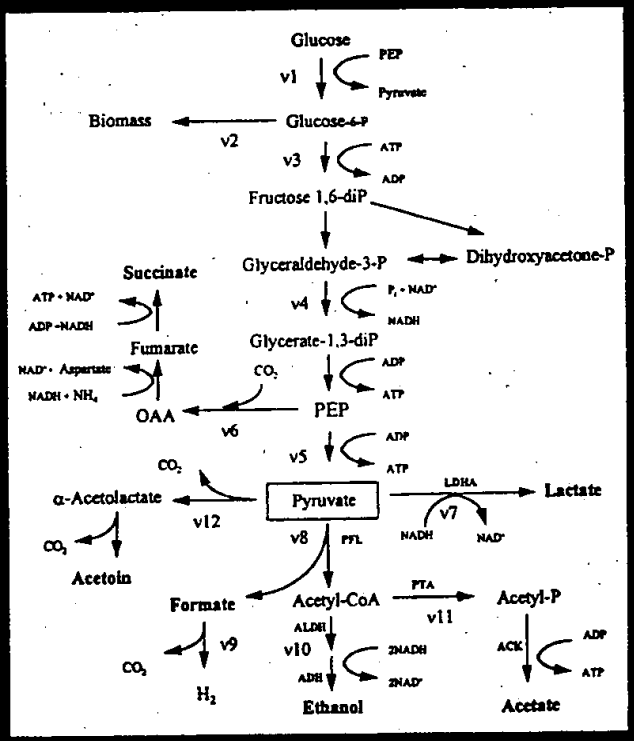

ACADEMIC PRESS

Metabolic Engineering

Cover figure. Central anaerobic metabolic pathway of *E. coli*. The fermentation end-products include acetoin produced by cells containing the ALS plasmid. The fluxes through each pathway are designated v_1 through v_{12}. (For details, see the paper by Yang *et al.* (1999), *Metab. Eng.* **1**, 26–34.)

THE JOURNAL OF BIOLOGICAL CHEMISTRY
Vol. 257, No. 3, Issue of February 10, pp. 1189–1195, 1982
Printed in U.S.A.

^{13}C Nuclear Magnetic Resonance Studies of the Biosynthesis by *Microbacterium ammoniaphilum* of L-Glutamate Selectively Enriched with Carbon-13*

(Received for publication, July 13, 1981)

T. E. Walker, C. H. Han, V. H. Kollman, R. E. London, and N. A. Matwiyoff‡

From the Los Alamos National Laboratory, University of California, Los Alamos, New Mexico 87545

^{13}C NMR of isotopically enriched metabolites has been used to study the metabolism of *Microbacterium ammoniaphilum*, a bacterium which excretes large quantities of L-glutamic acid into the medium. Biosynthesis from 90% [1-^{13}C]glucose results in relatively high specificity of the label, with [2,4-$^{13}C_2$]glutamate as the major product. The predominant biosynthetic pathway for synthesis of glutamate from glucose was determined to be the Embden Meyerhof glycolytic pathway followed by P-enolpyruvate carboxylase and the first third of the Krebs cycle. Different metabolic pathways are associated with different correlations in the enrichment of the carbons, reflected in the spectrum as different ^{13}C-^{13}C scalar multiplet intensities. Hence, intensity and ^{13}C-^{13}C multiplet analysis allows quantitation of the pathways involved. Although blockage of the Krebs cycle at the α-ketoglutarate dehydrogenase step is the basis for the accumulation of glutamate, significant Krebs cycle activity was found in glucose grown cells, and extensive Krebs cycle activity in cells metabolizing [1-^{13}C]acetate. In addition to the observation of the expected metabolites, the disaccharide α,α-trehalose and α,β-glucosylamine were identified from the ^{13}C NMR spectra.

Several varieties of bacteria have been described which utilize glucose or acetate as a sole carbon source and which excrete large quantities of amino acids (1). One of these is *Microbacterium ammoniaphilum*, which has an impaired Krebs cycle due to a reduced activity of the enzyme(s) necessary for processing α-ketoglutarate and its metabolites. It can be induced to excrete L-glutamate late in the growth cycle of cells cultured in media of high nitrogen content at sufficiently low concentrations of biotin that the cells develop altered membranes which allow facile transport of L-glutamate formed by transamination of α-ketoglutarate (2–4). We concluded that these characteristics of *M. ammoniaphilum* made it an excellent potential vehicle for the biosynthesis of L-glutamate selectively labeled with ^{13}C, if it were grown on specifically enriched glucose or acetate as the predominant source of carbon.

Our interest in these systems developed in the continuing program at the Los Alamos National Laboratory on the use of microorganisms and cell-free extracts for the large scale synthesis of natural products, uniformly or specifically labeled with ^{13}C (5). Current work is focused on those L-amino acids for which efficient organic synthesis methods are not now available and for which there is a need either in human metabolic and nutritional studies or in the investigation of the structure and dynamics of proteins enriched with labeled amino acids. In the use of biological systems for the selective enrichment of natural products, there are two prime practical considerations: 1) the optimization of the incorporation of the ^{13}C label from the precursor into the product; and 2) the minimization of the degree to which the label becomes randomized in the product due to the flux of the precursor and its metabolites through various pools. Especially at high levels of enrichment of products for mass spectrometric and nuclear magnetic resonance studies, randomization of the label leads to complications arising from multiple isotope clusters and ^{13}C nuclear spin coupling patterns (6–8).

In this paper we address the latter consideration in a ^{13}C NMR analysis of the flow of ^{13}C label through the Krebs cycle, the phosphogluconate pathway, and the glyoxylate shunt into selectively labeled L-glutamate excreted by *M. ammoniaphilum* grown in media containing [1-^{13}C]glucose or [1-^{13}C]acetate as the predominant carbon source. The work illustrates the general utility of selective, in contrast to random, ^{13}C labeling of natural products biosynthetically. In addition it is of interest because it demonstrates that it is not generally valid to assume in biosynthetic labeling experiments that the label from ^{13}C-enriched precursors will occupy the sites of a natural product in a statistically independent manner.

EXPERIMENTAL PROCEDURES

Materials—[1-^{13}C]Glucose enriched to 90 atom % (9) and [1-^{13}C]acetate (10) enriched to 70 atom % were gifts of V. Kerr and T. Sanchez, respectively, both of the Los Alamos National Laboratory. Corn steep liquor was a gift of Grain Processing Company of Muscatine, IA. Cultures of *M. ammoniaphilum* (ATCC 15354) were obtained from the American Type Culture Collection, Rockville, MD.

Nuclear Magnetic Resonance Spectroscopy—Pulsed ^{13}C NMR spectra were obtained with a Varian XL-100-15 spectrometer (25.2 MHz) interfaced to a Data General SuperNova computer. The spectra were recorded at 25 °C with a spectral width of 5000 Hz and 4096 spectral points. The lock signal was obtained from ~5% D_2O contained in the sample. Spectra of the production media were obtained on the supernatant after removing the cells by centrifugation at 12,000 × *g* for 10 m. The supernatant could then be run directly, appropriately diluted, or concentrated by reducing the pH and evaporating *in vacuo*. Standard samples were dissolved in 0.05 M potassium phosphate buffer and the pH adjusted to 7.5. Proton NMR spectra for

* This work was performed under the auspices of the United States Department of Energy. The proton NMR spectra were obtained at the Colorado State University Regional NMR Center, funded by the National Science Foundation Grant CHE-78-18581. The costs of publication of this article were defrayed in part by the payment of page charges. This article must therefore be hereby marked "*advertisement*" in accordance with 18 U.S.C. Section 1734 solely to indicate this fact.

‡ Recipient of National Institutes of Health Research Grant RR-00962-05 from the Division of Research Resources, Department of Health, Education and Welfare.

D_2O solutions were obtained on a Nicolet spectrometer in the FT mode operating at 360 MHz. ^{13}C chemical shifts were measured with respect to external tetramethyl silane and ^1H shifts with respect to the methyl resonance of internal trimethylsilylpropanesulfonic acid.

^{13}C NMR Spectroscopy of Cell Suspensions—M. ammoniaphilum was grown on a slant of nutrient agar at 30 °C for 3–4 days. One loopfull of the microorganism was precultured in 30 ml of a rich medium containing 5% corn steep liquor, 5% casein, 0.1% $MgSO_4 \cdot 7H_2O$ and 0.1% KH_2PO_4 at pH 7.3 for 24 h at 30 °C in a 500-ml Erlenmeyer flask in a shaker. The fermentation was carried out at 30 °C in a baffled 500-ml Erlenmeyer flask containing 30 or 60 ml in a production medium (pH 7.3) which contained 5% glucose, 1.2% urea, 0.5% KH_2PO_4, 0.1% $MgSO_4 \cdot 7H_2O$, 0.001% $FeSO_4 \cdot 7H_2O$, 0.001% $MnSO_4 \cdot 4H_2O$, biotin (1.5 μg/liter), and a 2% innoculum of the preculture medium.

M. ammoniaphilum cells were grown for 24 h at 300 rpm in an orbital shaker, harvested by centrifugation at 12,000 × *g* for 10 min, washed twice with 0.2% KCl, and suspended in fresh media containing [1-^{13}C]glucose or [1-^{13}C]acetate. Aeration was provided by continuously bubbling a stream of pure oxygen gas through a very thin capillary tube which reached to within 1–2 mm of the bottom of the spinning 12-mm NMR tube. The total volume in the NMR tube was 4 ml to prevent bubbles breaking the surface from disturbing the magnetic field, and to allow for evaporation of sample due to oxygen bubbling. Other details are given in the figure captions. Spectra were continually obtained for 2–3 h increments over a 20-h period, at which time all of the glucose had been consumed and the glutamate level was reasonably stable.

RESULTS

^{13}C and ^1H NMR Spectra—The time dependence of the ^{13}C NMR spectra of a suspension of *M. ammoniaphilum* containing [1-^{13}C]glucose near the stationary phase of growth is summarized in Fig. 1. Since the production of glutamate in large quantities by this microorganism does not begin until that stage is attained (1), the initial growth was accomplished with a natural abundance of glucose to minimize loss of the ^{13}C label. In addition to the expected resonances from ^{13}C-enriched bicarbonate, glutamate, succinate, and lactate, the spectra in Fig. 1 exhibit prominent peaks from two unusual ^{13}C-labeled products which are eventually consumed: trehalose and glucosylamine. The accumulation of trehalose, which presumably functions as a storage carbohydrate, has been observed previously by ^{13}C NMR in growing yeast (11, 12), bacteria (13), and differentiating amoeba cultures (14). To our knowledge, glucosylamine formation in cell culture has not been observed and, at present, we do not know whether its synthesis is under enzyme control and what role it plays in the control of glucose or nitrogen metabolism.[1] The formation of lactate and succinate by *M. ammoniaphilum* depends on the oxygen tension which, for the cultures appropriate to Fig. 1, fell sharply in the later stages of glucose consumption. In fully aerated cultures, the lactate and succinate levels are sharply reduced (Fig. 2). The time dependence of the ^{13}C NMR spectra of the cell-free production media (see "Experimental Procedures") obtained under fully aerobic and partially anaerobic conditions was quantitatively like the spectra of the cell suspensions. This observation, together with the lack of ^{13}C-enriched resonances in the spectra of medium-free packed cells obtained at the end of the metabolism experiments, suggests that the ^{13}C spectra monitored (Figs. 1 and 2) were those of extracellular substrates and metabolites. A qualitative appreciation of the flow of labeled carbon in this system can be obtained from the summary of the time dependence of the intensities of the ^{13}C resonances of the glucose substrate and the ^{13}C-labeled metabolites tabulated in Fig. 3

[1] The appearance of glucosylamine in the ^{13}C NMR spectra of metabolizing cells is not inconsistent with the ease of its formation under a variety of conditions (15–17). In addition, cell-free extracts of *M. ammoniaphilum* will catalyze the formation of α,β-[1-^{13}C,^{15}N] glucosylamine from [1-^{13}C]glucose and [$^{15}N_2$]urea.

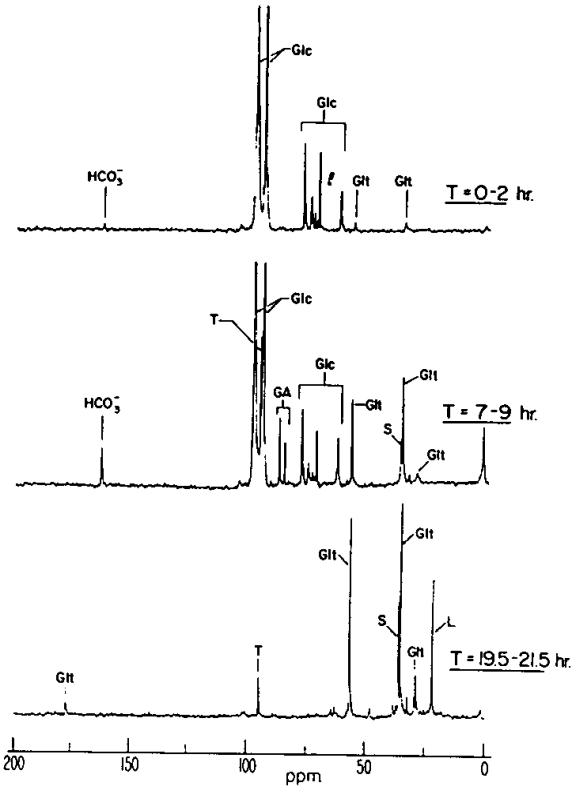

FIG. 1. **Time dependence of the proton-decoupled Fourier transform ^{13}C NMR spectra (25.2 MHz) of a suspension of *M. ammoniaphilum* initially containing [1-^{13}C (90 atom %)]glucose.** *T* = time interval for accumulation of the spectra after transfer of the cells to fresh medium containing [1-^{13}C]glucose (see "Experimental Procedures"). Enriched ^{13}C resonances are: HCO_3^- ion; *Glc*, α and β anomers of [1-^{13}C]glucose; *T*, C-1 of α,α-[1,1′-$^{13}C_2$]trehalose; *Glt*, C-2 (56.0 ppm), C-4 (34.6 ppm), and C-3 (28.3 ppm) of glutamate; *S*, C-2 of succinate; *L*, C-3 of lactate; and *GA*, β- and α- C-1 resonances of glucosylamine. In the *T* = 0–2 h and 7–9 h spectra, the glucose C-1 resonances are truncated and the natural abundance glucose resonances are apparent.

for a particular experiment. The yield of glutamate from labeled glucose in experiments like these typically is 35–40%. The ^{13}C chemical shifts of the metabolites are tabulated in Table I.

The 360 MHz proton NMR spectrum of a solution of [1,2,3,4-$^{13}C_4$]glutamate derived from *M. ammoniaphilum* grown on [1-^{13}C]glucose is shown in Fig. 4*A*. Despite the high level of ^{13}C incorporation demonstrated by the proton spectrum, the C-2 and C-4 resonances in the ^{13}C spectrum are predominantly singlets (Fig. 4*B*), suggesting that the ^{13}C label is introduced into specific sites (C-2, C-4) with a minimum of scrambling to other sites. This site specificity is even greater in the early production phase of glutamate. A plot of the intensity ratio of C-3 to C-4 *versus* time is presented in Fig. 5, which shows that C-3 is more highly labeled at later times. An even higher degree of site-specific incorporation is illustrated in Fig. 6, which is a reproduction of the ^{13}C NMR spectrum of a solution of [1,5-$^{13}C_2$]glutamate obtained from *M. ammoniaphilum* grown on [1-^{13}C]acetate.

Major Metabolic Pathways in M. ammoniaphilum—The metabolic pathways of *M. ammoniaphilum* have been established primarily through ^{14}C labeling studies carried out by Shiio and co-workers (Fig. 7). A glucose carbon source is metabolized primarily via the Embden Meyerhof pathway to phosphoenolpyruvate and pyruvate (18, 19). Accumulation of

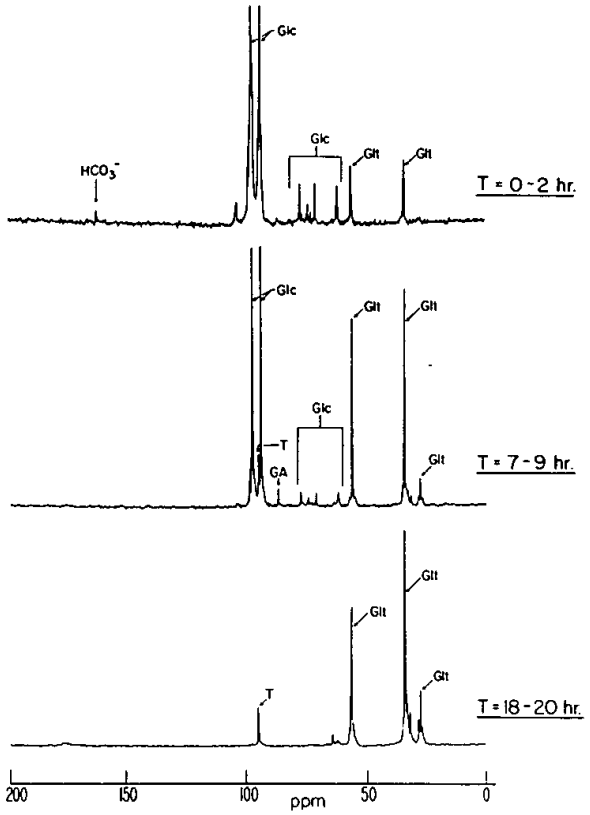

FIG. 2. **Time dependence of the proton-decoupled ^{13}C NMR spectra of a fully aerated suspension of *M. ammoniaphilum* grown on [1-^{13}C (90 atom %)]glucose.** See Fig. 1 legend.

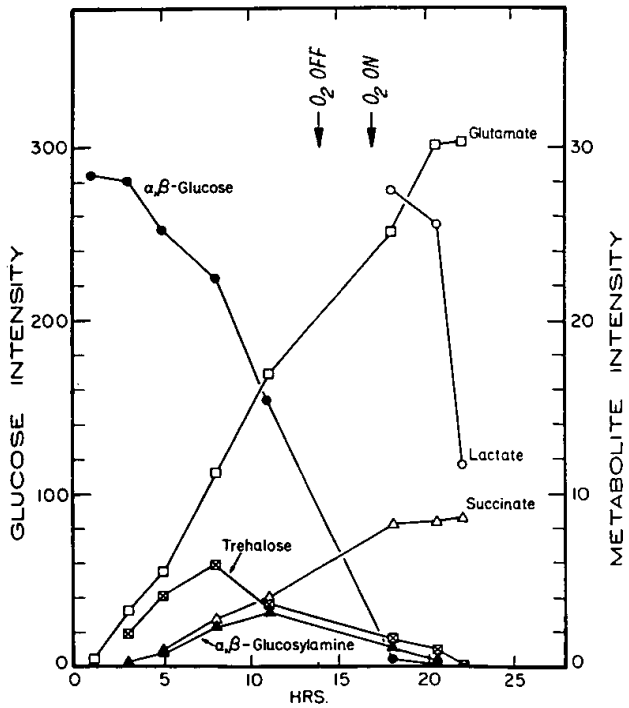

FIG. 3. **Time dependence of the intensities of the ^{13}C resonances of the enriched glucose substrate and the metabolites identified in Fig. 1.** See text also.

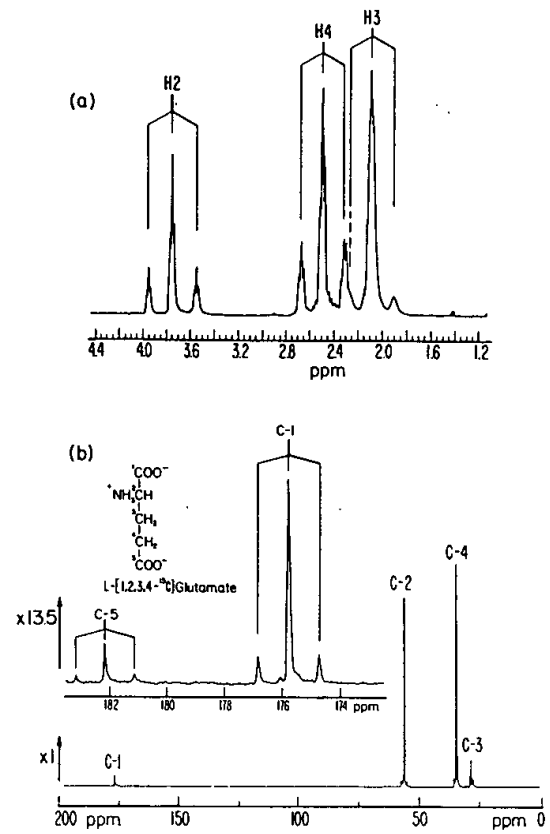

FIG. 4. **Proton NMR and proton-decoupled ^{13}C NMR spectra of [1,2,3,4-$^{13}C_4$]glutamate.** *a*, proton NMR spectrum (360 MHz) of [1,2,3,4-$^{13}C_4$]glutamate derived from *M. ammoniaphilum* grown on [1-^{13}C (90 atom %)]glucose. For each proton, the center of the multiplet arises from ^{12}C-H moieties with fine structure caused by H-H scalar interactions. The doublets with similar fine structure are due to the ^{13}C-H splitting from moieties containing the ^{13}C label. The ^{13}C populations calculated from the ratio of the doublet to the singlet intensities are: C-2, 34%; C-4, 39%; and C-3, 14%. *b*, proton-decoupled ^{13}C NMR spectrum (25.2 MHz) of [1,2,3,4-$^{13}C_4$]glutamate derived from *M. ammoniaphilum* grown on [1-^{13}C (90 atom %)]glucose. The spectrum illustrates the nonrandom distribution of the ^{13}C label among the C-2, C-3, and C-4 sites. If the label were distributed randomly with the ^{13}C abundances derived from the spectra in B, then, for example, the C-1 and C-5 signals should consist of approximate 1:2:1 multiplets.

glutamate is due primarily to the reduced activity of α-ketoglutarate dehydrogenase (20) which, in effect, shuts down the Krebs cycle. As a result, α-ketoglutarate levels are elevated and, in the presence of sufficient ammonia, glutamate levels will consequently become elevated. Excretion of glutamate into the medium is found to be dependent on growth on limiting biotin levels (2, 3); the effect of the biotin is related to the production of faulty, "leaky" membranes which permit this excretion (21).

As is apparent from Fig. 7, several pathways connecting glucose to glutamate are available to the organism. The shortest pathway for direct conversion follows the glycolytic degradation of glucose to pyruvate and phosphoenolpyruvate, formation of acetyl CoA and oxaloacetate via decarboxylation and carboxylation, respectively, and the first third of the Krebs cycle which combines the oxaloacetate and acetyl CoA to yield citrate and, subsequently, α-ketoglutarate. On the basis of this pathway, the glutamate ^{13}C-labeling pattern resulting from any initial glucose ^{13}C-labeling pattern is readily determined: [1-^{13}C]glucose leads to the synthesis of [3-^{13}C]

TABLE I

^{13}C NMR chemical shifts of metabolites

Samples were dissolved in water or 0.05 M phosphate buffer, pH ~7 to 7.5, 25 °C.

Compound	Chemical shift					
	C-1	C-2	C-3	C-4	C-5	C-6
α-D-Glucose	93.2	72.5	73.9	70.7	72.5	61.7
β-D-Glucose	97.0	75.3	76.9	70.7	76.9	61.8
α,α-Trehalose[a]	94.2	73.2	73.7	70.8	72.2	61.7
α-D-Glucosylamine[b]	84.2					
β-D-Glucosylamine[b]	86.2					
L-Glutamate	175.8	55.8	28.3	34.6	182.2	
L-Glutamine	175.0	55.4	27.5	32.0	178.5	
L-Lactate	183.4	69.7	21.3			
Succinate	183.3	35.3	35.3	183.3		

[a] Assignments are from Ref. 14.

[b] Shifts for α,β-glucosylamine C-2 through C-6 were not observed.

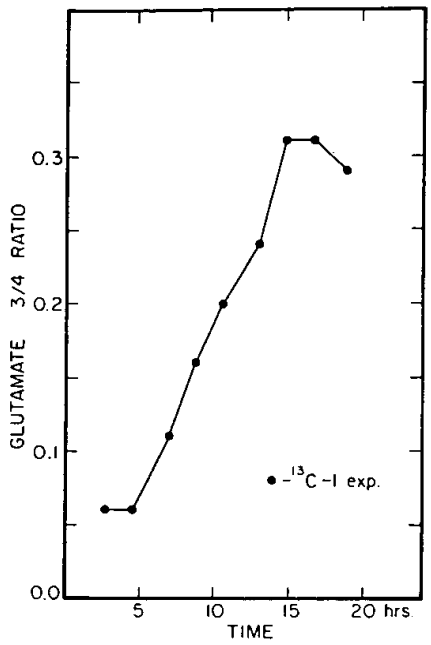

FIG. 5. **Time-dependent ratio of C-3 to C-4 intensities in [^{13}C] glutamate.** Data were taken from the ^{13}C NMR spectra of the experiment depicted in Fig. 2.

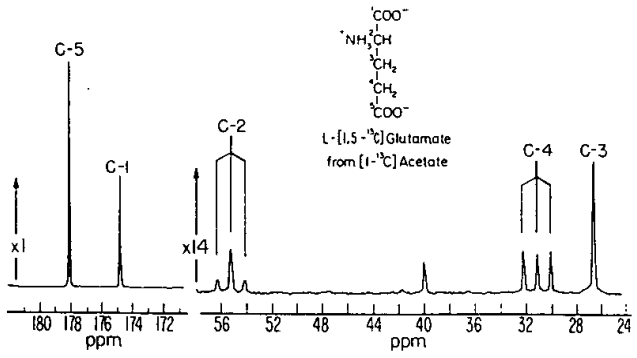

FIG. 6. **Proton-decoupled ^{13}C NMR (25.2 MHz) spectrum of [1,5-$^{13}C_2$]glutamate obtained from *M. ammoniaphilum* grown on [1-^{13}C (70 atom %)]acetate.** The cells were grown on natural abundance glucose for 24 h and then transferred to the medium containing [1-^{13}C]acetate and cultured for an additional 96 h. Only C-1 and C-5 are labeled. From the multiplet to singlet intensities of C-4, the ^{13}C enrichment at C-5 is calculated to be 70 atom %. From the corresponding intensities for the C-2 resonance, the ^{13}C enrichment at C-1 is calculated to be 35 atom %.

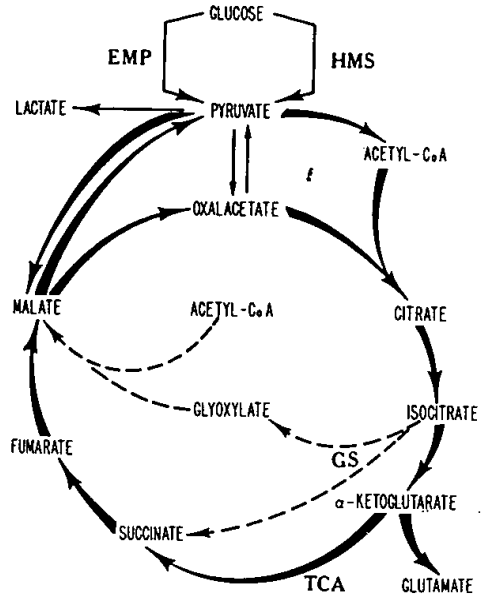

FIG. 7. **Major metabolic pathways in *M. ammoniaphilum* involving glucose, acetate, and glutamate.** Glucose labeled at C-1 produces [3-^{13}C]pyruvate via the Embden-Meyerhof pathway (*EMP*) and unlabeled pyruvate via the hexose monophosphate shunt (*HMS*). [3-^{13}C]Pyruvate enters the tricarboxylic acid (*TCA*) and glyoxylate shunt (*GS*) cycles as [3-^{13}C]oxaloacetate and/or [2-^{13}C] acetate, and can result in the formation of [2-^{13}C]glutamate, [4-^{13}C] glutamate, and [2,4-^{13}C]glutamate via α-ketoglutarate formed in a third of a turn of the TCA cycle. Formation of glutamate after one or more turns of the TCA cycle will tend to randomize the label because of the formation of the symmetrical intermediates, succinate and fumarate. Similar scrambling will occur through the flow of citrate through the glyoxylate cycle.

pyruvate and [2-^{13}C]acetate and, consequently, to [2,4-$^{13}C_2$]-labeled glutamate. Reference to Fig. 4 for the glutamate released into the medium indicates a pattern which is substantially in agreement with this prediction, supporting this as the predominant route of glutamate synthesis from glucose.

As is apparent from Fig. 7, the pathway summarized above is not the only route of glutamate synthesis, and the importance of other pathways is suggested by deviations from the above pattern, *e.g.* labeling of C-1 and C-3 of glutamate, which also occurs to a limited extent. In the following section, we consider the general approach of estimating the contributions of alternative pathways from the available NMR data.

Quantitative NMR Analysis of Metabolic Pathways—Quantitation of the ^{13}C population at specific sites in multiply labeled molecules requires the accurate evaluation of the ratios of singlet-to-multiplet intensities in both ^{1}H and ^{13}C NMR spectra. This is usually a straightforward task, but it must be recognized that the satellite resonances can exhibit different T_1 and/or nuclear Overhauser effect values than the center resonance. The differential T_1 effect in ^{1}H NMR spectra can be quite significant. For example, a center band (^{12}C-*H*) to satellite (^{13}C-*H*) ^{1}H T_1 ratio greater than 4 has been observed for a ^{13}C-enriched sugar methine proton (22). In such cases, the pulse delay must be sufficiently long that the center band is not overpulsed. A similar, but smaller effect occurs in the ^{13}C NMR spectra of enriched molecules. Although the ^{13}C-^{13}C dipolar interaction is negligible, relative to the ^{13}C-H dipolar interaction for proton bearing carbon atoms (23), the former interaction can be large for quaternary carbons and lead to significant differences in the satellite (^{13}C-^{13}C) and center band (^{13}C-^{12}C) T_1 values. Again, if the pulse delay is not long enough, the intensity of the center band will be

underestimated due to overpulsing. Another related potential source of error in the analysis of ^{13}C multiplet intensities of quaternary carbon atoms is a reduction in the nuclear Overhauser effect value due to ^{13}C-^{13}C dipolar interactions and which leads to a reduction in the satellite (^{13}C-^{13}C)/center band (^{13}C-^{12}C) intensity ratio (7). In the evaluation of the relative intensities of the multiplets discussed in the following, these potential problems have been avoided.

The satellite-to-center band intensities, in the ^1H NMR spectrum (Fig. 4*a*) of the L-[1,2,3,4-$^{13}C_4$]glutamate derived from *M. ammoniaphilum* grown on [1-^{13}C]glucose, directly give the *total* ^{13}C enrichment of C-2 (34 atom %), C-4 (39 atom %), and C-3 (14 atom %). Although the relative *total* integrated intensities of the ^{13}C resonances of C-2, C-3, and C-4 are consistent with these enrichments, this high level of enrichment is not reflected in the ^{13}C-^{13}C multiplets in the ^{13}C NMR spectrum (Fig. 4*b*), as noted previously. The *apparent* discrepancy arises from the presence of ^{13}C isotopomers (*e.g.* $^{13}C_4{}^{12}C_3{}^{13}C_2$ and $^{12}C_4{}^{13}C_3{}^{13}C_2$), in which there is a high degree of negative correlation in the ^{13}C labeling that does not affect the proton spectrum, but has a major influence on the appearance of ^{13}C multiplets. For example, the C-2 enrichment obtained from the H-2 satellites is 34 atom %, whereas the *apparent* enrichment calculated from the C-1 satellites (Fig. 4*b*) is only 25 atom %. This apparent discrepancy can be explained by a negatively correlated labeling of C-1 and C-2: [3-^{13}C]oxaloacetate forms [2-^{13}C]glutamate via a ⅓ turn of the Krebs cycle, whereas in a single turn of the Krebs cycle, [4-^{13}C]oxaloacetate is formed which can be the precursor for [1-^{13}C]glutamate. Note that these reactions will not introduce label into C-1 and C-2 in the *same* molecule.

Having the absolute ^{13}C enrichments from the ^1H NMR spectra and the multiplet intensities from the ^{13}C NMR spectra, one can use several approaches to interpret the data *quantitatively*, on the basis of the metabolic pathways operative. In the present study, we have used the method of mixtures with the essential elements summarized below.

1) Variables are assigned to each alternative path with the sum normalized to 1.0. 2) a labeling pattern is associated with each path, based on the biochemical pathways expected. 3) a table is formulated in which the various possible labeled species resulting from each pathway are included. 4) from the above table, a second table giving the carbon enrichments and multiplet probabilities can be constructed and then compared with the data for quantitation.

The mixture analysis is most simply illustrated for the quantitation of the two competing pathways for glucose degradation. 1) the dominant Embden Meyerhof pathway, and 2) the hexose monophosphate shunt. We assign a probability f to the former pathway and $1 - f$ to the latter. If the labeling probability of the starting material [1-^{13}C]glucose is designated α_i, the labeling probability of pyruvate C-3 or the acetyl-CoA produced by pyruvate decarboxylation will be $\alpha_i/2$ due to the formation of two trioses via this pathway. The labeling of acetyl-CoA via pathway (2) will be zero since the label is removed as CO_2. Although the labelings of pyruvate or acetyl-CoA derived from pyruvate are not directly observed, analysis of the various biosynthetic pathways indicates that regardless of the particular path, glutamate C-4 is always labeled from C-2 of acetyl-CoA and so provides a direct measure of this pool. If the C-4 enrichment observed from the ^1H spectrum (Fig. 4*a*) is α_0, we have

$$f\cdot(\alpha_i/2) + (1 - f)\cdot 0 = \alpha_0 \qquad (1)$$

For the present study, $\alpha_i = 90\%$, $\alpha_0 = 39\%$, giving $f = 87\%$, or 13%, of the glucose is metabolized via the hexose monophosphate shunt.

Quantitation of the glyoxylate and Krebs cycle activities can be approached as above using a mixture analysis, although the case is somewhat more complex. Table II summarizes the important labeling pathways and the labeling patterns which result. As indicated in the table, several compromises have been made in the analysis since in some cases different labeling paths can result in identical labeling patterns and thus cannot be distinguished. In addition, a small quantity of the labeling patterns indicated under w and y can also be produced after

TABLE II

Possible labeling patterns for C-2, C-3, and C-4 of [^{13}C]glutamate derived from [1-^{13}C]glucose

Pathway designation	Labeling pattern[a]	Source of label	Pathway
			%
x	$^{0}C_1$-$^{*}C_2$-$^{*}C_3$-$^{*}C_4$	Phosphoenolpyruvate carboxylase + ⅓ Krebs cycle	58
y	$^{*}C_1$-$^{*}C_2$-$^{*}C_3$-$^{*}C_4$ $^{*}C_1$-$^{*}C_2$-$^{*}C_3$-$^{*}C_4$	Fumarase activity plus single turn of glyoxylate cycle	26
z	$^{*}C_1$-$^{*}C_2$-$^{*}C_3$-$^{*}C_4$	Multiple turns of Krebs or glyoxylate cycles	10
w	$^{*}C_1$-$^{*}C_2$-$^{*}C_3$-$^{*}C_4$	Single turn	
	$^{*}C_1$-$^{*}C_2$-$^{*}C_3$-$^{*}C_4$	Krebs cycle	6

[a] Asterisk (*) indicates a labeling probability α derived from the enriched pyruvate pool. Zero (^{0}) indicates a labeling probability β derived from the enrichment of the bicarbonate pool.

TABLE III

Glutamate labeling and multiplet probabilities

	Analytical expressions
Enrichments	
C-1	$x\beta + (z + w/2)\cdot\alpha$
C-2	$(x + y/2 + w/2)\cdot\alpha$
C-3	$(y/2 + z + w/2)\cdot\alpha$
C-4	$(x + y + z + w)\cdot\alpha = \alpha$
Multiplets	
C-1(doublet/singlet)	$(x\beta\alpha + z\alpha^2)/\left(x\beta(1-\alpha) + z\alpha(1-\alpha) + \frac{w}{2}\alpha\right)$
C-2(doublet/singlet)[a]	$[x\alpha\beta + 2z\alpha^2(1-\alpha)]/\left(x\alpha(1-\beta) + \frac{y}{2}\alpha + z\alpha(1-\alpha)^2 + \frac{w}{2}\alpha\right)$
C-2(quartet/singlet)[b]	$z\alpha^3/\left[x\alpha(1-\beta) + \frac{y}{2}\alpha + z\alpha(1-\alpha)^2 + \frac{w}{2}\alpha\right]$
C-3(doublet/singlet)	$\left[\frac{y}{2}\alpha^2 + 2z\alpha^2(1-\alpha) + \frac{w}{2}\alpha^2\right]\Big/\left[\frac{y}{2}\alpha(1-\alpha) + z\alpha(1-\alpha)^2 + \frac{w}{2}\alpha(1-\alpha)\right]$
C-3(triplet/singlet)	$z\alpha^3/\left[\frac{y}{2}\alpha(1-\alpha) + z\alpha(1-\alpha)^2 + \frac{w}{2}\alpha(1-\alpha)\right]$
C-4(doublet/singlet)	$\left(\frac{y}{2} + z + \frac{w}{2}\right)\alpha^2/\left[x\alpha + y\alpha\left(1 - \frac{\alpha}{2}\right) + z\alpha(1-\alpha) + w\alpha\left(1 - \frac{\alpha}{2}\right)\right]$

[a] Represents total doublet intensity, although two separate doublets are resolvable due to different J_{12} and J_{23} values.

[b] Quartet since $J_{12} \neq J_{23}$.

additional turns of the Krebs and glyoxylate cycles. Nevertheless, the approach summarized represents a reasonable approximation for quantitative pathway analysis. Since spectral inspection (Fig. 4*b*) indicates that the number of multiply enriched molecules (z) is small, these approximations are probably fairly good. As can be seen from the table, negative correlations of the labeling of C-2 and C-3 can result from the Krebs or glyoxylate cycle, or from back reactions which reach fumarase. Krebs cycle activity will also result in a negative correlation between C-1 and C-2 labeling. Analytical expressions for carbon labeling and relative multiplet probabilities can be derived in a straightforward manner, and the results are summarized in Table III. Using these expressions and the value of $\alpha_0 = 0.39$ and the relative multiplet intensities in the ^{13}C spectrum (Fig. 4*b*), values of 58, 26, 10 and 6% are obtained for x, y, z, and w, respectively. The relative contribution of these pathways should result in ^{13}C populations at C-2 and C-3 of 33 and 10%, respectively, in good agreement with those obtained directly from the ^1H NMR spectrum (Fig. 4*a*).

We were unable to grow *M. ammoniaphilum* on acetate as the sole carbon source; however, cells grown on unlabeled glucose were washed and incubated with [1-^{13}C]acetate. A ^{13}C NMR spectrum of the extracted glutamate is shown in Fig. 6. The primary features of this spectrum are the labeling ratio of 2:1 for C-5:C-1 and the absence of label for C-2, C-3, and C-4. These observations parallel the ^{14}C observations (24) on the glutamate labeling patterns obtained with another glutamate producer, *Brevibacterium flavum.*

DISCUSSION

Activity of the Hexose Monophosphate Shunt—The determination that 13% of the glucose metabolized by *M. ammoniaphilum* occurs via the hexose monophosphate shunt agrees well with the 10% value determined by analysis of the pyruvate carboxyl group in metabolically blocked cells (18, 19). The result is significantly lower than the 25% figure determined by recovering $^{14}CO_2$ from [1-^{14}C]- and [6-^{14}C]glucose-grown cells. There is a variety of approximations inherent in both approaches (25). In particular, the hexose monophosphate pathway may be somewhat underestimated since some of the pentose produced via this path will be used for nucleotide synthesis, rather than for production of pyruvate.

Activities of the Krebs and Glyoxylate Cycles in the Metabolism of [1-^{13}C]Glucose—The major metabolic routes found for the degradation of glucose involve glycolysis to pyruvate and phosphoenolpyruvate, formation of acetyl-CoA and oxaloacetate via decarboxylation and carboxylation, respectively, and the first third of the Krebs cycle to yield α-ketoglutarate and, subsequently, glutamate. Significant activity of the glyoxylate shunt is required to explain the C-3 labeling and reduced C-2 labeling of glutamate. The observed Krebs cycle activity was initially unexpected since this cycle is presumably shut down due to the reduction of α-ketoglutarate dehydrogenase activity. Evidence for the activity of this cycle comes primarily from the observed negative correlation in the labeling of C-1 and C-2 of glutamate.

The time dependence of the ^{13}C NMR spectra (Fig. 2) and the time-dependent increase in the C-3/C-4 intensity ratio (Fig. 5) is particularly interesting. Since the C-4 enrichment level is constant ($\alpha_0 = 0.39$), this time-dependent ratio reflects a time-dependent increase in the relative contributions of the y, z, and/or w pathways. Although, in principle, it is possible to quantitate these as a function of time, there are several problems with this approach in practice. 1) the spectra correspond to cumulative pools of glutamate and therefore reflect cumulative average pathways; 2) ^1H NMR spectra of purified glutamate in parallel with the ^{13}C data were not obtained; 3) the signal/noise in the 2-h spectra was insufficient to permit analysis of the C-1 multiplet, which is of value for the demonstration of Krebs cycle activity. In view of these problems, a simplified approach was taken in which the glyoxylate and Krebs cycle activities were both represented by y since it becomes impossible to distinguish between y and w in the absence of C-1 data. Based on this analysis, the cumulative contribution from the y pathway increases from ~0 to a steady state value of ~35%, with z increasing to ~12% and x decreasing to a value of ~53%. This increased cycling may reflect the decreasing glucose concentration which might release the inhibition of enzymes in both the glyoxylate and Krebs cycles, *i.e.* the time-dependent changes may reflect catabolite repression. A similar time-dependent result was recently reported in a study of the glutamate derived from rat hearts perfused with [2-^{13}C]acetate (26).

Another interesting result is that the ^{13}C spectra show that the labeling at C-4 also appears to show a negative correlation with C-5. On the surface, there is no immediately obvious route for C-5 to be labeled, and one would expect C-5 to be at natural abundance regardless of the labeling at C-4. Instead, the analysis of the doublet center band intensities at C-5 leads to an enrichment of 32 atom % ^{13}C at C-4, compared to the higher value of 39 atom % obtained by the ^1H satellites. This apparent discrepancy can be explained using the following pathway in which oxaloacetate breaks down to acetyl-CoA, which leads to an anticorrelated (*vis a vis* C-4) C-5 enrichment of glutamate (Structure 1).

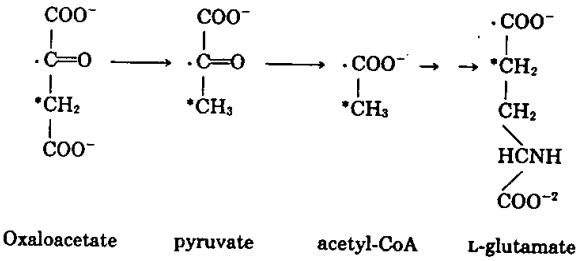

STRUCTURE 1

The amount by which the acetyl-CoA pool is diluted with material derived from the oxaloacetate pool can be calculated from Equation 2.

$$D/S = \frac{(1-f)z\alpha^2 + f\alpha\gamma}{(1-f)\left[\left(\frac{y+w}{2}\right)\alpha + z\alpha(1-\alpha)\right] + f\gamma(1-\alpha)} \quad (2)$$

where D/S is the doublet to singlet ratio for ^{13}C-5, f is the fraction of acetyl-CoA derived directly from glucose, $1-f$ the fraction of acetyl-CoA derived from oxaloacetate, α, y, z, and w are as defined in Table II, and γ is the natural abundance ^{13}C level for C-5. Solving this equation for f from the data in Table II gives a value of ~96%, suggesting that only ~4% of the acetyl-CoA pool is derived from oxaloacetate. Finally, given f, one can calculate the enrichment at C-5 from Equation 3.

$$\%\ ^{13}C\text{-}5 \approx f\gamma + \alpha(1-f)(y/2 + w/2 + z) \quad (3)$$

This value cannot be directly measured from the data, but a value of 1.8% ^{13}C can be obtained from Equation 3. Using a different approach, one can also calculate the enrichment at C-5 from the apparent enrichment at C-4 using the C-5 multiplets and the actual enrichment at C-4 using the proton data. The discrepancy between these two values and the known distribution of label between the C-5 doublet and singlet from the amount of negatively correlated labeling at C-2 and C-3 of oxaloacetate, allow one to calculate an enrich-

ment of 1.7% at C-5, in excellent agreement with the value determined from Equation 3.

Metabolism of [1-^{13}C]Acetate—In principle, it is possible to explain the 1:2 ratio for the C-1/C-5 labeling of glutamate derived from [1-^{13}C]acetate on the basis of a contribution of the unlabeled metabolites initially present in the cell, which would dilute the C-1 label to a greater extent than C-5. However, this explanation proves inadequate since the concentration of initial unlabeled metabolites is far less than would be necessary to produce the observed difference. Thus, the labeling difference must reflect a steady state phenomenon in which the C-1 label is systematically diluted. This conclusion can be made more convincingly in the case of *B. flavum*, in which acetate can be used as the sole carbon source, eliminating the possible complication of an initial pool of unlabeled metabolites.

A steady state analysis of the acetate labeling experiments indicates that the data can be explained on the basis of significant Krebs cycle activity. This reflects the fact that only half of the C-1 carbons processed through the w pathway become labeled (Table II). The possibility of high Krebs cycle activity as an explanation for similar carbon-14 acetate growth results was considered by Shiio and Tsunoda (24), but subsequently rejected on the basis of the demonstrated inhibition of this cycle under glucose growth conditions. The alternative possibility of two acetate pools was proposed. In view of our demonstration of the existence of Krebs cycle activity in the glucose growth experiment, the possibility of increased activity on acetate medium seems reasonable. In contrast, the possibility of two acetate pools for a prokaryotic cell seems less likely. We thus conclude that, as in the apparent time-dependent nature of the labeling, differences in carbon source may also have a significant effect on the relative contributions of the different pathways, possibly reflecting catabolite repression.

Acknowledgments—We gratefully acknowledge the technical assistance of W. E. Wageman and several helpful discussions with Dr. David LeMaster.

REFERENCES

1. Yamada, K., Kinoshita, S., Tsunoda, T., and Aida, K. (eds) (1972) *The Microbial Production of Amino Acids*, pp. 3–537, Halsted Press, New York
2. Shiio, I., Otsuka, S., and Katsuya, N. (1963) *J. Biochem.* (*Tokyo*) **53**, 333–340
3. Otsuka, S., Miyajimay, R., and Shiio, I. (1965) *J. Gen. Appl. Microbiol.* **11**, 295–301
4. Kimura, K. (1963) *J. Gen. Appl. Microbiol.* **9**, 205–212
5. Kollman, V. H., Hanners, J. L., London, R. E., Adame, E. G., and Walker, T. E. (1979) *Carbohydr. Res.* **73**, 193–202
6. London, R. E., Kollman, V. H., and Matwiyoff, N. A. (1975) *J. Am. Chem. Soc.* **97**, 3565–3573
7. London, R. E., Matwiyoff, N. A., Kollman, V. H., and Mueller, D. D. (1975) *J. Magn. Reson.* **18**, 555–557
8. Tran-Dinh, S., Fermandjian, S., Sala, E., Mermet-Bouvier, R., Cohen, M., and Formageot, P. (1974) *J. Am. Chem. Soc.* **96**, 1484–1493
9. Serianni, A. S., Nunez, H. A., and Barker, R. (1979) *Carbohydr. Res.* **72**, 71–78
10. Ott, D. G., and Kerr, V. N. (1976) *J. Labelled Compd. Radiopharm.* **12**, 119–125
11. Eakin, R. T., Morgan, L. O., Gregg, C. T., and Matwiyoff, N. A. (1972) *FEBS Lett.* **28**, 259–264
12. Kainosho, M., Ajisaka, K., and Nakazawa, H. (1977) *FEBS Lett.* **80**, 385–389
13. Burton, G., Baxter, R. L., Gunn, J. M., Sidebottom, P. J., Fagerness, P. E., Shishido, K., Lee, J. Y., and Scott, A. I. (1980) *Can. J. Chem.* **85**, 1839–1846
14. Deslauriers, R., Jarrell, H. C., Byrd, R. A., Smith, I. C. P. (1980) *FEBS Lett.* **118**, 185–190
15. Kort, M. J. (1970) *Adv. Carbohydr. Chem. Biochem.* **25**, 311–349
16. Isbell, H. S., and Frush, H. L. (1951) *J. Res. Natl. Bur. Standards* **46**, 132–144
17. Isbell, H. S., and Frush, H. L. (1951) *J. Res. Natl. Bur. Standards* **47**, 239–247
18. Shiio, I., Otsuka, S., and Tsunoda, T. (1960) *J. Biochem.* (*Tokyo*) **47**, 414–421
19. Shiio, I., Otsuka, S., and Tsunoda, T. (1960) *J. Biochem.* (*Tokyo*) **48**, 110–120
20. Shiio, I., Otsuka, S., and Takahashi, M. (1961) *J. Biochem.* (*Tokyo*) **50**, 164–165
21. Otsuka, S., and Shiio, I. (1968) *J. Gen. Appl. Microbiol.* **14**, 135–146
22. London, R. E., Walker, T. E., Kollman, V. H., and Matwiyoff, N. A. (1977) *J. Magn. Reson.* **26**, 213–218
23. Moreland, C. G., and Carroll, F. I. (1974) *J. Magn. Reson.* **15**, 596–599
24. Shiio, I., and Tsunoda, T. (1961) *J. Biochem.* (*Tokyo*) **49**, 141–147
25. Cheldelin, V. H. (1961) *Metabolic Pathways in Microorganisms*, pp. 1–89, John Wiley & Sons, New York
26. Bailey, I. A., Gadian, D. G., Matthews, P. M., Radda, G. K., and Seeley, P. J. (1981) *FEBS Lett.* **123**, 315–318

FEBRUARY 10, 1982 VOLUME 257 NUMBER 3

ISSN 0021-9258
JBCHA3 257(3) 1107-1563 (1982)

THE Journal of Biological Chemistry

Published by The American Society of Biological Chemists, Inc.

FOUNDED BY CHRISTIAN A. HERTER

AND SUSTAINED IN PART BY THE CHRISTIAN A. HERTER MEMORIAL FUND

VOLUME 14 NUMBER 5 • MAY 1996

nature biotechnology

FORMERLY BIO/TECHNOLOGY

Terminating chromosome elongation

Lighting up gene transfer

A yeast screen for functional antagonists

Biotechnology: A $30 billion dollar enterprise?

Vaccine approval times

D t rmination of th Flux s in the C ntral M tabolism of *Corynebacterium glutamicum* by Nuclear Magnetic R sonanc Sp ctroscopy Combined with M tabolit Balancing

Doc. Ref. AT2
Appl. No. To be assigned

Achim Marx, Albert A. de Graaf,* Wolfgang Wiechert, Lothar Eggeling, and Hermann Sahm
Institut für Biotechnologie, Forschungszentrum Jülich GmbH D-52425, Jülich, Germany

Received March 28, 1995/Accepted August 8, 1995

To determine the in vivo fluxes of the central metabolism we have developed a comprehensive approach exclusively based on the fundamental enzyme reactions known to be present, the fate of the carbon atoms of individual reactions, and the metabolite balance of the culture. No information on the energy balance is required, nor information on enzyme activities, or the directionalities of reactions. Our approach combines the power of ^{1}H-detected ^{13}C nuclear magnetic resonance spectroscopy to follow individual carbons with the simplicity of establishing carbon balances of bacterial cultures. We grew a lysine-producing strain of *Corynebacterium glutamicum* to the metabolic and isotopic steady state with [1-^{13}C]glucose and determined the fractional enrichments in 27 carbon atoms of 11 amino acids isolated from the cell. Since precursor metabolites of the central metabolism are incorporated in an exactly defined manner in the carbon skeleton of amino acids, the fractional enrichments in carbons of precursor metabolites (oxaloacetate, glyceraldehyde 3-phosphate, erythrose 4-phosphate, etc.) became directly accessible. A concise and generally applicable mathematical model was established using matrix calculus to express all metabolite mass and carbon labeling balances. An appropriate all-purpose software for the iterative solution of the equations is supplied. Applying this comprehensive methodology to *C. glutamicum,* all major fluxes within the central metabolism were determined. The result is that the flux through the pentose phosphate pathway is 66.4% (relative to the glucose input flux of 1.49 mmol/g dry weight h), that of entry into the tricarboxylic acid cycle 62.2%, and the contribution of the succinylase pathway of lysine synthesis 13.7%. Due to the large amount and high quality of measured data in vivo exchange reactions could also be quantitated with particularly high exchange rates within the pentose phosphate pathway for the ribose 5-phosphate transketolase reaction. Moreover, the total net flux of the anaplerotic reactions was quantitated as 38.0%. Most importantly, we found that in vivo one component within these anaplerotic reactions is a back flux from the carbon 4 units of the tricarboxylic acid cycle to the carbon 3 units of glycolysis of 30.6%.
Key words: intracellular fluxes • metabolite balance • carbon labeling balance • lysine • anaplerotic reactions • NMR spectroscopy

INTRODUCTION

Amino acid production has a long tradition in biotechnology. In particular, the bacterium *Corynebacterium glutamicum* as well as mutants derived from this species are of industrial interest for the production of L-lysine and L-glutamate.[24,29] Currently, enzymatic and genetic analysis of this species is mostly directed to a single reaction[6,15,34,45] or to a very limited set of reactions.[7,39] However, the effective implementation of any targeted genetic engineering of such overproducers requires a basic understanding of the central metabolism as a whole. Therefore, it is imperative to quantify the actual fluxes in vivo through all the reactions of the central metabolism. Unfortunately, experimental access to these reactions in particular (e.g., citrate synthase) is difficult to achieve in vivo.

One useful approach which has very recently attracted great attention is metabolite balancing.[8,32,53] Flux estimations are obtained using measurements of substrate consumption and product formation, while taking into account the known demands of precursor metabolites for cellular growth (oxaloacetate, pyruvate, α-ketoglutarate, etc.). This approach can be well suited for particular purposes, i.e., when only specific pathways need to be considered[53,60] or if the contribution of flux for cellular growth is weak, as with hybridoma cells[49,65] and entire organs.[21] However, in the more complex bacterial systems, where product formation often occurs simultaneously with growth and the consequent use of the entire set of metabolic pathways is required, the large number of branching points in the metabolic network usually prevents a detailed analysis.[43] In such cases, the application of metabolite balancing either requires sets of reactions to be lumped together[59] or forces the

* To whom all correspondence should be addressed.

CCC 0006-3592/96/020111-19

use of data from in vitro enzyme assays to answer such an important question as, for instance, that on the in vivo use of the glyoxylate cycle. Moreover, additional assumptions on the energy balance of the cell have to be included, thus leading to further uncertainties.[23,31]

Therefore, additional experimental data are required to establish a reliable stationary flux analysis. Isotopic tracer experiments are a prominent candidate for such a purpose. This technique is well established for differentiating between the relative use of two pathways, such as between the pentose phosphate pathway and glycolysis.[18,63] The use of ^{13}C-labeled substrate combined with nuclear magnetic resonance (NMR) spectroscopy is particularly instrumental, since the isotopic labeling of individual carbons is directly accessible. As an example, the measured incorporation of label from [1-^{13}C]glucose into L-glutamate derived from the precursor metabolite α-ketoglutarate was proof of an in vivo activity of the tricarboxylic acid (TCA) cycle in a *Corynebacterium* strain,[60] where previous in vitro studies had suggested that it was inactive.[50] In a similar approach, the quantification of glyoxylate cycle and TCA cycle usage was possible.[61] We used ^{13}C NMR to determine the fractional enrichments in carbons of L-alanine (derived from pyruvate) and L-lysine (derived from pyruvate and oxaloacetate) produced by *C. glutamicum*.[52] This enabled us to quantitate the relative use of the two competing pathways of L-lysine synthesis present in this bacterium. The data indicated that about three-quarters of the total flux of L-lysine occurs in vivo through the succinylase variant, although the activities of the enzymes involved are about 10 times less than that of the competing dehydrogenase variant. This once more illustrates the power of the NMR technique and presents a case where including information from in vitro analyses to decide on in vivo fluxes clearly would be invalid.

The aim of the present study was to provide basic quantitative information on the in vivo fluxes of as many reactions in the central metabolism of *C. glutamicum* as possible. We chose an L-lysine producer of *C. glutamicum* for flux analysis, which has high productivity in batch culture,[45] is very well characterized with respect to its genetic situation,[7,33] and for which data on its flux characteristics already exist.[52] In addition, information is also available on other L-lysine-secreting strains of *C. glutamicum*.[15,18,29,53]

Here we present and apply an experimental methodology to make maximum and simultaneous use of the balancing and NMR technique, which allows the fluxes to be determined in an overall network of reactions. A generally applicable, completely automated methodology for data handling and analysis was developed. In contrast to other studies, we grew *C. glutamicum* to metabolic steady state as well as to isotopic steady state to increase the reliability of the metabolite balance and the isotopic balances as much as possible, thereby avoiding the inherent uncertainties of a dynamic study. Furthermore, we made full use of the fact that the carbon skeletons of the central metabolites are fixed at clearly predetermined positions in amino acids. Therefore the particularly valuable ^{13}C labeling of central metabolites is obtainable, to which access is otherwise difficult.

To obtain very precise and accurate labeling information, we determined ^{13}C enrichments by ^{1}H NMR spectroscopy. Due to the high information content of the labeling data, neither assumptions on the stoichiometry of the energy metabolism (e.g., Y_{ATP}, P/O ratio, H^+/e ratio), which are a matter of controversial debate,[31,42] nor assumptions based on any in vitro enzyme activity have to be taken into account. The metabolic model uses only the well-established chemistry of the carbon transitions in the enzyme reactions of the central metabolism. Our description takes full account of label scrambling reactions where symmetrical molecules occur and also of back fluxes. The formalization developed by us is of general validity and ready to be applied to other systems. It enables a detailed picture of the in vivo fluxes to be obtained under L-lysine-producing conditions in *C. glutamicum*.

MATERIALS AND METHODS

Organism and Cultivation

The organism used was the L-lysine-producing *Corynebacterium glutamicum* strain MH20-22B.[44,45] To stabilize the Leu$^-$ character of the strain, the plasmid pKK74I2[33] was introduced via conjugation into MH20-22B. Twelve kanamycin-resistant clones were obtained due to vector sequences integrated in the chromosome since pKK74I2 is nonreplicative in *C. glutamicum*. Because this plasmid carried an internal *leuA* fragment of 647 bp, the vector was integrated into the chromosomal *leuA* locus. The resulting strains were confirmed to be inactive in the *leuA* encoding isopropylmalate synthase, thus securing the stability of the Leu$^-$ character and ensuring that no leucine biosynthetic intermediate accumulates. The resulting strain *C. glutamicum* MH20-22B *leuA* was pregrown in a medium containing 3.7% brain–heart infusion (Difco, Detroit, MI), 2% glucose, and 20 mg/L kanamycin.

Continuous cultivation was started by inoculating 120 mL of a late exponential growth phase culture into the cultivation vessel containing 205 mL medium with (amounts per liter): 2 g urea, 150 mg leucine, 20 mg kanamycin monosulfate, 30 mg protocatechuic acid, 0.2 mg biotin, 75 mg Titriplex II, 0.02% polypropylene glycol, 10 g $(NH_4)_2SO_4$, 1.5 g $NaH_2PO_4 \cdot H_2O$, 1 g KCl, 250 mg $MgSO_4 \cdot {}_{H_2}O$, 1 mg $ZnSO_4 \cdot 7H_2O$, 0.5 mg $CuSO_4$, 0.2 mg $NiCl_2 \cdot 6H_2O$, and 0.12% HCl. The medium was supplemented with 7.55 g/L of either unlabeled glucose (Sigma, St. Louis, MO) or [1-^{13}C]glucose (99% enriched, Cambridge Isotope Laboratories, Cambridge, MA).

Continuous culture with a dilution rate of 0.10 h^{-1} and 325 mL culture volume was carried out in a BioFlo C30 reactor (New Brunswick Scientific Co., Edison, NJ) in a 20% O_2 and 80% N_2 synthetic air atmosphere at 30°C. The

rotation speed was 400 rpm and the aeration rate was 41.0 L/h. The pH of the culture was maintained at 7.0 with 2 *N* NaOH by an automatic pH control system (Bioengineering AG, Wald, Switzerland). Peristaltic pumps were used for media supply and withdrawal. On-line observation of the CO_2 concentration in the effluent gas indicated metabolic steady-state conditions after 77 h of cultivation so that the medium containing unlabeled glucose was changed to a medium supplemented with [1-^{13}C]glucose while maintaining the other components unchanged. After 30 h of subsequent cultivation, the cells were harvested by centrifugation, washed twice, lyophilized, and stored at −20°C. Unless otherwise stated, all chemicals were obtained from Merck (Darmstadt, Germany) or Boehringer Mannheim (Germany).

Analytical Methods

Dry weights were obtained after centrifuging 5 mL of 8-mL samples (13000*g*, 10 min), washing the pellets twice with 50 m*M* KH_2PO_4/K_2HPO_4 buffer, pH 7.0, and drying for 48 h at 100°C. The supernatants were analyzed for glucose and amino acids. Amino acids were analyzed as *ortho*-phthaldialdehyde derivatives by reversed-phase liquid chromatography.[45] Glucose was assayed enzymatically.[3] The carbon dioxide content of the effluent air was measured with an infrared CO_2 analyzer (Hartmann und Braun, Frankfurt, Germany). The total carbon content of the freeze-dried biomass was determined using a CHNS 932 elemental analyzer (Leco Co., St. Joseph, MI). The $^{13}CO_2/^{12}CO_2$ ratio in the purified gas phase[12] of the culture was estimated by analyzing the head space with a Sira II mass spectrometer (Fisions VG Isotech Instruments, Middlewich, United Kingdom).

Preparation of Amino Acids for NMR Spectroscopy

Lyophilized cells prepared from 55-mL culture volume were resuspended in 160 mL of 6 *N* HCl and hydrolyzed at 110°C in a sealed glass for 12 h. After the addition of 480 mL of demineralized water the hydrolysate was evaporated to dryness and redissolved in 8 mL of 0.2 *M* triethylamine (pH 2.5). Amino acids were fractionated[52] by cation exchange chromatography on an Ultrapac 11-μm resin column (Pharmacia Biotech GmbH, Freiburg, Germany) with triethylamine buffer (0.2 *M*, pH 3.2–10.5) used for elution. Freeze-dried powders of the amino acids were dissolved in 700 μL D_2O and passed through a 0.2-μm Dyna Gard filter (Microgon Inc., CA) to remove insoluble impurities.

NMR Spectroscopy

All NMR experiments were performed using a Bruker AMX 400-WB spectrometer equipped with a 5-mm inverse probe head for ^{1}H. Carbon-13 enrichments were determined from normal and ^{13}C-decoupled 400-MHz proton NMR spectra by relating the area of the ^{13}C satellite signals in the difference spectrum to the area of the corresponding proton signals in the decoupled spectrum as described.[52] Broadband ^{13}C decoupling was accomplished using the GARP-1 composite pulse decoupling scheme.[48]

RESULTS

Biochemical Flux Model

The fluxes connecting the various precursor metabolites within the central metabolism are given in Figure 1. These basic pathways have been identified by a variety of biochemical analyses carried out with *C. glutamicum*.[24] This network of reactions provides the biochemical model for the flux analysis. The established pathways are that of glycolysis, the pentose phosphate pathway (PPP), TCA cycle, and glyoxylate cycle. The anaplerotic reactions are currently a matter of much debate. Phosphoenolpyruvate carboxylase, of which the existence had been shown by enzyme studies,[9] was concluded to be of utmost importance in *C. glutamicum* from metabolite balance studies[53] but can be deleted without any consequences for product formation,[14,34] although an alternative reaction replenishing the TCA cycle has not yet been identified.[20] According to the various enzyme determinations, the principal catalytic activities carrying fluxes connecting phosphoenolpyruvate with oxaloacetate, pyruvate with oxaloacetate, and pyruvate with malate are present in *C. glutamicum*.

For our purpose of in vivo flux analysis, not relying on in vitro activities, we regarded phosphoenolpyruvate plus pyruvate as one pool, which seems justified because the determined ^{13}C enrichments were equal within experimental error (Table I). Oxaloacetate and malate were also treated as a single pool. The notation of all fluxes is given in Table II. The metabolite branch points included in the model are identified by rectangles in Figure 1. Because, in our model, acetyl coenzyme A is always directly and exclusively derived from pyruvate while no reverse flux of acetyl coenzyme A to pyruvate can occur, its ^{13}C labeling must exactly reflect that in pyruvate. Therefore, acetyl coenzyme A was not considered to be a metabolic branch point and was not incorporated as a separate metabolite pool in our model. Likewise, all other metabolites not representing branch points (e.g., 6-phosphogluconate, succinate, etc.) were not included as separate pools in the model. In no way does this approach affect the ^{13}C distribution in our network. Of course, for, e.g., experiments with acetate supply in the medium, one definitely would require a separate acetyl coenzyme A pool to be included in the model.

Within the biosynthetic reactions removing metabolites for synthesis of the macromolecular components, CO_2 generating and consuming reactions occur. Therefore, in total 11 anabolic reactions were incorporated into the model

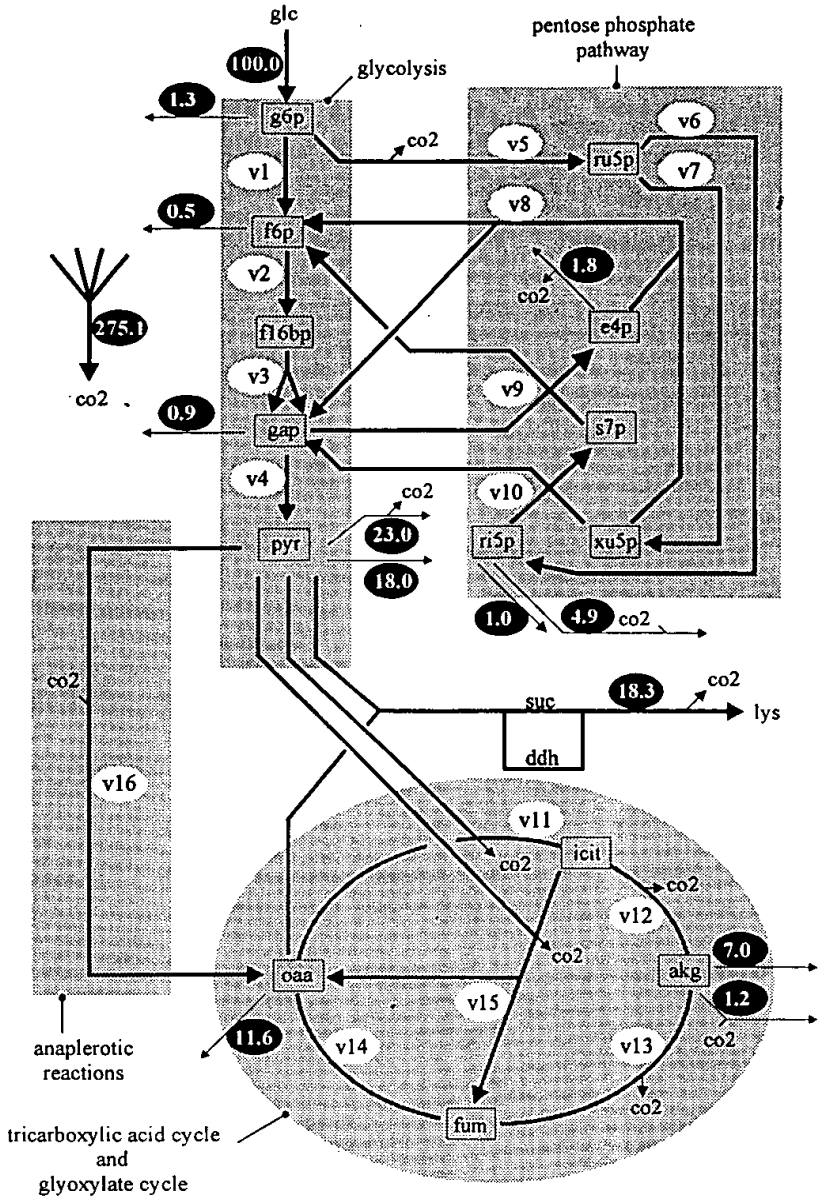

Figure 1. Metabolic model and metabolite balance used for in vivo flux determination in the L-lysine-producing *Corynebacterium glutamicum* strain MH20-22B *leuA*. Numbers in oval black symbols state measured fluxes of substrate, products, and biomass precursor metabolites. The latter were inferred from the measured biomass concentration using the stoichiometric approach described in the text. All fluxes are expressed as percentage of the glucose uptake rate (1.49 mmol/g dry weight h). Flux identifiers indicated (v_1, v_2, . . .) refer to the enzyme reactions listed in Table I. Abbreviations: glc, glucose; lys, lysine; co2, CO_2; g6p, glucose 6-phosphate; f16bp, fructose 1,6-bisphosphate; f6p, fructose 6-phosphate; gap, glyceraldehyde 3-phosphate; pyr, pyruvate; oaa, oxaloacetate; fum, fumarate; icit, isocitrate; akg, α-ketoglutarate; ru5p, ribulose 5-phosphate; ri5p, ribose 5-phosphate, xu5p, xylulose 5-phosphate; s7p, sedoheptulose 7-phosphate; e4p, erythrose 4-phosphate; ddh, diaminopimelate dehydrogenase pathway; suc, succinylase pathway.

(Fig. 1). The anabolic contribution was determined from the observed biomass yield on glucose and stoichiometric data (see below). It is important to note that all reaction steps shown, as well as all the concomitant carbon dioxide fluxes, were included in the metabolite balances as well as in the ^{13}C label distribution calculations. Thus, for example, the CO_2 balance included carbon dioxide released and/or fixed in the oxidative PPP, in the TCA cycle, in anaplerosis, as

Table I. Carbon-13 label data for central metabolic intermediates derived from the ^{13}C enrichments of the purified amino acids by ^{1}H NMR (Table IV).

	^{13}C enrichment (%) by carbon position					
Metabolite	C-1	C-2	C-3	C-4	C-5	C-6
e4p	2.0 ± 1.0	3.6 ± 1.0	2.0 ± 1.0	16.7 ± 2		
gap	2.9 ± 0.2	2.6 ± 0.1	26.7 ± 0.2			
pep	n.d.	2.5 ± 0.5	26.5 ± 1.0			
pyr	n.d.	3.0 ± 1.0	26.4 ± 0.5			
akg	n.d.	24.1 ± 0.3	11.1 ± 0.5	28.1 ± 0.6	n.d.	
oaa	n.d.	7.7 ± 2.0	20.9 ± 2.0	16.8 ± 2.7		
lys	n.d.	6.8 ± 0.2	21.9 ± 0.3	18.9 ± 1.0	22.2 ± 1.0	5.6 ± 0.3
CO_2	23.0 ± 0.4					

Note: ^{13}C fractional enrichment of CO_2 was determined by mass spectroscopy. Abbreviations (see Fig. 1): pep, phosphoenolpyruvate; n.d., not determined.

well as in the anabolic reactions. The resulting net CO_2 production of the culture was measured.

Depending on thermodynamic considerations as found in standard biochemistry textbooks, in our model a number of reactions were formulated as being reversible (see below) while others were considered irreversible. This was done because the presence of back reactions may severely influence ^{13}C labeling.

Strain and Quantification of Extracellular Fluxes

Corynebacterium glutamicum strain MH20-22B is an excellent L-lysine producer,[45] which is characterized by a *lysC* mutation and thereby feedback-resistant aspartate kinase. This and an altered export carrier[6,45] result in a high flux of aspartate to L-lysine with this strain. In addition this strain is auxotrophic for L-leucine,[7,33] but this character has been observed to be susceptible to reversion. Therefore, we introduced the defined *leuA* mutation into strain MH20-22B by gene-directed mutagenesis as described in the Materials and Methods section. The resulting strain was cultivated in a chemostat at a dilution rate of 0.1 h^{-1} and found to be stable for at least 107 h. L-Lysine production was not reduced with cultivation time, as is often observed with overproducers.[25] L-Lysine determinations were made, as well as dry weight determinations, and the CO_2 release was followed on-line.

Table II. Enzyme reactions corresponding to the flux identifiers in the biochemical model of Figure 1.

v_1	glucose 6-phosphate isomerase
v_2	phosphofructokinase
v_3	fructose 1,6-bisphosphate aldolase, triose phosphate isomerase
v_4	glyceraldehyde 3-phosphate dehydrogenase, bisphosphoglycerate kinase, phosphoglycerate mutase, enolase, pyruvate kinase, phosphoenolpyruvate:sugar phosphotransferase system
v_5	glucose 6-phosphate dehydrogenase, lactonase, 6-phosphogluconate dehydrogenase
v_6	ribose 5-phosphate isomerase
v_7	ribulose 5-phosphate epimerase
v_8	transketolase (xu5p + e4P ↔ gap + f6p)
v_9	transaldolase (gap + s7p ↔ e4p + f6p)
v_{10}	transketolase (xu5p + ri5p ↔ s7p + gap)
v_{11}	pyruvate dehydrogenase complex, citrate synthase, aconitase
v_{12}	isocitrate dehydrogenase
v_{13}	α-ketoglutarate dehydrogenase, succinate thiokinase, succinate dehydrogenase
v_{14}	fumarase, malate dehydrogenase
v_{15}	isocitrate lyase, malate synthase, fumarase, malate dehydrogenase
v_{16}	phosphoenolpyruvate carboxylase, phosphoenolpyruvate carboxykinase, malic enzyme, oxaloacetate decarboxylase
ddh	transaminase A, aspartate kinase, aspartate semialdehyde dehydrogenase, dihydrodipicolinate synthase, dihydrodipicolinate reductase, diaminopimelate dehydrogenase, diaminopimelate decarboxylase (lysine production over the diaminopimelate dehydrogenase pathway)
suc	same as ddh, except diaminopimelate dehydrogenase replaced by the sequence of enzyme reactions tetrahydrodipicolinate succinylase, succinyl aminoketopimelate transaminase, succinyl diaminopimelate desuccinylase, diaminopimelate epimerase (lysine production via the succinylase pathway)

Because all glucose was consumed in the culture, the uptake rate for glucose could be directly calculated as 1.49 ± 0.03 mmol/g dry weight h from the dry weight content of the broth (2.8 g dry weight/L), glucose concentration in the medium (7.55 g glucose/L), and the dilution rate (0.1 h^{-1}). For simplicity, this value was normalized to 100% and all fluxes reported in this study are molar fluxes expressed as percentage values of this glucose uptake rate. The L-lysine concentration accumulating in the culture was 7.66 m*M*. This corresponds to an L-lysine excretion flux of 18.3 ± 0.4%. The CO_2 efflux was determined from the measured CO_2 release (4.10 mmol CO_2/g dry weight h) to be 275.1 ± 13.8%. From the biomass concentration in the fermentor (2.80 g dry weight/L) and the carbon content of the biomass (0.408 g carbon/g dry weight) it was concluded that 35.3% of the carbon originating from glucose was used for anabolic purposes. Furthermore, it was calculated that of the total supplied carbon 45.8% was converted to CO_2 and 18.3% was used for the synthesis of L-lysine. Therefore, after summation, the carbon balance was closed up to 99.4%. Accordingly, only traces of other amino acids, keto acids, or organic acids were detected. Trehalose, often found with L-lysine producers,[59] could not be detected either.

Fluxes for Precursor Use

As determined, in the culture about one-third of the carbon is used for cellular growth. Therefore, the requirements of pyruvate and oxaloacetate and that of the other precursor metabolites which are removed at various steps in the central metabolism have to be quantitated. For the *Escherichia coli* cell a detailed stoichiometric approach is described where the cell is decomposed into 12 precursor metabolites.[30] These data have been used in a metabolite balance study with *C. glutamicum* ATCC 21253.[59] We directly quantitated the amino acid composition of *C. glutamicum* MH20-22B (Table III) to obtain the amounts of the 12 precursor metabolites required for amino acid synthesis. These requirements are based on the standard biosynthetic path-

Table III. Precursor and carbon dioxide requirements (μmol/g dry weight) for biomass synthesis of *C. glutamicum*.

		Stoichiometry												
Precursor	Amount	g6p	f6p	ri5p	e4p	gap	pga	pep	pyr	accoa	oaa	akg	co2	nadph
Ala	606								1					1
Arg	189											1	1	4
Asx	399										1			1
Cys	87						1							5
Glx	806											1		1
Gly	361						1							1
His	71			1										1
Ile	202								1		1		−1	5
Leu	0								2	1			−2	2
Lys	202								1		1		−1	4
Met	146										1			8
Phe	133				1			2					−1	2
Pro	170											1		3
Ser	225						1							1
Thr	275										1			3
Trp	54			1	1			1					−1	2
Tyr	81				1			2					−1	2
Val	284								2				−1	2
Dmp	146								1		1			4
Protein		0	0	125	268	0	673	482	1,724	0	1,370	1,165	−767	9,718
RNA				630			368				262		630	427
DNA				100			50				50		100	200
Lipids						129	129			2,116			−2,116	3,612
LPS		51	16	24			24	24		329			−329	470
Peptidoglycan			55					28	83	55	28	28	−55	193
Glycogen		154												0
Cl-units							49							49
Polyamines												59		180
Precursor		g6p	f6p	ri5p	e4p	gap	pga	pep	pyr	accoa	oaa	akg	co2	nadph
Total		205	71	879	268	129	1,293	534	1,807	2,500	1,710	1,252	−2,537	14,849

Note: The amino acid composition was determined from *C. glutamicum* strain MH20-22B *leuA* grown in continuous culure as described. The data account for the very high intracellular glutamate pool of 160 m*M* present in this strain. The data on other cellular constituents were taken from ref. 30. The experimentally determined specific glucose consumption was 14,949 μmol/g dry weight. Abbreviations (see Fig. 1): pep, phosphoenolpyruvate; accoa, acetyl coenzyme A; nadph, β-nicotinamide adenine dinucleotide phosphate (reduced form).

ways of amino acids which are identical to those in *E. coli* (except for L-lysine synthesis[45]). The total amino acid content represents the major part (64%) of the carbon content of *C. glutamicum*. Together with data on the other cellular polymers[30] which are also shown in Table III, a good fit to the experimentally determined total carbon content of the cells was found, confirming once more the established total carbon balance.

The demands of precursor metabolites as determined using the stoichiometric data in Table III in combination with the measured biomass yield on glucose for *C. glutamicum* MH20-22B, as well as the directly measured fluxes, are given in the black ovals of Figure 1. Inspection of the proposed anabolic pathways[30] shows that with a number of reaction steps involved CO_2 is released or fixed. Therefore, careful account was taken of the fluxes of carbon dioxide associated with those reactions in order to keep accurate metabolite balances and take accurate account of the concomitant transfer of ^{13}C label. The stoichiometric parameters for these fluxes are also included in Table III. Thus, where appropriate, anabolic precursor metabolite fluxes were split up into two components: one with involvement of carbon dioxide release (or fixation) and one without such involvement. This is indicated in Figure 1.

As an example, the total flux of pyruvate withdrawn from the central metabolism for anabolic purposes, which was calculated to be 41.0%, is composed of a flux of 23.0% involving the release of CO_2 and of a flux of 18.0% where no carbon dioxide is involved. These values were determined as follows: The total stoichiometric demand for glyceraldehyde 3-phosphate, phosphoenolpyruvate, pyruvate, and acetyl coenzyme A (Table III), all condensed into pyruvate, is 6,132 μmol C3 unit/g biomass, which amounts to 41% of the measured specific glucose uptake of 14,949 μmol/g dry weight. Of this total of 6,132 μmol/g dry weight, 3,456 μmol C3 unit/g dry weight, or 23% normalized on specific glucose consumption, is involved in decarboxylating biosynthetic reactions, i.e., with release of CO_2. This value of 3,456 μmol C3 unit/g dry weight is obtained by summing the contributions given in Table III for the synthesis of L-isoleucine, L-lysine, L-phenylalanine, L-tryptophane, L-tyrosine, L-valine, lipids, lipopolysaccharids, and peptidoglycan. The remaining 18% represents reactions where the complete C3 unit is incorporated in cellular constituents. Likewise, the total flux of α-ketoglutarate diverted from the central metabolism was 8.2%, of which a component of 1.2% involves CO_2 fixation for L-arginine biosynthesis (Table III).

Quantification of Fractional Enrichments in Precursor Metabolites

In the steady state of the culture identical to that from which the metabolite balance was made, the unlabeled glucose was replaced by [1-^{13}C]glucose and the cells were grown for a further 30 h, which is equivalent to three complete volume changes. Stability of the culture was ensured by monitoring the L-lysine concentration, cell density, and CO_2. Applying first-order wash-out kinetics, the 95% isotopic equilibration calculated was accounted for in the data analysis. The cells were harvested and hydrolyzed, and the amino acids were isolated on a preparative scale by cation exchange chromatography. Since the amino acids are synthesized by predetermined, exactly defined pathways from precursor metabolites, as established for *E. coli*[30] and confirmed in all studies with *C. glutamicum*[24] the fractional enrichments in individual carbons of the amino acids directly reflect the fractional enrichments in the precursors. (In fact, all determinations were in full accord with the standard biosynthetic pathways). For instance, the α-ketoglutarate skeleton is directly accessible by analysis of L-glutamate (Table IV), or glyceraldehyde 3-phosphate by analysis of L-serine.

Because in several cases one specific precursor metabolite is incorporated in several amino acids, redundant measurements were possible, further increasing the accuracy of the determinations. For example, pyruvate was accessible by analysis of L-alanine, L-valine, and L-isoleucine. We determined the fractional ^{13}C enrichments by ^{1}H NMR spectroscopy from the protonated carbons of purified L-glutamate, L-aspartate, L-threonine, L-lysine, L-leucine, L-isoleucine, L-alanine, L-valine, L-serine, L-glycine, and L-phenylalanine. Thirty-one out of the 52 carbons of these amino acids were measured. The results are shown in Table IV. From these data the ^{13}C enrichments of the precursor metabolites erythrose 4-phosphate, glyceraldehyde 3-phosphate, pyruvate, oxaloacetate, and α-ketoglutarate were available. The condensed results are given in Table I. A typical recorded NMR spectrum is shown in Figure 2. Further important information was the fractional enrichment in the carboxyl group of glycine, which is identical to the C-1 position of glyceraldehyde 3-phosphate. This was obtained with ^{1}H NMR by quantitating the small fractional splitting of the H-2 signal unequivocally attributable to heteronuclear scalar coupling to ^{13}C-1 of glycine. As additional information, the ^{13}C fractional enrichment of CO_2 was also determined. This was achieved by mass spectroscopy and the enrichment estimated as 23.0 ± 0.4%.

Computer Modeling of the Metabolite Balance and ^{13}C Label Distribution

Manual inspection of the data already provides useful information. Thus, the label in C-2 of pyruvate cannot be explained by assuming the sole transfer of carbon step by step through glycolysis or the PPP. Instead a back flux within the PPP or a back flux from the TCA cycle to pyruvate is necessarily required. Similarly, inspection of the label distribution in erythrose 4-phosphate conclusively shows that back fluxes occur in vivo within the PPP. However, for accurate quantification by detailed simultaneous consideration of metabolite, as well as ^{13}C label balances throughout the complete metabolic network, a general mathematical formalism had to be developed. The mathematical principles and a simple application example are de-

Table IV. Carbon-13 label data of the purified amino acids as determined by ^{1}H NMR.

Amino acid	^{13}C enrichment (%) by carbon position					
	C-1	C-2	C-3	C-4	C-5	C-6
Gly	2.9 ± 0.2	2.6 ± 0.1				
Ser	n.d.	1.5 ± 1.5	26.7 ± 0.2			
Ala	n.d.	3.0 ± 1.0	26.4 ± 0.5			
Val	n.d.	n.d.	n.d.	26.3 ± 0.5	26.3 ± 0.5	
Ile	n.d.	7.9 ± 2.0	n.d.	n.d.	16.5 ± 0.8	26.0 ± 0.8
Leu[a]	n.d.	1.1 ± 0.3	0.9 ± 0.7	1.1 ± 0.6	1.0 ± 0.2	1.0 ± 0.2
Glu	n.d.	24.1 ± 0.3	11.1 ± 0.5	28.1 ± 0.6	n.d.	
Asp	n.d.	7.8 ± 2.0	20.5 ± 2.0	n.d.		
Thr	n.d.	7.4 ± 1.0	21.3 ± 0.9	16.8 ± 2.7		
Lys	n.d.	6.8 ± 0.2	21.9 ± 0.3	18.9 ± 1.0	22.2 ± 1.0	5.6 ± 0.3
Phe[b,c]	n.d.	2.5 ± 0.5	26.5 ± 1.0	n.d.		

Note: Measurement inaccuracy varied strongly due to differences in overlap between the spectra. Abbreviation: n.d., not determined.

[a]Leucine with natural abundance, since it was supplied in the medium (see Methods section).

[b]The average enrichment of Phe C-5 and C-9 was 21.6 ± 1.0%, where one of these carbons is derived from phosphoenolpyruvate C-3 and therefore should be labeled according to Phe C-3.

[c]Of the remaining three carbons Phe C-6, C-7, and C-8, which are derived from erythrose 4-phosphate, 0.047 are ^{13}C.

scribed in the Appendix. According to the biochemical network of *C. glutamicum*, the three fluxes corresponding to nonstationary metabolite pools (glucose, lysine, CO_2), as well as 11 depleting fluxes for biomass synthesis, were defined as well as 14 nonaccumulating metabolite pools (identified by squares in Fig. 1), which are connected by 16 fluxes v_i (Table II). For instance, the PPP was not simply represented as a glycolysis bypass, but instead included the

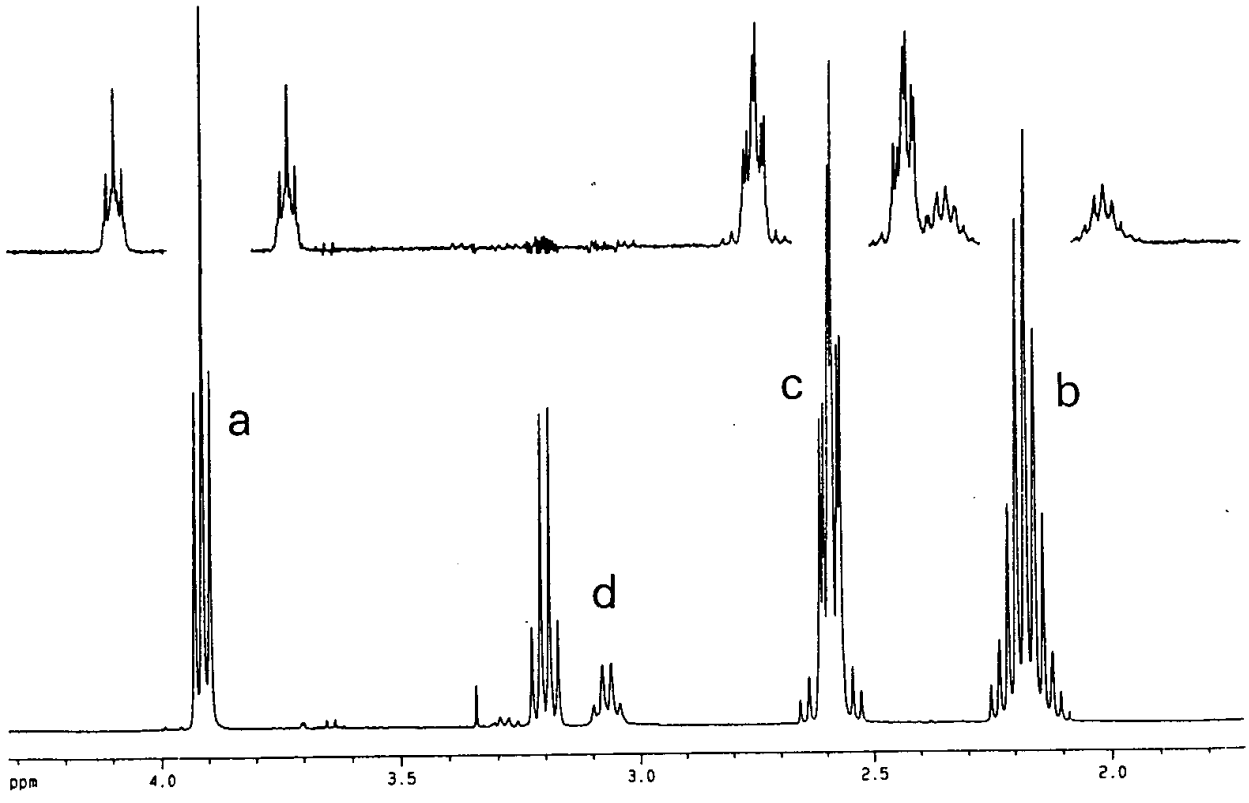

Figure 2. Illustrative ^{1}H NMR spectrum of L-glutamate extracted from the isotopically enriched cell protein of *C glutamicum* strain MH20-22B *leuA*. Lower trace, ^{13}C decoupled spectrum. Upper trace, difference between normal and ^{13}C decoupled spectra showing the ^{13}C satellites (2.6 times enlarged). Signal assignments: a, b, c: H-2, H-3, and H-4 of glutamate, respectively; d: CH_2 of residual triethylamine buffer used for elution.

metabolites glucose 6-phosphate, ribulose 5-phosphate, ribose 5-phosphate, xylulose 5-phosphate, sedoheptulose 7-phosphate, erythrose 4-phosphate, glyceraldehyde 3-phosphate and fructose 6-phosphate together with the reactions of glucose 6-phosphate isomerase, ribulose 5-phosphate epimerase, ribose 5-phosphate isomerase, transketolase, transaldolase, as well as the enzymes of the oxidative PPP branch. Except for the oxidative branch, all the PPP reactions were modeled as being reversible; i.e., they were allowed to carry a back flux simultaneously with a forward flux. This enabled the correct modeling of exchange fluxes as well as of their influence on ^{13}C label distribution in these reactions (see Appendix). In addition, the reactions v_1, v_3, v_4, and v_{16} (Table II) were considered to be reversible, as was the reaction sequence of fumarase and malate dehydrogenase (v_{14}). The extent to which a reaction runs in a reversible manner is represented by the exchange rate, which we define as the ratio of the flux component running simultaneously backward and forward in a reaction to the net forward flux.

Whereas in most studies only extreme situations have been analyzed so far, i.e., there is either no exchange or very large exchange rates prevail,[46] our analysis also models intermediate exchanges, simply because the exact dependence on the exchange flux of the ^{13}C label of the intermediates involved is adequately described by our mathematical equation system. In addition, full label scrambling was assumed within the reactions converting α-ketoglutarate to fumarate and fumarate to oxaloacetate. In total, 82 carbon atoms are included in the model and 26 corresponding measurement values were available. In addition, since we supplied the culture with CO_2-free gas to make use of the respective fractional enrichment in evolved CO_2, also the origin and fate of CO_2 in the biosynthetic pathways.was individually included in the model and formulated accordingly as described above. The assumptions used for modeling are given in Table V.

Table V. Special features of the in vivo flux analysis for *C. glutamicum* and assumptions used for flux estimations.

1. Only data for metabolite and carbon atom balances are used. Energy consideration are excluded.
2. Specific enzyme activities and kinetic information on enzymes, as obtained from in vitro studies, are excluded.
3. No directionality is preset for any of the fluxes.
4. In specific cases fluxes are preset to be irreversible, but with arbitrary directionality. (These fluxes appear without hexagonal symbol in Fig. 3.)
5. The conversion of citrate to α-ketoglutarate is accompanied by a conserved orientation of the citrate carbon skeleton (i.e., no scrambling of carbons).
6. The orientation of carbons in reactions involving fumarate is randomized, i.e., the carbons C-1 and C-4 as well as C-2 and C-3 of fumarate are scrambled.
7. The conversion of tetrahydrodipicolinate to diaminopimelate through the succinylase variant of L-lysine synthesis is accompanied by scrambling of the carbons C-1 and C-7, C-2 and C-6, and C-3 and C-5.

Based on the experimental data and the metabolic network, the ^{13}C labeling in all carbons of all branch point metabolites was related to the flux and exchange parameters of the metabolic model. This was coupled to an optimization program that, in addition to the net fluxes, also optimized the exchange rates such that altogether the predicted ^{13}C labelings fitted best to the experimentally observed values. The optimal estimations for fluxes and exchange rates were obtained by minimizing the sum of squares of the deviations between model values and the measured data (for fluxes as well as ^{13}C labelings). These deviations were normalized to the experimental errors, i.e., a difference (for a given single carbon label or single flux value) of equal magnitude to the experimental error in the corresponding measurement value contributed one unit to the total residual sum of squares.

Estimated Fluxes in Central Metabolism

A series of flux estimations was made using different sets of starting values. Independent of starting values, reproducible results were obtained for the entire fluxes of the glycolysis, PPP, TCA cycle, glyoxylate cycle, and split pathway of L-lysine synthesis. Therefore, the fluxes in these pathways of the central metabolism seemed to be well defined by the experimental data. For instance, a nonoxidative PPP flux for the supply of erythrose 4-phosphate and ribose 5-phosphate is also possible,[54,63] but evidently did not occur, although our model is well able to accommodate it. As can be seen from Table VI, the experimentally determined enrichments are in excellent agreement with the corresponding enrichments as estimated by the parameter fitting algorithm.

In Figure 3 the values for the net fluxes are given in the black ovals. Thus, of the 100.0% glucose flux entering the cell, 32.2% is metabolized over glycolysis (v_1) and 66.4% over the oxidative branch of the PPP (v_5). The remaining flux of 1.3% was used for cell material synthesis. The net flux from glyceraldehyde 3-phosphate to pyruvate is 160.9%, which is higher than the glucose input flux, since of course 2 mol of C3 unit can basically be generated per mole of glucose. Thus, 39.1% of flux, expressed in C3 unit flux, had been withdrawn from glycolysis and the PPP for biomass synthesis and CO_2 formation. The flux entering the TCA cycle (v_{11}) is 62.2%. The glyoxylate cycle flux is weak (0.2%) but is significantly and reproducibly greater than zero. This is proof that the current assumptions used for modeling on the in vivo use of the TCA cycle are reasonable. The flux of pyruvate and oxaloacetate toward exported lysine was 4.9% through the dehydrogenase reaction and 13.7% through the succinylase reaction.

The estimated values for the exchange rates are stated in hexagonal symbols in Figure 3. As stated before, exchange rates were normalized to the net flux, i.e., a value of 10 means that the reaction back flux is 10 times larger than the net flux v_i. It has been shown[46] that large exchange rates can only be estimated within large confidence bounds. However, the existence and approximate magnitude can be well

Table VI. Estimated ^{13}C enrichments of central metabolic intermediates resulting from the best fit to the experimental data.

	^{13}C enrichment (%) by carbon position					
Metabolite	C-1	C-2	C-3	C-4	C-5	C-6
e4p	2.5	2.0	1.9	15.3		
gap	2.7	2.6	26.3			
pyr	2.8	2.7	26.3			
akg	17.3	22.6	9.8	26.3	2.7	
oaa	7.2	9.8	22.6	17.3		
lys	5.5	7.1	24.0	17.3	24.9	5.3
CO_2	21.6					

Note: Abbreviations: see Table I.

assessed. Such very high exchange rates of 8.8 in the glucose 6-phosphate isomerase reaction, 387.1 in the glyceraldehyde 3-phosphate to pyruvate conversions, and 46.8 in the ribose 5-phosphate transketolase reaction were found. Intermediate high exchange rates of 0.1–1.7 for the ribulose 5-phosphate epimerase, transaldolase, and fumarase/malate dehydrogenase reaction sequence were estimated, indicating that exchange fluxes in these reactions were of the same order of magnitude as the net fluxes.

The biological complexity of anaplerotic reactions and interconnections with decarboxylating reactions is demonstrated in various organisms.[20,22] As already stated in the biochemical model description (Fig. 1), several enzyme reactions carrying fluxes that connect phosphoenolpyruvate with oxaloacetate and pyruvate with oxaloacetate, or pyruvate with malate, are present in *C. glutamicum*.[9,15,19,34,57] However, since we wished to retain the limited set of assumptions as given in Table V, i.e., not speculate which anaplerotic enzyme plays the most important role in vivo, we regarded phosphoenolpyruvate and pyruvate as one network pool as well as malate and oxaloacetate. This approach was also prompted by the measured identical fractional enrichments in the carbon atoms of phosphoenolpyruvate and pyruvate (Table I). In all parameter estimates the estimates yielded a reproducible, positive value of 38.0% for the net anaplerotic flux of C3 units to C4 units. Moreover, an exchange rate of 0.8 was consistently estimated, implying that the total forward in vivo flux of C4 unit generation was 68.6% (1.8 times 38.0%) [while a back flux of 30.6% (0.8 times 38.0%) simultaneously decarboxylated the C4 units oxaloacetate and/or malate]. This finding is in accord with the view that cycling occurs through the anaplerotic reactions in mammals,[22,37] though to date no quantitative information is available for bacteria.

DISCUSSION

Our approach to determine the fractional enrichments of individual carbons of precursor metabolites in the metabolic and isotopic steady state by amino acid analysis yields detailed information on the fluxes in the central metabolism. The method has crucial advantages over the methods conventionally applied for stationary flux determination using NMR or metabolite balancing. Zupke and Stephanopoulos[65] showed consistency between results obtained from metabolite balancing and information gained from ^{13}C NMR tracer data. While these authors conducted the two types of data analysis separately, in our approach the data can be analyzed simultaneously.

In *C. glutamicum* MH20-22B we quantified the entry of the glucose 6-phosphate flux into the PPP as 66.4%, whereas 32.2% enters the glycolysis, at an absolute glucose consumption rate of 1.49 mmol/g dry weight h set as 100.0%. Current data available on the relative use of both pathways in *Corynebacterium* species vary from 11 to 65%. In these cases the metabolic state differed greatly from our situation since washed cells[18] or strains producing histidine[17] or glutamate[60] were assayed. Moreover, cultivation–time-dependent variations of fluxes are documented for L-lysine[52] and L-glutamate synthesis[60] with *Corynebacterium* species, which we prevent in our continuous culture study. Data obtained from the early lysine production phase in a batch study based solely on metabolite balances may be most readily compared to our data with respect to the flux distribution and absolute flux rate at the glucose 6-phosphate branch point.[59] However, the other fluxes reported in the latter study are entirely different from ours, probably due to the fact that in our continuous culture study glucose was completely consumed, whereas in the batch culture a large excess of glucose was present.

In studies with hybridomas[27,49] or bacteria[13,59] the reduced forms of nicotinamide adenine dinucleotide (NAD/H) or NAD phosphate (NADP/H) balances were included since this information was required as an additional constraint on metabolism in order to be able to solve the flux network equation system. Since we do not need this information in our analysis, we can use our estimates to calculate the amount of energy and redox equivalents used and generated during metabolism. With respect to adenine triphosphate (ATP) and NADH this calculation is probably not useful for *C. glutamicum*, since for this organism the number of coupling sites in the respiratory chain is questionable.[23,51] Furthermore, in addition to the various possible anaplerotic reactions, other well-defined biochemical reactions have been identified that have the potential to operate in a futile cycle for ATP hydrolysis accompanied by proton translo-

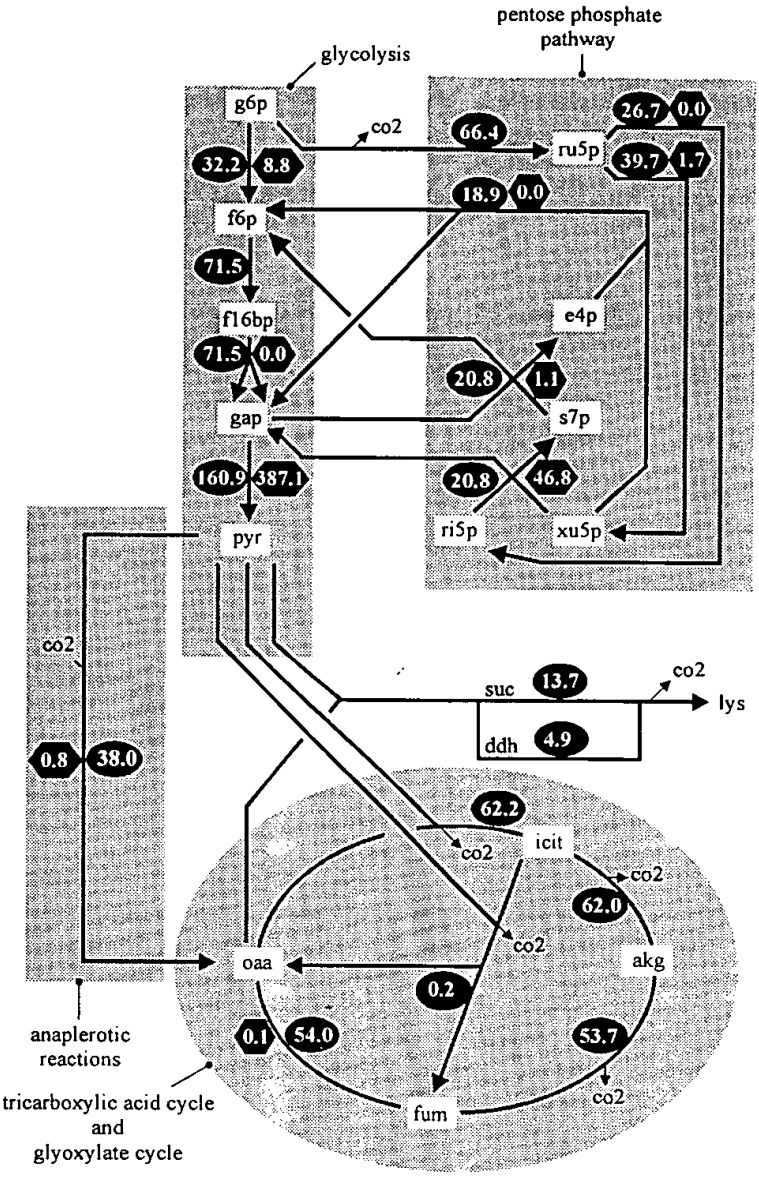

Figure 3. In vivo flux distribution in the central metabolism of the lysine-producing *C. glutamicum* strain MH20-22B *leuA* resulting from the best fit to the experimentally determined fluxes and ^{13}C labeling data. Numbers in oval symbols state the estimated net fluxes. Numbers in hexagonal symbols state the estimated exchange rates in reversible reactions expressed as multiples of the net flux. All net fluxes are expressed as a percentage of the glucose uptake rate (1.49 mmol/g dry weight h).

cation.[59] However, for NADP/H the situation is different and our analysis allows an independent check on the balance of its synthesis and requirement.

It is documented that in *C. glutamicum* the PPP enzymes glucose 6-phosphate dehydrogenase[55] and 6-phosphogluconate dehydrogenase[56] are NADP linked. This is also the case for the isocitrate dehydogenase[10] of *C. glutamicum*. Thus, with the flux distribution shown in Figure 3 the total flux of NADPH synthesis is 194.8%. NADP is regenerated in the biosynthetic reactions with a stoichiometry (Table III) of 14,849 μmol per 14,949 μmol of glucose (i.e., 99.3% molar flux), as well as in lysine biosynthesis, with a flux of 74.4% (Fig. 3, Table III). Thus, according to our calculation, an excess of 194.8 − 99.3 − 74.4 = 21.1% molar flux relative to the glucose consumption rate is the result. This questions the use of a fixed NADP stoichiometry for flux determination. Instead, we have to conclude that *C. glutamicum* possibly regenerates NADP in vivo by an oxidase, or that alternative reactions are present whose operation in vivo still has to be demonstrated. A carboxylating enzyme requiring NADPH (the malic enzyme) could in theory be a candidate. However, this seems extremely unlikely since the thermodynamic equilibrium favors the reverse reaction from oxaloacetate plus NADP to pyruvate plus CO_2

and NADPH.[54] Thus, at present the problem of the observed NADPH imbalance cannot be resolved.

An important advantage over metabolic balancing is trivially and obviously that our method can handle bidirectionality of fluxes where this is impossible with metabolic balancing since it leads to singularities in the equation system.[58] We detected enrichment in C-4 of erythrose 4-phosphate. Since the biochemistry dictates that this C-atom originates from C-5 of ribulose 5-phosphate, and ribulose 5-phosphate is not labeled via the oxidative part of the PPP, this is proof that an in vivo exchange of the glyceraldehyde 3-phosphate pool with that of ribulose 5-phosphate occurs via the ribose 5-phosphate transketolase and epimerase reaction. Such exchange activities have been demonstrated in vitro in extracts of erythrocytes[4] and rat liver[11] by following the appearance of the ^{13}C label originally present in an added sugar phosphate in new sugar phosphates of the PPP. Whereas in those studies exchange could only be investigated in isolated enzyme reactions *in vitro*, our approach allowed exchange reactions to be quantitated as they are embedded in the complete network of the operative PPP in vivo. Since the PPP serves as a source of NADPH, ribose 5-phosphate as well as erythrose 4-phosphate, all of which are required in different stoichiometric quantities for anabolism, restructuring of the excess generated polyol-phosphates with glyceraldehyde 3-phosphate from the PPP and glycolysis is necessary to arrive again at the precursor metabolite phosphoenolpyruvate.[54] The exchange rate carried by the ribose 5-phosphate transketolase reaction exceeds the net flux by about 30-fold. Intermediate exchange rates are present for the ribulose 5-phosphate epimerase and the transaldolase, where the exchange fluxes are in the range of the net flux.

From current data on the quantification of the exchange reactions of the separated enzymes based on in vitro measurements,[11] it is concluded that in various tissue preparations the transketolase can exceed the net flux through PPP from 7- to 600-fold. Our finding of label mixing within the PPP also implies that using label in glyceraldehyde 3-phosphate solely for the calculation of the PPP flux can lead to falsified net fluxes. The withdrawal of precursors for biosynthesis is fully accounted for in our model, which is not the case in many NMR studies. The flux of ribulose 5-phosphate and erythrose 4-phosphate withdrawal for anabolism also alters the fluxes and labeling patterns as already concluded by Walker et al. in the study on glutamate production with the coryneform *Microbacterium ammoniaphilum*.[60] Disregarding the withdrawal for anabolism, we would only calculate a value of 58.7% entering the PPP. Further high exchange rates are determined in the glycolysis for the reactions involved in converting glyceraldehyde 3-phosphate into pyruvate, which is in accord with full reversibility of these reactions as quantified within erythrocytes.[28]

In recent attempts to quantify the in vivo fluxes in *C. glutamicum* it had to be assumed that the glyoxylate cycle is inactive, since due to the restricted information on metabolite balances and/or label incorporation, calculations of fluxes would otherwise be impossible. A quantification of the in vivo glyoxylate cycle flux for *E. coli* during growth on acetate was done by Walsh and Koshland.[61] Attention was drawn here to the fact that knowledge of C-1 labeling in glutamate is essential to differentiate between the TCA cycle and glyoxylate cycle flux. These authors point out that flux information is also present in the amount of CO_2 release, which correlates with TCA cycle activity. In our analysis the fractional enrichment in C-1 of glutamate was not directly determined since it carries no protons. However, this C-atom corresponds to the C-4 atom of oxaloacetate (which became available by the quantitation of the enrichments in threonine und aspartate). This is incorporated in our analysis as well as the quantitation of the CO_2 labeling. We always found a small but reproducible nonzero value for the glyoxylate cycle flux. Apparently, the low activity of the isocitrate lyase determined in vitro (0.01–0.02 μmol/mg protein min)[40] and of malate synthase[41] is sufficient to carry the flux entry in the glyoxylate cycle when *C. glutamicum* grows with glucose as substrate. Those in vitro activities are in the range of the α-ketoglutarate dehydrogenase activity (0.02–0.03 μmol/mg protein min), which in our study carries a flux of 53.7%, or 0.013 μmol/mg dry weight min. Walker already concluded for *M. ammoniaphilum* that the glyoxylate cycle may be active in vivo.[60]

It would in principle be possible to replenish the TCA cycle via the glyoxylate cycle, but this is ruled out by the low glyoxylate cycle activity. Therefore, carboxylating anaplerotic reactions are required to replenish the loss of TCA cycle metabolites for anabolic processes. The metabolite balance dictates that this anaplerotic net flux in *C. glutamicum* MH20-22B is 38.0%. This largely explains the labeling of α-ketoglutarate in C-2. In the anaplerotic reactions, it cannot be differentiated whether a carboxylation of phosphoenolpyruvate or of pyruvate occurs, since we regarded these metabolites as one pool in our analysis, as we also did for malate and oxaloacetate. Which enzyme(s) carry the anaplerotic flux in vivo is currently a matter of much debate.[20,34]

It is questionable whether the phosphoenolpyruvate carboxylase plays a major role in replenishing the TCA cycle, as originally concluded,[53] since a defined deletion mutant of this enzyme was not altered in L-lysine production,[14,34] a situation in which there is a high demand for oxaloacetate. At this point, however, attention should be drawn to the fact that any flux analysis by deletion mutants is questionable since the flux is severely disturbed and the cell may react very flexibly. This is shown within the central metabolism of *C. glutamicum*, not only for phosphoenolpyruvate carboxylase, but also for glutamate dehydrogenase[5] and pyruvate kinase.[15] To quantify the in vivo fluxes of anaplerosis in the undisturbed situation, a detailed NMR study, such as an isotopomer analysis, would be particularly instrumental, as was used for the metabolism in the heart, where it was found that the carboxylation of pyruvate mainly contributes to the replenishment of the TCA cycle.[26]

It was pointed out as early as 1982[60,61] that the C-5

carbon of glutamate (which is directly derived from pyruvate C-2) becomes ^{13}C labeled by a back flux from oxaloacetate to acetyl coenzyme A. This back flux was ignored in subsequent studies of fluxes in *C. glutamicum* because C-5 of glutamate was not included in the equations for tracer data analysis. Our study fully accounts for this important futile cycling and conclusively reveals that there is a back flux from the C-4 pool (oxaloacetate and malate) to the C-3 pool (phosphoenolpyruvate and pyruvate) amounting to 30.6%. According to the literature,[60] this back flux is reflected in the presence of ^{13}C label in C-5 of α-ketoglutarate, which is necessarily derived from C-2 of pyruvate since the sole synthesis of α-ketoglutarate results from pyruvate (acetyl coenzyme A) plus oxaloacetate. Indeed, flux variation studies showed that the ^{13}C labels in pyruvate C-2 and oxaloacetate C-2 reacted significantly to the exchange rate of the anaplerotic flux. At infinite exchange rates, these two labels would in fact become equal. Thus within *C. glutamicum* not only are high exchange rates present within glycolysis, or PPP (simply for thermodynamic reasons), but also within the complex sets of reactions exchanging carbon between phosphoenolpyruvate, pyruvate, oxaloacetate, and malate. It is speculated that such futile cycling serves to waste ATP.[37] It could also serve as a peculiar regulatory device, since in the presence of two regulated enzymes, one catalyzing the negative and one the positive flux, a regulatory signal has a stronger effect on the net flux than if only the enzyme exclusively catalyzing the positive flux were present.[54] A flux from pyruvate to oxaloacetate was also quantified in rats, being as in our case of approximately the same size as that from oxaloacetate to phosphoenolpyruvate.[22]

Our observed labeling data, especially the enrichment in α-ketoglutarate C-2, could in principle also be partly explained by the presence of channeling through the reactions catalyzed by succinate thiokinase, succinate dehydrogenase, and fumarase (directed transfer of C-2, -3, -4, -5 of α-ketoglutarate to C-1, -2, -3, -4 of oxaloacetate), which seems to occur in eukaryotic cells.[35] However, the labeling data are in full accord with our current model based on the assumptions given in Table V, which includes full label scrambling through the TCA cycle reactions that are assumed to go without channeling. Based on this model, we also determined that only a small fraction of the oxaloacetate formed by the anaplerotic reactions is subjected to label scrambling by back flux to fumarate and subsequent reconversion to oxaloacetate. If ever it should be confirmed that channeling is present in *C. glutamicum*, our data would be consistently interpreted by an increased exchange of the anaplerotically formed oxaloacetate with the symmetrical intermediate fumarate. The presence of back fluxes greatly influences the ^{13}C label distribution. For instance, it has been reported[61] that the flux through the isocitrate dehydrogenase derived from ^{13}C label data differed by more than 10% depending on whether complete equilibration of the oxaloacetate and fumarate pools was assumed or no equilibration at all. This illustrates how, in most cases, simplified models are used[46] that address the situation where either no back flux or complete equilibration is assumed. In contrast, our model, by virtue of its comprehensiveness and the large amount of experimental data, actually allows the in vivo exchange rates to be estimated from measured data.

In summary, the approach presented here is a straightforward method for deriving detailed information on metabolic fluxes in growing cultures. Many NMR studies conducted thus far used labeling models that describe only a limited part of the central metabolism[27,60,61] (especially the TCA cycle and anaplerotic reactions) and, even so, did not fully take into account all possible carbon transitions, as stated by the authors themselves.[60,63] Consequently, these models could not be generalized[11,17,18,49] to other metabolic systems.

In contrast, our equation system is fully comprehensive of all carbon transtitions and the mathematical formulation can be generally applied to other systems. Our approach offers the advantage of well-defined physiological conditions. We perform measurements under isotopic steady state of intracellular metabolites, whereas in batch fermentation conditions this is generally not the case, even after a 10-h period of incubation with the labeled substrate.[60] It should prove useful to combine genetic analysis with the analysis of consequences on intracellular fluxes. This is of special interest for those mutants of the central metabolism where no balance disturbances occur. Furthermore, our approach provides the basis for comparing well-defined isogenic strains of *C. glutamicum*, which display great differences with respect to amino acid overproduction.

Thanks are due to K. Sonntag for NMR measurements and to J. Engelmann for supporting the fermentations. H. Förstel at the IRA Forschungszentrum Jülich GmbH is thanked for the mass spectrometry analysis of carbon dioxide. We are grateful to J. Föhles at the Deutsches Wollforschungsinstitut RWTH Aachen for the analysis of the biomass amino acid composition and to G. Küppers at the ZCH Forschungszentrum Jülich GmbH for the CHNO analysis of the biomass. The authors appreciate discussions with N. D. Lindley INSA, Toulouse, and B. Eikmanns. We are grateful to J. Carter-Sigglow for critical reading of the manuscript.

APPENDIX: MATHEMATICAL DETAILS OF FLUX DETERMINATION

Intracellular flux determination under stationary conditions as applied in this contribution is based on a general model quantitatively explaining the relations between fluxes and ^{13}C labels. This mathematical model, the automatic generation of model equations, and the data analysis procedure are now briefly described to give an understanding of the theoretical background.

Modeling Frameworks for Carbon Isotope Labeling Systems

Carbon isotope labeling studies fall within the category of tracer experiments. General models and tools for tracer analysis were already developed in the 1970s; an excellent textbook is that by Anderson.[2] However, there are some new aspects in stationary carbon isotope labeling systems

that have not been explicitly taken into account before. In particular, the fluxes of all carbon atoms participating in the same reaction step are closely linked by an identical flux rate which considerably reduces the number of independently varying variables in the system. Furthermore, as will be shown below, reversible reaction steps can significantly influence the label patterns in metabolic intermediates. Although this has been described previously,[2,46] metabolic exchange fluxes are considered in their complete generality for the first time in our approach. Moreover (as in refs. 64, 65) a computer-supported framework for modeling, simulation, and data analysis is supplied.

A Simple Example

Before formulating a general (but rather abstract) mathematical model, the equations will be introduced for the case of the very simple example network shown in Figure 4. It was designed to demonstrate the effect of a bidirectional reaction step with a minimal number of carbon atoms. Although oversimplified, the example may be interpreted as a prototype of two branching pathways with different fates of carbon atoms. For example, in the central metabolism a comparable branching situation is encountered at the level of pyruvate. The bidirectional flux v_2 in Figure 4 then corresponds to the anaplerotic flux between pyruvate and oxaloacetate while the unidirectional flux v_3 represents the alternative transformation of pyruvate via acetyl coenzyme A through the citric acid cycle where carbon atoms change positions. The example motivates how in principle the information on exchanging fluxes can be obtained from labeling data.

In Figure 4 the substrate uptake v_1 as well as the fractional labels in carbon atoms B_1 and C_2 are assumed to be measurable. The intracellular flux v_2 takes place in both directions while v_3 is assumed to be irreversible. Finally, fluxes across the system borders (here v_1, v_4) must always be assumed to be irreversible.

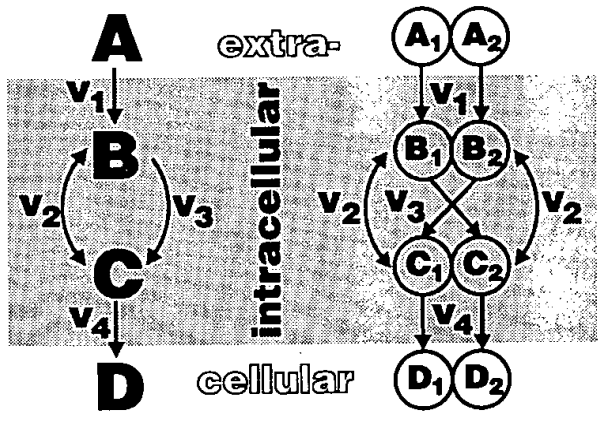

Figure 4. Simple example network. Left: metabolite view. Right: carbon atom view. The extracellular flux v_1 and the labels B_1, C_2 are assumed to be measurable. Input labels A_1, A_2 are known.

The system will be described in terms of fluxes v_i and labels x_j. Both flux directions of a bidirectional reaction step must be accounted for. In the example the forward and backward fluxes of v_i are represented by the symbols $v_i^{\rightarrow}$, $v_i^{\leftarrow}$. The irreversibility assumptions are then represented by $v_1^{\leftarrow} = 0$, $v_3^{\leftarrow} = 0$, $v_4^{\leftarrow} = 0$ while the corresponding net fluxes are $v_i^{\text{net}} = v_i^{\rightarrow} - v_i^{\leftarrow}$.

The fractional labels at each carbon atom position of intracellular metabolites are denoted by $B_1, B_2, C_1, C_2 \in [0,1]$. Additionally the known input to the system is specified by A_1, A_2. For example, a substrate A, which is 100 % labeled only at the first carbon atom position, is described by $A_1 = 1, A_2 = 0$. Clearly, the terminal nodes D_1, D_2 are not required for flux balancing.

The metabolite net fluxes from and to an intracellular metabolite pool must add up to zero in the stationary state. This gives rise to the following linear metabolite flux balance equations at stages B and C:

$$\begin{aligned} B:&\quad v_1^{\rightarrow} + v_2^{\leftarrow} = v_2^{\rightarrow} + v_3^{\rightarrow} \\ C:&\quad v_4^{\rightarrow} + v_2^{\leftarrow} = v_2^{\rightarrow} + v_3^{\rightarrow} \end{aligned} \tag{1}$$

from which follows

$$v_4^{\rightarrow} = v_1^{\rightarrow} \quad \text{and} \quad v_3^{\rightarrow} = v_1^{\rightarrow} - v_2^{\rightarrow} + v_2^{\leftarrow} = v_1^{\rightarrow} - v_2^{\text{net}}. \tag{2}$$

This leaves $v_2^{\leftarrow}$, $v_2^{\rightarrow}$ to be determined (remembering that $v_1^{\rightarrow} = v_1^{\text{net}}$ is measured directly). To this end the carbon isotope balance equations are established. As an example the flux $v_3^{\rightarrow}: B_1 \rightarrow C_2$ (interpreted as a molar carbon atom flux rather than a molar flux of metabolites as shown in the left and right part of Fig. 4, respectively) carries the amount of $v_3^{\rightarrow} \cdot B_1$ labeled carbon atoms per unit time. This term contributes to the label balances of B_1 and C_2, but with opposite signs. The complete set of equations for the pools B_1, B_2, C_1, C_2 is now

$$\begin{aligned} B_1:&\quad 0 = v_1^{\rightarrow}A_1 - v_2^{\rightarrow}B_1 + v_2^{\leftarrow}C_1 - v_3^{\rightarrow}B_1 \\ B_2:&\quad 0 = v_1^{\rightarrow}A_2 - v_2^{\rightarrow}B_2 + v_2^{\leftarrow}C_2 - v_3^{\rightarrow}B_2 \\ C_1:&\quad 0 = v_2^{\rightarrow}B_1 - v_2^{\leftarrow}C_1 + v_3^{\rightarrow}B_2 - v_4^{\rightarrow}C_1 \\ C_2:&\quad 0 = v_2^{\rightarrow}B_2 - v_2^{\leftarrow}C_2 + v_3^{\rightarrow}B_1 - v_4^{\rightarrow}C_2. \end{aligned} \tag{3}$$

From these equations it becomes clear that negative flux values do not produce a meaningful system description which has to be taken into account for flux determination.

In the example the flux determination problem can be solved explicitly. We have finished when $v_2^{\rightarrow}$, $v_2^{\leftarrow}$ have been computed from $v_1^{\rightarrow}$, B_1, C_2. The label conservation equations

$$A_1 + A_2 = B_1 + B_2 = C_1 + C_2$$

can be derived from Equations (2) and (3). Using this, the unknown fluxes are calculated to be

$$v_2^{\leftarrow} = \frac{B_1 - A_1}{A_1 + A_2 - B_1 - C_2} \cdot v_1^{\rightarrow}$$

$$v_2^{\rightarrow} = \frac{C_2 - B_1}{A_1 + A_2 - 2B_1} \cdot (v_2^{\leftarrow} + v_1^{\rightarrow}).$$

This shows how both rates of bidirectional reactions can in principle be computed from labeling data. With conventional measurement techniques nothing more than the quantity $v_1^{\rightarrow} = v_4^{\rightarrow} = v_2^{\rightarrow} - v_2^{\leftarrow} + v_3^{\rightarrow}$ can be observed!

General Flux Model

A general model for arbitrary metabolic networks is now formulated. Based on this model, fractional labels can be computed when all fluxes are known. This enables ^{13}C isotope labeling experiments to be simulated. The model makes extensive use of matrix calculus to obtain a concise notation. All matrices are constant and represent structural qualities of the underlying network,[38] i.e., they do not depend on the state variables. Furthermore, they are more or less sparsely populated, which can be exploited for reduction of memory requirements and speedup of numerical computations.

To begin with, the state vectors have to be introduced. The flux vectors

$$\mathbf{v}^{\rightarrow}, \mathbf{v}^{\leftarrow}$$

(of equal dimension) comprise both directions of all the molar fluxes in the reaction network. In the example of Figure 4 these fluxes are $\mathbf{v}^{\rightarrow} = (v_1^{\rightarrow}, v_2^{\rightarrow}, v_3^{\rightarrow}, v_4^{\rightarrow})^T$ and $\mathbf{v}^{\leftarrow} = (v_1^{\leftarrow}, v_2^{\leftarrow}, v_3^{\leftarrow}, v_4^{\leftarrow})^T$. From these vectors the composite overall flux vector (of twice the dimension) and the corresponding net flux vector is formed:

$$\mathbf{v} = \begin{pmatrix} \mathbf{v}^{\rightarrow} \\ \mathbf{v}^{\leftarrow} \end{pmatrix} \qquad \mathbf{v}^{\text{net}} = \mathbf{v}^{\rightarrow} - \mathbf{v}^{\leftarrow}.$$

This is how in our analysis full account can be taken of bidirectional fluxes. On the other hand, it will be explained in the section on exchange fluxes how available knowledge can be incorporated by introducing irreversibility or rapid equilibrium assumptions.

Finally, the vector of intracellular fractional labels of each (enumerated) carbon atom in the intracellular metabolites as well as the vector of input labels comprising the known fractional labels of all carbon atoms fed into the system are required. These two vectors are denoted by

$$\mathbf{x}, \mathbf{x}^{\text{in}}$$

In the example $\mathbf{x} = (B_1, B_2, C_1, C_2)^T$ and $\mathbf{x}^{\text{in}} = (A_1, A_2)^T$.

The metabolite flux balances are formulated using the well-known stoichiometric matrix $\mathbf{N}$ and Equation (4), which leads to the linear equation system

$$\mathbf{N} \cdot \mathbf{v}_{\text{net}} = \mathbf{N} \cdot \mathbf{v}^{\rightarrow} - \mathbf{N} \cdot \mathbf{v}^{\leftarrow} = \mathbf{0}. \qquad (5)$$

In the example equations (1) lead to

$$\mathbf{N} = \begin{pmatrix} 1 & -1 & -1 & \cdot \\ \cdot & 1 & 1 & -1 \end{pmatrix}$$

where points denote zeroes. The carbon isotope label balance equations (3) have a bilinear structure with respect to $\mathbf{x}$ and $\mathbf{v}$; i.e., all terms of type $\pm \mathbf{x}_j \mathbf{v}_i$ containing a certain flux $\mathbf{v}_i$ and some involved pool variable $\mathbf{x}_j$. The corresponding coefficients ± 1 can therefore be collected in a square matrix $\mathbf{P}_i$ and a rectangular matrix $\mathbf{P}_i^{\text{in}}$ associated with $\mathbf{v}_i$. Here, $\mathbf{P}_i$ describes transitions between intracellular pools, while $\mathbf{P}_i^{\text{in}}$ describes transitions involving one extracellular partner. In the example [compare to Equation (3)]

$$\mathbf{P}_2^{\rightarrow} = \begin{pmatrix} -1 & \cdot & \cdot & \cdot \\ \cdot & -1 & \cdot & \cdot \\ 1 & \cdot & \cdot & \cdot \\ \cdot & 1 & \cdot & \cdot \end{pmatrix}$$

$$\mathbf{P}_2^{\leftarrow} = \begin{pmatrix} \cdot & 1 & \cdot & \cdot \\ \cdot & \cdot & 1 & \cdot \\ \cdot & -1 & \cdot & \cdot \\ \cdot & \cdot & -1 & \cdot \end{pmatrix}$$

$$\mathbf{P}_1^{\text{in}} = \begin{pmatrix} 1 & \cdot \\ \cdot & 1 \\ \cdot & \cdot \\ \cdot & \cdot \end{pmatrix}.$$

Using matrix notation the carbon pool balance equations can now be written as

$$\left(\sum_i \mathbf{v}_i \cdot \mathbf{P}_i\right) \cdot \mathbf{x} + \left(\sum_i \mathbf{v}_i \cdot \mathbf{P}_i^{\text{in}}\right) \cdot \mathbf{x}^{\text{in}} = \mathbf{0}. \qquad (6)$$

From these equations it follows immediately that

$$\mathbf{x} = \mathbf{x}(\mathbf{v}) = -\left(\sum_i \mathbf{v}_i \cdot \mathbf{P}_i\right)^{-1} \left(\sum_i \mathbf{v}_i \cdot \mathbf{P}_i^{\text{in}}\right) \cdot \mathbf{x}^{\text{in}} \qquad (7)$$

is a function of $\mathbf{v}$. This equation is the key to the numerical simulation of ^{13}C tracer experiments.

Flux Estimation

Clearly, flux estimation is an inverse problem associated with Equation (7); i.e., a flux vector $\mathbf{v}$ has to be found that reproduces all the measured fluxes and labels. Unlike the example, the flux determination problem cannot always be solved explicitly because the nonlinear equation system is too greatly entangled. In this situation a parameter fitting approach is suitable, as is now described.

The measurement matrices $\mathbf{M}_{\mathbf{v}}^{\text{net}}$, $\mathbf{M}_{\mathbf{x}}$ are used to describe which net fluxes and intracellular labels are measured. They are both composed of unit vectors. In the example v_1^{net}, B_1, C_2 are measured, and therefore we have

$$\mathbf{M}_v^{net} = (1 \quad \cdots) \qquad \mathbf{M}_x = \begin{pmatrix} 1 & \cdots & \\ & \cdots & 1 \end{pmatrix}.$$

The complete measurement equations are then

$$\mathbf{w} = \mathbf{M}_v^{net} \cdot \mathbf{v}^{net} + \epsilon_v$$

$$\mathbf{y} = \mathbf{M}_x \cdot \mathbf{x} + \epsilon_x. \tag{8}$$

Here $\mathbf{w}$, $\mathbf{y}$ denote the vectors of measured fluxes and labels; ϵ_v, ϵ_x are normally distributed measurement noise terms with expectation $\mathbf{0}$ and covariance matrices $\mathbf{\Sigma}_v$, $\mathbf{\Sigma}_x$.

The familiar least-squares flux estimator is constructed from Equations (8) by minimizing the sum-of-squares function

$$\kappa(\upsilon) = \|\mathbf{w} - \mathbf{M}_v^{net} \cdot (\mathbf{v}^{\rightarrow} - \mathbf{v}^{\leftarrow})\|^2_{\Sigma_v} + \|\mathbf{y} - \mathbf{M}_x \cdot \mathbf{x}(\mathbf{v})\|^2_{\Sigma_x} \tag{9}$$

where $\|\xi\|^2_\Sigma = \xi^T \cdot \mathbf{\Sigma}^{-1} \cdot \xi$ denotes the squared weighted norm corresponding to a covariance matrix $\mathbf{\Sigma}$. Putting equations (5), (7), and (8) together we are left with a linearly constrained minimization problem for flux estimation:

$$\begin{aligned} &\text{minimize} && \kappa(\mathbf{v}) \\ &\text{with respect to} && \mathbf{N} \cdot \mathbf{v}^{net} = \mathbf{0} \quad \text{and} \quad \mathbf{v} \geqslant \mathbf{0}. \end{aligned} \tag{10}$$

The resulting flux estimator is denoted by $\hat{\mathbf{v}}$. Numerical algorithms for solving this problem are described later.

Exchange Fluxes

In the example from Figure 4 only one intracellular flux was assumed to be bidirectional as expressed by the flux variables $v_2^{\rightarrow}$ and $v_2^{\leftarrow}$. If v_3 would also split into two directions, the available amount of measured quantities would no longer be sufficient for flux determination. In general, the number of unknown flux variables must not exceed the number of measured values.

To prevent the investigated labeling system from being underdetermined, reversibility assumptions on fluxes must be introduced. Three types of assumptions are frequently encountered in the literature:

1. If a reaction step is known to be highly reversible (i.e. $\mathbf{v}_i^{\rightarrow} + \mathbf{v}_i^{\leftarrow} \gg \mathbf{v}_i^{net}$), we can eliminate some variables by using a rapid equilibrium technique.[46]
2. When reaction steps cross the system border (e.g., a substrate uptake step), they are assumed to be irreversible.
3. Reaction steps exposing a large ΔG^0 value in vitro may be assumed to be irreversible in vivo too, which means that either $\mathbf{v}_i^{\rightarrow}$ or $\mathbf{v}_i^{\leftarrow}$ is zero.

A formal notation is needed to express these assumptions, i.e., to introduce further numerical constraints on the flux vector $\mathbf{v}$ in the minimization equation (10). To this end a quantity must be defined that describes the degree of reversibility for some bidirectional reaction step. For example, the quantity $\mathbf{v}_i^{\rightarrow} + \mathbf{v}_i^{\leftarrow}$ was introduced elsewhere[46] to study the rapid equilibrium behavior $\mathbf{v}_i^{\rightarrow} + \mathbf{v}_i^{\leftarrow} \to \infty$. However, this is not a useful formalism when irreversibility has to be expressed since in that case it depends on $\mathbf{v}_i^{net}$. For this reason we define the exchange flux of the ith reaction to be

$$\mathbf{v}_i^{ex} = \min(\mathbf{v}_i^{\rightarrow}, \mathbf{v}_i^{\leftarrow}), \tag{11}$$

which means that $\mathbf{v}_i^{ex}$ is the amount of flux that is common to both reaction directions in relation to $\mathbf{v}_i^{net}$. This makes it easy to express the above-mentioned modeling assumptions.

$\mathbf{v}_i^{ex} = 0$ means irreversibility of step i

$\mathbf{v}_i^{ex} = \infty$ means rapid equilibrium of step i.

Clearly, any other value for $\mathbf{v}_i^{net}$ can be fixed for simulation purposes. On the other hand, if nothing is kept fixed, both flux directions can be freely varied. The reversibility assumptions made for a given metabolic network must be carefully documented to ensure reproducibility of the results. In our case they are given within Figure 3 where bidirectional fluxes are indicated by hexagonal symbols while all other fluxes are assumed to be irreversible. For better readability the numbers given in the hexagons are the normalized exchange fluxes $|\mathbf{v}_i^{ex}/\mathbf{v}_i^{net}|$.

In previous approaches, exchange fluxes could not be taken into extensive consideration because not enough measurement information was available to quantify fluxes and exchanges simultaneously. As a consequence, previously obtained results may be biased due to oversimplifying assumptions concerning irreversibility or rapid equilibria that had to be made. The experimental technique presented in this contribution supplies a previously unattainable amount of (stationary) flux and label measurements that enables to quantitate both net fluxes and exchange rates with only a few assumptions.

Numerical Algorithms

Presentation of the rather technical details of incorporating additional constraints and their computational treatment exceeds the scope of this article. Thus only some basic principles will be given here and more details will be published elsewhere.

It is well known from general tracer kinetics[2] that the system matrix $\sum_{i=1}^{n} \mathbf{v}_i \cdot \mathbf{P}_i$ of Equation (6) is diagonally dominant and thus can be treated by iterative methods.[15] On the other hand, it can be proven that high exchange fluxes lead to ill-conditioned system matrices, so that QR decomposition far outperformed an iterative solution for solving Equation (7).[16, 64]

Having established a simulation algorithm, the flux estimation equation (10) can be solved by iterative optimization methods.[47] The linear constraints given by Equation (5) are treated by singular value decomposition.[36,58] It should be recognized that the inequality $\mathbf{v} \geqslant 0$ has to be strictly recognized and that exchange fluxes as defined by Equation

(11) are not everywhere differentiable with respect to **v**. This makes flux estimation a delicate numerical problem. As a first practicable approach, a robust derivative-free method was used to solve the minimization problem at the cost of high computation times. Further work is devoted to the development of a modified Gauss–Newton type algorithm that enables the almost everywhere differentiable, linearly constrained problem to be treated.

The most important property of exchange fluxes with respect to the parameter fitting algorithm is that a fixed exchange flux does not prescribe a reaction direction; i.e., the sign of the corresponding net flux can still vary freely. For this reason, the algorithm will find the reaction direction that best fits the data.

Automatic Generation of Equations

As shown in this Appendix all model equations required for describing the isotope labeling system can be built up from certain vectors and matrices. However, the dimensions can become quite large (about 100 for a reasonably complex metabolic network). A manual input of these structures would be time consuming and susceptible to errors. Moreover, model variation studies would be quite time consuming if manual input were used. For these reasons a compiler program was implemented that generates the required structures from a text file describing the biochemical network together with the measured data in a convenient way.[62] The following formal notation is used therein:

1. Each reaction is expressed using the familiar biochemical sum notation. The atom transitions are specified afterward. For example, the transaldolase reaction from the PPP is written as

```
x9 : gap    + s7p       > e4p    + f6p
     #ABC + #abcdefg > #defg + #abcABC .
```

This means that the first carbon atom of gap (denoted A) is taken over to the fourth carbon atom of f6p and so on.

2. It now becomes clear how integer stoichiometric coefficients other than 1 can be expressed. If a metabolite occurs twice, it has to be repeated. For example, the conversion of fructose 1,6-bisphosphate to glyceraldehyde 3-phosphate is simply written as

```
x3 : f16bp      > gap    + gap
     #ABCDEF > #CBA + #DEF .
```

Similarly the scrambling reaction of fumarate can be expressed by

```
x14 : fum     + fum     > oaa     + oaa
      #ABCD + #UVWX > #ABCD + #XWVU .
```

3. Sometimes noninteger coefficients have been used to express biomass composition.[58] Such equations make no sense when carbon atoms have to be traced through the network. However, they can be easily replaced by a set of equations that describe the incorporation of each precursor metabolite into biomass. For example, incorporation of glucose 6-phosphate is written as

```
b1: g6p       > g6pBiomass
    #ABCDEF > #ABCDEF .
```

The corresponding "noninteger coefficient" is then supplied separately as a flux measurement value computed from biomass composition and growth rate. This is in any case the more natural way to take biomass composition into account.

The NMRFlux program translates this text input to the vector and matrix notation described above by using the recursive descent method as a standard technique for compiler construction.[1]

A companion program takes the generated vectors and matrices as input and performs the numerical computations as described above. For performing simulation runs, all linear independent flux parameters can be interactively changed. Similarly, the exchange fluxes can be fixed to given values. This led to valuable insight concerning the sensitivity of estimated exchange fluxes. Finally, the iterative optimization procedure can be set up and all results are written to a protocol file for further use.

References

1. Aho, A. V., Sethi, R., Ullman, J. D. 1986. Compilers—principles, techniques and tools. Addison-Wesley, London.
2. Anderson, D. H. 1983. Compartmental modelling and tracer kinetics. In: S. Levin (ed.), Lecture notes in biomathematics. Springer-Verlag, Berlin.
3. Bergmeyer, H. U., Bernt, E., Schmidt, F., Stork, H. 1974. pp. 1196–1201. In: H. U. Bergmeyer (ed.), Methods of enzymatic analysis, 2nd edition. Academic Press, New York.
4. Berthon, H. A., Bubb, W. A., Kuchel P. W. 1993. ^{13}C n.m.r. isotopomer and computer-simulation studies of the non-oxidative pentose phosphate pathway of human erythrocytes. Biochem. J. **296**: 379–387.
5. Börmann-El Kholy, E. R., Eikmanns, B. J., Gutmann, M., Sahm, H. 1993. Glutamate dehydrogenase is not essential for glutamate formation by *Corynebacterium glutamicum*. Appl. Environ. Microbiol. **59**: 2329–2331.
6. Bröer, S., Eggeling, L., Krämer, R. 1993. Strains of *Corynebacterium glutamicum* with different lysine productivities may have different lysine excretion systems. Appl. Environ. Microbiol. **59**: 316–321.
7. Cremer, J., Eggeling, L., Sahm, H. 1991. Control of the lysine biosynthesis sequence in *Corynebacterium glutamicum* as analysed by overexpression of the individual corresponding genes. Appl. Environ. Microbiol. **60**: 1746–1752.
8. Diaz-Ricci, J. C., Tsu, M., Bailey, J. E. 1992. Influence of expression of the *pet* operon on intracellular metabolic fluxes of *Escherichia coli*. Biotechnol. Bioeng. **39**: 59–65.
9. Eikmanns, B. J., Follettie, M. T., Girot, M. U., Sinskey, A. J. 1989. The phosphoenolpyruvate carboxylase gene of *Corynebacterium glutamicum:* Molecular cloning, nucleotide sequence and expression. Mol. Gen. Genet. **218**: 330–339.
10. Eikmanns, B. J., Rittmann, D., Sahm, H. 1995. Cloning, sequence

analysis, expression, and inactivation of the *Corynebacterium glutamicum icd* gene encoding isocitrate dehydrogenase and biochemical characterization of the enzyme. J. Bacteriol. **177**: 774–782.
11. Flanigan, I., Collins, J. G., Arora, K. K., MacLeod, J. K., Williams, J. F. 1993. Exchange reactions catalysed by group-transferring enzymes oppose the quantitation and the unravelling of the identity of the pentose pathway. Eur. J. Biochem. **213**: 477–485.
12. Folkerts, M., Ney, U., Kneifel, H., Stackebrandt, E., Witte, E. G., Fõrstel, H., Schoberth, S. M., Sahm, H. 1989. *Desulfovibrio furfuralis* sp. nov., a furfural degrading strictly anaerobic bacterium. System. Appl. Microbiol. **11**: 161–169.
13. Goel, A., Ferrance, J., Jeong, J., Ataai, M. M. 1993. Analysis of metabolic fluxes in batch and continuous cultures of *Bacillus subtilis*. Biotechnol. Bioeng. **42**: 686–696.
14. Gubler, M., Park, S. M., Jetten, M., Stephanopoulos, G., Sinskey, A. J. 1994. Effects of phosphoenol pyruvate carboxylase deficiency on metabolism and lysine production in *Corynebacterium glutamicum*. Appl. Microbiol. Biotechnol. **40**: 857–863.
15. Gubler, M., Jetten, M., Lee, S. H., Sinskey, A. J. 1994. Cloning of the pyruvate kinase gene (*pyk*) of *Corynebacterium glutamicum* and site-specific inactivation of *pyk* in a lysine-producing *Corynebacterium lactofermentum* strain. Appl. Environ. Microbiol. **60**: 2501–2507.
16. Hager, W. W. 1988. Applied numerical linear algebra. Prentice-Hall, Englewood Cliffs, NJ.
17. Ishino, S., Kuga, T., Yamaguchi, K., Shirahata, K., Araki, K. 1986. ^{13}C NMR studies of histidine fermentation with a *Corynebacterium glutamicum* mutant. Agric. Biol. Chem. **50**: 307–310.
18. Ishino, S., Shimomura-Nishimuta, J., Yamaguchi, K., Shirahata, K., Araki, K. 1991. ^{13}C NMR studies of glucose metabolism in L-glutamic acid and L-lysine fermentation by *Corynebacterium glutamicum*. J. Gen. Appl. Microbiol. **37**: 157–165.
19. Jetten, M. S. M., Sinskey, A. J. 1989. Characterisation of phosphoenolpyruvate carboxykinase from *Corynebacterium glutamicum*. FEMS Microbiol. Lett. **111**: 183–188.
20. Jetten, M. S. M., Pitoc, G. A., Follettie, M. T., Sinskey, A. J. 1994. Regulation of phospho(enol)-pyruvate- and oxaloacetate-converting enzymes in *Corynebacterium glutamicum*. Appl. Microbiol. Biotechnol. **41**: 47–52.
21. Kashiwaya, Y., Sato, K., Tsuchiya, N., Thomas, S., Fell, D. A., Veech, R. L., Passonneau, J. V. 1994. Control of glucose utilization in working perfused rat heart. J. Biol. Chem. **269**: 25502–25514.
22. Katz, J., Wals, P., Lee, W.-N. P. 1993. Isotopomer studies of gluconeogenesis and the Krebs cycle with ^{13}C-labeled lactate. J. Biol. Chem. **268**: 25509–25521.
23. Kawahara, Y., Tanaka, T., Ikeda, S., Sone, N. 1988. Coupling sites of the respiratory chain of *Brevibacterium lactofermentum*. Agric. Biol. Chem. **52**: 1979–1983.
24. Kinoshita, S., Tanaka, K. 1972. Glutamic acid. pp. 263–324. In: K. Yamada (ed.), The microbial production of amino acids. Wiley, New York.
25. Kiss, R. D., Stephanopoulos G. 1992. Culture instability of auxotrophic amino acid producers. Biotechnol. Bioeng. **40**: 75–85.
26. Malloy, C. R., Sherry, A. D., Jeffrey, F. M. H. 1988. Evaluation of carbon flux and substrate selection through alternative pathways involving the citric acid cycle of the heart by ^{13}C NMR spectroscopy. J. Biol. Chem. **263**: 6964–6971.
27. Mancuso, A., Sharfstein, S. T., Tucker, S. N., Clark, D. S., Blanch, H. W. 1994. Examination of primary metabolic pathways in murine hybridoma with carbon-13 nuclear magnetic resonance spectroscopy. Biotechnol. Bioeng. **44**: 563–585.
28. Minikami, S., Yoshikawa, H. 1965. Thermodynamic considerations of erythrocyte glycolysis. Biochem. Biophys. Res. Commun. **18**: 345–349.
29. Nakayama, K. 1985. Lysine. pp. 607–620. In: M. Moo-Young (ed.), Comprehensive biotechnology. Pergamon, Oxford.
30. Neidhardt, F. C., Ingraham, J. L., Schaechter M. 1990. Physiology of the bacterial cell. pp. 133–173. Sinauer Associates, Sunderland, MA.
31. Neijssel, O. M., Teixeira de Mattos, M. J. 1994. The energetics of bacterial growth: A reassessment. Mol. Microbiol. **13**: 179–182.
32. Papoutsakis, E. T., Meyer, C. L. 1985. Equations and calculations of product yields and preferred pathway for butanediol and mixed-acid fermentations. Biotechnol. Bioeng. **27**: 50–66.
33. Pátek, M., Krumbach, K., Eggeling, L., Sahm, H. 1994. Leucine synthesis in *Corynebacterium glutamicum:* Enzyme activities, structure of *leuA*, and effect of *leuA* inactivation on lysine synthesis. Appl. Environ. Microbiol. **60**: 133–140.
34. Peters-Wendisch, P. G., Eikmanns, B. J., Thierbach, G., Bachmann, B., Sahm, H. 1993. Phosphoenolpyruvate carboxylase in *Corynebacterium glutamicum* is dispensable for growth and lysine production. FEMS Microbiol. Lett. **112**: 269–274.
35. Portais, J.-C., Schuster, R., Merle, M., Canioni, P. 1993. Metabolic flux determination in C6 glioma cells using carbon-13 distribution upon [1-^{13}C]glucose incubation. Eur. J. Biochem. **217**: 457–468.
36. Press, W. H., Flannery, B. P., Teukolsk, S. A., Vetterling W. T. 1988. Numerical recipes in C—the art of scientific computing. Cambridge University Press, Cambridge.
37. Rabkin, M., Blum, J. J. 1985. Quantitative analysis of intermediary metabolism in hepatocytes incubated in the presence and absence of glucagon with a substrate mixture containing glucose, ribose, fructose, alanine and acetate. Biochem. J. **225**: 761–786.
38. Reder, C. 1988. Metabolic control theory: A structural approach. J. Theor. Biol. **135**: 175–201.
39. Reinscheid, D. J., Kronemeyer, W., Eggeling, L., Eikmanns, B. J., Sahm, H. 1994. Stable expression of *hom-l-thrB* in *Corynebacterium glutamicum* and its effect on the carbon flux to threonine and related amino acids. Appl. Environ. Microbiol. **60**: 126–132.
40. Reinscheid, D. J., Eikmanns, B. J., Sahm, H. 1994. Characterisation of the isocitrate lyase gene from *Corynebacterium glutamicum* and biochemical analysis of the enzyme. J. Bacteriol. **176**: 3474–3483.
41. Reinscheid, D. J., Eikmanns, B. J., Sahm, H. 1994. Malate synthase from *Corynebacterium glutamicum:* Sequence analysis of the gene and biochemical characterization of the enzyme. Microbiology **140**: 3099–3108.
42. Russel, J. B., Cook, G. M. 1995. Energetics of bacterial growth: Balance of anabolic and catabolic reactions. Microbiol. Rev. **59**: 48–62.
43. Savinell, J. M., Palsson, B. O. 1992. Optimal selection of metabolic fluxes for in vivo measurement. I. Development of mathematical methods. J. Theor. Biol. **155**: 201–214.
44. Schrumpf, B., Schwarzer, A., Kalinowski, J., Pühler, A., Eggeling, L., Sahm, H. 1991. Functionally split pathway for lysine synthesis in *Corynebacterium glutamicum*. J. Bacteriol. **173**: 4510–4516.
45. Schrumpf, B., Eggeling, L., Sahm, H. 1992. Isolation and prominent characteristics of an L-lysine hyperproducing strain of *Corynebacterium glutamicum*. Appl. Microbiol. Biotechnol. **37**: 566–571.
46. Schuster, R., Schuster, S., Holzhütter, H.-G. 1992. Simplification of complex kinetic models used for the quantitative analysis of nuclear magnetic resonance or radioactive tracer studies. J. Chem. Soc. Faraday Trans. **88**: 2837–2844.
47. Seber, G. A. F., Wild, C. J. 1989. Nonlinear regression. Wiley, New York.
48. Shaka, A. J., Barker, P. B., Freeman, R. 1985. Computer-optimized decoupling scheme for wideband applications and low-level operation. J. Magn. Reson. **64**: 547–552.
49. Sharfstein, S. T., Tucker, S. N., Mancuso, A., Blanch, H. W., Clark, D. S. 1994. Quantitative in vivo nuclear magnetic resonance studies of hybridoma metabolism. Biotechnol. Bioeng. **43**: 1059–1074.
50. Shiio, I., Ujigawa-Takeda, K. 1980. Presence and regulation of α-ketoglutarate dehyrogenase complex in a glutamate-producing bacterium, *Brevibacterium flavum*. Agric. Biol. Chem. **44**: 1897–1904.
51. Shvinka, Yu. E., Viestur, U. E., Toma, M. K. 1979. Alternative pathways of oxidation in the respiratory chain of *Brevibacterium flavum*. Microbiology **48**: 4–10.
52. Sonntag, K., Eggeling, L., de Graaf, A. A., Sahm, H. 1993. Flux

partitioning in the split pathway of lysine synthesis in *Corynebacterium glutamicum:* Quantification by ^{13}C- and ^{1}H-NMR spectroscopy. Eur. J. Biochem. **213**: 1325–1331.
53. Stephanopoulos, G., Vallino, J. J. 1991. Network rigidity and metabolic engineering in metabolic overproduction. Science **252**: 1675–1680.
54. Stryer, L. 1988. Biochemistry, 3rd edition. W. H. Freeman, New York.
55. Sugimoto, S.-I., Shiio, I. 1987. Regulation of glucose-6-phosphate dehydrogenase in *Brevibacterium flavum*. Agric. Biol. Chem. **51**: 101–108.
56. Sugimoto, S. I., Shiio, I. 1987. Regulation of 6-phosphogluconate dehydrogenase in *Brevibacterium flavium*. Agric. Biol. Chem. **51**: 1257–1263.
57. Tosaka, O., Morioka, H., Takinami, K. 1979. The role of biotin dependent pyruvate carboxylase in L-lysine production. Agric. Biol. Chem. **43**: 1513–1519.
58. Vallino, J. J., Stephanopoulos, G. 1990. Flux determination in cellular bioreaction networks: Application to lysine fermentation. pp. 205–219. In: S. K. Sikdar, M. Bier, and P. Todd (eds.), Frontiers in bioprocessing. CRC Press, Boca Raton, FL.
59. Vallino, J. J., Stephanopoulos, G. 1993. Metabolic flux distributions in *Corynebacterium glutamicum* during growth and lysine overproduction. Biotechnol. Bioeng. **41**: 633–646.
60. Walker, T. E., Han, C. H., Kollman, V. H., London, R. E., Matwiyoff, N. A. 1982. ^{13}C NMR studies of the biosynthesis by *Microbacterium ammoniaphilum* of L-glutamate selectively enriched with carbon-13. J. Biol. Chem. **257**: 1189–1195.
61. Walsh, K., Koshland, Jr., D. E. 1984. Determination of flux through the branch point of two metabolic cycles. J. Biol. Chem. **259**: 9646–9654.
62. Wiechert, W. 1994. Design of a software framework for flux determination by ^{13}C NMR isotope labeling experiments. pp. 305–310. In: E. Gnaiger, F. N. Gellerich, and M. Wyss (eds.), Modern trends in biothermokinetics. Innsbruck University Press, Innsbruck.
63. Wood, T. 1985. The pentose phosphate pathway. Academic, Orlando, FL.
64. Zupke, C., Stephanopoulos, G. 1994. Modeling of isotope distributions and intracellular fluxes in metabolic networks using atom mapping matrices. Biotechnol. Prog. **10**: 489–498.
65. Zupke, C., Stephanopoulos, G. 1995. Intracellular flux analysis in hybridomas using mass balances and in vitro ^{13}C NMR—human fibronectin IgG-producing hybridoma cell culture intracellular flux analysis by mass balance. Biotechnol. Bioeng. **45**: 292–303.

JOURNAL OF BACTERIOLOGY, Apr. 1997, p. 2724–2730
0021-9193/97/$04.00+0

Vol. 179, No. 8

Interruption of the Phosphoglucose Isomerase Gene Results in Glucose Auxotrophy in *Mycobacterium smegmatis*

DAVID TUCKMAN,[1] ROBERT J. DONNELLY,[2] FENG X. ZHAO,[3] WILLIAM R. JACOBS, JR.,[1] AND NANCY D. CONNELL[3,4]*

Departments of Microbiology and Molecular Genetics,[3] National Tuberculosis Center, Department of Medicine,[4] and Department of Pathology and Laboratory Medicine,[2] UMDNJ, New Jersey Medical School, Newark, New Jersey, and Howard Hughes Medical Institute and Department of Microbiology and Immunology, Albert Einstein Medical School, Bronx, New York[1]

Received 24 October 1996/Accepted 10 February 1997

Two glycerol utilization mutants of *Mycobacterium smegmatis* that were unable to utilize most carbon sources except glucose were isolated. Supplementation of these media with small amounts of glucose restored growth in the mutants; these strains are therefore glucose auxotrophs. The mutant phenotype is complemented by the gene encoding phosphoglucose isomerase (*pgi*), and direct measurement of enzyme activities in the mutants suggests that this gene product is absent in the auxotrophic strains. Mapping of the mutant allele by Southern analysis demonstrates the presence of a 1-kb deletion extending into the coding sequence of *pgi*. The possible roles of phosphoglucose isomerase in mycobacterial cell wall synthesis and metabolic regulation are discussed.

The resurgence of diseases caused by mycobacteria has spurred a new interest in these acid-fast organisms. Although current research is largely directed towards virulence mechanisms in pathogenic strains of mycobacteria, basic biochemical information about these organisms is essential for understanding their interactions with their hosts and for developing new therapeutics. Knowledge of intermediary metabolism of the mycobacteria has been fragmentary, in large part due to the low growth rates, tendency to clump in culture, and lack of genetics systems of members of this genus. Mycobacteria exhibit unusual and complex patterns of carbohydrate utilization. In *Mycobacterium tuberculosis*, *Mycobacterium phlei*, and *Mycobacterium smegmatis*, glycerol utilization is blocked until all other carbon sources, including glutamate and asparagine, have been consumed (3, 23, 38). Nevertheless, glycerol is considered the preferred carbon source under laboratory conditions. Growth of most species on this substrate results in greater mass per unit volume of growth medium (32).

Glycerol and its metabolic derivatives are at the interface of catabolic (glycolytic and oxidative pathways) and anabolic (lipid biosynthesis and gluconeogenesis) processes and therefore play important growth regulatory roles in cells grown on a variety of carbon sources. In addition, glycerol is an important precursor of key cell wall constituents. The presence of glycolipids such as the acyl glycerols and acylglucoses varies widely depending on the carbon source in the medium (4). A number of the enzymes of glycolysis, the hexose monophosphate shunt, and the Entner-Doudoroff pathways have been studied (reviewed in reference 26). However, carbon metabolism in mycobacteria has not been characterized at the genetic level and few genes encoding glycolytic enzymes have been cloned.

We have initiated a genetic approach to the study of carbohydrate metabolism in *M. smegmatis* by isolating and characterizing mutants unable to utilize certain substrates as sole carbon sources. In this study, we describe two strains obtained in a screen for glycerol utilization mutants. Unexpectedly, these mutants are unable to use any carbohydrate except glucose as a sole carbon source. Genetic complementation of the growth defect on glycerol was accomplished by expression of the gene encoding phosphoglucose isomerase (*pgi*), which we have cloned and sequenced. The mutants lack detectable levels of Pgi, a key enzyme in glycolysis that functions at the juncture of gluconeogenesis and catabolism. Finally, we demonstrate that *pgi* mutants in *M. smegmatis* are defective in the utilization of many carbohydrates as sole carbon sources because they are actually auxotrophic for glucose.

* Corresponding author. Mailing address: Departments of Microbiology and Molecular Genetics, UMDNJ/New Jersey Medical School, 185 South Orange Ave., Newark, NJ 07103. Phone: (201) 982-3759. Fax: (201) 982-3644. E-mail: connell@umdnj.edu.

MATERIALS AND METHODS

Bacterial strains and plasmids. The bacterial strains and plasmids used are shown in Table 1. *M. smegmatis* mc^{2}155 (27) was used for all mycobacterial experiments. *Escherichia coli* DH5α was used to propagate DNA for cloning, sequencing, and transforming *M. smegmatis*. mc^{2}743 and mc^{2}744 were derived in this study. The plasmids used were pYUB18 and a cosmid library contained therein (13), pMVI203 (28), and pDT252, created in this study, which is pMVI203 bearing a 1.9-kb fragment of mc^{2}155 DNA encoding the *pgi* gene.

Media. *M. smegmatis* was grown as described previously (6). The complete medium used was Middlebrook 7H9 (liquid) or 7H10 (agar; Difco). Minimal media were composed of basal salts medium (0.1% KH_2PO_4, 0.25% $NaHPO_4$, 0.5% NH_4Cl, 0.2% K_2SO_4) supplemented with either glucose (1.0%) or glycerol (0.5%). For auxotrophy studies, glucose was added at a concentration of 0.01%, a level insufficient to support growth in the absence of another carbon source. All liquid cultures were supplemented with 0.05% Tween 80 (Sigma Chemical Co.). Kanamycin sulfate (Sigma) was used at 50 μg/ml.

Mutant isolation. *M. smegmatis* (mc^{2}155) was mutagenized by treatment with *N*-methyl-*N'*-nitro-*N*-nitrosoguanidine (MNNG; Sigma) at 100 μg/ml in basal salts medium. After treatment at 30°C for 2 h, the cells were pelleted and washed three times in basal salts medium with 0.05% Tween 80. The cells were resuspended in Middlebrook 7H9 medium with glycerol at 5 g/liter and glucose at 10 g/liter and incubated at 37°C for 3 h to allow expression of mutant gene products and then diluted onto minimal plates containing glucose and glycerol with 0.05% Tween 80 to facilitate replica plating. Colonies were replica plated onto minimal glycerol plates, and those that did not grow on glycerol were collected from the master plates.

Enzyme assays. Cell extracts were prepared by growing cells in the designated minimal medium to an A_{600} of 0.8 to 1.0. Cells were harvested by centrifugation at 3,000 × *g* for 10 min at 4°C and washed in 10 mM potassium phosphate buffer (1 mM EDTA and 1 mM dithiothreitol). The cell pellet was resuspended in an equal volume of buffer, and the cells were disrupted by passage twice through a French press at 18,000 lb/in^2. The extracts obtained were dialyzed overnight at 4°C in the same phosphate buffer and stored at −70°C.

Glucose phosphate isomerase activity was determined spectrophotometrically by measuring the decrease in A_{340} caused by reduction of β-NADP. Reactions of a total volume of 3 ml contained 42 mM glycylglycine, 3.3 mM D-fructose-6-

TABLE 1. Strains and plasmids used

Strain or plasmid	Description	Reference
Strains		
E. coli K-12 DH5α	*endA1 hsdR17*(r_K^- m_K^+) *supE44 thi-1 recA1 gyrA*(Nal^r) *relA1* Δ(*lacIZYA-argF*)*U169* *deoR* [ϕ80d*lac* Δ(*lacZ*)M15]	12
M. smegmatis		
mc^{2}155	*ept-1*	27
mc^{2}743	*ept-1* Δ1(*pgi*)	This work
mc^{2}744	*ept-1 pgi2*	This work
Plasmids		
pYUB18		24
pMVI203		28
pDT252		This work

phosphate, 0.67 mM β-NADP, 3.3.mM $MgCl_2$, and 5.0 U of glucose-6-phosphate (G6P) dehydrogenase (8).

Triose phosphate isomerase activity was determined spectrophotometrically by measuring the decrease in A_{340} caused by reduction of β-NADP. Reactions of a total volume of 3 ml contained 280 mM triethanolamine, 245 mM glyceraldehyde-3-phosphate, 0.132 mM β-NADP, and 4 U of α-glycerolphosphate dehydrogenase (19).

α-Glycerol phosphate dehydrogenase activity was determined spectrophotometrically by measuring the decrease in A_{340} caused by reduction of β-NADP. Reactions of a total volume of 3 ml contained 290 mM triethanolamine, 2.5 mM dihydroxyacetone phosphate, and 0.13 mM β-NADP (14).

Complementation of mutants with wild-type genomic libraries. The carbohydrate utilization mutant strains mc^{2}743 and mc^{2}744 were transformed with a cosmid library prepared from mc^{2}155 (wild-type) DNA. This library was constructed by ligating 32- to 40-kb fragments of genomic DNA into pYUB18 (24). Transformants were plated on glucose minimal medium to estimate the transformation efficiency and on glycerol minimal medium to select complementing cosmids. mc^{2}743 was complemented for growth on glycerol by 12 cosmids (of 3×10^4 screened), and mc^{2}744 was complemented by 7 cosmids (of 6×10^3 screened). Cosmid DNA was isolated from two representative Glp$^+$ colonies of strains mc^{2}743 and mc^{2}744 and amplified in *E. coli* DH5α. These four cosmid DNAs were then used to transform mc^{2}743 and mc^{2}744. Each was fully capable of complementing mc^{2}743 and mc^{2}744 for growth on glycerol minimal plates. Two of the cosmids were then partially digested with *Sau*3A, and fragments in the range of 1,500 to 5,000 bp were isolated from an agarose gel. The *Sau*3A fragments were ligated into the *Bam*HI site of pMVI203. The resulting recombinant plasmids were pooled and used to transform mc^{2}743 and mc^{2}744. Nine plasmids were recovered. All nine complemented the glycerol-negative phenotype of mc^{2}743; mc^{2}744 was complemented fully by four plasmids. The four plasmids which complemented the glycerol-negative phenotype of both mc^{2}743 and mc^{2}744 showed identical restriction maps; the smallest of these, pDT252, bearing a 1.5-kb insert, was chosen for sequencing. That five plasmids did not complement both mutant strains suggests that mc^{2}744 may have an alternate or additional lesion, and this will be investigated further.

DNA sequencing and deletion mapping. The Erase-a-Base system (Promega) was used to generate a series of deletions from one end of the 1.5-kb insert in pDT252. The plasmid was digested with *Not*I and *Kpn*I and treated with exonuclease III for 0.5 to 10 min. Samples of the reaction were removed at 30-s intervals and separated on an agarose gel. DNA fragments differing by 200 bp in length were collected, treated with S1 nuclease and Klenow large fragment to introduce blunt ends, and self-ligated to produce a series of plasmids for sequencing. Sequencing was performed with an automated sequencer (Applied Biosystems).

Southern hybridization was performed to determine whether sequences found in the wild-type *pgi* region were missing in the mutant chromosome of mc^{2}743. Two micrograms of genomic DNA prepared from mc^{2}155 and mc^{2}743 was digested with various restriction enzymes and analyzed on agarose gels. The Southern transfer procedure used was described previously (15). The probe used for Southern analysis was the plasmid pDT252 containing the entire *pgi* gene.

Nucleotide sequence accession number. The 1,928-bp sequence bearing the phosphoglucose isomerase gene of *M. smegmatis* was deposited in GenBank under accession number U88433.

RESULTS

Isolation and complementation of glycerol utilization mutants. Glycerol-nonutilizing mutants of *M. smegmatis* were isolated as described in Materials and Methods. Of 40,000 colonies screened, two isolates, mc^{2}743 and mc^{2}744, were unable to use glycerol as a sole carbon source. mc^{2}743 and mc^{2}744 had colony morphologies and growth rates on glucose minimal plates similar to those of the wild-type parental strain, mc^{2}155 (data not shown).

Strains mc^{2}743 and mc^{2}744 were transformed with a cosmid library of mc^{2}155 (wild-type) DNA (see Materials and Methods). Several cosmids which complemented the glycerol deficiency in both strains were isolated. Analysis of restriction enzyme digests of four of the cosmids revealed overlapping inserts of similar sizes from the cosmids. An insert of 1.9 kb which complemented the deficiencies in strains mc^{2}743 and mc^{2}744 was subcloned from one of the complementing cosmids. The insert was cloned into pMVI203 to create pDT252. Initial restriction mapping of the clone and construction of internal deletions indicated that the entire 1.9 kb was required for complementation of growth on glycerol for both mutants (data not shown).

Characterization of the mycobacterial gene encoding phosphoglucose isomerase. The sequence of the region of wild-type *M. smegmatis* DNA complementing the two glycerol utilization mutants is shown in Fig. 1. The fragment contains a large single open reading frame (ORF) on one strand and two smaller ORFs on the opposite strand (data not shown). The single long ORF encodes a putative protein of 442 amino acids, beginning with GTG (Val) at position 420, with a predicted molecular mass of 47,649 Da. An alternative start codon is found at position 471, with a methionine codon (ATG), predicting a polypeptide product of 425 amino acids or 45,818 Da. The codon usage pattern is consistent with that of other mycobacterial genes, namely, a G+C content of >65%, due largely to G or C in the third position (36). To determine the identity of the ORF contained in the complementing fragment, we translated the 442-codon ORF and subjected the derived amino acid sequence to a homology search in GenBank by using FASTA. The predicted *M. smegmatis* sequence shows striking homology to that of the products of genes encoding the enzyme phosphoglucose isomerase (Pgi). Multiple sequence alignment demonstrated extensive amino acid homology between the *M. smegmatis* protein and the amino acid sequences of Pgi from *Homo sapiens* (37), *Saccharomyces cerevisiae* (31), *Leishmania mexicana* (22), *Bacillus stearothermophilus* (30), and *E. coli* (11) (data not shown). For example, human Pgi has 49.4% identity over a 447-amino-acid overlap, *S. cerevisiae* has 50.7% identity over a 436-amino-acid overlap, and *E. coli* has 52.9% identity over a 448-amino-acid overlap.

The mutant allele of mc^{2}743 was characterized by designing six pairs of primers to amplify the mutant gene in six overlapping fragments. It was observed that the 3′ end of the mc^{2}743 allele was resistant to amplification by PCR. Southern analysis identified a deletion of approximately 1 kb in the 3′ end of the *pgi* gene. Chromosomal DNA from wild-type and mutant cells was restricted with three enzymes (*Nco*I, *Pst*I, and *Sph*I) recognizing internal sites suggested by the sequence of the cloned fragment carrying the wild-type gene (data not shown). In all cases, there is an approximately 1-kb reduction in the size of one band of the mutant allele; a restriction map of the region is shown in Fig. 2. This result is consistent with the reversion frequency measured for this mutant, which is $<10^{-8}$ (data not shown). Precise determination of the deletion endpoints in the

```
      10        20        30        40        50        60        70        80        90       100
12345678901234567890 12345678901234567890 12345678901234567890 12345678901234567890 12345678901234567890
GGATCCACAGTCCGGTGGGG ACGGATGAAATCAGGTCTTC GATGCGCATACATCCATCAT GTACACCCTCGACACGTTCA CCGCACTAAGGTCGACACAA  100

TGAGCGCTGACATCACCGAA ACTCCCGCATGGCAGGCTTT GTCGGACCACCACGCCGAGA TCGGCGACCGGCATCTGACA GAACTGTTTGCTGACGATCC  200

CGCGCGGGGAACCGAGTTGG CGTTGACCGTCGGGGATCTC TACATCGACTACAGCAAGCA CCGCGTCACGCGGCGCACCC TGGACCTGCTCGTCGACCTG  300

GCGCGCGCGGCCGGGTTGGA GGAGCGCCGGGATGCGATGT TCGCCGGCGAGCACATCAAC ACCTCCGAGGACCGCGCGGT GCTGCACACCGCGCTGCGCT  400

CCCGCGGGACGCCAAGCTGG TGGTGGACGGTCAGGACGTG GTCGCCGATGTGCACGACGT GCTGGACCGCATGGGCGATT TCACCGATCGGTTGCGCAGC  500
                  V  V  D  G  Q  D  V  V  A  D  V  H  D  V  L  D  R  M  G  D  F  T  D  R  L  R  S
GGAGAGTGGACCGGCGCCAC CGGCGAACGCATCACCACGG TGGTCAACATCGGCATCGGC GGCTCGGATCTGGGTCCGGT GATGGTGTACGACGCGCTGC  600
G  E  W  T  G  A  T   G  E  R  I  T  T  V   V  N  I  G  I  G   G  S  D  L  G  P  V   M  V  Y  D  A  L  R
GCCATTACGCCGACGCCGGC ATCTCGGCGCGCTTCGTGTC CAACGTCGACCCCGCCGATC TGGTCGCCAAACTCGACGGC CTGGAGCCGGCGAAGACGTT  700
  H  Y  A  D  A  G   I  S  A  R  F  V  S   N  V  D  P  A  D  L   V  A  K  L  D  G   L  E  P  A  K  T  L
GTTCATCGTCGCCTCCAAGA CGTTCTCGACGCTGGAGACG CTGACCAATGCGACCGCGGC GCGGCGCTGGCTCACCGACG CCCTGGGTGACGCCGCGGTG  800
 F  I  V  A  S  K  T   F  S  T  L  E  T   L  T  N  A  T  A  A   R  R  W  L  T  D  A   L  G  D  A  A  V
GCCAAGCATTCGTCGCGGTG TCCACCAACAAGAAGCTGGT CGACGAAGTTCGGCATCAAC ACCGACAACATGTTCGGGTT CTGGGACTGGGTGGGCGGGC  900
A  K  H  S  S  R  C   P  P  T  R  S  W  S   T  K  F  G  I  N   T  D  N  M  F  G  F   W  D  W  V  G  G  R
GCTACTCGGTGGACAGTGCG ATCGGGTTGAGCGTGATGGC CGTGATCGGCAAGGAACGCT TCGCCGAGTTCCTGGCCGGG TTCCACATCGTCGACGAGCA 1000
 Y  S  V  D  S  A   I  G  L  S  V  M  A   V  I  G  K  E  R  F   A  E  F  L  A  G   F  H  I  V  D  E  H
CTTCCGCACCGCCCCGCTGC ACCAGAACGCTCCGGCGCTG CTGGGGCTGATCGGGCTGTG GTACTCGAATTTCTTTGGCG CGCAATCCCGTGCGGTGCTG 1100
 F  R  T  A  P  L  H   Q  N  A  P  A  L   L  G  L  I  G  L  W   Y  S  N  F  F  G  A   Q  S  R  A  V  L
CCCTACTCCAACGACCTGTC ACGGTTCGCGGCGTACCTGC AGCAGTTGACCATGGAATCC AACGGCAAGTCGGTACGCGC CGACGGCACACCGGTGTCCA 1200
P  Y  S  N  D  L  S   R  F  A  A  Y  L  Q   Q  L  T  M  E  S   N  G  K  S  V  R  A   D  G  T  P  V  S  T
CCGACACCGGTGAGATCTTC TGGGGCGAGCCGGGCACCAA CGGCCAGCACGCCTTCTACC AGTTGCTGCACCAGGGCACC CGACTGGTGCCCGCGGACTT 1300
 D  T  G  E  I  F   W  G  E  P  G  T  N   G  Q  H  A  F  Y  Q   L  L  H  Q  G  T   R  L  V  P  A  D  F
CATCGGGTTCTCCCAGCCCA CCGACGACCTGCCCCACGGCC GATGGCACCGGCAGCATGCA CGACCTGCTGATGAGCAACT TCTTCGCCCAGACCCAGGTG 1400
 I  G  F  S  Q  P  T   D  D  L  P  T  A   D  G  T  G  S  M  H   D  L  L  M  S  N  F   F  A  Q  T  Q  V
CTGGCATTCGGAAAGACCGC CGACGCAATAGCTTCCGAGG GCACCCCCGCAGATGTGGTG CCGCACAAGGTGATGCCCGG CAACCGGCCCACCACCAGCA 1500
L  A  F  G  K  T  A   D  A  I  A  S  E  G   T  P  A  D  V  V   P  H  K  V  M  P  G   N  R  P  T  T  S  I
TCCTCGCCACCAAGCTCACC CCGTCGGTCGTCGGGCAGTT GATCGCCCTCTACGAACATC AGGTGTTCACCGAAGGCGTG ATCTGGGGCATCGACTCGTT 1600
 L  A  T  K  L  T   P  S  V  V  G  Q  L   I  A  L  Y  E  H  Q   V  F  T  E  G  V   I  W  G  I  D  S  F
CGACCAGTGGGGCGTGGAAC TCGGCAAGACGCAGGCCAAG GCCCTGCTCCCGGTTCTGAC CGGCGACAAATCTCCTGCCG CGCAGTCGGATACGTCCACC 1700
 D  Q  W  G  V  E  L   G  K  T  Q  A  K   A  L  L  P  V  L  T   G  D  K  S  P  A  A   Q  S  D  T  S  T
GACGCCCTGGTGCGGCGCTA CCGGACCGAGCGGGGCCGGC CCGCTTAGGCTTCGGCGTCG GCTTCTGCGTCCGAACGCCT GGTCCAGCCCAGGATCATCG 1800
D  A  L  V  R  R  Y   R  T  E  R  G  R  P   A  .
CGGGCAGGCAGCTGCCGATC ATCAAGGCCGCCAAGGCCAT CAGCGCACCGGCATAGGCCA GGTCGCGGATGGTCTTGGCG TCGGCGCCGGTTCAGCTGCG 1900

TCGACACGATGATCCAGCTG CAGAATTC                                                                            1928
```

FIG. 1. Nucleotide and deduced amino acid sequences of the *Eco*RI-*Bam*HI fragment containing the phosphoglucose isomerase gene of *M. smegmatis*. Two putative start codons are underlined.

pgi gene of mc^{2}743 and characterization of the mutant allele of mc^{2}744 are under way.

Characterization of *pgi* mutants. The enzyme Pgi exerts considerable control at a pivotal point at the juncture of three metabolic pathways, i.e., the Embden-Meyerhoff-Parnass, the Entner-Doudoroff, and the phosphogluconate pathways (Fig. 3) (see Discussion). We examined the growth of the parental strain (mc^{2}155) and the two glycerol utilization mutants (mc^{2}743 and mc^{2}744) on nine carbon sources, which is summarized in Table 2. Each of the three strains carries the *E. coli*-mycobacterium shuttle vector, pMVI203, containing a kanamycin resistance gene and a multiple cloning site (28).

The noncomplemented mutant strains mc^{2}743 and mc^{2}744 grow only on glucose and poorly on galactose: no other carbohydrate tested (glycerol, fructose, succinate, Casamino Acids, gluconate, sorbitol, or ribose) was able to serve as a sole carbon source for growth. This suggests that the metabolic requirement is G6P or some derivative thereof, since of the nine carbon sources tested, only galactose typically enters the glycolytic pathway above G6P (Fig. 3). Pgi, which catalyzes the conversion of G6P to fructose-6-phosphate, is the only source of G6P during growth on substrates other than glucose or galactose.

We tested the growth of the wild-type and mutant strains carrying the complementing plasmid, pDT252, on these carbon sources. Table 2 shows that the wild-type and mutant strains grow equally well on glycerol minimal media in the presence of *pgi* carried on a multicopy plasmid (pDT252). This indicates

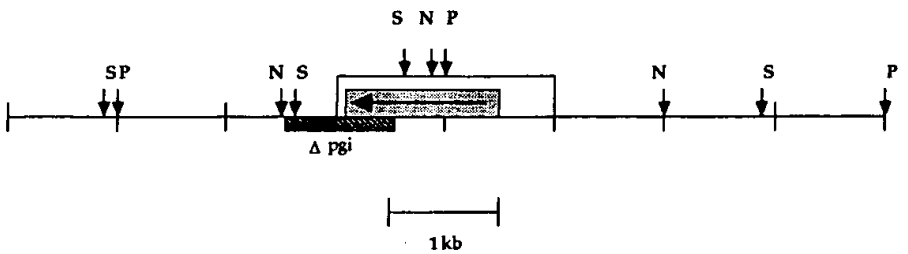

FIG. 2. Restriction map of the *pgi* region of *M. smegmatis*. *Pst*I (P), *Nco*I (N), and *Sph*I (S) were used to analyze chromosomal DNA of mc^{2}155 and mc^{2}743 by Southern analysis (see Materials and Methods). The sequenced region is indicated by an unshaded box. A horizontal arrow indicates the direction of transcription of the *pgi* ORF (shaded area). A hatched bar indicates the extent of deletion in mutant strain mc^{2}743.

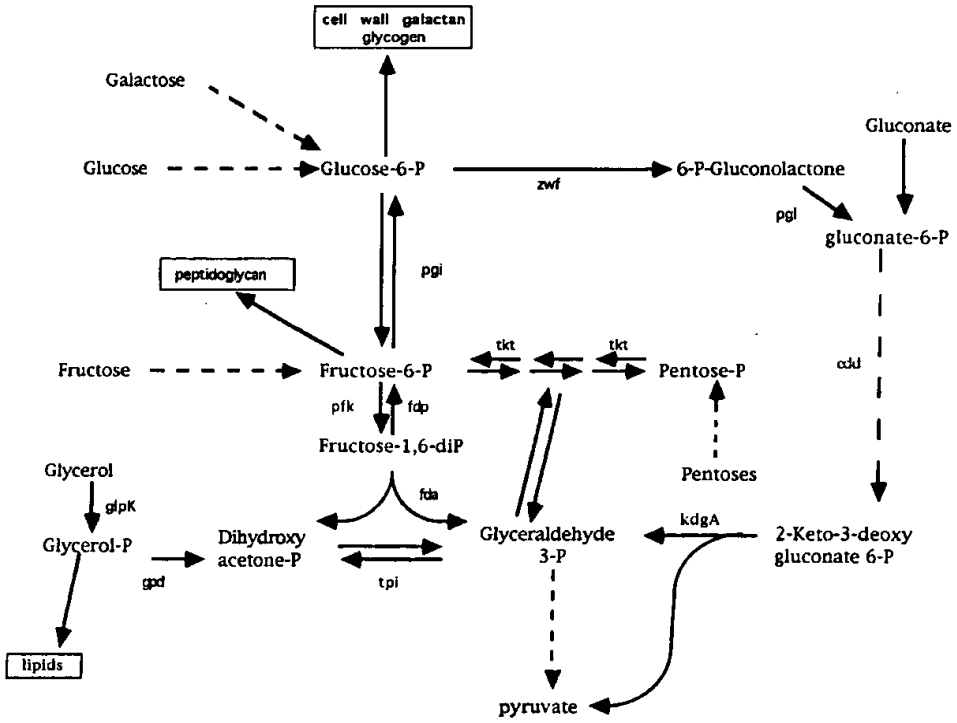

FIG. 3. Intermediary metabolic pathways in bacteria known to be present in mycobacteria (26). The routes to cell wall components are indicated.

that the *pgi* gene is sufficient to restore wild-type growth abilities to the two mutants.

To corroborate these phenotypic observations, levels of three glycerol and glucose metabolic enzymes were measured in extracts prepared from wild-type cells, the *pgi* mutants, and all three strains carrying the cloned copy of the *pgi* gene. We prepared extracts from wild-type and mutant cells carrying either the cloning vector pMVI203 or the *pgi* plasmid pDT252 growing in either glucose or glycerol. Table 3 shows the levels of Pgi in wild-type cells and in mc^{2}743 and mc^{2}744. The wild-type strain had high levels of Pgi in both glycerol and glucose minimal medium, indicating constitutive expression of the enzyme. However, the mutant strains mc^{2}743 and mc^{2}744 showed at least a 1,000-fold reduction in Pgi activity when grown on glucose. In contrast, the presence of the cloned copy of the complementing gene restored Pgi activity to the mutant strains.

As controls for the cell extracts and growth conditions, we measured the levels of α-glycerol phosphate dehydrogenase (GlpD) and triose phosphate isomerase (Tpi). The former should be regulated in response to a carbon source (i.e., repressed by glucose) (3), whereas the latter should be constitu-

TABLE 2. Growth patterns of the wild type and glycerol mutants on various substrates[a]

Carbon source (concn)	Growth pattern[b]					
	mc^{2}155(pMVI203)	mc^{2}743(pMVI203)	mc^{2}744(pMVI203)	mc^{2}155(pDT252)	mc^{2}743(pDT252)	mc^{2}744(pDT252)
Glucose	+	+	+	+	+	+
Glycerol	+	−	−	+	+	+
Glucose + glycerol	+	+	+	+	+	+
Fructose	+	−	−	+	+	+
Sorbitol	+	−	−	+	+	+
Ribose	+	−	−	+	+	+
Galactose	+	±	±	+	+	+
Gluconate	+	−	−	+	+	+
Succinate	+	−	−	+	+	+
Succinate + glycerol	+	−	−	+	+	+
Casamino Acids	+	−	−	+	+	+
Glucose (0.1%)	±	±	±	ND[c]	ND	ND
Glucose (0.01%)	−	−	−	ND	ND	ND
Glycerol + glucose (0.01%)	+	+	+	ND	ND	ND

[a] Cells were streaked for single colonies on minimal basal salts plates supplemented with the indicated carbon sources at 10 g/liter, except as indicated.
[b] Symbols: +, large single colonies; ±, small single colonies; −, no single colonies.
[c] ND, not done.

TABLE 3. Levels of phosphoglucose isomerase, triose phosphate isomerase, and α-glycerol phosphate dehydrogenase activities in wild-type and mutant strains with and without the *pgi* gene carried on plasmid pMVI203[a]

Strain	Activity[b]		
	Pgi	Tpi	GlpD
Glycerol grown			
mc²155(pMVI203)	59.6 ± 0.5	16.3 ± 0.2	12.4 ± 0.4
mc²743(pMVI203)	NG[c]	NG	NG
mc²744(pMVI203)	NG	NG	NG
mc²155(pDT252)	120.9 ± 0.1	9.8 ± 0.03	12.5 ± 0.6
mc²743(pDT252)	81.0 ± 0.8	14.5 ± 0.1	12.4 ± 0.4
mc²744(pDT252)	78.2 ± 0.2	7.9 ± 0.05	0.9 ± 0.1
Glucose grown			
mc²155(pMVI203)	51.8 ± 0.8	10.8 ± 0.2	<0.6
mc²743(pMVI203)	<0.6	8.2 ± 0.2	<0.6
mc²744(pMVI203)	<0.6	8.5 ± 0.3	<0.6
mc²155(pDT252)	141.7 ± 0.3	11.3 ± 0.3	<0.6
mc²743(pDT252)	95.2 ± 0.5	11.0 ± 0.9	<0.6
mc²744(pDT252)	82.4 ± 0.3	9.4 ± 0.1	<0.6

[a] Assays were performed three times on two extracts.
[b] Activity is expressed in units per milligram of cell extract.
[c] NG, no growth (mutants do not grow in glycerol minimal medium).

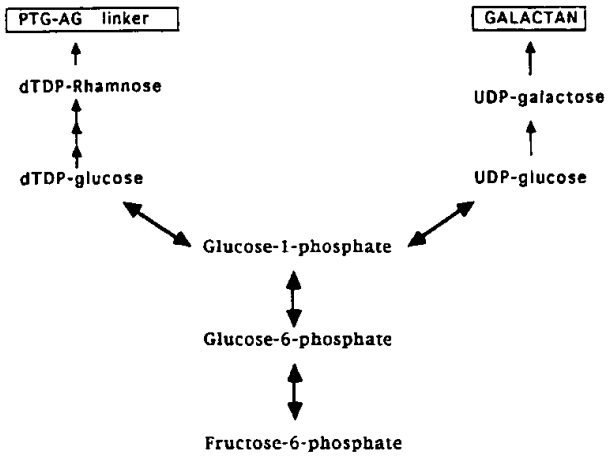

FIG. 4. Relevant cell wall synthetic pathways. Enzymes whose activity has been identified in mycobacteria are indicated (see Discussion).

tively expressed. Tpi is found at similar levels in extracts from all six strains (Table 3). As expected, GlpD levels were barely detectable in glucose-grown cells of all six strains, suggesting that the mutants bear no severe regulatory defects with respect to glycerol and glucose regulation of glycerol enzymes (3). However, mc²744(pDT252), which exhibits wild-type levels of Pgi activity, does show slightly reduced levels of GlpD activity when grown on glycerol (Table 3). The basis of this sole difference between the two *pgi* mutants is under examination.

Pgi mutants of *M. smegmatis* are glucose auxotrophs. Since the *pgi* mutants of *M. smegmatis* grow only on glucose, we tested the possibility that they actually require glucose for growth. We supplied extremely low concentrations of glucose in media composed of other carbon sources. Glucose at a concentration of 0.01% is not sufficient to support the growth of wild-type *M. smegmatis* in the absence of another carbon source (Table 2). When this low concentration of glucose was added to glycerol (Table 2) or to the other carbon sources listed in Table 2, mc²743 and mc²744 grew at wild-type levels in every case (data not shown). This experiment demonstrates that low levels of glucose are required for growth of mycobacterial *pgi* mutants on substrates other than glucose, indicating an absolute requirement in these mutants for glucose or G6P.

DISCUSSION

We have isolated mutants of *M. smegmatis* lacking a functional gene encoding the enzyme phosphoglucose isomerase (*pgi*). These mutants can grow only on glucose or galactose as a sole carbon source. However, any carbon source will support wild-type levels of growth if glucose is provided in trace amounts. We used the mutants to clone the gene encoding *pgi* and showed that its sequence is highly homologous to that of the *pgi* genes of other species. We measured the levels of Pgi in the wild type and mutants and showed that there is no detectable activity of Pgi in the mutants. Complementation of the mutants with the cloned copy of *pgi* restored both intracellular levels of Pgi and the wild-type growth phenotype when tested on a large number of carbon sources. Finally, we demonstrated that the *pgi* mutants are glucose auxotrophs, since (i) the mutants grow only on glucose as the sole carbon source and (ii) supplementation of carbon sources other than glucose with trace amounts of glucose restores wild-type growth.

The absolute requirement for glucose by *pgi* mutants of *M. smegmatis* may be explained by examining the structure of the mycobacterial cell wall and its synthetic pathways. The major polysaccharide is arabinogalactan (AG), a large polymer positioned by covalent linkage between the peptidoglycan (PTG) and mycolic acid (MA) (18). MA, constituting close to 50% by weight of the cell wall mass, is likely responsible for the notorious impermeability of the mycobacterial cell. The ability to synthesize any of the components of the PTG-AG-MA network, or cell wall core, is expected to be essential, and the enzymes involved in its synthesis are targets of current or future antimycobacterial drugs (17).

A key feature in this covalent polymeric network is the linker disaccharide phosphate which links the PTG to the AG (16). The structure of the PTG-AG linker is L-rhamnose-(1-3)-D-*N*-acetylglucosamine-(1-P-6)-D-muramic acid (16). As illustrated in Fig. 4, G6P, via glucose-1-phosphate, is the precursor for the L-rhamnose component of the linker molecule. The donor of this component, dTDP-rhamnose, is synthesized from glucose-1-phosphate and TTP (18) in the same manner as it is in gram-negative bacteria, which use dTDP-rhamnose to insert rhamnose into lipopolysaccharide (LPS) O antigens (39). Thus, inability to synthesize G6P will inhibit cell wall core formation and lead to loss of viability of the cell.

A second component of the mycobacterial cell wall requiring G6P for its synthesis is the galactan residue of AG. Again, by analogy with other polysaccharide synthetic systems (33, 34), G6P is converted to G1P and thence to UDP-glucose; an activity has been identified in mycobacteria which converts UDP-glucose to UDP-galactose for transfer into the AG complex (16). Inhibition of AG synthesis is lethal for the mycobacterial cell and is most likely the mechanism of action of ethambutol (29).

Pgi is a key enzyme in the pathway of cell wall biosynthesis in mycobacteria. Our observation that 0.01% glucose (10^{-5} g/ml) supplies sufficient precursor for cell wall core synthesis is supported by calculations of the amount of carbon directed into L-rhamnose and galactan from G6P, assuming that there is 1 rhamnose molecule for every 33 galactose molecules and that

the cell wall galactan is 1% of the dry weight of the cell (approximately 3×10^{-6} g/ml of saturated culture) (17a, 21).

Phosphoglucose isomerase mutants have been well characterized in a number of other genetic systems. The salient phenotypes of *Bacillus subtilis* (25) and *E. coli* (35) mutants lacking phosphoglucose isomerase are (i) very slow growth on glucose and galactose, (ii) normal growth on carbon sources entering glycolysis below the block, such as fructose and glycerol, and (iii) normal growth on gluconate, which is metabolized via either the Entner-Doudoroff pathway or the hexose monophosphate shunt. The slow growth on glucose is presumed to be the result of the inefficiency of growth on these latter pathways. *pgi* mutants of *E. coli* can grow on gluconate as the sole carbon source because they do not require G6P or any of its derivatives for growth (8, 18); gluconate is metabolized via the pentose phosphate or Entner-Doudoroff pathways (Fig. 3). The glucose auxotrophy of the *pgi* mutants of *M. smegmatis* described here predicts that these mutants cannot grow on gluconate, since the enzymes leading from G6P to gluconate-6-phosphate are unidirectional (Fig. 3). Table 2 shows that this is indeed the case.

In contrast, *pgi1* mutants of *S. cerevisiae* cannot grow on glucose as the sole carbon source, yet they are glucose auxotrophs (1). *pgi1* null mutants of *S. cerevisiae* have been well characterized. These strains cannot grow on glucose, presumably because flux through the hexose monophosphate shunt is inadequate to support growth (5). Yet, *pgi1* null cells also require glucose for growth and sporulation on other substrates (1). Indeed, the locus is also known as *CDC30*, since *cdc30* and *pgi1* cells arrest late in nuclear division at the nonpermissive temperature (7). A number of *CDC* genes encode intermediary metabolic genes. For example, *CDC19* encodes a temperature-sensitive pyruvate kinase (20). The sensitivity of *S. cerevisiae pgi1* null strains to high concentrations of glucose may explain the cell cycle phenotype as the result of accumulation of G6P in arrested cells, since many phosphorylated intermediates are toxic when allowed to accumulate (1).

In addition to its involvement in yeast cell cycle control, phosphoglucose isomerase has recently been implicated in growth phase gene regulation in *E. coli*. The *pgi* gene was identified in a screen for insertions which affect in *trans* the expression of a *lacZ* fusion to *osmY*, a gene regulated by the stationary-phase sigma factor RpoS (2). The authors of the *E. coli* study propose that UDP-glucose, a derivative of G6P, is an intracellular signal molecule in the control of expression of a number of *rpoS*-regulated genes. While the mycobacterial *rpoS* itself has not been cloned, a mycobacterial homolog of *sigF* (*B. subtilis* and *Streptomyces coelicolor*) and *sigB* (*B. subtilis*) has recently been cloned (13) and the regulatory targets of this and other putative stationary-phase and stress response regulatory molecules will soon be identified. It will be interesting to see whether *pgi* mutants of *M. smegmatis* are similarly altered in expression of *rpoS*-regulated genes, and these experiments are under way.

That *E. coli* and *S. typhimurium pgi* null mutants can grow, albeit slowly, on glucose suggests that there is no requirement for G6P and its derivatives in these species (35). Thus, *pgi* mutants of *S. typhimurium* grown on gluconate have incomplete LPS, since G6P cannot be formed from gluconate (9). In *pgi* mutants of *E. coli*, complete polymers of LPS or glycogen are produced only in the presence of glucose, and this feature can be exploited in the study of LPS or glycogen synthesis (10). Similarly, the mutants described here could serve as useful labeling strains. *M. smegmatis* appears to have an absolute requirement for glucose or a derivative thereof: growth of the cells on succinate or glycerol with trace labels of high-specific-activity [^{14}C]glucose would direct radiolabel only into those lipid moieties derived from glucose. We have initiated the construction of *pgi* deletion mutants to investigate the roles of *pgi* in carbohydrate metabolism and cell wall synthesis in the pathogenic slow-growing species such as *M. tuberculosis* and *Mycobacterium bovis*.

ACKNOWLEDGMENTS

We thank M. Brandriss, J. Flynn, and C. Newlon for helpful discussions and reading of the manuscript and R. Coles for performing the enzyme assays.

This work was supported in part by Public Health Service grants R29AI34436 to N.C. and AI26170 to W.R.J.

REFERENCES

1. **Aguilera, A.** 1986. Deletion of the phosphoglucose isomerase structural gene makes growth and sporulation glucose dependent in *Saccharomyces cerevisiae*. Mol. Gen. Genet. **204**:310–316.
2. **Boehringer, J., D. Fischer, G. Mosler, and R. Hengge-Aronis.** 1995. UDP-glucose is a potential intracellular signal molecule in the control of expression of σ^S and σ^S-dependent genes in *Escherichia coli*. J. Bacteriol. **177**:413–422.
3. **Bowles, J. A., and W. Segal.** 1965. Kinetics of utilization of organic compounds in the growth of *Mycobacterium tuberculosis*. J. Bacteriol. **90**:157–163.
4. **Brennan, P. J., D. P. Lehane, and D. W. Thomas.** 1970. Acylglucoses of the corynebacteria and mycobacteria. Eur. J. Biochem. **13**:117–123.
5. **Bruinenberg, P. M., G. W. Waslander, J. P. van Dijken, and W. A. Scheffers.** 1986. A comparative radiospirometric study of glucose metabolism in yeasts. Yeast **2**:117–121.
6. **Connell, N. D.** 1994. Mycobacterium: isolation, maintenance, transformation, and mutant selection, p. 107–125. *In* D. G. Russell (ed.), Methods in cell biology. Academic Press, Inc., New York, N.Y.
7. **Dickinson, J. R., and A. S. Willimas.** 1987. The *cdc30* mutation in *Saccharomyces cerevisiae* results in a temperature-sensitive isoenzyme of phosphoglucose isomerase. J. Gen. Microbiol. **133**:135–140.
8. **Fraenkel, D. G., and B. I. Horecker.** 1964. Pathways of D-glucose metabolism in *Salmonella typhimurium*. J. Biol. Chem. **239**:2765–2769.
9. **Fraenkel, D. G., M. J. Osborn, B. L. Horecker, and S. M. Smith.** 1963. Metabolism and cell wall structure of a mutant of *Salmonella typhimurium* deficient in phosphoglucose isomerase. Biochem. Biophys. Res. Commun. **11**:423–428.
10. **Fraenkel, D. G., and R. T. Vinopal.** 1973. Carbohydrate metabolism in bacteria. Annu. Rev. Microbiol. **27**:69–100.
11. **Froman, B. E., R. C. Tait, and L. D. Gottlieb.** 1989. Isolation and characterization of the phosphoglucose isomerase gene from *Escherichia coli*. Mol. Gen. Genet. **217**:126–131.
12. **Hanahan, D.** 1983. Studies on transformation of *Escherichia coli* with plasmids. J. Mol. Biol. **166**:557–580.
13. **Jacobs, W. R. J., G. V. Kalpana, J. D. Cirillo, L. Pascopella, S. B. Snapper, R. A. Udani, W. Jones, R. G. Barletta, and B. R. Bloom.** 1991. Genetic systems for mycobacteria. Methods Enzymol. **204**:537–555.
14. **Lin, E. C. C., and B. Magasanik.** 1960. The activation of glycerol dehydrogenase from *Aerobacter aerogenes* by monovalent cations. J. Biol. Chem. **235**:1820–1823.
15. **Maniatis, T., E. F. Fritsch, and J. S. Sambrook.** 1982. Molecular cloning: a laboratory manual. Cold Spring Harbor Laboratory, Cold Spring Harbor, N.Y.
16. **McNeil, M., M. Daffe, and P. J. Brennan.** 1990. Evidence for the nature of the link between the arabinogalactan and peptidoglycan of mycobacterial cell walls. J. Biol. Chem. **265**:18200–18206.
17. **McNeil, M. R.** 1996. Targeted preclinical drug development for *Mycobacterium avium* complex: a biochemical approach, p. 263–283. *In* J. A. Korbick and C. A. Benson (ed.), Mycobacterium avium complex infection. Marcel Dekker, Inc., New York, N.Y.

17a. **McNeil, M. R.** Personal communication.

18. **McNeil, M. R., G. S. Besra, and P. J. Brennan.** 1996. Chemistry of the mycobacterial cell wall, p. 171–186. *In* W. N. Rom and S. M. Garay (ed.), Tuberculosis. Little, Brown & Co., New York, N.Y.
19. **Misset, O., and F. R. Opperdoes.** 1984. Simultaneous purification of hexokinase class I fructose-bisphosphate aldolase, triosephosphate isomerase and phosphoglycerate kinase from *Trypanosoma brucei*. Eur. J. Biochem. **144**:475–483.
20. **Moore, P. A.** 1990. Multiple copies of the pyruvate kinase gene affect yeast cell growth. J. Gen. Microbiol. **136**:2359–2366.
21. **Neidhardt, F. C., and H. E. Umbarger.** 1996. Chemical composition of *Escherichia coli*, p. 13–16. *In* F. C. Neidhardt, R. Curtiss III, J. L. Ingraham, E. C. C. Lin, K. B. Low, Jr., B. Magasanik, W. S. Reznikoff, M. Riley, M. Schaechter, and H. E. Umbarger (ed.), *Escherichia coli* and *Salmonella*:

cellular and molecular biology, 2nd ed. ASM Press, Washington, D.C.
22. **Nyame, K., C. D. Do-Thi, F. R. Opperdoes, and P. A. Michels.** 1994. Subcellular distribution and characterization of glucosephosphate isomerase in *Leishmania mexicana*. Mol. Biochem. Parasitol. **67**:269–279.
23. **Padh, H., and T. A. Venkitasubramanian.** 1976. Adenosine 3′:5′-monophosphate in *Mycobacterium phlei* and *Mycobacterium tuberculosis* H37Ra. Microbios **16**:183–189.
24. **Pascopella, L., F. M. Collins, J. M. Martin, M. H. Lee, G. F. Hatfull, C. K. Stover, B. R. Bloom, and W. R. Jacobs, Jr.** 1994. Use of in vivo complementation in *Mycobacterium tuberculosis* to identify a genomic fragment associated with virulence. Infect. Immun. **62**:1313–1319.
25. **Prasad, C., M. Diesterhaft, and E. Freese.** 1972. Initiation of spore germination in glycolytic mutants of *Bacillus subtilis*. J. Bacteriol. **110**:321–328.
26. **Ratledge, C.** 1982. Nutrition, growth and metabolism, p. 186–212. *In* C. Ratledge and J. Stanford (ed.), The biology of the mycobacteria. Academic Press, Ltd., London, United Kingdom.
27. **Snapper, S. B., R. E. Melton, S. Mustafa, T. Kieser, and W. R. J. Jacobs.** 1990. Isolation and characterization of efficient plasmid transformation mutants of *Mycobacterium smegmatis*. Mol. Microbiol. **4**:1911–1919.
28. **Stover, C. K., V. F. de la Cruz, T. R. Fuerst, J. E. Burlein, L. A. Benson, L. T. Bennet, G. P. Bansal, J. F. Young, M. H. Lee, G. F. Hatfull, S. B. Snapper, R. G. Barletta, W. R. Jacobs, and B. R. Bloom.** 1991. New use of BCG for recombinant vaccines. Nature (London) **351**:456–460.
29. **Takayama, K., and J. O. Kilburn.** 1989. Inhibition of synthesis of arabinogalactan by ethambutol in *Mycobacterium smegmatis*. Antimicrob. Agents Chemother. **33**:1493–1499.
30. **Tao, W., L. Wang, R. Shen, and Z. Sheng.** 1989. Complete nucleotide sequence of two phosphoglucoseisomerase isozymes from *Bacillus stearothermophilus*. Nucleic Acids Res. **17**:10107–10108.
31. **Tekamp-Olson, P., R. Najarian, and R. Burke.** 1988. The isolation, characterization and nucleotide sequence of the phosphoglucoseisomerase gene of *Saccharomyces cerevisiae*. Gene **73**:153–161.
32. **Tepper, B. S.** 1968. Differences in the utilization of glycerol and glucose by *Mycobacterium phlei*. J. Bacteriol. **95**:1713–1717.
33. **Trejo, A. G., G. J. F. Chittenden, J. G. Buchanan, and J. Baddiley.** 1970. Uridine diphosphate α-D-galactofuranose, an intermediate in the biosynthesis of galactofuranosyl residues. Biochem. J. **117**:637–639.
34. **Trejo, A. G., J. W. Haddock, G. J. F. Chittenden, and J. Baddiley.** 1971. The biosynthesis of galactofuranosyl residues in galactocarlose. Biochem. J. **122**: 49–57.
35. **Vinopal, R. T., J. D. Hillman, H. Schulman, W. S. Reznikoff, and D. G. Fraenkel.** 1975. New phosphoglucose isomerase mutants of *Escherichia coli*. J. Bacteriol. **122**:1172–1174.
36. **Wada, K., Y. Wada, Y. Ishibashi, T. Gojobori, and T. Ikemura.** 1992. Codon usage tabulated from the GenBank genetic sequence data. Nucleic Acids Res. **20**:S2111–S2118.
37. **Walker, J. I., P. Faik, and M. J. Morgan.** 1990. Characterization of the 5′ end of the gene for human glucose phosphate isomerase (GPI). Genomics **7**:638–643.
38. **Winder, F. G., and P. J. Brennan.** 1966. Initial steps in the metabolism of glycerol by *Mycobacterium tuberculosis*. J. Bacteriol. **92**:1846–1847.
39. **Xiang, S. H., A. M. Haase, and P. R. Reeves.** 1993. Variation of the *rfb* gene clusters in *Salmonella enterica*. J. Bacteriol. **175**:4877–4884.

Volume 49, Number 2, January 20, 1996

Biotechnology and Bioengineering

ISSN 0006-3592

WILEY
Publishers Since 1807